

9-27-1961

An Acoustic Simulator For Modeling Backscatter of Electromagnetic Waves

Allen R. Edison

Follow this and additional works at: https://digitalrepository.unm.edu/ece_etds



Part of the [Electrical and Computer Engineering Commons](#)

Recommended Citation

Edison, Allen R.. "An Acoustic Simulator For Modeling Backscatter of Electromagnetic Waves." (1961).
https://digitalrepository.unm.edu/ece_etds/429

This Dissertation is brought to you for free and open access by the Engineering ETDs at UNM Digital Repository. It has been accepted for inclusion in Electrical and Computer Engineering ETDs by an authorized administrator of UNM Digital Repository. For more information, please contact disc@unm.edu.

UNIVERSITY OF NEW MEXICO-UNIVERSITY LIBRARIES



A14429 095774

AN ACOUSTIC
SIMULATOR
OR MODELING
BACKSCATTER
OF ELECTRO-
MAGNETIC
WAVES

EDISON

EDISON

78.789
ln310e
1962
cop. 2

THE LIBRARY
UNIVERSITY OF NEW MEXICO



Call No.

378.789

Un310e

1962

cop.2

Accession
Number

285033

A14409 152051

DATE DUE

5w LTD

FEB 15 1966

APR 10 '88

DEMCO 38-297

LIBRARY

UNIVERSITY OF TORONTO

UNIVERSITY OF NEW MEXICO LIBRARY

MANUSCRIPT THESES

Unpublished theses submitted for the Master's and Doctor's degrees and deposited in the University of New Mexico Library are open for inspection, but are to be used only with due regard to the rights of the authors. Bibliographical references may be noted, but passages may be copied only with the permission of the authors, and proper credit must be given in subsequent written or published work. Extensive copying or publication of the thesis in whole or in part requires also the consent of the Dean of the Graduate School of the University of New Mexico.

This thesis by Allen R. Edison
has been used by the following persons, whose signatures attest their acceptance of the above restrictions.

A Library which borrows this thesis for use by its patrons is expected to secure the signature of each user.

NAME AND ADDRESS

DATE

Loaned to U. S. Dept. of the Interior,
Geological Survey, Washington, D. C.
June 19, 1962.

Loaned to U. S. Navy Underwater Sound
Laboratory, Fort Trumbull, New London,
Connecticut 12 February, 1965.

AN ACOUSTIC SIMULATOR FOR MODELING BACKSCATTER OF
ELECTROMAGNETIC WAVES



By
Allen R. Edison

A Dissertation
Submitted in Partial Fulfillment of the
Requirements for the Degree of
Doctor of Science in Electrical Engineering

The University of New Mexico

1961

AN ACOUSTIC SIMULATOR FOR MODELLING BACKSCATTER OF

ELECTROMAGNETIC WAVES



By

Allen R. Edson

A Dissertation

Submitted in Partial Fulfillment of the

Requirements for the Degree of

Doctor of Science in Electrical Engineering

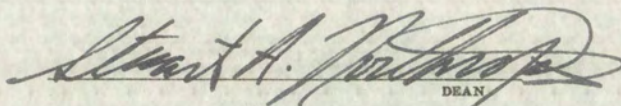
The University of New Mexico

1951

378.789
Un310e
1962
cop. 2

This dissertation, directed and approved by the candidate's committee, has been accepted by the Graduate Committee of the University of New Mexico in partial fulfillment of the requirements for the degree of

DOCTOR OF SCIENCE


DEAN

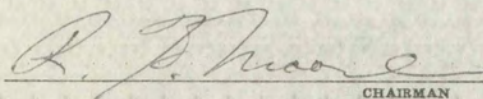
September 27, 1961
DATE

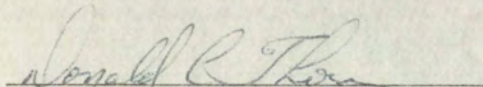
AN ACOUSTIC SIMULATOR FOR MODELING BACKSCATTER OF
ELECTROMAGNETIC WAVES

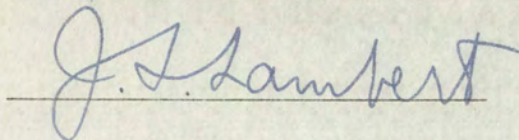
By

Allen R. Edison

Committee


CHAIRMAN





285083

This dissertation directed and approved by the candidate's committee, has been accepted by the Graduate Committee of the University of New Mexico in partial fulfillment of the requirements for the degree of

DOCTOR OF SCIENCE




AN ACOUSTIC SIMULATOR FOR MODELING BACKSCATTER OF
ELECTROMAGNETIC WAVES

BY

Allen R. Ellison

Committee



282883

TABLE OF CONTENTS

	Page
LIST OF TABLES	iv
LIST OF ILLUSTRATIONS	v
Chapter	
I INTRODUCTION	1
II THEORY OF MODELS	13
2.1 Dimensional and Inspectional Analysis	14
2.2 Linear Modeling	17
2.3 Nonlinear Modeling	23
2.4 Modeling Considerations	30
III ANALOGIES	33
3.1 Wave Equations	34
3.2 Spherical Waves	36
3.3 Plane Waves	43
3.4 Plane-Wave Reflection	46
3.5 Applications of the Analogies	53
3.6 A Scattering Model	64
3.7 Summary of Model Validity	68
IV RADAR SYSTEM SCALE FACTORS	70
4.1 Pulsed Radar	71
4.2 FM Radar System	79
4.3 Doppler Frequency Radar	84
4.4 Forward Scatter Model	87
V THE ACOUSTIC SIMULATOR	91
5.1 Pulsed Radar Simulator.	92
5.2 Doppler Radar Device	100
5.3 Frequency Modulated Radar Device	103
5.4 Sound Absorbing Materials for Tank Walls	104
5.5 Acoustic Tank and Targets	106
5.6 Transducers	111
5.7 Antenna Pattern for Flat Disk Transducer	118
5.8 Pattern Shaping Devices	120
5.9 Recommendations for an Acoustic Simulator	131

Page	
iv	LIST OF TABLES
v	LIST OF ILLUSTRATIONS
	Chapter
i	INTRODUCTION
ii	THEORY OF MODELS
14	2.1 Dimensional and Spectral Analysis
17	2.2 Linear Modeling
22	2.3 Nonlinear Modeling
30	2.4 Modeling Considerations
32	ANALOGIES
34	3.1 Wave Equations
35	3.2 Spherical Waves
36	3.3 Plane Waves
37	3.4 Plane-Wave Reflection
38	3.5 Applications of the Analogies
39	3.6 A Scattering Model
40	3.7 Summary of Model Validity
40	RADAR SYSTEM SCALE FACTORS
41	4.1 Pulsed Radar
42	4.2 FM Radar System
43	4.3 Doppler Frequency Radar
44	4.4 Forward Scatter Model
44	THE ACOUSTIC SIMULATOR
45	5.1 Pulsed Radar Simulator
46	5.2 Doppler Radar Device
47	5.3 Frequency Modulated Radar Device
48	5.4 Sound Absorbing Materials for
49	Tank Walls
50	5.5 Acoustic Tank and Targets
51	5.6 Transducers
52	5.7 Antenna Pattern for Flat Disk
53	Transducer
54	5.8 Pattern Shaping Devices
55	5.9 Recommendations for an Acoustic
56	Simulator

Chapter		Page
VI	EXPERIMENTAL RESULTS	135
	6.1 Geometrical Effects	136
	6.2 Fading Statistics	146
	6.3 Radar Cross Sections	156
	6.4 Recommendations	160
VII	THE ACOUSTIC SIMULATOR AS AN ANALOG COMPUTER	163
	7.1 The FM Altimeter Analog	165
	7.2 FM Altimeter Results.	171
VIII	CONCLUSIONS.	184
APPENDIX		
	A. FADING OF RADAR SIGNALS.	190
	B. REPEATABILITY OF FADING RECORDS . . .	199
BIBLIOGRAPHY		202

VI	EXPERIMENTAL RESULTS	135
	6.1 Geometrical Effects	135
	6.2 Fading Statistics	140
	6.3 Radar Cross Sections	150
	6.4 Recommendations	160
VII	THE ACOUSTIC SIMULATOR AS AN ANALOG COMPUTER	163
	7.1 The FM Altimeter Analogy	165
	7.2 FM Altimeter Results	171
VIII	CONCLUSIONS	184
APPENDIX		
	A. FADING OF RADAR SIGNALS	190
	B. REPEATABILITY OF FADING RECORDS	199
	BIBLIOGRAPHY	202

LIST OF TABLES

Table	Page
3-1 Analogies - Acoustic Double Source and Short Current Element	41
3-2 Analogies - Elementary Spherical Source and Short Current Element	42
3-3 Analogies - Acoustic Dipole and Short Current Element	44
3-4 Plane Wave Analogies	45
3-5 Acoustic Impedance Ratios for Several Materials	53
4-1 Scaled Parameters for Pulse Radar	72
4-2 Scaling Relations for a Pulse Radar System	76
4-3 Example of Pulse Radar Scaling	77
4-4 Scaled Parameters for FM Radar	80
4-5 Scaling Relations for an FM Radar System .	85
4-6 Scaled Parameters for a Doppler Radar . . .	86
4-7 Scaling Relations for a Doppler Radar System	88
5-1 Beamwidths for Flat Disk Transducers . . .	120
6-1 Radar Terrain Return Fading Data	148
6-2 Acoustic Simulator Fading Data	149
6-3 Effective Fading Frequencies	154
6-4 Target Recommendations	162
7-1 Frequency Modulated Altimeter Model	165
7-2 FM Altimeter Experimental Results	177

LIST OF TABLES

Table	Page
3-1 Analogies - Acoustic Double Source and Short Current Element	41
3-2 Analogies - Elementary Spherical Source and Short Current Element	42
3-3 Analogies - Acoustic Dipole and Short Current Element	44
3-4 Plane Wave Analogies	45
3-5 Acoustic Impedance Ratios for Several Materials	53
4-1 Scaled Parameters for Pulse Radar	73
4-2 Scaling Relations for a Pulse Radar System	76
4-3 Example of Pulse Radar Scaling	77
4-4 Scaled Parameters for FM Radar	80
4-5 Scaling Relations for an FM Radar System	82
4-6 Scaled Parameters for a Doppler Radar	86
4-7 Scaling Relations for a Doppler Radar System	88
5-1 Beamwidths for Flat Disk Transducers	130
6-1 Radar Terrain Return Fading Data	148
6-2 Acoustic Simulator Fading Data	149
6-3 Effective Fading Frequencies	154
6-4 Target Recommendations	163
7-1 Frequency Modulated Altimeter Model	165
7-2 FM Altimeter Experimental Results	177

LIST OF FIGURES

Figure	Page
2-1 Nonlinear Modeling of Transmission Line . .	27
3-1 Short Current Element	37
3-2 Acoustic Double Source	38
3-3 Boundary Conditions on Perfect Plane Surfaces	54
3-4 Coordinate System for EM Wave	55
3-5 Coordinate System for Acoustic Wave	56
3-6 H-Field Incident on Plane	60
3-7 Particle Velocity Incident on Plane	61
3-8 Reflection Coefficients for TM and TE Waves	63
3-9 Reflection Coefficients for Acoustic Waves	63
3-10 Scattering Model	65
3-11 Geometry for Incident Acoustic and EM Fields	66
4-1 Piece-Wise Linear Modulation	80
4-2 FM Difference Frequency	82
5-1 Pulsed Radar Acoustic Simulator - Block Diagram	93
5-2 Pulsed Oscillator	94
5-3 Acoustic Simulator Equipment Setup	94
5-4 Duplexer	96
5-5 Sample Film Strip Showing Successive Pulses	99
5-6 Sample Film Strip Showing Fading Record . .	99

LIST OF FIGURES

Figure	
2-1	Nonlinear Modeling of Transmission Lines
2-2	Short Current Element
2-3	Acoustic Double Source
2-4	Boundary Conditions on Perfect Plane Surface
2-5	Coordinate System for EM Wave
2-6	Coordinate System for Acoustic Wave
2-7	H-Field Incident on Plane
2-8	Particle Velocity Incident on Plane
2-9	Reflection Coefficients for TM and TE Waves
2-10	Reflection Coefficients for Acoustic Waves
2-11	Scattering Model
3-1	Geometry for Incident Acoustic and EM Fields
3-2	Piece-Wise Linear Modulation
3-3	FM Difference Frequency
3-4	Pulsed Radar Acoustic Simulator Block Diagram
3-5	Pulsed Oscillator
3-6	Acoustic Simulator Equipment Setup
3-7	Duplexer
3-8	Sample Film Strip Showing Successive Frames
3-9	Sample Film Strip Showing Fading Record

Figure		Page
5-7	Doppler Frequency Radar - Block Diagram .	102
5-8	Frequency Modulated Radar - Block Diagram	102
5-9	Water Tank, Platform, and Transducer . . .	107
5-10	City Target in the Tank	107
5-11	Rough Sand Target	109
5-12	Close-up of Rough Sand Target	109
5-13	Mountain Target	112
5-14	City Target	112
5-15	Electro-Mechanical Transducer Diagram . .	115
5-16	Transducer Equivalent Circuit	117
5-17	Transducers and Lenses	122
5-18	Lens and Antenna Pattern	123
5-19	Extension Lens	124
5-20	Fan-Beam Reflector and Antenna Pattern . .	126
5-21	Broad-Beam Reflector and Antenna Pattern .	127
5-22	Aperture Mask	128
5-23	Collimators	129
5-24	Shaped Transducers	130
6-1	Transmitter Pulses	140
6-2	Short Pulse - Narrow Beam - No Motion . .	140
6-3	Short Pulse - Narrow Beam - Motion	140
6-4	Wide Pulse - Narrow Beam - No Motion . . .	141
6-5	Wide Pulse - Narrow Beam - Motion	141
6-6	Narrow Pulse - Wide Beam - No Motion . . .	141
6-7	Narrow Pulse - Wide Beam - Motion	141

- 5-7 Doppler Frequency Radar
- 5-8 Frequency Modulated Radar
- 5-9 Water Tank, Platform, and Radar
- 5-10 City Target in the Tank
- 5-11 Rough Sand Target
- 5-12 Close-up of Rough Sand Target
- 5-13 Mountain Target
- 5-14 City Target
- 5-15 Electro-Mechanical Transducer Diagram
- 5-16 Transducer Equivalent Circuit
- 5-17 Transducers and Joints
- 5-18 Lens and Antenna Pattern
- 5-19 Extension Lens
- 5-20 Fan-Beam Reflector and Lens
- 5-21 Broad-Beam Reflector and Antenna Pattern
- 5-22 Aperture Mask
- 5-23 Collimators
- 5-24 Shaped Transducers
- 6-1 Transmitter Pulses
- 6-2 Short Pulse - Narrow Beam
- 6-3 Short Pulse - Narrow Beam
- 6-4 Wide Pulse - Narrow Beam
- 6-5 Wide Pulse - Narrow Beam
- 6-6 Narrow Pulse - Wide Beam
- 6-7 Narrow Pulse - Wide Beam

Figure		Page
6-8	Wide Pulse - Wide Beam - No Motion	142
6-9	Wide Pulse - Wide Beam - Motion	142
6-10	Signal vs. Altitude over Smooth Surface .	144
6-11	Signal vs. Altitude over Rough Surface . .	145
6-12	Variance Spectrum for Wooded Terrain . . .	151
6-13	Variance Spectrum for Rough Sand	152
6-14	Pulse-Radar Altitude Indication over City	156
6-15	Typical Radar Back-Scattering Cross Sections	158
6-16	Radar Back-Scattering Cross Sections Over Cities	159
7-1	FM Altimeter System - Block Diagram . . .	167
7-2	Amplifier and Clipper Circuit	168
7-3	Transmitted and Received Frequencies as a Function of Time	169
7-4	Counting Rate Circuit	171
7-5	Smooth Steel Target with Offset	179
7-6	Rough Sand Target - Antenna Tilted	179
7-7	Rough Sand Target - 6 degree Beamwidth . .	180
7-8	Rough Sand Target - 12 degree Beamwidth .	181
7-9	Rough Sand Target - Altitude Increasing .	182
7-10	City Target - 6 degree Beamwidth	183
B-1	FM Fading Records which Demonstrate Repeatability	200
B-2	Pulse Fading Records which Demonstrate Repeatability	201

Page	Figure
142	6-8 Wide Pulse - Wide Beam - No Motion
143	6-9 Wide Pulse - Wide Beam - Motion
144	6-10 Signal vs. Altitude over Smooth Surface
145	6-11 Signal vs. Altitude over Rough Surface
151	6-12 Variance Spectrum for Wooded Terrain
152	6-13 Variance Spectrum for Rough Sand
156	6-14 Pulse-Radar Altitude Indication over City
158	6-15 Typical Radar Back-Scattering Cross Section
159	6-16 Radar Back-Scattering Cross Section Over Cities
167	7-1 FM Altimeter System - Block Diagram
168	7-2 Amplifier and Clipper Circuit
169	7-3 Transmitted and Received Waveforms as a Function of Time
171	7-4 Counting Rate Circuit
173	7-5 Smooth Steel Target with Offset
175	7-6 Rough Sand Target - Antenna Tilted
176	7-7 Rough Sand Target - 0 degree Beamwidth
181	7-8 Rough Sand Target - 12 degree Beamwidth
182	7-9 Rough Sand Target - Altitude Indication
183	7-10 City Target - 6 degree Beamwidth
200	B-1 FM Radar Records which Demonstrate Repeatability
201	B-2 Pulse Radar Records which Demonstrate Repeatability

CHAPTER I

INTRODUCTION

Model experiments are commonly employed in situations where a full-scale experiment is uneconomical and where exact theoretical analysis is very difficult. The physical problem is scaled to convenient laboratory dimensions and a means is provided for controlling and measuring the parameters of the experiment. Measurements made in the model system are required to provide information on the time and space variations of functions which describe the real system. When interpreting results it is frequently necessary to consider "scale effects" which arise from certain parameters exerting a different influence in the model than in the real system.

The purpose of this investigation is to study and develop the technique of using acoustic waves in water to simulate electromagnetic waves in air.^{1,2} This requires

¹An investigation of acoustic modeling of radar systems was started at the University of New Mexico in 1959 with financial support from the Naval Ordnance Test Station, China Lake, California.

²Water was selected as the acoustic medium largely because of its availability and ease of handling.

CHAPTER 1

INTRODUCTION

Model experiments are commonly employed in situations where a full-scale experiment is uneconomical and where exact theoretical analysis is very difficult. The physical problem is scaled to convenient laboratory dimensions and a means is provided for controlling and measuring the parameters of the experiment. Measurements made in the model system are required to provide information on the time and space variations of functions which describe the real system. When interpreting results it is frequently necessary to consider "scale effects" which arise from certain parameters exerting a different influence in the model than in the real system.

The purpose of this investigation is to study and develop the technique of using acoustic waves in water to stimulate electromagnetic waves in air.^{1,2} This requires

¹An investigation of acoustic modeling of radar systems was started at the University of New Mexico in 1959 with financial support from the Naval Ordnance Test Station, China Lake, California.

²Water was selected as the acoustic medium largely because of its availability and ease of handling.

an application of the theory of modeling and the use of analogies which exist between electromagnetic and acoustic waves.¹ The final result is the development of an acoustic simulator which serves as an analog computer to investigate radar, navigational equipment, and altimeter design problems. Appropriate scale factors are required in order to model complete systems and to ascertain their operating characteristics with a variety of targets.² The modeling technique is demonstrated for several systems using both pulse and frequency modulation. The results show that appropriate targets scatter acoustic signals in such a manner that the statistical properties are similar to those obtained with radars in the real system.

Designing and testing a new radar, altimeter, or navigational device is an involved and expensive procedure. It is therefore desirable to take advantage of any modeling techniques which can aid in the selection of the appropriate system parameters in a more economical manner. The acoustic simulator is suited to this application for the following reasons:

(1) By scaling distance the system environment is reduced to a size which is easily accommodated in a water tank in the laboratory (typical range scales vary from 10^2

¹Moore, R.K., Traveling-Wave Engineering, McGraw-Hill Book Company, New York, 1960.

²Moore, R.K., Radar Design Using Acoustical Simulation as a Tool, University of New Mexico, Engineering Experiment Station Report No. EE-22, April 1959.

an application of the theory of modeling and the use of analogies which exist between electromagnetic and acoustic waves.¹ The final result is the development of an acoustic simulator which serves as an analog computer to investigate radar, navigational equipment, and altimeter design problems. Appropriate scale factors are required in order to model complete systems and to ascertain their operating characteristics with a variety of targets.² The modeling technique is demonstrated for several systems using both pulse and frequency modulation. The results show that appropriate targets scatter acoustic signals in such a manner that the statistical properties are similar to those obtained with radar in the real system.

Designing and testing a new radar, altimeter, or navigational device is an involved and expensive procedure. It is therefore desirable to take advantage of any modeling techniques which can aid in the selection of the appropriate system parameters in a more economical manner. The acoustic simulator is suited to this application for the following reasons:

- (1) By scaling distance the system environment is reduced to a size which is easily accommodated in a water tank in the laboratory (typical range scales vary from 10^2

¹ Moore, R.K., Traveling Wave Engineering, McGraw-Hill Book Company, New York, 1957.

² Moore, R.K., Radar Design Using Acoustical Simulation as a Tool, University of New Mexico, Engineering Experiment Station Report No. EE-52, April 1959.

to 10^4),

(2) by scaling time the carrier frequency, modulation frequency, and antenna velocity are adjusted to give readily obtained values in the model (typical values are: 1. carrier frequency, 1 mc/sec; 2. modulation frequency, 20 cps; and 3. antenna velocity, 5 cm/sec), and

(3) scattering of electromagnetic signals is reproduced in the model by the scattering of acoustic waves from a rough target. This allows an investigation of the effects of antenna patterns, flight paths, and other parameters on the system operation. An example of the kind of system studies that are possible, using the acoustic simulator, is given in Chapter VII. In this example an FM altimeter system is modeled and experimental results, which show the effects of area scattering on the altitude indication, are given.

The greatest advantages of the acoustic simulator are: (1) the speed with which results can be obtained, (2) the economy as compared to full-scale experiments, and (3) the fact that data reruns over a target are almost completely repeatable. This makes it possible to change a single parameter and then repeat the previous run over the target. When flight testing equipment, it is virtually impossible to make separate data runs that are similar to the extent that the signal fading records are identical. The repeatability of acoustic simulator data is shown in Appendix B.

to 10⁴ (2) by scaling the carrier frequency, modulation frequency, and antenna velocity are adjusted to give results obtained values in the model (typical values are: 1 carrier frequency, 1 m/sec; 1 modulation frequency, 10 cps; and 1 antenna velocity, 1 cm/sec) and

(3) scattering of electromagnetic signals is repro-

duced in the model by the scattering of acoustic waves from a rough target. This allows an investigation of the effects of antenna patterns, flight paths, and other parameters on the system operation. An example of the kind of system studies that are possible, using the acoustic

analog, is given in Chapter VII. In this example an FM altimeter system is modeled and experimental results, which show the effects of area scattering on the altitude indication, are given.

The greatest advantages of the acoustic simulator are:

- (1) the speed with which results can be obtained, (2) the economy as compared to full-scale experiments, and (3) the fact that data returns over a target are almost completely repeatable. This makes it possible to change a single parameter and then repeat the previous run over the target. When flight testing equipment, it is virtually impossible to make separate data runs that are similar to the extent that the signal fading records are identical. The repeatability of acoustic simulator data is shown in Appendix B.

The acoustic simulator is also useful as a research tool for studying the scattering of waves from a rough surface. In this capacity the model has a definite limitation since acoustic waves are longitudinal in nature, while electromagnetic waves are transverse.¹ The effects of polarization are, therefore, not considered when acoustic waves are used. However, there are a number of cases of interest where polarization effects are either of secondary importance or can be accounted for in other ways. For example, physical theories of the scattering of electromagnetic waves frequently begin with a plane wave approximation using linear polarization. Since a linearly polarized plane wave can be described in terms of one component of a vector, it is essentially scalar in nature and the acoustic analogy is adequate. As a second example, randomly polarized waves may be modeled, for in this case the vector nature of the waves is not evident. As an example of forward scattering, consider the case of modeling the propagation of electromagnetic waves through a nonhomogeneous medium, where the scattering pattern is to be determined. The scattering formulas developed by Booker and Gordon² for linearly polarized electromagnetic waves differ from similar formulas

¹The acoustic wave can be described by one vector, the particle velocity, and one scalar, the dynamic pressure. The electromagnetic wave can be described in terms of two vectors, the electric and magnetic field intensities.

²Booker, H. G. and Gordon, W. E., "A Theory of Radio Scattering in the Troposphere," Proc. IRE, No. 38, 1950, pp. 401-412.

The acoustic simulator is also useful as a research tool for studying the scattering of waves from a rough surface. In this capacity the model has a definite limitation since acoustic waves are longitudinal in nature, while electromagnetic waves are transverse.¹ The effects of polarization are, therefore, not considered when acoustic waves are used. However, there are a number of cases of interest where polarization effects are either of secondary importance or can be accounted for in other ways. For example, physical theories of the scattering of electromagnetic waves frequently begin with a plane wave approximation using linear polarization. Since a linearly polarized plane wave can be described in terms of one component of a vector, it is essentially scalar in nature and the acoustic analogy is adequate. As a second example, randomly polarized waves may be modeled, for in this case the vector nature of the waves is not evident. As an example of forward scattering, consider the case of modeling the propagation of electromagnetic waves through a nonhomogeneous medium, where the scattering pattern is to be determined. The scattering formulas developed by Booker and Gordon² for linearly polarized electromagnetic waves differ from similar formulas

¹The acoustic wave can be described by one vector, the particle velocity, and one scalar, the dynamic pressure. The electromagnetic wave can be described in terms of two vectors, the electric and magnetic field intensities.

²Booker, H. G. and Gordon, W. E., "A Theory of Radio Scattering in the Troposphere," Proc. IRE, No. 38, 1950, pp. 401-412.

developed for acoustic waves¹ by only a trigonometric term which accounts for the polarization. This trigonometric term can be used to modify the experimental results obtained with the acoustic simulator so they apply to the electromagnetic case.² As a final example, the reflection coefficients for the two types of polarization do not differ appreciably for many materials until the angle of incidence exceeds about 30 degrees; therefore, the acoustic model is adequate at near-vertical incidence. The acoustic-electromagnetic analogies are discussed in detail in Chapter III.

Modeling techniques have been used for many years as an aid in investigating electromagnetic scattering problems³ in cases where direct experiments are more difficult and costly to perform. In some of these cases the analogies between acoustic and electromagnetic waves were used in the study. Jordan used acoustic waves at a frequency of 600 cps in air to simulate patterns of various directional antenna arrays in 1941.⁴ Another investigation has been started

¹Chernov, Lev A., Wave Propagation in a Random Medium, McGraw-Hill Book Co., New York, 1960, p. 53. Translated from Russian by R. A. Silverman.

²Several methods are available for creating a suitable nonhomogeneous medium. One of these methods is to use a heat source which will create turbulence due to convection of heated water.

³Sinclair, George, "Theory of Models of Electromagnetic Systems," Proc. IRE, Vol. 36, No. 11, Nov. 1948, pp. 1364-70.

⁴Jordan, Edward C., Acoustic Models of Radio Antennas, Ohio State University, Engineering Experiment Station Bulletin No. 108, May 1941.

developed for acoustic waves¹ by only a trigonometric term which accounts for the polarization. This trigonometric term can be used to modify the experimental results obtained with the acoustic analogies so they apply to the electromagnetic case.² As a final example, the reflection coefficients for the two types of polarization do not differ appreciably for many materials until the angle of incidence exceeds about 50 degrees; therefore, the acoustic model is adequate at near-vertical incidence. The acoustic-electromagnetic analogies are discussed in detail

in Chapter III.

Modeling techniques have been used for many years as an aid in investigating electromagnetic scattering problems, in cases where direct experiments are more difficult and costly to perform. In some of these cases the analogies between acoustic and electromagnetic waves were used in the study. Jordan used acoustic waves at a frequency of 600 cps in air to simulate patterns of various directional antennas arrays in 1941.³ Another investigation has been started

¹Chernov, Lev A., Wave Propagation in a Random Medium, McGraw-Hill Book Co., New York, 1950, p. 53. Translated from Russian by R. A. Silverman.

²Several methods are available for creating a suitable nonhomogeneous medium. One of these methods is to use a heat source which will create turbulence due to convection of heated water.

³Stanciar, George, "Theory of Models of Electromagnetic Systems," Proc. IRE, Vol. 35, No. 11, Nov. 1948, pp. 1364-70.

⁴Jordan, Edward C., Acoustic Models of Radio Antennas, Ohio State University, Engineering Experiment Station Bulletin No. 103, May 1941.

within the past year to model antenna patterns using acoustic waves in water at a frequency of 200 kc/sec.¹ Acoustic waves have also been used in reverberation chambers to simulate reflection losses of microwaves from different surfaces at statistical angles of incidence.²

Useful results are derived from models because of the mathematical similarity which exists between the real and the model system. A priori arguments for the validity of the model are generally based on "dimensional analysis" and on "inspectional analysis" of the describing equations. Bridgman³ wrote the classic work on dimensional analysis; however, many others^{4,5,6} have made valuable contributions in this area. The term inspectional analysis is due to

¹Maestri, A., Hydroacoustic Simulation of Antenna Radiation Characteristics, Melpar Inc., Falls Church, Va., Technical Report TP-1-26, 1961.

²Meyer, Erwin, "Experiments on CM Waves with Acoustic Techniques Made in Gottingen," Jour. Acoust. Soc. of Am., Vol. 30, No. 7, July 1958, pp. 624-32.

³Bridgman, P. W., Dimensional Analysis, New Haven, 2nd. ed., 1931.

⁴Buckingham, E., "On Physically Similar Systems; Illustrations of the Use of Dimensional Equations," Physical Review, Vol. 4, No. 4, 1914, pp. 345-76.

⁵Tolman, R.C., "The Principle of Similitude," Physical Review, Vol. 3, No. 4, 1914k pp. 244-55.

⁶Campbell, Norman, "Dimensional Analysis," Phil. Mag., Vol. 47, 1924, pp. 481-94.

within the last year to model antenna patterns using acoustic waves in water at a frequency of 500 Kc/sec.¹ Acoustic waves have also been used in transmission channel experiments to simulate reflection losses of microwaves from dielectric surfaces at statistical angles of incidence.

Useful results are derived from models because of the mathematical similarity which exists between the real and the model system. A priori arguments for the validity of the model are generally based on "dimensional analysis" and on "asymptotic analysis" of the describing equations. Bridgman² wrote the classic work on dimensional analysis; however, many others^{3,4,5} have made valuable contributions in this area. The term asymptotic analysis is due to

¹ Messeri, A., "Hydrodynamic Simulation of Antenna Radiation Characteristics," Master's Thesis, Johns Hopkins Univ., Baltimore, Md., 1954.

² Meyer, R. W., "Experiments on CM Waves with Acoustic Techniques Made in Gortland," Phys. Rev., Vol. 50, No. 2, July 1942, pp. 241-247.

³ Bridgman, P. W., Dimensional Analysis, New Haven, 2nd ed., 1921.

⁴ Buckingham, E., "On Physically Similar Systems: Illustrations of the Use of Dimensional Equations," Physical Review, Vol. 4, No. 4, 1914, pp. 349-356.

⁵ Tolman, R. C., "The Principles of Similarity," Physical Review, Vol. 4, No. 4, 1914, pp. 344-355.

⁶ Campbell, Norman, "Dimensional Analysis," Phil. Mag., Vol. 47, 1924, pp. 481-94.

Ruark¹ although the method was used by earlier investigators. Birkhoff defines inspectional analysis as "testing for invariance under the appropriate transformation, every fundamental equation on which a given theory is based."²

The conditions of dimensional and inspectional analysis can be satisfied by an appropriate set of linear transformations which are used to transform the describing equations for the real system into the model system. This is called linear modeling since only linear transformations are involved. The same scale factor must be used for every basic or derived quantity of each type in linear modeling.

Linear modeling may not always be feasible, as for example in scaling a high altitude radar experiment into the dimensions of a laboratory. It is, in this case, necessary to scale range and wavelength separately in order to achieve both a realistic model size and a realistic model carrier frequency. The modeling is termed "nonlinear," when the wavelength and the range are scaled separately, since a nonlinear transformation must be introduced between certain variables in the real and model systems in order to maintain the differential equations invariant under the transformation. Theoretical implications of non-linear modeling have been

¹Ruark, A.E., "Inspectional Analysis: A Method Which Supplements Dimensional Analysis,": Journal Elisha Mitchell Science Soc., Vol. 51, 1935, pp. 127-33.

²Birkhoff, Garrett, Hydrodynamics, Dover Publications, Inc., 1955, pp. 90.

Rank¹ although the method was used by earlier authors.
 gators. Birkhoff defines mathematical analysis as "testing
 for invariance under the appropriate transformation, every
 fundamental equation on which a given theory is based."
 The conditions of dimensional and mathematical
 analysis can be satisfied by an appropriate set of linear
 transformations which are used to transform the describing
 equations for the real system into the model system. This
 is called linear modeling since only linear transformations
 are involved. The same scale factor must be used for every
 basic or derived quantity of each type in linear modeling.
 Linear modeling may not always be feasible, as for
 example in scaling a high speed radar experiment into the
 dimensions of a laboratory. It is, in this case, necessary
 to scale range and wavelength separately in order to achieve
 both a realistic model size and a realistic model carrier
 frequency. The modeling is termed "nonlinear," when the
 wavelength and the range are scaled separately, since a
 nonlinear transformation must be introduced between certain
 variables in the real and model systems in order to maintain
 the differential equations invariant under the transformation.
 Theoretical implications of nonlinear modeling have been

¹Rank, A.E., "Mathematical Analysis: A Method Which
 Supplements Dimensional Analysis," Journal of the
 Science Soc., Vol. 51, No. 1, pp. 1-12, 1948.

²Birkhoff, Garrett, Hydrodynamic Theory, Princeton
 Inc., 1955, pp. 90.

investigated by Ritt¹ and numerous examples are reported by Belyea, Low and Siegel.² Non-linear modeling has the advantage of making certain experiments economical to perform; however, it has the disadvantage of being more difficult to interpret. In some cases, where only statistical information is required, the nonlinearity does not contribute an extra complication. This is the case in this investigation where most of the targets considered are rough surfaces such as those presented by terrain. It is necessary to describe such random type surfaces in a statistical manner.

There are two separate and distinct types of modeling which can be described as:

(1) "replica modeling" where the same physical phenomenon is used in the model as in the real system, and

(2) "analogy modeling" where the physical phenomenon in the model and in the real system are different. In the first case, the model is described by the same type of equations as those which describe the real system; in the second case the analogy between the two phenomena must be considered. The use of acoustic waves in water to simulate electromagnetic waves in air is an application of analogy

¹Ritt, R.K., "The Modeling of Physical Systems," IRE Trans. on Ant. and Prop., Vol. AP-4, No. 3, July 1956.

²Belyea, J.E., Low, R.D., and Siegel, K.M., Non-Linear Modeling of Maxwell's Equations, University of Michigan, Rad. Lab. Rpt. No. 38, December 1959.

investigated by Ritt¹ and numerous examples are reported by Bel'ev, Iov and Stedel'. Non-linear modeling has the advantage of making certain experiments economical to perform; however, it has the disadvantage of being more difficult to interpret. In some cases, where only statistical information is required, the nonlinearity does not contribute an extra complication. This is the case in this investigation where most of the targets considered are rough surfaces such as those presented by terrain. It is necessary to describe such random type surfaces in a statistical manner.

There are two separate and distinct types of modeling which can be described as:

- (1) "replica modeling" where the same physical phenomenon is used in the model as in the real system, and
- (2) "analogy modeling" where the physical phenomenon in the model and in the real system are different. In the first case, the model is described by the same type of equations as those which describe the real system; in the second case the analogy between the two phenomena must be considered. The use of acoustic waves in water to simulate electromagnetic waves in air is an application of analogy.

¹Ritt, R.K., "The Modeling of Physical Systems," IRE Trans. on Ant. and Prop., Vol. AP-4, No. 3, July 1956.

²Bel'ev, I.E., Iov, R.P., and Stedel', K.M., "Non-linear Modeling of Maxwell's Equations," University of Michigan, Rad. Lab. Rep. No. 38, December 1959.

modeling. The use of "millimeter" electromagnetic waves to model "centimeter" electromagnetic waves is an example of replica modeling.

The application of acoustic modeling to a complete radar system involves a number of scaling relationships. The scale factors are so determined that the experiment is economical to perform and the similitude requirements are satisfied. The basic relationship between scale factors is

$$R = V J$$

where R is the range scale, J is the time scale and V is the velocity scale.¹ The velocity scale factor is fixed by the ratio of the velocity of propagation of electromagnetic waves in air to the velocity of propagation of acoustic waves in water. Normally the range scale factor is selected for a particular problem and the time scale factor is thereby determined. When linear modeling is employed, all distances associated with the radar system are scaled using the scale factor, R . This means that the distance in space occupied by a pulse packet (or a cycle of any kind of modulation) will scale the same as wavelength and range. When non-linear modeling is employed, two different scale factors are involved for scaling distance. The range scale is still selected in the same manner as above; however, the wavelength is scaled sep-

¹Moore, op. cit., EE-22.

modeling. The use of "millimeter" electromagnetic waves
to model "centimeter" electromagnetic waves is an example
of replica modeling.

The application of acoustic modeling to a complete
radar system involves a number of scaling relationships.
The scale factors are so determined that the experiment
is economical to perform and the similitude requirements
are satisfied. The basic relationship between scale

$$R = V \lambda$$

where R is the range scale, λ is the time scale and V is
the velocity scale.¹ The velocity scale factor is fixed
by the ratio of the velocity of propagation of electro-
magnetic waves in air to the velocity of propagation of
acoustic waves in water. Normally the range scale factor
is selected for a particular problem and the time scale
factor is thereby determined. When linear modeling is
employed, all distances associated with the radar system
are scaled using the scale factor, R . This means that
the distance in space occupied by a pulse packet (or a
cycle of any kind of modulation) will scale the same as
wavelength and range. When non-linear modeling is employed,
two different scale factors are involved for scaling dis-
tance. The range scale is still selected in the same
manner as above; however, the wavelength is scaled sep-

¹ Moore, op. cit., EE-22.

arately in order to give a realistic model carrier frequency. This also has the effect of introducing a second time scale factor since the wavelength, carrier frequency, and time scale are closely related. The scaling relationships are discussed in Chapter IV.

Experimental results using the acoustic simulator can be grouped into two classifications: (1) those involving theoretical questions regarding the scattering of waves from a rough surface, and (2) those involving practical system design problems associated with signals returned from targets.

Theoretical questions that have been investigated are those concerning the variation of signal strength with altitude over a rough surface and the variation of back-scattered power as a function of the angle of incidence. Problems that concern particular radar, altimeter, or navigational systems involve such things as the effects of pulse length on the return signal and the effects of antenna pattern and flight path on the fading statistics. Results of experiments dealing with these problems are presented in Chapter VI.

This study shows that certain general classes of terrain can be successfully modeled to the extent that several important signal statistics are reproduced in the model system. The statistics that are reproduced are:

- (1) the backscattering radar cross section as a function

erately in order to give a realistic model carrier frequency. This also has the effect of introducing a second time scale factor since the wavelength, carrier frequency, and time scale are closely related. The scaling relationships are discussed in Chapter IV.

Experimental results using the acoustic simulator can be grouped into two classifications: (1) those involving theoretical questions regarding the scattering of waves from a rough surface; and (2) those involving practical system design problems associated with signals returned from targets.

Theoretical questions that have been investigated are those concerning the variation of signal strength with attitude over a rough surface and the variation of back-scattered power as a function of the angle of incidence. Problems that concern particular radar, altimeter, or navigational systems involve such things as the effects of pulse length on the return signal and the effects of antenna pattern and flight path on the fading statistics. Results of experiments dealing with these problems are presented in Chapter VI.

This study shows that certain general classes of terrain can be successfully modeled to the extent that several important signal statistics are reproduced in the model system. The statistics that are reproduced are: (1) the backscattering radar cross section as a function

of angle of incidence, and (2) the probability distribution function for the signal power returned. Also geometrical effects due to such things as pulse widths, pulse shapes, and antenna patterns are reproduced. The backscattering radar cross section per unit area for woods is nearly constant with angles of incidence between zero and 30 degrees (measured from the vertical). Also, the range of fading, defined as the range between the level exceeded by 95% of the return signals and the level exceeded by only 5% of the return signals, is on the order of 18 db. A Rayleigh probability distribution function, to a good approximation, describes the statistics of signal returned from rough terrain, such as woods and most farmland areas. Relatively flat wooded terrain is properly modeled by a flat plywood target with a dense covering of sand particles that are on the order of a wavelength in size.

On the other hand, the backscattering radar cross section per unit area for farmland generally decreases by two orders of magnitude as the angle of incidence changes from 0 to 30 degrees. The range of fading is usually between 14 and 18 db for these areas. A proper model target for flat terrain of this type is a flat piece of plywood with a sparse distribution of sand particles (one to five wavelengths between particles). Certain very flat terrain areas have backscattering cross sections per unit area that decrease by two orders of magnitude as the angle of incidence goes

of angle of incidence, and (2) the probability distribution function for the signal power returned. Also geometrical effects due to such things as pulse widths, pulse shapes, and antenna patterns are reproduced. The backscattering radar cross section per unit area for woods is nearly constant with angles of incidence between zero and 30 degrees (measured from the vertical). Also, the range of fading, defined as the range between the level exceeded by 95% of the return signals and the level exceeded by only 5% of the return signals, is on the order of 18 db. A Rayleigh probability distribution function, to a good approximation, describes the statistics of signal returned from rough terrain, such as woods and most farmland areas. Relatively flat wooded terrain is properly modeled by a flat plywood target with a dense covering of sand particles that are on the order of a wavelength in size. On the other hand, the backscattering radar cross section per unit area for farmland generally decreases by two orders of magnitude as the angle of incidence changes from 0 to 30 degrees. The range of fading is usually between 14 and 18 db for these areas. A proper model target for flat terrain of this type is a flat piece of plywood with a sparse distribution of sand particles (one to five wavelengths between particles). Certain very flat terrain areas have backscattering cross sections per unit area that decrease by two orders of magnitude as the angle of incidence goes

from 0 to 10 degrees. The range of fading is usually less than 12 db for these terrain areas. A smooth piece of plywood provides a suitable model target.

The frequency range between 200 kc/sec and 5 mc/sec is best suited to acoustic modeling experiments. The attenuation in the water becomes a significant factor at higher frequencies. When the frequency is reduced to a low value the wave length is large and proper scaling is impractical for a small water tank. Typical model targets are on the order of 4 feet square and the range in the model may vary between about 30 cm and 3 meters.

from 0 to 10 degrees. The range of fading is usually less than 12 dB for these test areas. A smooth piece of plywood provides a suitable model target. The frequency range between 200 kc/sec and 5 mc/sec is best suited to acoustic modeling experiments. The attenuation in the water becomes a significant factor at higher frequencies. When the frequency is reduced to a low value the wave length is large and proper scaling is impractical for a small water tank. Typical model targets are on the order of 4 feet square and the range in the model may vary between about 50 cm and 5 meters.

CHAPTER II

THEORY OF MODELS

The use of a model experiment becomes quite important when the full scale experiment is uneconomical to perform. A model experiment is justified on the basis of the mathematical similarity that exists between the differential equations describing the behavior of the real and the model systems. The experiment may make use of an equivalent system, as when an electric circuit is replaced by another circuit which is equivalent in external behavior to the original. An artificial transmission line which simulates a real transmission line is an example of an equivalent system. On the other hand, the experiment may make use of an analogous system as when the diffusion of heat in a body is simulated by an appropriate transmission line. In the first case it is a sufficient condition to show that the describing equations remain invariant under the desired transformations. In the second case, it is also necessary to investigate analogous behavior in a second physical medium and to determine to what extent the model reproduces the behavior of the real system.

It is generally desirable, although not necessarily a requirement, that the differential equations describing

CHAPTER II

THEORY OF MODELS

The use of a model experiment becomes quite important when the full scale experiment is unobtainable to perform. A model experiment is justified on the basis of the mathematical simplicity that exists between the differential equations describing the behavior of the real and the model systems. The experiment may make use of an equivalent system as when an electric circuit is replaced by another circuit which is equivalent in external behavior to the original. An artificial transmission line which simulates a real transmission line is an example of an equivalent system. On the other hand, the experiment may make use of an analogous system as when the behavior of heat in a body is simulated by an appropriate transmission line. In the first case it is a sufficient condition to show that the describing equations remain invariant under the desired transformations. In the second case, it is also necessary to investigate analogous behavior in a second physical medium and to determine to what extent the model reproduces the behavior of the real system. It is generally desirable, although not necessarily a requirement, that the differential equations describing

the real system also apply to the model system.¹ When this condition is met, the problem reduces to one of finding the necessary transformations and then applying them to the problem at hand. When this condition is not met, it is necessary to resort to physical analogies between the two situations.

It is desired that measurements on a model provide certain information on the time and space variations of functions describing the real system. This information may or may not be complete or exact. The degree to which it is useful depends upon the possibility of reaching a better understanding of the real physical situation through the use of the model experiment.

2.1 Dimensional and Inspectional Analysis

Dimensional analysis has been discussed in detail by many authors.² It is well known that equations describing physical situations are dimensionally homogeneous; that is, of the same dimensions in every term of the equation. This fact is commonly used as a check on the validity of calculations. Dimensional homogeneity is, of course, a necessary but not a sufficient condition for the correctness of the equation. The dimensions of a quantity "are a code for telling us how the numerical value of a quantity changes

¹Belyea, et al, op. cit.

²Bridgeman, op. cit.

the real system also apply to the model system. When this condition is met, the problem reduces to one of finding the necessary transformations and then applying them to the problem at hand. When this condition is not met, it is necessary to resort to physical analogies between the two situations.

It is desired that measurements on a model provide certain information on the time and space variations of functions describing the real system. This information may or may not be complete or exact. The degree to which it is useful depends upon the possibility of reaching a better understanding of the real physical situation through the use of the model experiment.

2.1 Dimensional and Inspectional Analysis

Dimensional analysis has been discussed in detail by many authors. It is well known that equations describing physical situations are dimensionally homogeneous; that is, of the same dimensions in every term of the equation. This fact is commonly used as a check on the validity of calculations. Dimensional homogeneity is, of course, a necessary but not a sufficient condition for the correctness of the equation. The dimensions of a quantity are a code for telling us how the numerical value of a quantity changes

when the basic units of measurement are subjected to prescribed changes."^{1,2}

The term "inspectional analysis" means to investigate the describing equations of the phenomenon for invariance under the scaling relationships. Inspectional analysis is commonly used to check an equation describing a model system for consistent scale factors.

When the basic units are changed in an equation describing a physical situation, the numerical value of each of the units is altered by a factor K_i where $i = 1, 2, 3, \dots, n$, and n is the number of different units in the equation. The factor K_i is called a scale factor and can be interpreted as the factor which relates two corresponding measures of a quantity in a real system and a model system.

As an example, consider a simple experiment such as measuring the distance that an object falls from rest in a vacuum in a given period of time. The distance is given by

¹Langhaar, H.L., Dimensional Analysis and Theory of Models, John Wiley and Sons, Inc., New York, 1951, p. 5.

²Terms frequently encountered in discussions of dimensional analysis are defined as:

(1) A quantity is that property of anything that can be measured, increased or divided. Angle, area, volume and force are examples of mechanical quantities, and capacitance, current, charge and resistance are examples of electrical quantities. Quantities are defined as being either "primary" or "secondary" in nature. The primary (basic) quantities are those found to be most useful in developing a mathematical description of the physical system; all other quantities are secondary (derived). The usual primary quantities are length, mass, time, charge and temperature.

(2) A unit is a standard amount of a quantity normally used in measuring the quantity. Examples of units are the inch, centimeter, meter, ampere, farad and degree centigrade.

(3) A dimension is a symbol used to designate a primary quantity. The usual dimensions are $[L]$, $[M]$, $[T]$, $[Q]$ and $[\Theta]$.

when the basis and a of measurement are prescribed changes. The term "dimensional analysis" is used to describe the describing equations of the phenomena. Under the scaling relations, it is commonly used to check an equation. A system for consistent units is used.

When the basis units are changed in an equation, describing a physical situation, the numerical value of each of the units is altered. The factor N_i and n is the number of the unit in the equation. The factor N_i is called a scale factor and be interpreted as the factor which relates the measures of a quantity in a unit system to the measures. As an example, consider a speed of 100 ft/sec.

measuring the distance in feet and time in seconds. The distance in a given period of time is 100 ft/sec.

1. Dimensional Analysis and Units

1. A quantity is that property of a system that can be measured. It is a scalar quantity. Examples of scalar quantities are mass, length, time, temperature, etc. Quantities are divided into two categories: "primary" or "secondary". In nature, the primary quantities are those found to be most fundamental. A mathematical description of the physical system, all other quantities are secondary. They are derived from the primary quantities. Examples of secondary quantities are velocity, acceleration, etc.
2. A unit is a standard amount of a quantity. It is used in measuring the quantity. Examples of units are inch, centimeter, meter, second, etc.
3. A dimension is a physical quantity. It is a scalar quantity. Examples of dimensions are length, mass, time, etc.

$$S = \frac{1}{2} g t^2 \quad (2-1)$$

where

g is acceleration due to gravity, and

t is time.

The object will fall a distance of

$$S = \frac{1}{2} (32.2 \frac{\text{ft}}{\text{sec}^2}) 1 \text{sec}^2 = 16.1 \text{ft.} \quad (2-2)$$

in one second when the experiment is performed on the surface of the earth and English units are used. Now if the MKS system is employed the result is

$$S = \frac{1}{2} (9.80 \frac{\text{m}}{\text{sec}^2}) 1 \text{sec}^2 = 4.90 \text{m} \quad (2-3)$$

The difference between these numerical results is just the "conversion factor" which changes feet into meters. This conversion factor is given by

$$K_1 = \frac{16.1 \text{ft.}}{4.90 \text{m}} = 3.28 \frac{\text{ft.}}{\text{m}} \quad (2-4)$$

Now suppose that the experiment is performed on a planet where the gravitational acceleration is only 9.80 ft/sec^2 .

In this situation the object will fall a distance of

$$S = \frac{1}{2} (9.80 \frac{\text{ft}}{\text{sec}^2}) 1 \text{sec}^2 = 4.90 \text{ft.} \quad (2-5)$$

in a time of one second. This last experiment could be considered as a model experiment of the original problem. Real time is used in all cases and the distance is scaled by a factor

$$K_1 = 3.28$$

$$S = \frac{1}{2} g t^2$$

where

g is acceleration due to gravity, and

t is time.

The object will fall a distance of

$$S = \frac{1}{2} (32.2 \text{ ft/sec}^2) (1.67)^2 = 16.1 \text{ ft.} \quad (2-2)$$

in one second when the experiment is performed on the

surface of the earth and English units are used. Now if

the MKS system is employed the result is

$$S = \frac{1}{2} (9.80 \text{ m/sec}^2) (1.67)^2 = 13.6 \text{ m.} \quad (2-3)$$

The difference between these numerical results is just the

"conversion factor" which changes feet into meters. This

conversion factor is given by

$$K = \frac{1.67 \text{ m}}{4.92 \text{ ft}} = 0.338 \frac{\text{m}}{\text{ft}} \quad (2-4)$$

Now suppose that the experiment is performed on a planet

where the gravitational acceleration is only 9.80 ft/sec^2 .

In this situation the object will fall a distance of

$$S = \frac{1}{2} (9.80 \text{ ft/sec}^2) (1.67)^2 = 13.6 \text{ ft.} \quad (2-5)$$

in a time of one second. This last experiment could be

considered as a model experiment of the original problem.

Real time is used in all cases and the distance is scaled

by a factor

$$K = 0.338$$

where, in this case, κ_1 is a dimensionless scale factor. The transformations which relate the model system results to those in the real system are given by

$$\begin{aligned} s &= \kappa_1 s', \\ t &= \kappa_2 t', \text{ and} \\ a &= \kappa_3 a' \end{aligned} \tag{2-6}$$

where the primed quantities are measured in the model system. In this case, time is not scaled so the factor κ_2 is unity and the factor κ_3 must be equal to κ_1 to maintain Equation 2-1 dimensionally homogeneous under the transformations of Equation 2-6.

2.2 Linear Modeling

A physical problem can be formulated in terms of a number of basic independent quantities q_i . The number of basic quantities is one or more and is a matter of definition and convenience.¹ Three basic quantities are found to be most satisfactory when working with mechanical systems, and a fourth quantity is added when electrical systems are included. As a matter of convenience in visualizing and solving problems, a number of derived quantities, Q_i , are also used in describing the physical phenomenon.

¹Focken, C.M., Dimensional Methods and Their Applications, Edward Arnold and Co., London, 1953, p. 23.

where, in this case, K_1 is a dimensionless scale factor. The transformations which relate the model system results to those in the real system are given by

$$\begin{aligned} x &= K_1 x', \\ t &= K_2 t', \text{ and} \\ z &= K_3 z'. \end{aligned} \quad (2-6)$$

where the primed quantities are measured in the model system. In this case, time is not scaled so the factor K_2 is unity and the factor K_3 must be equal to K_1 to maintain Equation 2-1 dimensionally homogeneous under the transformations of Equation 2-6.

2.2 Linear Modeling

A physical problem can be formulated in terms of a number of basic independent quantities q_i . The number of basic quantities is one or more and is a matter of definition and convenience.¹ Three basic quantities are found to be most satisfactory when working with mechanical systems, and a fourth quantity is added when electrical systems are included. As a matter of convenience in visualizing and solving problems, a number of derived quantities, Q_i , are also used in describing the physical phenomenon.

¹Peckol, C.M., Dimensional Methods and Their Applications, Edward Arnold and Co., London, 1957, p. 23.

An equation describing a physical system is dimensionally homogeneous; that is, of the same dimensions in each term of the equation, and any transformations used in modeling must lead to similarly consistent equations. These concepts of dimensional analysis have commonly formed the basis for modeling theory.¹ A general form of the equation governing a physical situation where modeling may be desirable can be written as:

$$\sum_{j=1}^J C_j \left(q_1^{\alpha_1} q_2^{\alpha_2} \cdots q_n^{\alpha_n} \right)_j \left(Q_{n+1}^{\alpha_{n+1}} Q_{n+2}^{\alpha_{n+2}} \cdots Q_{n+m}^{\alpha_{n+m}} \right)_j = 0 \quad (2-7)$$

where:

c is a dimensionless constant,

q is a basic quantity,

Q is a derived quantity,

α is the dimension of the quantity,

j is the term number index,

J is the number of terms in the equation,

n is the number of basic quantities, and

m is the number of derived quantities.^{2,3}

¹Buckingham, op. cit.

²Equations describing physical situations where modeling may be desirable will always contain at least one derived quantity so "m" is not less than unity in this discussion.

³As an example, the one dimensional wave equation for a lossless transmission line is given by

$$\frac{\partial^2 v}{\partial x^2} - LC \frac{\partial^2 v}{\partial t^2} = 0$$

Using the notation of Equation 2-7, this equation becomes

$$\frac{\partial^2 (v^{[ML^2T^{-2}Q^{-1}]})}{\partial (x^{[L]})^2} - L \frac{[MLQ^{-2}]}{C} \frac{\partial^2 (v^{[ML^2T^{-2}Q^{-1}]})}{\partial (t^{[T]})^2} = 0$$

An equation describing a physical system is dimensionally homogeneous; that is, all the dimensions in each term of the equation, and any transformation used in modeling must lead to similarly consistent equations. These concepts of dimensional analysis have commonly formed the basis for modeling theory.¹ A general form of the equation governing a physical situation where modeling may be desirable can be written as:

$$\sum_{j=1}^J C_j Q_1^{x_1} Q_2^{x_2} \dots Q_n^{x_n} = 0 \quad (2-1)$$

where:

- C is a dimensionless constant,
- Q is a basic quantity,
- Q is a derived quantity,
- x is the dimension of the quantity,
- j is the term number index,
- J is the number of terms in the equation,
- n is the number of basic quantities, and
- m is the number of derived quantities.^{2,3}

¹ Buckingham, op. cit.

² Equations describing physical situations where modeling may be desirable will always contain at least one derived quantity so "m" is not less than unity in this discussion.

³ As an example, the one dimensional wave equation for a lossless transmission line is given by

$$\frac{\partial^2 V}{\partial x^2} - LC \frac{\partial^2 V}{\partial t^2} = 0$$

Using the notation of Equation 2-1, this equation becomes

$$\frac{1}{L^2} \left(\frac{V}{L} \right)^2 - C \left(\frac{V}{L} \right)^2 \left(\frac{t}{t} \right)^2 = 0$$

Equation 2-7 can be converted to dimensionless form by dividing through by the term J which results in

$$\sum_{j=1}^{J-1} \frac{C_j (g_1 g_2 \dots g_n)_j (Q_{n+1} Q_{n+2} \dots Q_{n+m})_j}{C_J (g_1 g_2 \dots g_n)_J (Q_{n+1} Q_{n+2} \dots Q_{n+m})_J} + 1 = 0 \quad (2-8)$$

Any number of the independent quantities, q , in Equation 2-7 can be scaled according to the transformation

$$T(q_i) = K_i q_i, \quad K > 0, \quad i = 1, 2, 3, \dots, n \quad (2-9)$$

where K is a dimensionless scaling factor. In mechanics $n = 3$ and the independent quantities are length, time and mass although in some cases force replaces mass as a basic unit.¹ The derived quantities, Q , must now be scaled according to the transformation

$$T(Q_{n+i}) = K_{n+i} Q_{n+i}, \quad i = 1, 2, 3, \dots, m \quad (2-10)$$

where the scale factors K in the transformed and dimensionless equation of the form of Equation 2-8, must be related by expressions of the form

$$\frac{(K_1 K_2 \dots K_n K_{n+1} K_{n+2} \dots K_{n+m})_j}{(K_1 K_2 \dots K_n K_{n+1} K_{n+2} \dots K_{n+m})_J} = R_j \quad (2-11)$$

where R_j is equal to unity. This is the important case of linear modeling which exists when all the values $R_j = 1$. Linear modeling has been considered most frequently in the past.

¹Langhaar, op. cit.

Equation 2-7 can be converted to dimensionless form

by dividing through by the term 1 which results in

$$(2-8) \quad \sum_{j=1}^{n-1} \frac{Q_j(Q_{n-1} \dots Q_{n-m})}{Q_j(Q_{n-1} \dots Q_{n-m})} + 1 = 0$$

Any number of the independent quantities, Q , in

Equation 2-7 can be scaled according to the transformation

$$(2-9) \quad T(Q_i) = K_i Q_i, \quad K_i > 0, \quad i = 1, 2, 3, \dots, n$$

where K_i is a dimensionless scaling factor. In mechanics $n = 5$ and the independent quantities are length, time and mass although in some cases force replaces mass as a basic unit. The derived quantities, Q , must now be scaled

according to the transformation

$$(2-10) \quad T(Q_{n+i}) = K_{n+i} Q_{n+i}, \quad i = 1, 2, 3, \dots, m$$

where the scale factors K in the transformed and dimensionless equation of the form of Equation 2-8, must be related by expressions of the form

$$(2-11) \quad \frac{(K_1 K_2 \dots K_n K_{n+m})}{(K_1 K_2 \dots K_n K_{n+m})} = R_j$$

where R_j is equal to unity. This is the important case of linear modeling which exists when all the values $R_j = 1$. Linear modeling has been considered most frequently in

the past.

The special case of linear modeling will now be considered in an example where the describing equation remains invariant under the specified transformations. Consider the case where the real system is described by

$$g_1 + Q_3 g_2 = 0 \quad (2-12)$$

and the model system is described by

$$g'_1 + Q'_3 g'_2 = 0 \quad (2-13)$$

In dimensionless form these equations become

$$\frac{g_1}{Q_3 g_2} + 1 = 0 \quad (2-14)$$

and

$$\frac{g'_1}{Q'_3 g'_2} + 1 = 0 \quad (2-15)$$

An allowable set of transformations can be written as

$$g'_1 = K_1 g_1 \quad (2-16)$$

$$g'_2 = K_2 g_2 \quad (2-17)$$

and

$$Q'_3 = K_3 Q_3 \quad (2-18)$$

Application of these transformations to Equations 2-15 results in

$$\frac{K_1}{K_2 K_3} \frac{g_1}{g_2 Q_3} + 1 = 0 \quad (2-19)$$

The special case of linear modeling will now be considered in an example where the describing equation remains invariant under the specified transformations. Consider the case where the real system is described by

$$y + Q_2 y = 0 \quad (2-12)$$

and the model system is described by

$$y' + Q_2 y' = 0 \quad (2-13)$$

In dimensionless form these equations become

$$\frac{y}{Q_2} + 1 = 0 \quad (2-14)$$

and

$$\frac{y'}{Q_2} + 1 = 0 \quad (2-15)$$

An allowable set of transformations can be written as

$$y' = K_1 y \quad (2-16)$$

$$y' = K_2 y \quad (2-17)$$

and

$$Q_2' = K_3 Q_2 \quad (2-18)$$

Application of these transformations to Equations 2-15

results in

$$\frac{K_1}{K_2 K_3} \frac{y'}{Q_2} + 1 = 0 \quad (2-19)$$

Equation 2-11 requires that the scale factors satisfy an equation of the form

$$\frac{\kappa_1}{\kappa_2 \kappa_3} = 1 \quad (2-20)$$

which clearly reduces Equation 2-19 to the form of Equation 2-14. In this example two of the scale factors can be arbitrarily selected so that $\kappa > 0$ and the third scale factor is then determined by Equation 2-20. Given the appropriate set of scale factors κ_1, κ_2 and κ_3 and the measured results of an experiment in the model system, the transformation equations can be used to determine corresponding results in the real system. The a priori choice of linear relationships between the variables fixes the boundary conditions in the two systems. If a boundary value in the real system is given as q_{10} then in the model system the corresponding boundary value is

$$q'_{10} = \kappa_1 q_{10} \quad (2-21)$$

As an additional example of linear modeling let the real system be governed by

$$q_1 + Q_4 q_2 + Q_5 q_3 = 0 \quad (2-22)$$

and the model system be governed by

$$q'_1 + Q'_4 q'_2 + Q'_5 q'_3 = 0 \quad (2-23)$$

Now in dimensionless form these equations are

$$\frac{q_1}{Q_5 q_3} + \frac{Q_4 q_2}{Q_5 q_3} + 1 = 0 \quad (2-24)$$

and

$$\frac{g_1'}{Q_5' g_3'} + \frac{Q_4' g_2'}{Q_5' g_3'} + 1 = 0 \quad (2-25)$$

An allowable set of transformations can be written as

$$g_1' = K_1 g_1 \quad , \quad (2-26)$$

$$g_2' = K_2 g_2 \quad , \quad (2-27)$$

$$g_3' = K_3 g_3 \quad , \quad (2-28)$$

$$Q_4' = K_4 Q_4 \quad , \quad (2-29)$$

and

$$Q_5' = K_5 Q_5 \quad (2-30)$$

Application of these transformations to Equation 2-25 results in

$$\frac{K_1}{K_5 K_3} \frac{g_1'}{Q_5' g_3'} + \frac{K_4 K_2}{K_5 K_3} \frac{Q_4' g_2'}{Q_5' g_3'} + 1 = 0 \quad (2-31)$$

The scale factors now must satisfy two equations which are of the form of Equation 2-11 and are written as

$$\frac{K_1}{K_5 K_3} = 1 \quad (2-32)$$

and

$$\frac{K_4 K_2}{K_5 K_3} = 1 \quad (2-33)$$

The scale factors are governed by two equations so that K_1, K_2 and K_3 can be arbitrarily selected, provided they are greater than zero.

and

$$\frac{Q_1'}{Q_2 Q_3} + \frac{Q_2 Q_3}{Q_1 Q_2} + 1 = 0 \quad (2-25)$$

An allowable set of transformations can be written as

$$Q_1' = K_1 Q_1 \quad (2-26)$$

$$Q_2' = K_2 Q_2 \quad (2-27)$$

$$Q_3' = K_3 Q_3 \quad (2-28)$$

$$Q_4' = K_4 Q_4 \quad (2-29)$$

and

$$Q_5' = K_5 Q_5 \quad (2-30)$$

Application of these transformations to Equation 2-25

results in

$$\frac{K_1}{K_2 K_3} + \frac{K_2 K_3}{K_1 K_3} + 1 = 0 \quad (2-31)$$

The scale factors now must satisfy two equations which are

of the form of Equation 2-11 and are written as

$$\frac{K_1}{K_2 K_3} = 1 \quad (2-32)$$

and

$$\frac{K_2 K_3}{K_1 K_3} = 1 \quad (2-33)$$

The scale factors are governed by two equations so that

K_1, K_2 and K_3 can be arbitrarily selected, provided they

are greater than zero.

2.3 Nonlinear Modeling

In some equations which describe physical phenomena there is more than one magnitude associated with a given basic or derived quantity. As an example of interest, consider the one-dimensional wave equation for voltage on a transmission line. The basic quantity, length, appears as the coordinate and also as wavelength in the wave number. In the previous discussion these two magnitudes are both associated with one basic or derived quantity and therefore have the same scale factor, K .

Equation 2-11 has been written in a manner that suggests that R_j could have a value different from unity in some cases. Suppose now that the basic quantity, q_1 , has two different magnitudes in a particular equation and that different values of scaling factor, K_1 , are used for each of these magnitudes. In the case of the transmission line mentioned above this means that distance along the line (basic quantity length) and wavelength (basic quantity length) are scaled separately. For this situation one would expect, in general, to find values of R_j that are not unity. This implies that Equation 2-7 will not be invariant under linear transformations of all the parameters when a single basic quantity is scaled in two different ways. It is now necessary to seek a nonlinear transformation which can be applied to one of the quantities in the describing equation so the equation remains invariant under the set

In some equations which describe physical phenomena there is more than one magnitude associated with a given basic or derived quantity. As an example of interest, consider the one-dimensional wave equation for voltage on a transmission line. The basic quantity, length, appears as the coordinate and also as wavelength in the wave number. In the previous discussion these two magnitudes are both associated with one basic or derived quantity and therefore have the same scale factor, K .

Equation 2-11 has been written in a manner that suggests that R_1 could have a value different from unity in some cases. Suppose now that the basic quantity, q_1 , has two different magnitudes in a particular equation and that different values of scaling factor, K_1 , are used for each of these magnitudes. In the case of the transmission line mentioned above this means that distance along the line (basic quantity length) and wavelength (basic quantity length) are scaled separately. For this situation one would expect, in general, to find values of R_1 that are not unity. This implies that Equation 2-7 will not be invariant under linear transformations of all the parameters when a single basic quantity is scaled in two different ways. It is now necessary to seek a nonlinear transformation which can be applied to one of the quantities in the describing equation so the equation remains invariant under the set

of transformations. In the examples which follow, the quantity which transforms nonlinearly is selected as the dependent variable.

It will be more advantageous to consider specific examples rather than the more general situation. As an example, consider a real situation described by the equation

$$\frac{dg_1}{dg_2} - Q_3 g_1 = 0 \quad (2-34)$$

where the quantity q_1 is the dependent variable, and a model situation described by the equation

$$\frac{dg'_1}{dg'_2} - Q'_3 g'_1 = 0 \quad (2-35)$$

The transformations relating Equations 2-34 and 2-35 can be written as

$$\phi(g'_1) = g_1 \quad (2-36)$$

$$T(g'_2) = K_2 g'_2 = g_2 \quad (2-37)$$

$$T(Q'_3) = K_3 Q'_3 = Q_3 \quad (2-38)$$

Applying these transformations to Equation 2-34 results in

$$\frac{1}{K_2} \frac{d\phi}{dg'_2} - K_3 \phi Q'_3 = 0 \quad (2-39)$$

According to Equation 2-11 the scaling factors must satisfy an expression of the form

$$\frac{1}{K_2 K_3} = R \quad (2-40)$$

of transformations. In the examples which follow, a quantity which transforms nonlinearly is selected as the dependent variable.

It will be more advantageous to consider specific examples rather than the more general situation. For example, consider a real situation described by the equation

$$\frac{dy}{dx} - Q_2 y = 0$$

where the quantity y is the dependent variable, and the model situation described by the equation

$$\frac{dy'}{dx'} - Q_2' y' = 0$$

The transformations relating Equations (1) and (2) can be written as

$$\begin{aligned} y' &= y \\ x' &= x \\ T(y') &= y' \\ T(x') &= x \end{aligned}$$

Applying these transformations to Equation (1) results in

$$\frac{dy}{dx} - Q_2 y = 0$$

According to Equation (2) the scaling factors must satisfy an expression of the form

$$\frac{1}{h_2 h_3} = R$$

where R is a constant. Now the unspecified transformation relating the dependent variables in the real and model systems is given by Equation 2-39 and can be expressed as

$$\frac{d\phi}{d g_2'} = R Q_3' \phi \quad (2-41)$$

Equation 2-41 can now be written as

$$\frac{d\phi}{d g_1'} \frac{d g_1'}{d g_2'} = R Q_3' \phi \quad (2-42)$$

and then using Equation 2-35 it becomes

$$\frac{d\phi}{d g_1'} = \frac{R}{g_1'} \phi \quad (2-43)$$

which has a general solution

$$\phi(g_1') = C (g_1')^R \quad (2-44)$$

Initial conditions on q_1 and q_1' are given by q_{10} and q_{10}' so the general solution for the nonlinear transformation is given by

$$\phi(g_1') = g_{10} \left[\frac{g_1'}{g_{10}'} \right]^R \quad (2-45)$$

Now it is obvious that linear modeling exists when $R = 1$ since the transformation reduces to a linear form as in the previous example. When

$$R \neq 1$$

and

$$R > 0$$

where R is a constant. Now the unspecified transformation relating the dependent variables in the real and model systems is given by Equation 2-3 and can be expressed as

$$\frac{d\phi}{dt} = R\phi \quad (2-41)$$

Equation 2-41 can now be written as

$$\frac{d\phi}{dt} = R\phi \quad (2-42)$$

and then using Equation 2-3 it becomes

$$\frac{d\phi}{dt} = R\phi \quad (2-43)$$

which has a general solution

$$\phi(t) = C e^{Rt} \quad (2-44)$$

Initial conditions on ϕ and $\dot{\phi}$ are given by ϕ_0 and $\dot{\phi}_0$ so the general solution for the nonlinear transformation

is given by

$$\phi(t) = \phi_0 \left[\frac{\dot{\phi}_0}{\phi_0} \right] e^{Rt} \quad (2-45)$$

Now it is obvious that linear modeling exists when $R = 1$ since the transformation reduces to a linear form as in the

previous example. When

$$R \neq 1$$

and

$$R > 0$$

then nonlinear modeling exists and the dependent variables in the real and model systems are related by Equation 2-45.

Another interesting example of a problem in nonlinear modeling involves the one dimensional analog of the scalar wave equation which can be expressed as:

$$\frac{d^2 V}{dx^2} + k^2 V = 0 \quad (2-46)$$

where k is the wave number, $2\pi/\lambda$. The model system will also be described by a similar equation:

$$\frac{d^2 V_1}{dx^2} + k_1^2 V_1 = 0 \quad (2-47)$$

Let the transformations between the real and model system be expressed as

$$\begin{aligned} V &= \phi(V_1) \\ x &= K_1 x_1 \\ k &= K_2 k_1 \end{aligned} \quad (2-48)$$

where the product $K_1 K_2$ is not unity for this case of nonlinear modeling. The nonlinear relationship between V_1 and V can be determined by considering the situation on two transmission lines where the behavior is governed by Equations 2-46 and 2-47.

The phasor diagrams for the real and model lines provide a tool to use in determining the necessary nonlinear relationship between the rms voltages on the two systems.

then nonlinear modeling exists and the dependent variables in the real and model systems are related by Equation 2-45. Another interesting example of a problem in nonlinear modeling involves the one dimensional analog of the scalar wave equation which can be expressed as:

$$\frac{\partial^2 V}{\partial x^2} + K^2 V = 0 \quad (2-45)$$

where K is the wave number, $2\pi/\lambda$. The model system will also be described by a similar equation:

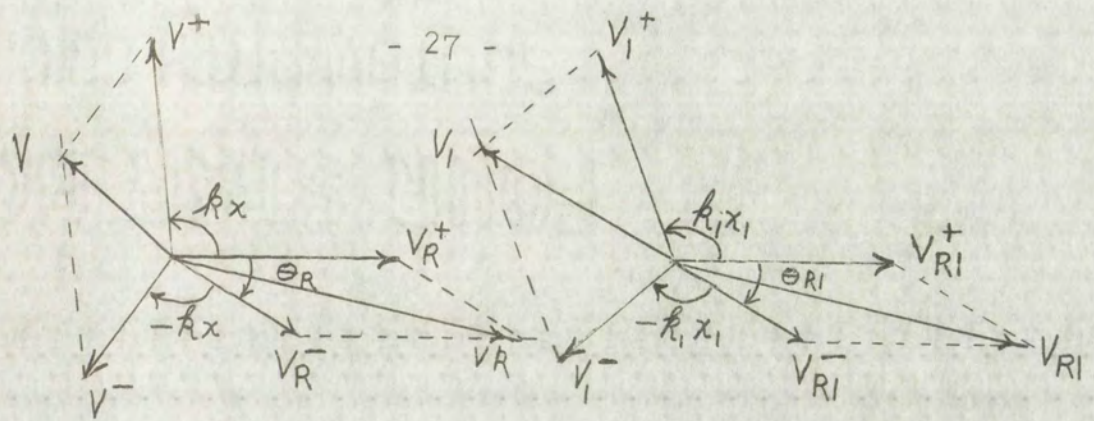
$$\frac{\partial^2 V}{\partial x^2} + K_1^2 V = 0 \quad (2-46)$$

Let the transformation between the real and model system be expressed as

$$\begin{aligned} V &= \phi(V_1) \\ x &= f_1(x_1) \\ K &= f_2(K_1) \end{aligned} \quad (2-47)$$

where the product $K_1 f_2$ is not unity for this case of nonlinear modeling. The nonlinear relationship between V and V_1 can be determined by considering the situation on two transmission lines where the behavior is governed by Equations 2-45 and 2-46.

The passor diagrams for the real and model lines provide a tool to use in determining the necessary nonlinear relationship between the two systems.



Real System

Model System

Nonlinear Modeling of Transmission Line

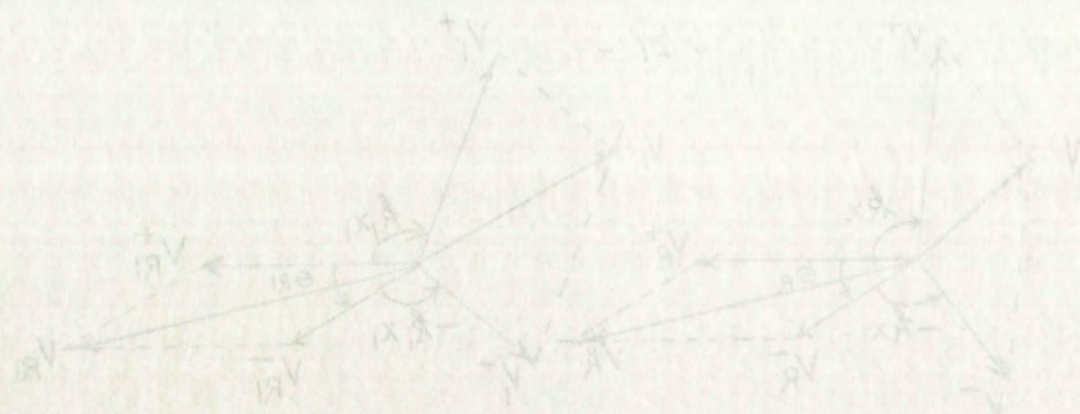
Figure 2-1

The positive traveling wave, V_R^+ , at the receiving end of the line is selected as the reference voltage. At a point x on the transmission line the positive traveling wave will be at an angle kx (measured counter-clockwise) from its position at the receiving end of the line. At the same point x the negative traveling wave will be at an angle $-kx$ (measured clockwise) from its position at the receiving end of the line.

Now let the positive traveling waves on the two systems be related by

$$V^+ = \gamma V_1^+ \quad (2-49)$$

where γ is a real positive constant. The voltage at any point on the real line can be expressed in terms of the magnitudes of the positive and negative traveling waves and the phase angle of the load by application of the law of cosines. The resulting voltage is given by



Model System

Real System

Nonlinear Modeling of Transmission Line

Figure 2-1

The positive traveling wave, V_R^+ , at the receiving end of the line is selected as the reference voltage. At a point x on the transmission line the positive traveling wave will be at an angle θ_x (measured counter-clockwise) from its position at the receiving end of the line. At the same point x the negative traveling wave will be at an angle $-\theta_x$ (measured clockwise) from its position at the receiving end of the line.

Now let the positive traveling waves on the two

systems be related by

$$V_R^+ = \gamma V_M^+ \quad (2-10)$$

where γ is a real positive constant. The voltage at any point on the real line can be expressed in terms of the magnitudes of the positive and negative traveling waves and the phase angle of the load by application of the law of cosines. The resulting voltage is given by

$$V = \left\{ V^{+2} + V^{-2} - 2V^{+}V^{-} \cos[\pi - (2kx - \theta_R)] \right\}^{1/2} \quad (2-50)$$

which can be simplified to give

$$V = V^{+} \left\{ (1 + \Gamma_R^2) + 2\Gamma_R \cos[2kx - \theta_R] \right\}^{1/2} \quad (2-51)$$

where $V^{-} = \Gamma_R V^{+}$ and Γ_R is the voltage reflection coefficient. Now using Equations 2-48 and 2-49, Equation 2-51 becomes

$$V = V_1^{+} \left\{ (1 + \Gamma_R^2) + 2\Gamma_R \cos[2K_1 K_2 k_1 x_1 - \theta_R] \right\}^{1/2} \quad (2-52)$$

This equation gives the voltage on the real line in terms of known constants and the position, $k_1 x_1$, on the model line. The voltage on the model line can be expressed as

$$V = V_1^{+} \left\{ (1 + \Gamma_{R1}^2) + 2\Gamma_{R1} \cos[2k_1 x_1 - \theta_{R1}] \right\}^{1/2} \quad (2-53)$$

which is similar to Equation 2-51. Now this equation can be solved for $k_1 x_1$ which gives

$$k_1 x_1 = \frac{1}{2} \cos^{-1} \left[\frac{V_1^2 - V^{+2} (1 + \Gamma_{R1}^2)}{2 V_1^{+2} \Gamma_{R1}} \right] + \frac{1}{2} \theta_{R1} \quad (2-54)$$

The magnitude of the voltage V on the real system is now expressed in terms of the voltage measured on the model line by substituting Equation 2-54 into Equation 2-52.

The result is the nonlinear relationship between the voltage on the model line and the voltage on the real line and is given by

$$V = \left\{ V^2 + V^2 - 2V^+ \cos[\pi - (2\lambda x - \theta_R)] \right\}^{1/2} \quad (2-50)$$

which can be simplified to give

$$V = V^+ \left\{ (1 + \Gamma_R^2) + 2\Gamma_R \cos[2\lambda x - \theta_R] \right\}^{1/2} \quad (2-51)$$

where $V = \Gamma_R V^+$ and Γ_R is the voltage reflection coefficient.

Now using Equations 2-48 and 2-49, Equation 2-51

becomes

$$V = V^+ \left\{ (1 + \Gamma_R^2) + 2\Gamma_R \cos[2\lambda x - \theta_R] \right\}^{1/2} \quad (2-52)$$

This equation gives the voltage on the real line in terms

of known constants and the position, λx , on the model

line. The voltage on the model line can be expressed as

$$V = V^+ \left\{ (1 + \Gamma_R^2) + 2\Gamma_R \cos[2\lambda x - \theta_R] \right\}^{1/2} \quad (2-53)$$

which is similar to Equation 2-51. Now this equation can

be solved for Γ_R which gives

$$\Gamma_R = \frac{1}{2} \cos^{-1} \left[\frac{V^2 - V^{+2} (1 + \Gamma_R^2)}{2 V^+ \Gamma_R} \right] + \frac{1}{2} \theta_R \quad (2-54)$$

The magnitude of the voltage V on the real system is now

expressed in terms of the voltage measured on the model

line by substituting Equation 2-54 into Equation 2-52.

The result is the nonlinear relationship between the voltage

on the model line and the voltage on the real line and is

given by

$$V = \sqrt{V_1^+} \left\{ \left(1 + \Gamma_R^2 \right) + 2 \Gamma_R \cos \left[K_1 K_2 \cos^{-1} \left(\frac{V - V_1^+ \sqrt{1 + \Gamma_R^2}}{2 V_1^+ \Gamma_R} \right) + K_1 K_2 \Theta_{R1} - \Theta_R \right] \right\}^{1/2} \quad (2-55)$$

Equation 2-55 can be used to determine the voltage at any point on the real transmission line by using results obtained from measurements on the model line. Now for proper results the model line must be terminated in such a manner that the magnitude and phase of the reflection coefficient at the receiving end on the line is the same as on the real line, therefore

$$\Gamma_{R1} = \Gamma_R \quad \text{and} \quad \Theta_{R1} = \Theta_R$$

It should be observed that under these conditions the non-linear transformation reduces to $V = \sqrt{V_1^+}$ for $K_1 K_2 = 1$, which is correct for linear modeling.

In certain cases the result of interest involves the mean value of voltage on the line as the boundary conditions are continuously changed. Let the terminating impedance vary with time over a range of values such that

$$-\pi \leq \Theta_R \leq \pi$$

and

$$0 \leq \Gamma_R \leq 1$$

with a uniform probability distribution for both parameters over the range. If Γ_R and Θ_R are assumed to be independent, then the time average value of V at a point on the real line will be given by

$$V = \sqrt{V_1^+} \quad (2-56)$$

$$V = \frac{1}{\sqrt{LC}} \left(\frac{1}{\omega} \cos \omega t + \frac{1}{\omega} \sin \omega t \right)$$

Equation 5-5 can be used to calculate the voltage

at any point on the test line. The voltage is obtained from measurements on the test line. Proper results are obtained in a manner that the measured voltage is of the order of coefficient of the test line. The test line is as on the test line, which is

$$V = \frac{1}{\sqrt{LC}} \left(\frac{1}{\omega} \cos \omega t + \frac{1}{\omega} \sin \omega t \right)$$

It should be observed that the voltage is linear transformation between the test line and which is correct for linear scaling.

In certain cases the test line is linear and the

the magnitude of voltage on the test line is the conditions are continuously changing and the impedance vary with time over a range of values.

$$V = \frac{1}{\sqrt{LC}} \left(\frac{1}{\omega} \cos \omega t + \frac{1}{\omega} \sin \omega t \right)$$

and

$$V = \frac{1}{\sqrt{LC}} \left(\frac{1}{\omega} \cos \omega t + \frac{1}{\omega} \sin \omega t \right)$$

With a uniform impedance distribution, the voltage over the range. If the test line is linear, then the line average voltage is given by

$$V = \frac{1}{\sqrt{LC}} \left(\frac{1}{\omega} \cos \omega t + \frac{1}{\omega} \sin \omega t \right)$$

where C is a constant. This average value will apply at any point on the line. It is therefore unnecessary to use the nonlinear transformation when the model is only intended to give time average values of voltage on the line.

2.4 Modeling Considerations

The terminology "linear" and "nonlinear" modeling has been obtained from the nature of the transformations used in scaling the experiment. In this paper the modeling is said to be linear when the wavelength and coordinate distances use the same scale factor. The modeling is said to be nonlinear when the wavelength scale is different from that used in scaling the range to the target. In linear modeling all similar basic and derived quantities use a single scale factor, while in the simplest case of nonlinear modeling a single pair of similar basic or derived quantities scale separately. The nonlinear transformation is taken between the dependent variables which are dynamic pressure or particle velocity in the case of acoustic waves and electric or magnetic field intensities in the case of electromagnetic waves. The target model remains geometrically similar to the real target in both cases since the nonlinear function relates only the reradiation fields in the real and model systems.

The radar targets of interest can be classified into two broad categories: (1) such as given by aircraft or missiles with a definite and known geometrical shape, and

where C is a constant. This average value will apply at any point on the line. It is therefore unnecessary to use the nonlinear transformation when the model is only intended to give time average values of voltage on the line.

2.4 Modeling Considerations

The terminology "linear" and "nonlinear" modeling has been obtained from the nature of the transformations used in scaling the experiment. In this paper the modeling is said to be linear when the wavelength and coordinate distances use the same scale factor. The modeling is said to be nonlinear when the wavelength scale is different from that used in scaling the range to the target. In linear modeling all similar basic and derived quantities use a single scale factor, while in the simplest case of nonlinear modeling a single pair of similar basic or derived quantities scale separately. The nonlinear transformation is taken between the dependent variables which are dynamic pressure or particle velocity in the case of acoustic waves and electric or magnetic field intensities in the case of electromagnetic waves. The target model remains geometrically similar to the real target in both cases since the nonlinear function relates only the radiation fields in the real and model systems.

The radar targets of interest can be classified into two broad categories: (1) such as given by aircraft or missiles with a definite and known geometrical shape, and

(2) random type areas such as terrain or perhaps thunderstorms where the target properties are known only in a statistical sense. It is this later class of targets that is considered in this paper.

Terrain acts primarily as a scatterer of electromagnetic energy at frequencies above a few hundred megacycles per second. The radar return signals are therefore subject to a considerable amount of fading in the usual application. Target irregularities for a surface such as that presented by terrain can be grouped into two categories: (1) small objects on the order of a few wavelengths or less in physical size, and (2) large objects on the order of hundreds of wavelengths or more in size. When the frequency range between a few hundred and a few thousand megacycles per second is considered the objects on the order of a few wavelengths will include natural surface roughness, such as that provided by vegetation and small changes in surface profile. Objects on the order of many wavelengths in size will include man-made structures such as cities or roads and natural irregularities such as hills, mountains, and rivers.

The large objects must be linearly scaled when constructing the target in order to preserve the proper time sequence in the reception of radar signals from the illuminated region. The small objects contribute signals with random phase which gives the return signal many characteristics of random noise. It is unrealistic to attempt to

[illegible]

construct a target which reproduces each of the many small scatterers so a random distribution of small objects is used in the model. The small-scale roughness can be adjusted by making the scatterers more or less dense, and to some extent it can be adjusted by varying their size.

When using either linear or nonlinear modeling techniques the large sized objects on the target must remain physically similar in shape to those in the real system, while the small scatterers are modeled with an appropriate random distribution of small objects. This means that the model target may appear optically different from the real target. The statistics of the acoustic signal must, however, be similar to those signal statistics obtained in the real system.

constructed a 12.5 cm. diameter, 1.5 m. long, cylindrical

accelerator with a vacuum chamber of 100 cm. diameter

used in the study of the small angle scattering of

adjusted by making the electron beam of 100 cm. length

to some extent it was the electron beam of 100 cm. length

When using a 100 cm. length of electron beam

techniques the same kind of results were obtained

mainly by using a 100 cm. length of electron beam

while the small angle scattering was observed with the

random distribution of small objects. This means that the

model of the electron beam of 100 cm. length

target. The electron beam of 100 cm. length

of similar to the electron beam of 100 cm. length

system

CHAPTER III

ANALOGIES

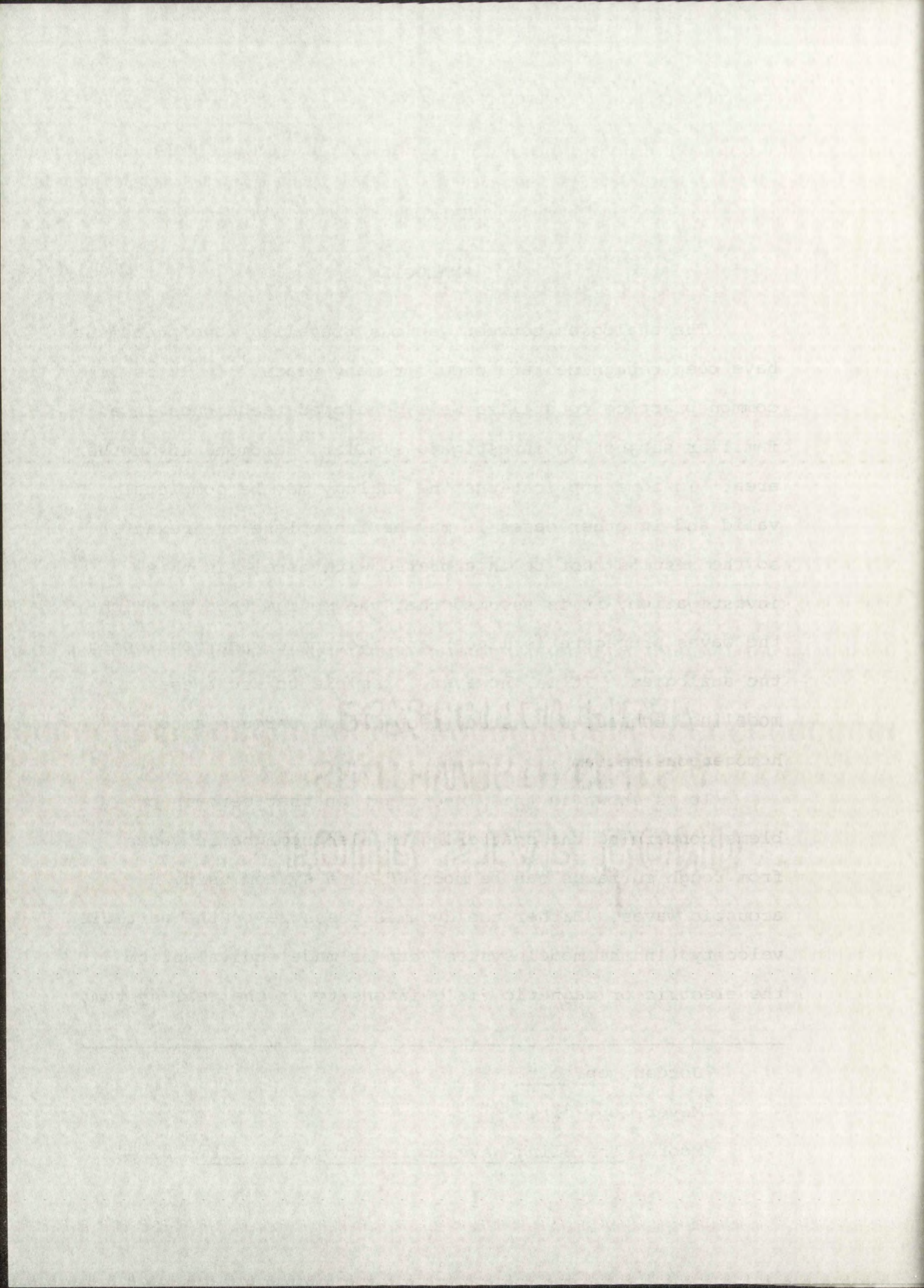
The analogies between various traveling wave phenomena have been recognized and used for many years.^{1,2} It is common practice to utilize well developed techniques in a familiar subject to investigate similar phenomena in another area. In some applications the analogy may be completely valid and in other cases it may be incomplete or inexact, so the results must be interpreted with care. In this investigation, it is assumed that the medium through which the waves propagate is linear and isotropic when developing the analogies. It is, however, possible to use these modeling techniques to study propagation through a non-homogeneous medium.

It is shown in this investigation that certain problems concerning the scattering of electromagnetic waves from rough surfaces can be modeled in a system using acoustic waves. Either the dynamic pressure or the particle velocity (in the model system) can be made equivalent to the electric or magnetic field intensity in the real system.³

¹Jordan, op. cit.

²Meyer, op. cit.

³Moore, Traveling-Wave Engineering, op. cit., p. 49.



The analogy is investigated for the case of electromagnetic waves in air and boundary conditions are considered. It is assumed that the acoustic carrier frequency is low enough that losses in the water remain negligible.¹

3.1 Wave Equations

Maxwell's equations in free space can be written as

$$\nabla \times \underline{E} = -\mu_0 \frac{\partial \underline{H}}{\partial t} \quad (3-1)$$

and

$$\nabla \times \underline{H} = \epsilon_0 \frac{\partial \underline{E}}{\partial t} \quad (3-2)$$

where \underline{E} is the electric field intensity (the bar indicates a vector quantity),

\underline{H} is the magnetic field intensity,

μ_0 is the permeability of free space, and

ϵ_0 is the dielectric constant of free space.

A corresponding pair of partial differential equations can be written to describe the pressure and velocity fields of an acoustic wave in a fluid.² Adiabatic compression and expansion are assumed.³ and the compressibility is considered

¹The plane wave attenuation in fresh water is approximately 0.2 db per meter at a frequency of 1 mc and it increases approximately with the square of the frequency.

²Morse, Philip M., Vibration and Sound, McGraw-Hill, 1948, Chapter 7.

³The compression and expansion are said to be adiabatic when the temperature changes and the heat energy does not change. The acoustic frequencies used are in the range of one megacycle per second which is high enough that heat flow is negligible during one cycle.

The first of these is a very simple one, and it is that the waves in the medium are longitudinal. This means that the particles of the medium move back and forth in the same direction as the wave itself. This is in contrast to transverse waves, where the particles move at right angles to the direction of the wave.

3.1 Wave Equation

Now we will derive the wave equation for a longitudinal wave. Let us consider a small element of the medium of length Δx and cross-sectional area A . The pressure on the left face of the element is p , and on the right face it is $p + \Delta p$. The net force on the element is $A \Delta p$.

and

$$\rho A \Delta x \frac{d^2 \xi}{dt^2} = A \Delta p$$

where ξ is the displacement of the element from its equilibrium position. The pressure p is related to the displacement ξ by the equation of state of the medium.

is the adiabatic exponent, and ρ is the density of the medium. The pressure p is the pressure of the medium.

is the adiabatic exponent, and ρ is the density of the medium. The pressure p is the pressure of the medium.

of an acoustic wave in a fluid. The pressure p is the pressure of the medium.

expansion and contraction, and the density ρ is the density of the medium.

The wave equation for a longitudinal wave in a fluid is

where c is the speed of sound in the medium. The wave equation for a longitudinal wave in a fluid is

to be much less than unity. These equations are

$$\nabla P = -\rho_0 \frac{\partial \underline{U}}{\partial t} \quad (3-3)$$

and

$$\nabla \cdot \underline{U} = -K \frac{\partial P}{\partial t} \quad (3-4)$$

where P is the dynamic acoustic pressure,

\underline{U} is the particle velocity,

ρ_0 is the density of the fluid, and

K is the compressibility of the fluid.

The wave equations for the two systems are readily obtained from Equations 3-1 and 3-2, and from Equations 3-3 and 3-4. These wave equations are

$$\nabla^2 \underline{E} = \mu_0 \epsilon_0 \frac{\partial^2 \underline{E}}{\partial t^2} \quad (3-5)$$

and

$$\nabla^2 \underline{H} = \mu_0 \epsilon_0 \frac{\partial^2 \underline{H}}{\partial t^2} \quad (3-6)$$

for the electromagnetic wave, and

$$\nabla^2 P = \rho_0 K \frac{\partial^2 P}{\partial t^2} \quad (3-7)$$

and

$$\nabla^2 \underline{U} + \nabla \times \nabla \times \underline{U} = \rho_0 K \frac{\partial^2 \underline{U}}{\partial t^2} \quad (3-8)$$

for the acoustic wave. Equation 3-8 can be simplified and written as

$$\nabla^2 \underline{U} = \rho_0 K \frac{\partial^2 \underline{U}}{\partial t^2} \quad (3-9)$$

to be much less than unity. These equations are

$$\nabla^2 p = -\rho \frac{\partial^2 u}{\partial t^2} \quad (2-3)$$

and

$$\nabla \cdot u = -K \frac{\partial p}{\partial t} \quad (2-4)$$

where p is the dynamic acoustic pressure,

u is the particle velocity,

ρ is the density of the fluid, and

K is the compressibility of the fluid.

The wave equations for the two systems are readily

obtained from Equations 2-1 and 2-2, and from Equations

2-3 and 2-4. These wave equations are

$$\nabla^2 E = \mu_0 \epsilon_0 \frac{\partial^2 E}{\partial t^2} \quad (2-5)$$

and

$$\nabla^2 H = \mu_0 \epsilon_0 \frac{\partial^2 H}{\partial t^2} \quad (2-6)$$

for the electromagnetic wave, and

$$\nabla^2 p = \rho K \frac{\partial^2 u}{\partial t^2} \quad (2-7)$$

and

$$\nabla^2 u + \nabla \times \nabla \times u = \rho K \frac{\partial^2 u}{\partial t^2} \quad (2-8)$$

for the acoustic wave. Equation 2-8 can be simplified and

written as

$$\nabla^2 u = \rho K \frac{\partial^2 u}{\partial t^2} \quad (2-9)$$

for cases where $\text{curl}(\text{curl } \underline{U})$ is small enough to neglect.¹

These wave equations form the basis for the useful analogy between acoustic and electromagnetic waves. It should be observed that electromagnetic waves are transverse while acoustic waves are longitudinal in nature. This basic difference between the two wave phenomena will prevent the analogy from being complete for all situations that might arise. Polarization effects are not present with acoustic waves. There are important phenomena, however, that are caused by the effects of interference. These effects are reproduced in the acoustic field and can be useful in predicting similar effects in the electromagnetic field.

3.2 Spherical Waves

The analogy between the electromagnetic wave and the acoustic wave is investigated first for the case of spherical geometry and for elementary sources. A short current element is used to establish an electromagnetic field. Several different acoustic sources are then considered and useful analogies are determined for each case.

3.21 Short Current Element - A short current element is located along the polar axis at the origin of a spherical coordinate system as shown in Figure 3-1.

¹Weinstein, M.S., On the Failure of Plane Wave Theory to Predict the Reflection of a Narrow Ultra Sonic Beam," Jour. Acoust. Soc. of Am., Vol. 24, No. 3, May 1952, pp. 284-87.

for cases where curl (curl \vec{E}) is small enough to neglect.

These wave equations form the basis for the useful

analogy between acoustic and electromagnetic waves. It

should be observed that electromagnetic waves are transverse

while acoustic waves are longitudinal in nature. This basic

difference between the two wave phenomena will prevent the

analogy from being complete for all situations that might

arise. Polarization effects are not present with acoustic

waves. There are important phenomena, however, that are

caused by the effects of interference. These effects are

reproduced in the acoustic field and can be useful in

predicting similar effects in the electromagnetic field.

3.2 Spherical Waves

The analogy between the electromagnetic wave and the

acoustic wave is investigated first for the case of spherical

geometry and for elementary sources. A short current

element is used to establish an electromagnetic field. Sev-

eral different acoustic sources are then considered and

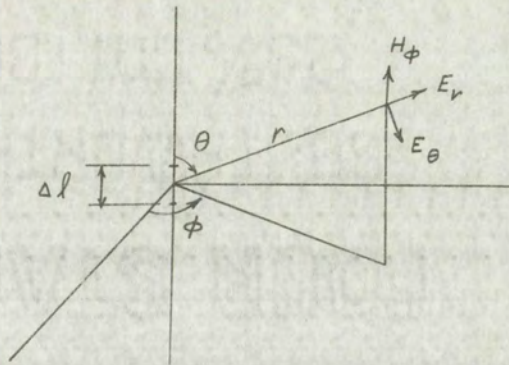
useful analogies are determined for each case.

3.2.1 Short Current Element - A short current element is

located along the polar axis at the origin of a spherical

coordinate system as shown in Figure 3-1.

¹Weinstein, M.S., "On the Failure of Plane Wave Theory to Predict the Reflection of a Narrow Ultra-Sonic Beam," Jour. Acoust. Soc. of Am., Vol. 24, No. 5, May 1952, pp. 184-187.



Short Current Element

Figure 3-1

A solution for the field distributions about the short wire carrying a sinusoidally oscillating current,^{1,2} can be expressed in spherical coordinates as

$$E_R = \frac{I_m \Delta l \eta}{2\pi} e^{-jkr} \left(\frac{1}{r^2} + \frac{\lambda}{2\pi j r^3} \right) \cos \theta \quad (3-10)$$

$$E_\theta = j \frac{I_m \Delta l \eta}{2\lambda} e^{-jkr} \left(\frac{1}{r} + \frac{\lambda}{2\pi j r^2} - \frac{\lambda^2}{4\pi^2 r^3} \right) \sin \theta \quad (3-11)$$

and

$$H_\phi = j \frac{I_m \Delta l}{2\lambda} e^{-jkr} \left(\frac{1}{r} + \frac{\lambda}{2\pi j r^2} \right) \sin \theta \quad (3-12)$$

where I_m is the peak value of the current,

¹Sinusoidally varying signals are represented by $e^{j\omega t}$ and the time variation is suppressed in the equations.

²Schelkunoff, S.A. and Friis, H.T., Antennas, Theory and Practice, John Wiley and Sons, New York, 1952, p. 120.

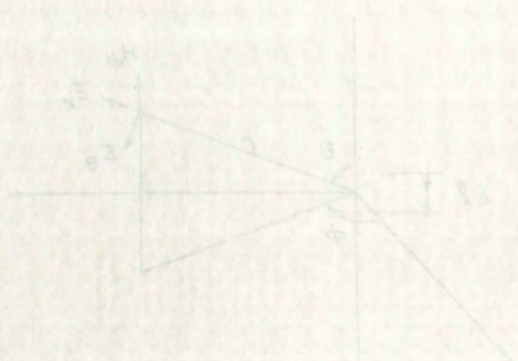


Figure 3-1 Short Current Element

Figure 3-1

A solution for the field distributions about the short wire carrying a sinusoidally oscillating current, $I_m e^{j\omega t}$, can be expressed in spherical coordinates as

$$E_r = \frac{I_m \Delta l}{2\pi} e^{-jkr} \left(\frac{1}{r^2} + \frac{j}{2\pi r^3} \right) \cos \theta \quad (3-10)$$

$$E_\theta = \frac{I_m \Delta l}{2\pi} e^{-jkr} \left(\frac{j}{r^2} + \frac{1}{2\pi r^3} \right) \sin \theta \quad (3-11)$$

and

$$H_\phi = \frac{I_m \Delta l}{2\pi} e^{-jkr} \left(\frac{1}{r} + \frac{j}{2\pi r^2} \right) \sin \theta \quad (3-12)$$

where I_m is the peak value of the current.

¹ Sinusoidally varying signals are represented by $e^{j\omega t}$ and the time variation is expressed in the equations.

² Schelkunoff, S.A. and Friis, H.T., Antennas, Theory and Practice, John Wiley and Sons, New York, 1952, p. 120.

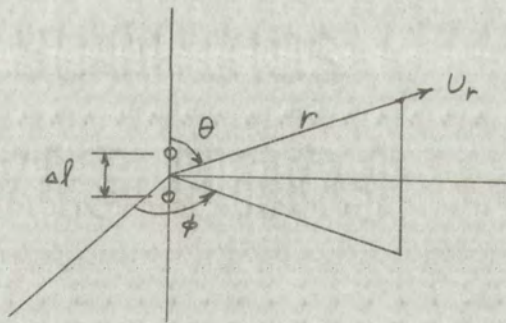
Δl is the length of the elementary conductor and is much shorter than a wavelength,

λ is the wave length,

k is the wave number, $2\pi/\lambda$, and

η is the intrinsic impedance of free space.

3.22 Double Acoustic Source - The analogies are developed first between the fields about a double acoustic source and the fields about the short current element. The double acoustic source consists of two elementary spherical sources operating 180° out of phase with each other and separated by a short distance Δl , where Δl is very small compared to the distance to the observation point.¹ The geometry is given in Figure 3-2.



Acoustic Double Source

Figure 3-2

A solution for the pressure and velocity fields about the source², using wave Equations 3-7 and 3-8, can be

¹The pulsing spheres are much smaller than a wavelength; however, Δl is not restricted to dimensions less than a wavelength in size.

²Randall, Robert H., An Introduction to Acoustics, Addison-Wesley, Cambridge, Mass., 1951, p. 58.

Δl is the length of the elementary conductor and is

much shorter than a wavelength,

λ is the wave length,

k is the wave number, $k = 2\pi/\lambda$, and

Z_0 is the intrinsic impedance of free space.

3.22 Double Acoustic Source - The analogies are developed

first between the fields about a double acoustic source and

the fields about the short current element. The double

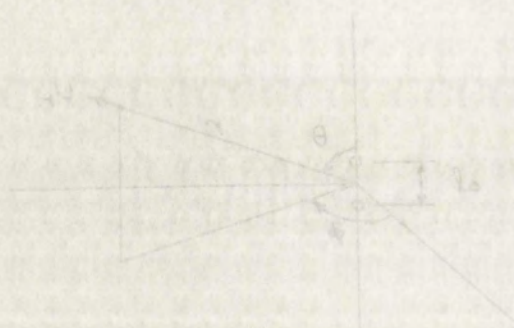
acoustic source consists of two elementary spherical sources

operating 180° out of phase with each other and separated

by a short distance Δl , where Δl is very small compared to

the distance to the observation point.¹ The geometry is

given in Figure 3-2.



Acoustic Double Source

Figure 3-2

A solution for the pressure and velocity fields about

the source,² using wave Equations 3-7 and 3-8, can be

¹The pulsing spheres are much smaller than a wavelength; however, Δl is not restricted to dimensions less than a wavelength in size.

²Randall, Robert H., An Introduction to Acoustics, Addison-Wesley, Cambridge, Mass., 1951, p. 58.

expressed in spherical coordinates for the case of sinusoidal variations as

$$P_1 = \frac{\pi A u_0 \Delta l z}{\lambda^2} e^{-jkr} \frac{1}{r} \cos \theta \quad (3-13)$$

and

$$U_r = \frac{\pi A u_0 \Delta l}{\lambda^2} e^{-jkr} \left(\frac{1}{r} + \frac{j}{2\pi f r^2} \right) \cos \theta \quad (3-14)$$

where P_1 is the dynamic pressure phasor,

U_r is the particle velocity phasor,

A is the area of one elementary sphere,

u_0 is the maximum value of the velocity of the surface of the source,

z is the specific acoustic impedance (product of the density and velocity of propagation), and

λ is the wave length.

There is an obvious partial analogy between the magnetic field intensity expressed by Equation 3-12 and the particle velocity expressed by Equation 3-14 with the exception that a $\sin \theta$ appears in one case and a $\cos \theta$ appears in the other case. The analogy between the electric field component, E_θ given by Equation 3-11 and the pressure, P_1 , given by Equation 3-13 is evident only when the distance r is large so that terms of the order $1/r^2$ are negligible. There is no component of the acoustic field that compares to the radial component of the electromagnetic field given by Equation 3-10.

expressed in spherical coordinates for the case of sinusoidal variations as

$$p = \frac{p_0}{r} e^{-i(kr - \omega t)} \cos \theta$$

and

$$u = \frac{u_0}{r} e^{-i(kr - \omega t)} \sin \theta$$

where p_0 is the dynamic pressure phasor,

u_0 is the particle velocity phasor,

A is the area of one elementary sphere,

u_0 is the maximum value of the velocity of the

surface of the source,

x is the specific acoustic impedance (product of the

density and velocity of propagation), and

λ is the wave length.

There is an obvious partial analogy between the magnetic

field intensity expressed by Equation 3-12 and the particle

velocity expressed by Equation 3-11 with the exception that

a sin θ appears in one case and a cos θ appears in the

other case. The analogy between the electric field component,

E_θ given by Equation 3-11 and the pressure, p , given by

Equation 3-12 is evident only when the distance r is large

so that terms of the order $1/r^2$ are negligible. There is

no component of the acoustic field that compares to the

radial component of the electromagnetic field given by

Equation 3-10.

There are several analogies between the electromagnetic wave and the acoustic wave that can be useful. The first analogy is

$$\frac{H_{\phi}}{r \sin \theta} \rightarrow \frac{U_r}{\cos \theta} \quad (3-15)$$

where terms of order $1/r$ and $1/r^2$ are considered. The peak value of the current is proportional to the peak particle velocity in the acoustic system. The analogy breaks down at the points where θ goes to zero or $\pi/2$, but is valid in the region somewhat closer to the source than the other analogies because terms of order $1/r^2$ are retained. The value of r , however, must still remain much greater than Δl as required for the solutions 3-13 and 3-14 to be valid.

Three additional analogies can be obtained for the case where r is large, so that terms of the order $1/r^2$ and $1/r^3$ can be neglected. These analogies are tabulated in Table 3-1. It should be observed from Figure 3-2 and Equations 3-13 and 3-14 that the radiation field from the acoustic dipole is a maximum along the axis of the dipole. This presents practical difficulties in realizing a suitable dipole source, since the transducer will interfere with the wave propagation because of its physical size. Because of these difficulties in obtaining an acoustic dipole source of this type, it is desirable to investigate the possible analogies using other acoustic sources.

There are several analogies between the electromagnetic wave and the acoustic wave that can be useful. The first analogy is

$$\frac{H_0}{\omega} \rightarrow \frac{V_0}{\omega} \quad (2-12)$$

where terms of order $1/r$ and $1/r^2$ are considered. The peak value of the current is proportional to the peak particle velocity in the acoustic system. The analogy breaks down at the points where θ goes to zero or $\pi/2$, but is valid in the region somewhat closer to the source than the other analogies because terms of order $1/r^2$ are retained. The value of r , however, must still remain much greater than Δ as required for the solutions 2-13 and 2-14 to be valid.

Three additional analogies can be obtained for the case where r is large, so that terms of the order $1/r$ and $1/r^2$ can be neglected. These analogies are tabulated in Table 2-1. It should be observed from Figure 2-2 and Equations 2-13 and 2-14 that the radiation field from the acoustic dipole is a maximum along the axis of the dipole. This presents practical difficulties in realizing a suitable dipole source, since the transducer will interfere with the wave propagation because of its physical size. Because of these difficulties in obtaining an acoustic dipole source of this type, it is desirable to investigate the possible analogies using other acoustic sources.

TABLE 3-1

ANALOGIES - ACOUSTIC DOUBLE SOURCE AND SHORT CURRENT ELEMENT

Analogy Pair	EM System	Acoustic System	Analogous Terms
1	$\frac{H_{\phi}}{j \sin \theta}$	$\frac{U_r}{\cos \theta}$	$1/r \quad 1/r^2$
2	$\frac{E_{\theta}}{j \sin \theta}$	$\frac{P_1}{\cos \theta}$	$1/r$
3	$\frac{H_{\phi}}{j \sin \theta}$	$\frac{P_1}{\cos \theta}$	$1/r$
4	$\frac{E_{\theta}}{j \sin \theta}$	$\frac{U_r}{\cos \theta}$	$1/r$

3.23 Elementary Spherical Source - Consider now the acoustic fields about an elementary pulsing sphere. Solutions to the wave equations for this simple source can be written as

$$P_1 = j \frac{AU_0 z}{2\lambda} e^{-jkr} \frac{1}{r} \quad (3-16)$$

and

$$U_r = j \frac{AU_0}{2\lambda} e^{-jkr} \left(\frac{1}{r} + \frac{\lambda}{2\pi j r^2} \right) \quad (3-17)$$

The analogy between the particle velocity in Equation 3-17 and the magnetic field intensity in Equation 3-12 extends through terms of order $1/r^2$ as in the case of the double acoustic source, and the $\sin \theta$ term is missing. The analogy between pressure and electric or magnetic field

TABLE 3-1

ANALOGIES - ACOUSTIC SOURCE AND SHORT CURRENT ELEMENT

Acoustic System	EM System	Analogy Pair
$\frac{U}{\cos \theta}$	$\frac{H_{\theta}}{1 \sin \theta}$	1
$\frac{I}{\cos \theta}$	$\frac{E_{\theta}}{1 \sin \theta}$	2
$\frac{p}{\cos \theta}$	$\frac{H_{\theta}}{1 \sin \theta}$	3
$\frac{U}{\cos \theta}$	$\frac{E_{\theta}}{1 \sin \theta}$	4

3.2.2 Elementary Spherical Source - Consider now the acoustic

field about an elementary pulsing sphere. Solutions to the

wave equation for this simple source can be written as

$$p = \frac{A}{r} e^{-jkr} \quad (3-16)$$

and

$$u_r = \frac{A}{r^2} e^{-jkr} \left(\frac{1}{r} + \frac{j}{kr} \right) \quad (3-17)$$

The analogy between the particle velocity in Equation 3-17

and the magnetic field intensity in Equation 3-12 extends

through terms of order $1/r^2$ as in the case of the doubleacoustic source, and the $\sin \theta$ term is missing. The

analogy between pressure and electric or magnetic field

intensity is valid only for the case of large range where terms of order $1/r^2$ and $1/r^3$ can be neglected. The $\sin \theta$ term is again missing in the expression for acoustic pressure.

The analogies that can be drawn between the acoustic wave equation solutions for an elementary spherical source and the electromagnetic fields about a short current carrying conductor are given in Table 3-2. These analogies appear to be fully as useful as those involving the more complicated acoustic double source discussed earlier.

TABLE 3-2
ANALOGIES-ELEMENTARY SPHERICAL SOURCE AND SHORT CURRENT ELEMENT

Analogy Pair	EM System	Acoustic System	Analogous Terms
1	$\frac{H_{\phi}}{\sin \theta}$	U_r	$1/r \quad 1/r^2$
2	$\frac{E_{\theta}}{\sin \theta}$	P_l	$1/r$
3	$\frac{H_{\phi}}{\sin \theta}$	P_l	$1/r$
4	$\frac{E_{\theta}}{\sin \theta}$	U_r	$1/r$

3.24 Acoustic Dipole - As the final example of an acoustic source consider an acoustic dipole which is defined as a sphere which vibrates along the polar axis in a prescribed manner. In this case the sphere is assumed to be small

compared to a wavelength and the vibration is assumed to be sinusoidal as in the previous examples (Refer to Figure 3-2 for the geometry).

The dynamic pressure can be expressed as

$$P_1 = \frac{-\pi A U_0 a}{2\lambda^2} e^{-jkr} \left(\frac{1}{r} + \frac{j}{2\pi f r^2} \right) \cos \theta \quad (3-18)$$

and the particle velocity can be expressed as

$$U_r = \frac{-\pi A U_0 a}{2\lambda^2} e^{-jkr} \left(\frac{1}{r} + \frac{j}{2\pi f r^2} - \frac{2\lambda^2}{4\pi^2 r^3} \right) \cos \theta \quad (3-19)$$

where "a" is the radius of the spherical source.¹

In this example the dynamic pressure equation is analogous to the magnetic field intensity equation for terms varying as $1/r$ and $1/r^2$. In the previous examples, it was the vector particle velocity that was analogous to this extent. The analogy between the particle velocity and the θ component of the electric field intensity about the short current element is valid for large values of range so that higher order terms are negligible. The terms in $1/r^2$ and $1/r^3$ are different from the corresponding terms in Equation 3-11 by only a factor of two. The analogies are tabulated in Table 3-3.

3.3 Plane Waves

The problem of analogies is somewhat simplified when plane waves with sinusoidal time variations are being considered. The wave equations can be written in rectangular

¹Morse, op. cit., p. 318.

compared to a wavelength and the vibration is assumed to be sinusoidal, as in the previous examples (Refer to figure 3-2 for the geometry).

The dynamic pressure can be expressed as

$$P = \frac{\pi A^2 \rho}{2\lambda} \left(\frac{1}{r} + \frac{1}{2\lambda} \right) \cos \theta \quad (3-18)$$

and the particle velocity can be expressed as

$$v_r = \frac{\pi A \rho}{2\lambda} \left(\frac{1}{r} + \frac{1}{2\lambda} \right) \cos \theta \quad (3-19)$$

where "a" is the radius of the spherical source.¹

In this example the dynamic pressure equation is

analogous to the magnetic field intensity equation for terms varying as $1/r$ and $1/\lambda$. In the previous examples, it was the vector particle velocity that was analogous to

this extent. The analogy between the particle velocity and the θ component of the electric field intensity about the short current element is valid for large values of

range so that higher order terms are negligible. The

terms in $1/\lambda^2$ and $1/\lambda^3$ are different from the corresponding terms in equation 3-11 by only a factor of two. The

analogies are tabulated in Table 3-3.

3.3 Plane Waves

The problem of analogies is somewhat simplified when plane waves with sinusoidal time variations are being considered. The wave equations can be written in rectangular

¹ Morse, op. cit., p. 218.

TABLE 3-3

ANALOGIES-ACOUSTIC DIPOLE AND SHORT CURRENT ELEMENT

Analogy Pair	EM System	Acoustic System	Analogous Terms
1	$\frac{H_{\phi}}{j \sin \theta}$	$\frac{P_l}{-\cos \theta}$	$1/r \quad 1/r^2$
2	$\frac{E_{\theta}}{j \sin \theta}$	$\frac{U_r}{-\cos \theta}$	$1/r$
3	$\frac{H_{\phi}}{j \sin \theta}$	$\frac{U_r}{-\cos \theta}$	$1/r$
4	$\frac{E_{\theta}}{j \sin \theta}$	$\frac{P_l}{-\cos \theta}$	$1/r$

coordinates as

$$\frac{d^2 E_y}{dx^2} + \omega^2 \mu_0 \epsilon_0 E_y = 0 \quad (3-20)$$

and

$$\frac{d^2 H_z}{dx^2} + \omega^2 \mu_0 \epsilon_0 H_z = 0 \quad (3-21)$$

for a linearly polarized electromagnetic wave, and

$$\frac{d^2 P_l}{dx^2} + \omega^2 \rho_0 K P_l = 0 \quad (3-22)$$

and

$$\frac{d^2 U_x}{dx^2} + \omega^2 \rho_0 K U_x = 0 \quad (3-23)$$

TABLE 3-3

ANALOGIES-ACOUSTIC DIPOLE AND SHORT CURRENT ELEMENT

Analogy Pair	EM System	Acoustic System	Analogous Terms
1	$\frac{H_\theta}{j \sin \theta}$	$\frac{p_l}{-\cos \theta}$	$1/r, 1/r^2$
2	$\frac{E_\theta}{j \sin \theta}$	$\frac{v_l}{-\cos \theta}$	$1/r$
3	$\frac{H_\phi}{j \sin \theta}$	$\frac{v_t}{-\cos \theta}$	$1/r$
4	$\frac{E_\phi}{j \sin \theta}$	$\frac{p_t}{-\cos \theta}$	$1/r$

coordinates as

$$\frac{\partial^2 E_z}{\partial x^2} + \omega^2 \mu_0 \epsilon_0 E_z = 0 \quad (3-20)$$

and

$$\frac{\partial^2 H_z}{\partial x^2} + \omega^2 \mu_0 \epsilon_0 H_z = 0 \quad (3-21)$$

for a linearly polarized electromagnetic wave, and

$$\frac{\partial^2 p}{\partial x^2} + \omega^2 \rho_0 K p = 0 \quad (3-22)$$

and

$$\frac{\partial^2 v_z}{\partial x^2} + \omega^2 \rho_0 K v_z = 0 \quad (3-23)$$

for the acoustic wave.¹ Solutions for the electric and magnetic field intensities are given by

$$E_y = E_m e^{-j\omega\sqrt{\mu_0\epsilon_0}x} \quad (3-24)$$

$$H_z = H_m e^{-j\omega\sqrt{\mu_0\epsilon_0}x} \quad (3-25)$$

and solutions for the dynamic acoustic pressure and particle velocity are given by

$$P_1 = P_m e^{-j\omega\sqrt{\rho_0 K}x} \quad (3-26)$$

$$U_x = U_m e^{-j\omega\sqrt{\rho_0 K}x} \quad (3-27)$$

The analogies for the plane wave case are Tabulated in Table 3-4

TABLE 3-4
PLANE WAVE ANALOGIES

Pair	EM System	Acoustic System
1	H_z	P_1
2	E_y	U_x
3	H_z	U_x
4	E_y	P_1

¹Moore, op. cit., EE-22.

for the acoustic wave. Solutions for the electric and

magnetic field intensities are given by

$$E_z = E_m e^{-j\omega \sqrt{\mu_0 \epsilon_0} x} \quad (3-24)$$

$$H_z = H_m e^{-j\omega \sqrt{\mu_0 \epsilon_0} x} \quad (3-25)$$

and solutions for the dynamic acoustic pressure and particle

velocity are given by

$$p_1 = p_m e^{-j\omega \sqrt{\rho_0 K} x} \quad (3-26)$$

$$u_x = u_m e^{-j\omega \sqrt{\rho_0 K} x} \quad (3-27)$$

The analogies for the plane wave case are tabulated

in Table 3-4

TABLE 3-4
PLANE WAVE ANALOGIES

Pair	EM System	Acoustic System
1	H_z	p_1
2	E_y	u_x
3	H_z	u_x
4	E_y	p_1

The analogies for the case of linearly polarized plane electromagnetic waves and plane acoustic waves are complete without the addition of trigonometric terms. This desirable situation will not always prevail, however, as will be evident when boundary conditions are considered.

In the discussion to this point the scalar nature of pressure has presented no particular difficulty. The analogy is exact when considering the radiation fields in space, providing the appropriate trigonometric relations are taken into account and both components of the electromagnetic radiation field can be determined from measurements of either the dynamic pressure or the particle velocity in the acoustic field.

3.4 Plane-Wave Reflection

The modeling problem at hand is essentially one of duplicating in an appropriate manner the boundary conditions experienced in the real system, since the propagating waves are adequately modeled. The general conditions that must be satisfied at the interface are given first and then several examples are considered.

3.41 Boundary Conditions - Boundary conditions that must be satisfied have similar characteristics in the two systems. Neglecting shear stresses in the liquid,¹ the boundary

¹The skin depth for the viscous wave in water at 20° C is about 0.5 micron.

The analogy for the case of longitudinal waves in a fluid is complete without the addition of a boundary condition. This desirable situation will be maintained as will be evident when considering the situation in this case. The pressure has been presented as a function of position and time, and is exact when considering the radiation field in space, provided the appropriate boundary conditions are taken into account and both components of the magnetic radiation field can be determined. The dynamic pressure or the radiation field in the acoustic field.

2.4. Plane-Wave Reflection

The modeling problem in this case is similar to that of the modeling problem in an acoustic system. The boundary conditions are experienced in the real system, since the radiation field is adequately modeled. The general conditions are satisfied at the interface and the radiation field is considered. Several examples are considered.

2.5. Boundary Conditions - Acoustic and Electromagnetic

As indicated have similar character in the two systems. Neglecting shear stresses in the fluid, the boundary conditions are:

¹The film depth for the acoustic wave is about 0.5 micron.

conditions can be expressed as

$$\underline{n} \times (\underline{E}_1 - \underline{E}_2) = 0 \quad (3-28)$$

and

$$\underline{n} \times (\underline{H}_1 - \underline{H}_2) = 0 \quad (3-29)$$

for the electromagnetic field, and as

$$P_1 = P_2 \quad (3-30)$$

and

$$\underline{n} \cdot (\underline{U}_1 - \underline{U}_2) = 0 \quad (3-31)$$

for the acoustic field, where \underline{n} is a unit vector normal to the surface. These equations state that the tangential components of \underline{E} and \underline{H} are continuous across the boundary as are the pressure, p , and the normal component of the particle velocity, \underline{u} .

The situation is considered first at theoretically perfect surfaces, and then realizable surfaces are investigated. Boundary conditions at a perfect conductor require the tangential electric field to be zero and the tangential magnetic field to be two times the incident field. On the other hand, at a perfectly elastic wall, (pressure release surface) the dynamic pressure is zero and the normal component of the total particle velocity is twice the normal component of the incident particle velocity. In each of these situations there is no wave propagation beyond the interface.

conditions can be expressed as

$$\mathbf{n} \times (\mathbf{E}_1 - \mathbf{E}_2) = 0 \quad (3-28)$$

and

$$\mathbf{n} \times (\mathbf{H}_1 - \mathbf{H}_2) = 0 \quad (3-29)$$

for the electromagnetic field, and as

$$p_1 = p_2 \quad (3-30)$$

and

$$\mathbf{n} \cdot (\mathbf{u}_1 - \mathbf{u}_2) = 0 \quad (3-31)$$

for the acoustic field, where \mathbf{n} is a unit vector normal to the surface. These equations state that the tangential components of \mathbf{E} and \mathbf{H} are continuous across the boundary as are the pressure, p , and the normal component of the particle velocity, \mathbf{u} .

The situation is considered first at theoretically perfect surfaces, and then realizable surfaces are investigated. Boundary conditions at a perfect conductor require the tangential electric field to be zero and the tangential magnetic field to be two times the incident field. On the other hand, at a perfectly elastic wall, (pressure release surface) the dynamic pressure is zero and the normal component of the total particle velocity is twice the normal component of the incident particle velocity. In each of these situations there is no wave propagation beyond the interface.

When a plane electromagnetic wave is normally incident on a perfectly conducting plane surface, the field components are both parallel to the surface, and the electric field component can be made equivalent to either the pressure or the particle velocity in the acoustic wave. When the electric field is made equivalent to pressure, a perfectly elastic boundary is required in the acoustic system in order to obtain the proper phase relationships. On the other hand, a perfectly rigid boundary is required when the electric field is made equivalent to the particle velocity in the acoustic wave.

3.42 Snell's Law - The boundary conditions require that the phase velocities be identical along the interface in both media. This requirement results in Snell's law which applies equally well to the electromagnetic or acoustic wave and is expressed as

$$k_1 \sin \theta_i = k_r \sin \theta_r = k_2 \sin \theta_t \quad (3-32)$$

where θ_i is the angle of incidence,

θ_r is the angle of reflection,

θ_t is the angle of transmission, and

k_1 and k_2 are the wave numbers ($2\pi/\lambda$) in the two media.

Snell's law for the acoustic wave is frequently written as

$$\sin \theta_t = \frac{v_2}{v_1} \sin \theta_i \quad (3-33)$$

since the phase velocities v_1 and v_2 are commonly available for different materials.

When a plane electromagnetic wave is normally incident on a perfectly conducting plane surface, the field components

are both parallel to the surface, and the electric field

component can be made equivalent to either the pressure or

the particle velocity in the acoustic wave. When the electric

field is made equivalent to pressure, a perfectly elastic bound-

ary is required in the acoustic system in order to obtain the

proper phase relationships. On the other hand, a perfectly

rigid boundary is required when the electric field is made

equivalent to the particle velocity in the acoustic wave.

3.42 Snell's law - The boundary conditions require that the

phase velocities be identical along the interface in both

media. This requirement results in Snell's law which applies

equally well to the electromagnetic or acoustic wave and is

expressed as

$$k_1 \sin \theta_1 = k_2 \sin \theta_2 \quad (3-32)$$

where θ_1 is the angle of incidence,

θ_2 is the angle of reflection,

θ_3 is the angle of transmission, and

k_1 and k_2 are the wave numbers ($2\pi/\lambda$) in the two media.

Snell's law for the acoustic wave is frequently written as

$$\sin \theta_1 = \frac{v_1}{v_2} \sin \theta_2 \quad (3-33)$$

since the phase velocities v_1 and v_2 are commonly available

for different materials.

3.43 Oblique Incidence Reflection - Linearly polarized plane electromagnetic waves will be considered in this section. In addition the electric field vector will be assumed to lie in the plane of incidence (TM wave). For this situation the tangential component of the electric field intensity is reduced by a factor, $\cos \theta$, where θ is the angle of incidence as measured from the normal to the surface. It is therefore necessary to let the vector particle velocity in the acoustic wave be equivalent to the electric field intensity in the electromagnetic wave, since the normal component of the particle velocity is also reduced by a factor, $\cos \theta$. The magnetic field intensity is parallel to the interface and the dynamic acoustic pressure is a scalar so neither of these quantities is affected by the angle of incidence.

The reflection coefficient is by definition the ratio of the tangential component of the reflected electric field to the tangential component of the incident electric field and can be written as

$$\Gamma_r^a = \frac{E_{r \tan}}{E_{i \tan}} \quad (3-34)$$

where the subscripts i and r refer to the incident and reflected fields respectively.¹ Superscripts a and w are used to refer to the electromagnetic field in air or to the acoustic field in water. In terms of the magnetic field the above reflection coefficient becomes

¹The reflection coefficient is ordinarily complex.

5.45 Oblique Incidence Reflection - Linearly Polarized

plane electromagnetic waves will be considered in this section. In addition the electric field vector will be assumed to lie in the plane of incidence (TM waves). For this situation the tangential component of the electric field intensity is reduced by a factor, $\cos \theta$, where θ is the angle of incidence as measured from the normal to the surface. It is therefore necessary to let the vector

particle velocity in the electric wave be equivalent to

the electric field intensity in the electromagnetic wave

since the normal component of the particle velocity is also

reduced by a factor, $\cos \theta$. The magnetic field intensity

is parallel to the interface and the dynamic acoustic pressure

is a scalar so neither of these quantities is affected by

the angle of incidence.

The reflection coefficient is by definition the ratio

of the tangential component of the reflected electric field

to the tangential component of the incident electric field

and can be written as

$$(5-54) \quad R = \frac{E_{\text{ref}}}{E_{\text{inc}}}$$

where the subscripts i and r refer to the incident and

reflected fields respectively. Subscripts s and w are

used to refer to the electromagnetic field in air or to the

acoustic field in water. In terms of the magnetic field the

above reflection coefficient becomes

The reflection coefficient is ordinarily complex.

$$\Gamma_r^a = - \frac{H_{r \tan}}{H_{i \tan}} \quad (3-35)$$

The reflection coefficient for the acoustic wave is defined here in a similar manner in terms of particle velocity as

$$\Gamma_r^w = \frac{U_{r \text{ norm}}}{U_{i \text{ norm}}} \quad (3-36)$$

The above reflection coefficient can also be expressed in terms of the dynamic pressure as

$$\Gamma_r^w = - \frac{P_{ir}}{P_{ii}} \quad (3-37)$$

At a perfect conductor the reflection coefficient for the E component of an electromagnetic wave is -1 as given by Equation 3-34. Since the tangential component of the E field must be zero on the surface, the corresponding situation for the acoustic wave occurs on a perfectly rigid wall where the normal component of particle velocity goes to zero. Therefore, Equation 3-36 corresponds to Equation 3-34, and the positive sign is used. It is now necessary to use a minus sign on Equation 3-35 and 3-37, since the tangential component of H and the pressure both double at the corresponding perfect surfaces.

The concept of directional impedance is useful when considering oblique incidence reflection of plane waves. The impedance in the x direction can be expressed as

(3-25)

$$\Gamma_v = \frac{H_{\text{refl}}}{H_{\text{inc}}}$$

The reflection coefficient for the acoustic wave is defined here in a similar manner in terms of particle velocity as

(3-26)

$$\Gamma_v = \frac{U_{\text{refl}}}{U_{\text{inc}}}$$

The above reflection coefficient can also be expressed in terms of the dynamic pressure as

(3-27)

$$\Gamma_p = \frac{P_{\text{refl}}}{P_{\text{inc}}}$$

At a perfect conductor the reflection coefficient for the z component of an electromagnetic wave is -1 as given by Equation 3-24. Since the tangential component of the E field must be zero on the surface, the corresponding situation for the acoustic wave occurs on a perfectly rigid wall where the normal component of particle velocity goes to zero. Therefore, Equation 3-26 corresponds to Equation 3-24, and the positive sign is used. It is now necessary to use a minus sign on Equation 3-25 and 3-27, since the tangential component of H and the pressure both double at the corresponding perfect surfaces. The concept of directional impedance is useful when considering oblique incidence reflection of plane waves. The impedance in the x direction can be expressed as

$$Z_{x1}^a = \frac{E_i \tan}{H_i} = \eta_i \cos \theta_i \quad (3-38)$$

for the electromagnetic field and

$$Z_{x1}^w = \frac{U_i \text{ norm}}{P_{i1}} = Z_i \cos \theta_i \quad (3-39)$$

for the acoustic field. It should be observed that the acoustic impedance has been defined as the ratio of the particle velocity to the dynamic pressure in this equation. This definition of acoustic impedance is just the reciprocal of that which is ordinarily used.¹ Since impedance is a defined quantity either definition is satisfactory, however, one definition must be consistently used in a particular problem.

The reflection coefficient for electromagnetic waves can also be expressed in terms of the directional impedances as

$$\Gamma_r^a = \frac{Z_{x2}^a - Z_{x1}^a}{Z_{x2}^a + Z_{x1}^a} \quad (3-40)$$

where the subscripts 1 and 2 refer to the media on opposite sides of the interface. For acoustic waves in water the reflection coefficient can be written in a similar manner² as

¹Some authors, however, have preferred to define specific acoustic impedance as the ratio of particle velocity to dynamic pressure, for example; Moore, Traveling-Wave Engineering, op. cit.

²The expression for the reflection coefficient comes out in the usual manner because it is defined here in terms of velocity and the impedance is defined as the ratio of particle velocity to dynamic pressure.

$$\frac{E_{1x}}{H_1} = \frac{E_{2x}}{H_2} = \eta \cos \theta$$

for the electromagnetic field and

$$\frac{v_{1x}}{p_1} = \frac{v_{2x}}{p_2} = \frac{1}{\rho c} \cos \theta$$

for the acoustic field. It should be observed that the

acoustic impedance has been defined as the ratio of the

particle velocity to the dynamic pressure in this equation.

This definition of acoustic impedance is just the reciprocal of

that which is ordinarily used.¹ Since impedance is a defined

quantity either definition is satisfactory, however, one

definition must be consistently used in a particular problem.

The reflection coefficient for electromagnetic waves

can also be expressed in terms of the directional impedances

$$R = \frac{\frac{E_{1x}}{H_1} - \frac{E_{2x}}{H_2}}{\frac{E_{1x}}{H_1} + \frac{E_{2x}}{H_2}} \quad (2-10)$$

where the subscripts 1 and 2 refer to the media on opposite

sides of the interface. For acoustic waves in water the

reflection coefficient can be written in a similar manner

as

¹Some authors, however, have preferred to define specific acoustic impedance as the ratio of particle velocity to dynamic pressure, for example, Moore, Traveling-Wave Engineering, p. 117.

The expression for the reflection coefficient comes out in the usual manner because it is defined here in terms of velocity and the impedance is defined as the ratio of particle velocity to dynamic pressure.

$$\Gamma^w = \frac{Z_{x2}^w - Z_{x1}^w}{Z_{x2}^w + Z_{x1}^w} \quad (3-41)$$

The reflection coefficient for either system can be written as

$$\Gamma_r = \frac{\cos \theta_t - \frac{Z_1}{Z_2} \cos \theta_i}{\cos \theta_t + \frac{Z_1}{Z_2} \cos \theta_i} \quad (3-42)$$

using Equation 3-38 (replace the Z's with η 's) or 3-39.

The reflection coefficient is properly modeled when the ratio of Z_1 to Z_2 in the acoustic system is the same as the ratio of η_1 to η_2 in the electromagnetic system. As an example, assume the dielectric constant of the earth to be $13 \epsilon_0$. The impedance is given by

$$\eta = \sqrt{\frac{\mu}{\epsilon(1 + \frac{\sigma}{j\omega\epsilon})}} \quad (3-43)$$

where μ is the permeability,

σ is the conductivity,

ϵ is the dielectric constant, and

ω is the angular frequency.

If it is assumed that the conductivity is small enough or that the frequency is high enough that $\sigma/j\omega \ll 1$ then the impedance is given by $\eta = \sqrt{\frac{\mu}{\epsilon}} \doteq 105 \text{ ohms}$.

Since the impedance of air to the electromagnetic plane wave is about 377 ohms, the air-earth impedance ratio is about 3.6/1. Typical impedance ratios for the model system are shown in Table 3-5. It should be observed that an impedance ratio of R or 1/R results in the same magnitude for the reflection coefficient; only the sign is changed.

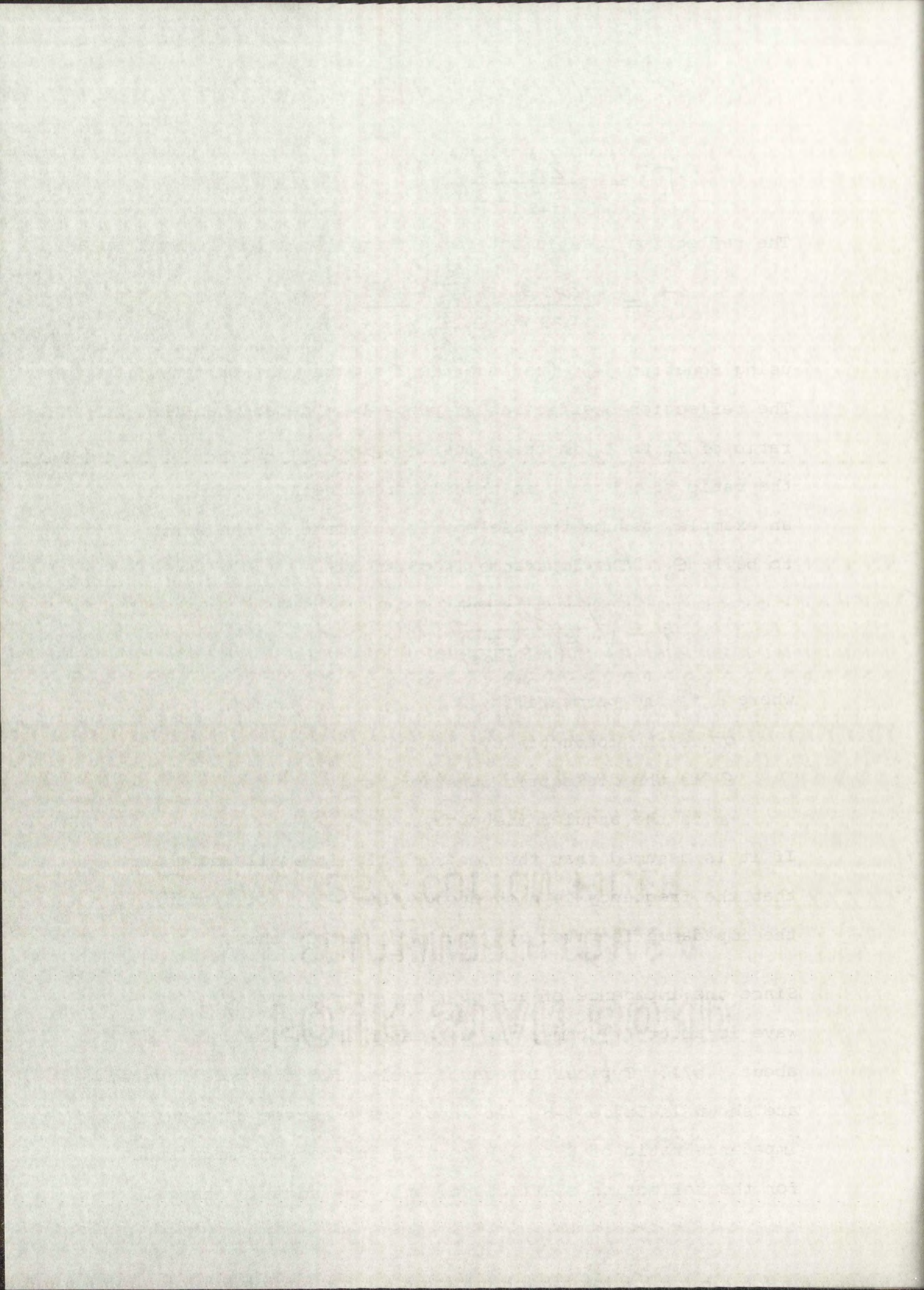


TABLE 3-5
ACOUSTIC IMPEDANCE^a RATIOS FOR SEVERAL MATERIALS

<u>Material</u>	<u>Impedance Ratio</u>
Water/Steel	31/1
Water/Glass	12/1
Water/Magnesium	6.5/1
Water/Elm Wood	1/2.7
Water/Bakelite	2.5/1
Water/Polystyrene	1.7/1

^aAcoustic impedance is defined as the ratio U/p in this table.

To summarize this section it should be noted that the TM wave can be replaced by a TE wave. In this case it is convenient to redefine the reflection coefficient in terms of dynamic pressure and to redefine the acoustic impedance as the ratio of the dynamic pressure to the particle velocity. This is done merely to maintain the symmetry of the equations in the real and model system.

The analogies for all cases where a plane linearly polarized electromagnetic wave is reflected from a perfectly conducting plane surface are shown in Figure 3-3.

3.5 Applications of the Analogies

To demonstrate an application of the analogies, it is desirable to consider a simple situation where the exact solution is known in both the real and the model

TABLE 3-5

ACOUSTIC IMPEDANCE RATIOS FOR SEVERAL MATERIALS

Material	Impedance Ratio
Water/Steel	37/1
Water/Glass	12/1
Water/Magnesium	6.5/1
Water/Birch Wood	1.2/1
Water/Bakelite	2.5/1
Water/Polyethylene	1.7/1

⁶Acoustic impedance is defined as the ratio U/p in this table.

To summarize this section it should be noted that the TM wave can be replaced by a TE wave. In this case it is convenient to redefine the reflection coefficient in terms of dynamic pressure and to redefine the acoustic impedance as the ratio of the dynamic pressure to the particle velocity. This is done merely to maintain the symmetry of the equations in the real and model system. The analogies for all cases where a plane linearly polarized electromagnetic wave is reflected from a perfectly conducting plane surface are shown in Figure 3-5.

3.5 Applications of the Analogies

To demonstrate an application of the analogies, it is desirable to consider a simple situation where the exact solution is known in both the real and the model

BOUNDARY CONDITIONS ON PERFECT PLANE SURFACES

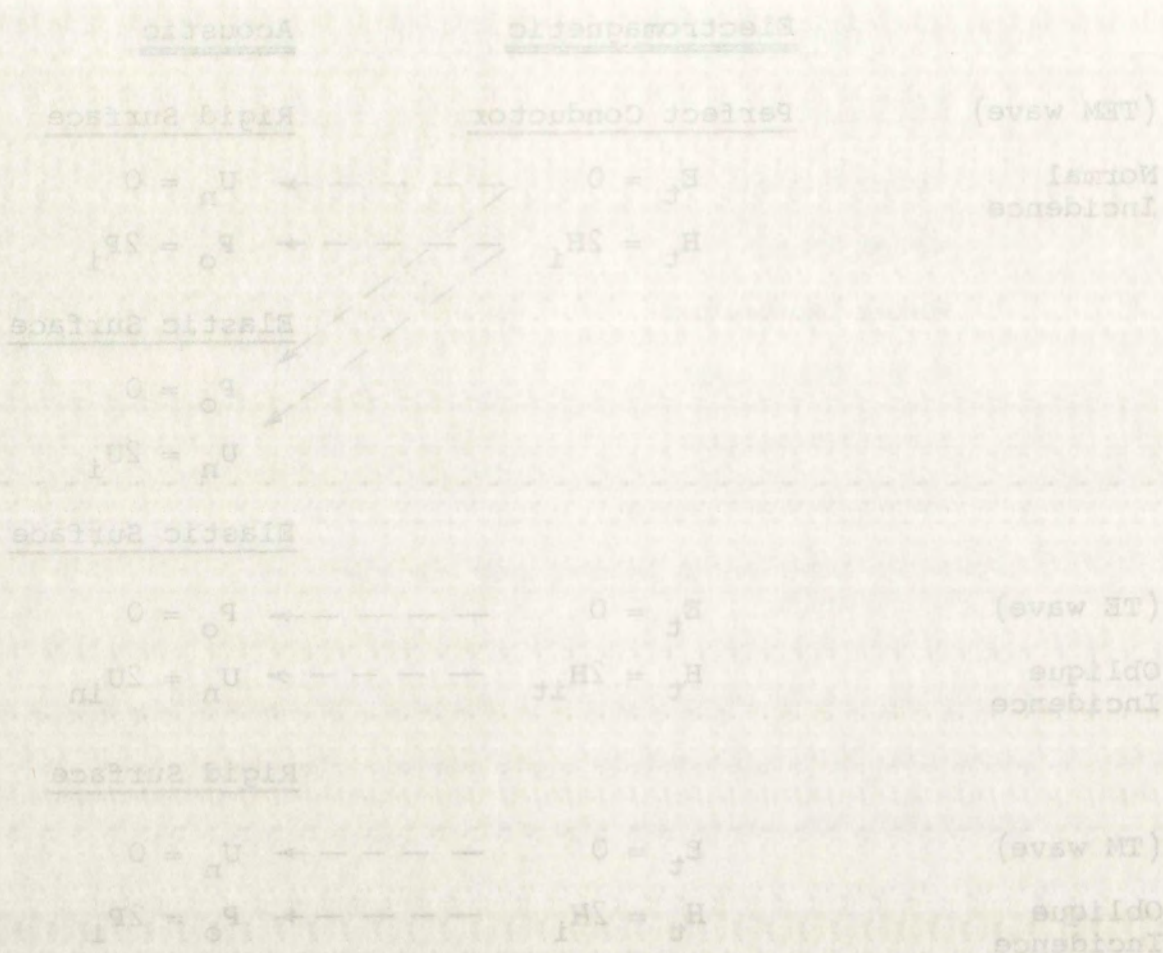
	<u>Electromagnetic</u>	<u>Acoustic</u>
(TEM wave)	<u>Perfect Conductor</u>	<u>Rigid Surface</u>
Normal Incidence	$E_t = 0$	$U_n = 0$
	$H_t = 2H_i$	$P_o = 2P_i$
		<u>Elastic Surface</u>
		$P_o = 0$
		$U_n = 2U_i$
		<u>Elastic Surface</u>
(TE wave)	$E_t = 0$	$P_o = 0$
Oblique Incidence	$H_t = 2H_{it}$	$U_n = 2U_{in}$
		<u>Rigid Surface</u>
(TM wave)	$E_t = 0$	$U_n = 0$
Oblique Incidence	$H_t = 2H_i$	$P_o = 2P_i$

Boundary Conditions on Perfect Plane Surfaces

Figure 3-3

systems. If an investigation of the problem indicates that correct experimental results will be obtained in the simple case then an extension to a more complicated problem is reasonable. Since only the correctness of the analogy is being investigated, no scaling is considered in this example. Also, the magnitude of the magnetic field intensity at unit distance in Equation 3-12 is set numerically equal

BOUNDARY CONDITIONS ON PERFECT PLANE SURFACES



Boundary Conditions on Perfect Plane Surfaces

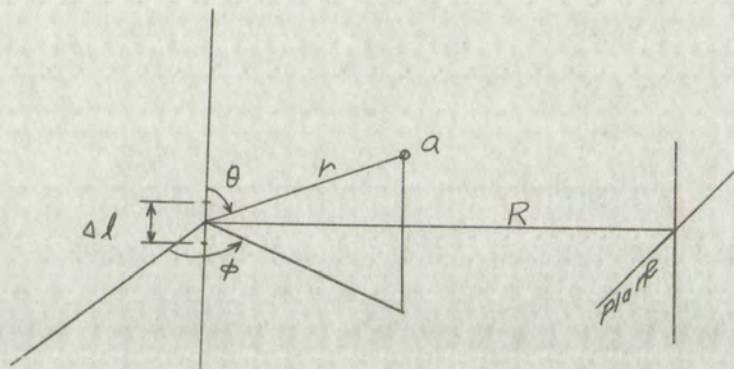
Figure 3-3

systems. If an investigation of the problem indicates that correct experimental results will be obtained in the simple case then an extension to a more complicated problem is reasonable. Since only the correctness of the analogy is being investigated, no scaling is considered in this example. Also the magnitude of the magnetic field intensity at unit distance in Equation 3-12 is set numerically equal

to the magnitude of the particle velocity at unit distance in Equation 3-14. The applications considered in Section 3.51 are theoretical only and were not investigated experimentally.

3.51 The Analogy with the Elementary Acoustic Source -

Consider a spherical coordinate system located in free space with an elementary current dipole located at the origin as shown in Figure 3-4.



Coordinate System for EM Wave

Figure 3-4

The problem is to determine the field at any point "a" which is located far enough from the origin so that $r \gg \Delta l$. Assume that the acoustic model is set up as shown in Figure 3-5.

Now the fields about the current element in the real system are specified by Equations 3-10, 3-11, and 3-12; and in the model system they are given by Equations 3-13 and 3-14. If the analogy is considered to be between

to the magnitude of the particle velocity at unit distance in Equation 3-14. The applications considered in Section 3-5 are theoretical only and were not investigated experimentally.

3.51 The Analogy with the Elementary Acoustic Source

Consider a spherical coordinate system located in free space with an elementary current dipole located at the origin as shown in Figure 3-1.

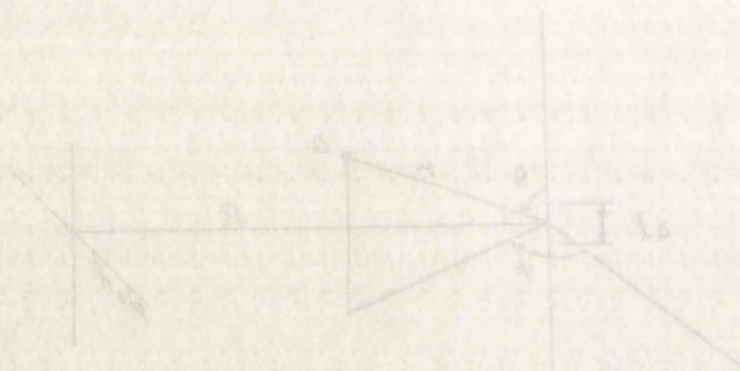


Figure 3-1 Coordinate System for EM Wave

Figure 3-2

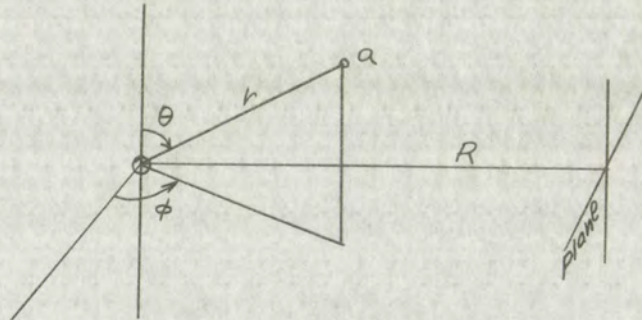
The problem is to determine the field at any point "A".

which is located far enough from the origin so that $r \gg \lambda$. Assume that the acoustic model is set up as

shown in Figure 3-5.

Now the fields about the current element in the real system are specified by Equations 3-10, 3-11, and 3-12; and in the model system they are given by Equations 3-13 and 3-14. If the analogy is considered to be between

H_ϕ and U_r a measurement of the particle velocity in the radial direction in the model system will allow the magnitude of the magnetic field component in the ϕ direction in the real system to be determined using pair 1 from Table 3-2.



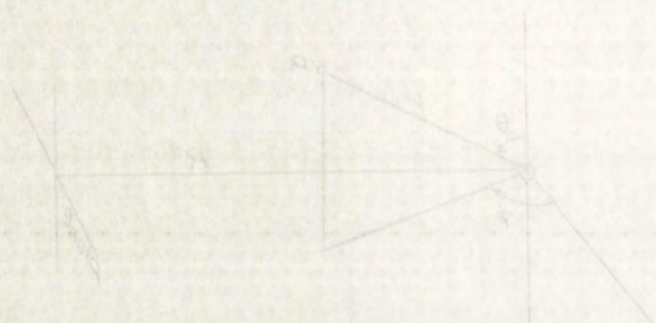
Coordinate System for Acoustic Wave

Figure 3-5

The particle velocity can be easily measured using a properly calibrated narrow beam pressure transducer to probe the field at the point "a". Both the magnitude and the direction of the particle velocity can be determined by this method. After H_ϕ has been determined from the measurement in the model system, Maxwell's equations can be used to determine the remaining field components.

Suppose now that in the real system a perfectly conducting infinite plane is located at a distance R from the origin as shown in Figure 3-4. Let the line R be normal to the plane and pass through the origin of the coordinate system. Assume that the reflected fields are required at the location of the origin.

H_z and U_z a measurement of the particle velocity in the radial direction in the model system will allow the magnitude of the magnetic field component in the z direction in the real system to be determined using pair 1 from Table 3-2.



Coordinate System for Acoustic Wave

Figure 3-5

The particle velocity can be easily measured using a properly calibrated narrow beam pressure transducer to probe the field at the point "a". Both the magnitude and the direction of the particle velocity can be determined by this method. After H_z has been determined from the measurement in the model system, Maxwell's equations can be used to determine the remaining field components. Suppose now that in the real system a perfectly conducting infinite plane is located at a distance R from the origin as shown in Figure 3-6. Let the line R be normal to the plane and pass through the origin of the coordinate system. Assume that the reflected fields are required at the location of the origin.

Using image theory and Equation 3-12, the reflected magnetic field intensity at the origin is given by

$$H_{\phi} = j \frac{I_m \Delta l}{2\lambda} e^{-j\beta 2R} \left(\frac{\Gamma}{2R} + \frac{\lambda \Gamma'}{2\pi j (2R)^2} \right) \sin \theta \quad (3-44)$$

where θ is equal $\pi/2$ (from the geometry),

Γ is the plane wave reflection coefficient, and

Γ' is a reflection coefficient determined for the $1/r^2$ term.¹

For the special case of a perfectly conducting interface both Γ and Γ' reduce to unity.

Now in the model system the particle velocity is equivalent to the field intensity in the real system. Equivalent boundary conditions for particle velocity require a perfectly elastic infinite plane boundary located at a distance R from the origin as shown in Figure 3-5. Again

¹For a dipole oriented horizontally above a plane surface the reflected magnetic field for the radiation term is equivalent to that radiated from an image dipole modified by the plane wave reflection coefficient. The term which varies as $1/r^2$ is modified by a factor

$$\frac{\eta-1}{\eta+1} \left(\frac{\eta^2 - 6\eta + 9 - \frac{4}{\eta}}{(\eta-1)^2} \right)$$

where

$$\eta = \sqrt{\frac{\epsilon - j \frac{\sigma}{\omega}}{\epsilon_0}}$$

The plane wave reflection coefficient is given by

$$\Gamma = \frac{\eta-1}{\eta+1}$$

Moore, R.K., Normal Incidence Reflection of Dipole Radiation from a Plane Interface, Sandia Corp. Tech. Memo 199-56-14. Sept., 1956.

Using image theory and Equation 3-12, the reflected magnetic field intensity at the origin is given by

$$H_0 = \frac{1}{2} \frac{I_0}{\lambda} e^{-\gamma R} \left(\frac{\Gamma}{2R} + \frac{\Gamma'}{2\gamma R^2} \right) \sin \theta \quad (3-14)$$

where θ is equal to $\pi/2$ (from the geometry),

Γ is the plane wave reflection coefficient, and Γ' is a reflection coefficient determined for the

$1/R^2$ term.

For the special case of a perfectly conducting interface

both Γ and Γ' reduce to unity.

Now in the model system the particle velocity is

equivalent to the field intensity in the real system. Equiv-

alent boundary conditions for particle velocity require a

perfectly elastic infinite plane boundary located at a

distance R from the origin as shown in Figure 3-5. Again

For a dipole oriented horizontally above a plane surface the reflected magnetic field for the radiation term is equivalent to that radiated from an image dipole modified by the plane wave reflection coefficient. The term which varies as $1/R^2$ is modified by a factor

$$\left(\frac{n-1}{n+1} \right) \left(\frac{n^2 - \epsilon n + \frac{1}{2}}{(n-1)^2} - \frac{n}{2} \right)$$

where

$$n = \sqrt{\frac{\epsilon - \frac{1}{2}}{\epsilon_0}}$$

The plane wave reflection coefficient is given by

$$\Gamma = \frac{n-1}{n+1}$$

using image theory and Equation 3-17 the reflected component of particle velocity at the origin is given by

$$U_r = j \frac{AU_0}{2\lambda} e^{-j k 2R} \left(\frac{1}{2R} + \frac{\lambda}{2\pi j (2R)^2} \right) \quad (3-45)$$

It is required that the level and phase of the electromagnetic field be determined by physical measurements of the acoustic field. A pressure transducer with a very narrow antenna pattern can be used to measure the particle velocity and direction at the origin of the acoustic system. The results of the measurement will obviously give the magnitude of Equation 3-45 and the direction will lie along the line R. The phase can be determined by comparing the received acoustic signal with the reference oscillator which controls the transmitter. In this model a component of particle velocity in the r direction corresponds to the component of magnetic field intensity in the ϕ direction. The magnitude of the particle velocity will be equal to the magnitude of the field intensity in consistent units since the trigonometric factor ($\sin \theta$) is unity.

An alternative method of measurement is to use a transducer calibrated to measure pressure. The resulting measurement will be the magnitude of

$$P_1 = j \frac{AU_0}{2\lambda z} e^{-j k 2R} \frac{1}{2R} \quad (3-46)$$

which is Equation 3-16 with the appropriate range inserted. It can be shown that the particle velocity for the case of sinusoidal variations is given by

using image theory and Equation 5-17 the reflected component of particle velocity at the origin is given by

$$U_r = \frac{A U_0}{2\lambda} e^{-j\lambda z} \left(\frac{1}{2R} + \frac{j}{2\pi f(2R)^2} \right) \quad (5-45)$$

It is required that the level and phase of the electromagnetic field be determined by physical measurements of the acoustic field. A pressure transducer with a very narrow antenna pattern can be used to measure the particle velocity and direction at the origin of the acoustic system. The results of the measurement will obviously give the magnitude of Equation 5-45 and the direction will lie along the line R. The phase can be determined by comparing the received acoustic signal with the reference oscillator which controls the transmitter. In this model a component of particle velocity in the x direction corresponds to the component of magnetic field intensity in the y direction. The magnitude of the particle velocity will be equal to the magnitude of the field intensity in constant units since the impedance factor ($\sin \theta$) is unity.

An alternative method of measurement is to use a transducer calibrated to measure pressure. The resulting measurement will be the magnitude of

$$P = \frac{A U_0}{2\lambda} e^{-j\lambda z} \frac{1}{2R} \quad (5-46)$$

which is Equation 5-16 with the appropriate range inserted. It can be shown that the particle velocity for the case of sinusoidal variations is given by

$$U_r = - \frac{1}{\rho_0 \omega} \frac{\partial P_1}{\partial r} \quad (3-47)$$

where P_1 is given by Equation 3-16. Evaluating Equation 3-47 results in Equation 3-45 when the range, $2R$, is substituted for r .

3.52 Boundary Considerations - In the previous models the analogy is exact since the describing equations are identical in the two systems, except for factors which are taken into account in the transformation, and the boundary conditions are simple and equivalent. The complete electromagnetic field can be determined from measurements made in the acoustic system because of the simplifications. This desirable situation will not continue when more interesting and useful problems are investigated.

Let a short dipole antenna carrying a sinusoidally varying current be located at the origin of a coordinate system as shown in Figure 3-6. Now assume a perfectly conducting surface is placed at a distance, h , from the origin, where $h \gg \lambda$. Assume also that irregularities on the surface cause it to deviate from a plane surface by an amount comparable to a few wavelengths. A typical problem of the backscatter of electromagnetic waves from a rough surface is encountered when one attempts to calculate the scattered fields at a point above the rough surface.

$$V_r = - \frac{1}{\rho_0 \omega} \frac{\partial P}{\partial r} \quad (3-47)$$

where P_r is given by Equation 3-16. Evaluating Equation 3-47 results in Equation 3-48 when the range, R , is substituted for r .

3.52 Boundary Considerations - In the previous models the

analogy is exact since the describing equations are identical

in the two systems, except for factors which are taken into

account in the transformation, and the boundary conditions

are simple and equivalent. The complete electromagnetic

field can be determined from measurements made in the acoustic

system because of the simplifications. This desirable sit-

uation will not continue when more interesting and useful

problems are investigated.

Let a short dipole antenna carrying a sinusoidally

varying current be located at the origin of a coordinate

system as shown in Figure 3-6. Now assume a perfectly

conducting surface is placed at a distance, h , from the

origin, where $h \gg \lambda$. Assume also that irregularities on

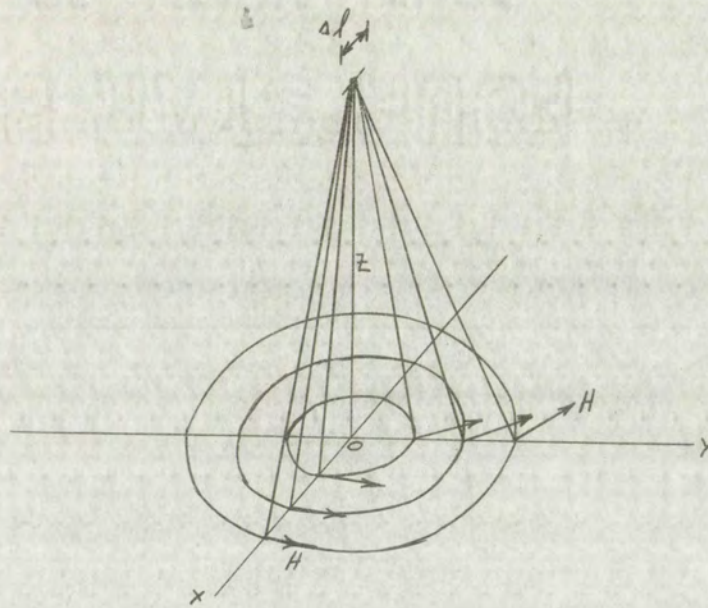
the surface cause it to deviate from a plane surface by an

amount comparable to a few wavelengths. A typical problem

of the backscatter of electromagnetic waves from a rough

surface is encountered when one attempts to calculate the

scattered fields at a point above the rough surface.



H-Field Incident on Plane

Figure 3-6

In Figure 3-6 the directions and relative magnitudes of the incident H vectors are shown as they reach the x, y plane where the rough boundary is located. The magnitude of the incident H vector varies inversely with the range to the point on the target. In addition the field is reduced by the size of the angle measured from the axis of the current element to the point on the target. This situation is to be compared to the incident particle velocity on the boundary in the case of an acoustic wave.

Figure 3-7 shows an elementary spherical source located on the z axis at a distance h from the origin. The relative magnitude and direction of the incident particle velocities are shown in the x, y plane where the rough boundary



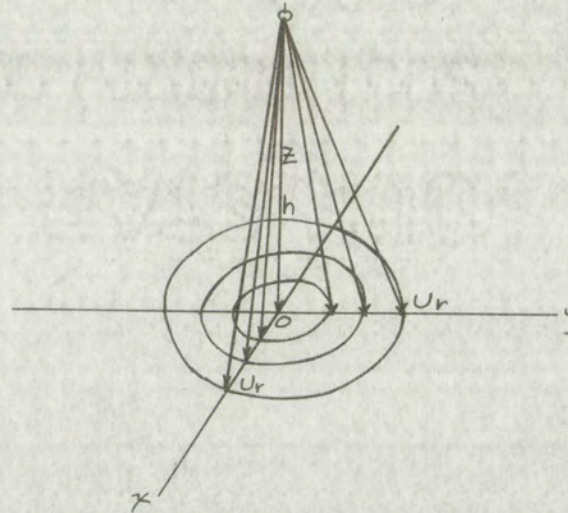
H-Field Incident on Plane

Figure 5-6

In Figure 5-6 the directions and relative magnitudes of the incident H vectors are shown as they reach the x,y plane where the rough boundary is located. The magnitude of the incident H vector varies inversely with the range to the point on the target. In addition the field is reduced by the size of the angle measured from the axis of the current element to the point on the target. This situation is to be compared to the incident particle velocity on the boundary in the case of an acoustic wave.

Figure 5-7 shows an elementary spherical source located on the z axis at a distance h from the origin. The relative magnitude and direction of the incident particle velocities are shown in the x,y plane where the rough boundary

is located. The magnitude of the velocities vary inversely with range and not with the angle of incidence. At each point on the target the particle velocity is normal to the direction of the corresponding H field vector in the electromagnetic field.



Particle Velocity Incident on Plane

Figure 3-7

It is apparent that the intensity of the incident signal is not faithfully reproduced in the acoustic model in this example. The scattering elements off the y axis have an incident field that should be reduced by a factor

$$\cos \left(\tan^{-1} \frac{x}{h} \right)$$

in each case. This is equivalent to saying that the antenna pattern of the elementary spherical acoustic source is different from the antenna pattern for the elementary current

is located. The magnitudes of the velocities vary inversely with range and not with the angle of incidence. At each point on the target the particle velocity is normal to the direction of the corresponding H field vector in the static magnetic field.



Particle Velocity Incident on Plane

Figure 2

It is apparent that the intensity of the incident signal is not faithfully reproduced in the acoustic model in this example. The scattered elements off the y axis have an incident field that should be reduced by a factor

$$\cos\left(\tan^{-1}\frac{x}{y}\right)$$

in each case. This is equivalent to saying that the pattern of the elementary spherical acoustic source is different from the antenna pattern for the elementary current

dipole. This situation can be remedied at least in part by choosing an acoustic source with a more appropriate antenna pattern.¹

There is, however, another discrepancy that cannot be removed by such a simple procedure. Consider a particular scattering element to consist of a small inclined plane surface. When this scattering model is used, the assumption is made that the surface consists of relatively plane areas that are several wavelengths in size; so that ray theory and the plane wave reflection coefficient can be used to approximate the direction, magnitude, and phase of the reflected wave. The incident magnetic field intensity can be separated into two components, one of which is in the plane of incidence on this particular scattering facet and one of which is normal to the plane of incidence. It is well known that the reflection coefficients for the two polarizations are different except for the case of normal incidence and at the grazing angle.

For the cases of fresh water and dry earth the approximate reflection coefficients for power for the two types of polarization² are shown in Figure 3-8. Typical reflection

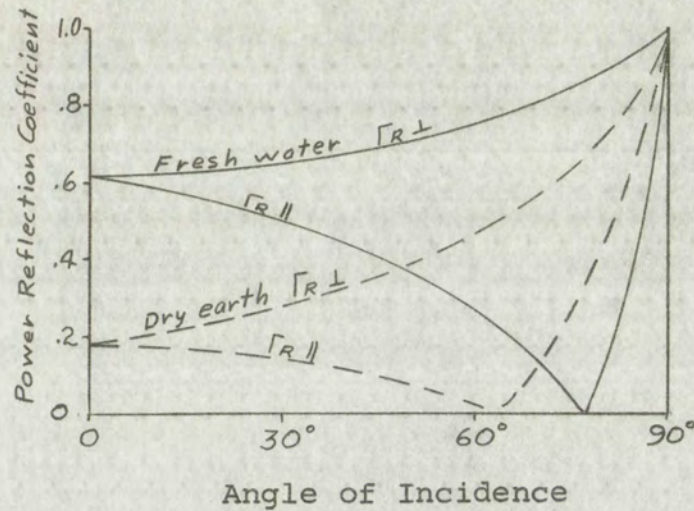
¹Hueter, T. F., and Bolt, R. H., Sonics, John Wiley and Sons, New York, 1955, p. 63.

²Stratton, J. A., Electromagnetic Theory, McGraw-Hill Book Company, New York, 1941, p. 510.

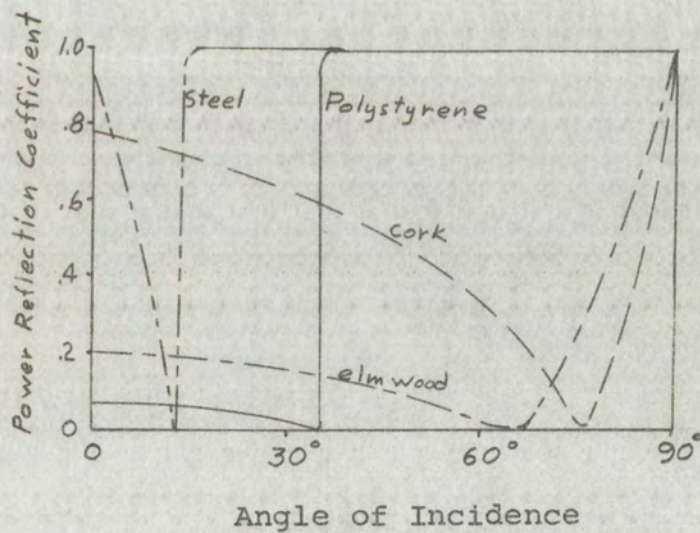
dipole. This situation can be considered at least in part
 by choosing an acoustic source with a more appropriate
 antenna pattern.
 There is, however, another discrepancy that cannot
 be removed by such a simple procedure. Consider a particu-
 lar scattering element to consist of a small inclined plane
 surface. When this scattering model is used, the assumption
 is made that the surface consists of relatively plane areas
 that are several wavelengths in size so that ray theory
 and the plane wave reflection coefficient can be used to
 approximate the direction, magnitude, and phase of the
 reflected wave. The incident magnetic field intensity can
 be separated into two components, one of which is in the
 plane of incidence on this particular scattering facet and
 one of which is normal to the plane of incidence. It is
 well known that the reflection coefficients for the two
 polarizations are different except for the case of normal
 incidence and at the grazing angle.
 For the cases of fresh water and dry earth the approxi-
 mate reflection coefficients for power for the two types of
 polarization are shown in Figure 5-8. Typical reflection

Hunter, T. W. and R. H. Sonics, John Wiley and
 Sons, New York, 1955, p. 57.
 Stratton, R. A., Electromagnetic Theory, McGraw-Hill
 Book Company, New York, 1941, p. 210.

coefficients¹ for sonic waves from several different boundary materials are given in Figure 3-9.



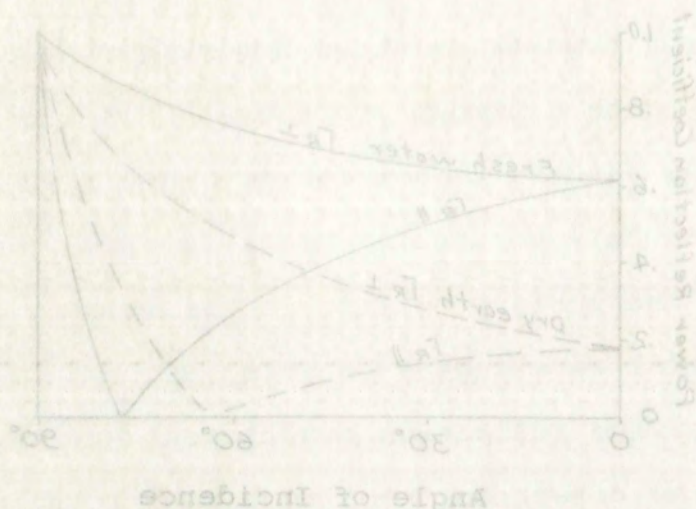
Reflection Coefficients for TM and TE Waves
Figure 3-8



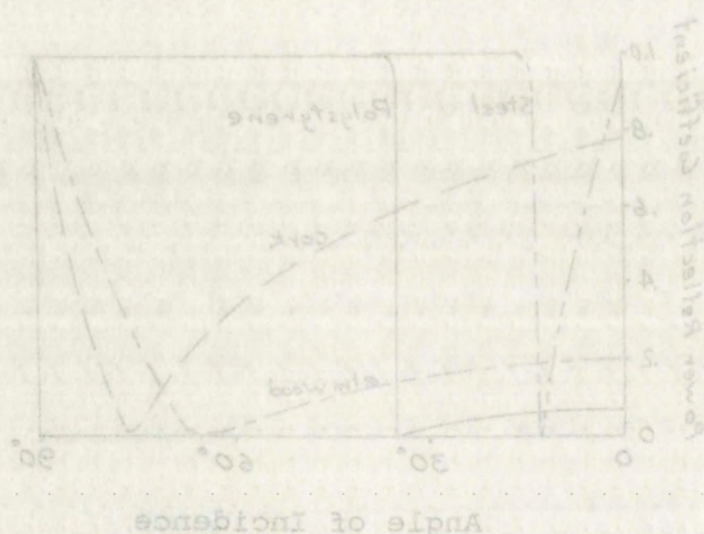
Reflection Coefficient for Acoustic Waves
Figure 3-9

¹These reflection coefficients are based upon an assumed lossless material.

coefficients¹ for sonic waves from several different boundary materials are given in Figure 3-9.



Reflection Coefficients for TM and TE Waves
Figure 3-8



Reflection Coefficient for Acoustic Waves
Figure 3-9

¹These reflection coefficients are based upon an assumed lossless material.

The difference in reflection coefficients for the two polarizations is not too significant for many materials, until the angle of incidence exceeds 30 degrees. From the standpoint of plane-wave reflections from an infinite plane surface the error introduced by ignoring polarization is not appreciable for the case of near-vertical incidence. It is important, however, to note that a scattering model based on the reflection coefficient of small plane facets is definitely limited in application. Use of this model requires that the slope of the surface change only slightly in a distance of several wavelengths. It may be desirable to use a different model to generate the scattered signal in which case the information on reflection coefficients will not be used.

3.6 A Scattering Model

In this section the acoustic-electromagnetic wave analogy is investigated for the case of rough targets where only the radiation field is considered. Radar signals are generally random in nature for this type of target; therefore, signal statistics such as the mean value and range of fading are of particular interest.

In the usual application the antenna pattern restricts radiation to a much smaller region than for the case of an elementary dipole and in many cases it is reasonable to assume that the pattern is circularly symmetric about a

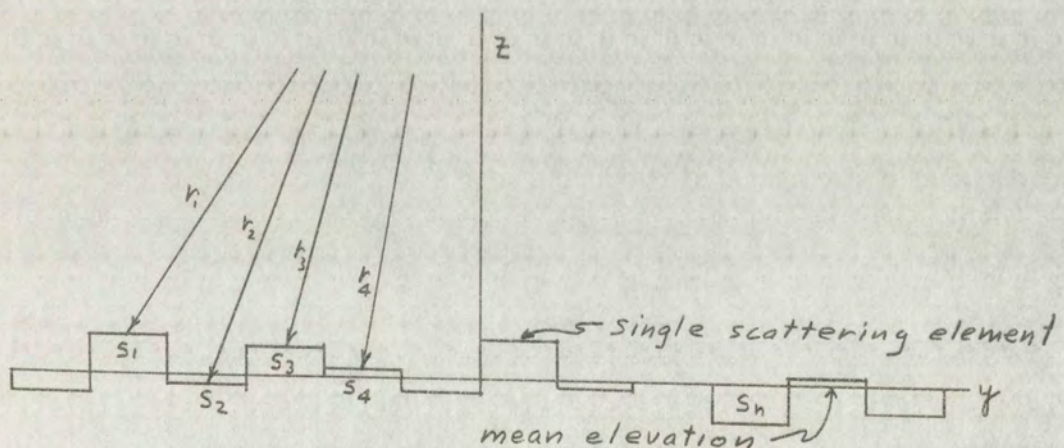
The difference in reflection coefficients for the two polarizations is not too significant for many materials, until the angle of incidence exceeds 30 degrees. From the standpoint of plane-wave reflections from an infinite plane surface the error introduced by ignoring polarization is not appreciable for the case of near-vertical incidence. It is important, however, to note that a scattering model based on the reflection coefficient of small plane facets is definitely limited in application. Use of this model requires that the slope of the surface change only slightly in a distance of several wavelengths. It may be desirable to use a different model to generate the scattered signal in which case the information on reflection coefficients will not be used.

3.6 A Scattering Model

In this section the acoustic-electromagnetic wave analogy is investigated for the case of rough targets where only the radiation field is considered. Radar signals are generally random in nature for this type of target; therefore, signal statistics such as the mean value and range of fading are of particular interest. In the usual application the antenna pattern restricts radiation to a much smaller region than for the case of an elementary dipole and in many cases it is reasonable to assume that the pattern is circularly symmetric about a

center line. The electric and magnetic field vectors are both at right angles to the range vector between the antenna and the particular scattering element under consideration, and have a magnitude determined by the range and antenna gain in that direction. In the acoustic model of the situation, the particle velocity vector is in the direction of the range vector to the scattering element under consideration and has a magnitude determined by range and antenna gain in that direction. Therefore, the incident acoustic particle velocity on a scattering element always bears a definite relationship to the incident electromagnetic field vectors on the corresponding scattering element in the real system.

Consider a scattering model for the rough surface where the individual scattering elements are located in a radius manner about a mean elevation as shown in Figure 3-10.

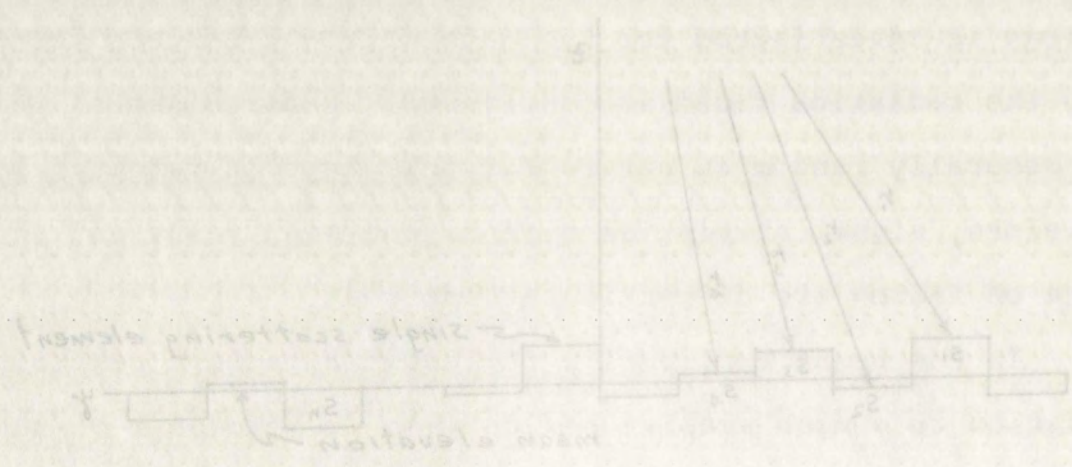


Scattering Model

Figure 3-10

center line. The electric and magnetic field vectors are both at right angles to the range vector between the antenna and the particular scattering element under consideration, and have a magnitude determined by the range and antenna gain in that direction. In the acoustic model of the situation, the particle velocity vector is in the direction of the range vector to the scattering element under consideration and has a magnitude determined by range and antenna gain in that direction. Therefore, the incident acoustic particle velocity on a scattering element always bears a definite relationship to the incident electromagnetic field vectors on the corresponding scattering element in the real system.

Consider a scattering model for the rough surface where the individual scattering elements are located in a radius manner about a mean elevation as shown in Figure 3-10.



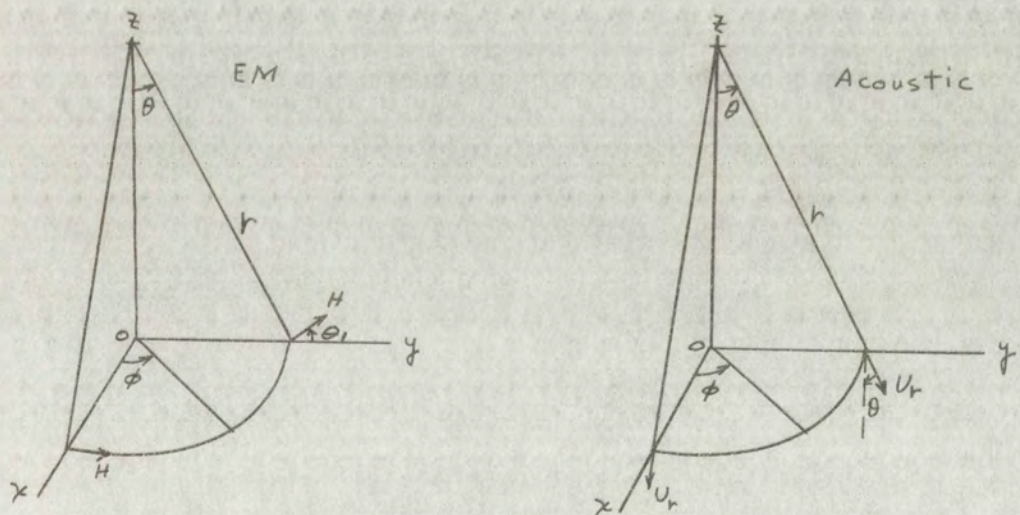
Scattering Model

Figure 3-10

In this rough surface model the range to each scattering element differs from the corresponding range to the mean elevation by some small amount, Δr_i . Each scatterer is assumed to be a Huygen's source. In addition, the excitation is assumed to be the same as though the scatterer were part of an infinite plane at that particular elevation. The electromagnetic wave is assumed to be polarized so the H vector always lies parallel to the y,z plane as shown in Figure 3-11. The tangential component of the H vector (which is effective in exciting Huygen's current sources in the boundary) varies with

$$\cos \theta_1 = \frac{1}{\sqrt{1 + \tan^2 \theta \sin^2 \phi}} \quad (3-48)$$

where θ_1 is measured between the incident H vector and the x,y plane.



Geometry for Incident Acoustic and EM Fields

Figure 3-11

In this rough estimate model the change in the element distance from the corresponding range to the elevation by some small amount, Δz . Each scattering element is assumed to be a Huygen's source. In addition, the excitation is assumed to be the same as though the scatterer were part of an infinite plane at that particular elevation. The electromagnetic wave is assumed to be polarized as the H vector always lies parallel to the y, z plane as shown in Figure 11. The tangential component of the H vector (which is effective in exciting Huygen's current sources in the secondary) varies with

$$\cos \theta_i = \frac{y}{\sqrt{y^2 + z^2}}$$

where θ_i is measured between the incident H vector and the x, y plane.



Geometry for Incident Acoustic and EM Fields

The radiation from the small element for the electromagnetic wave can be considered as caused by the incremental conduction or displacement current excited in the element by the incident field. These current elements establish fields of the type described earlier in Equations 3-10, 3-11, and 3-12. The radiation from the Huygen's current source varies with the sine of the angle, θ_2 , measured between its axis and the direction of the radiation. For signals received at the antenna this variation is given by

$$\sin \theta_2 = \sqrt{1 - \sin^2 \theta \cos^2 \phi} \quad (3-49)$$

Now the magnetic field intensity received at the antenna from a single source on the plane can be expressed as

$$H = \mathcal{H} \frac{e^{-j2kr}}{2r} \propto \cos \theta_1 \sin \theta_2 \quad (3-50)$$

where " \mathcal{H} " is the magnetic field intensity (radiation field) of the source at unit distance and \propto is a factor which accounts for absorption.

The geometry of Figure 3-11 indicates that the normal component of partial velocity (which is effective in exciting Huygen's sources in the boundary) varies with $\cos \theta$ over the surface. The radiation from the Huygen's velocity source is isotropic (above the boundary) and therefore does not vary with angle. Now, in a similar manner, the particle velocity at the antenna can be expressed as

$$U = \mathcal{U} \frac{e^{-j2kr}}{2r} \propto \cos \theta \quad (3-51)$$

The radiation from the small element for the electro-
magnetic wave can be considered as caused by the incremental
conduction or displacement current excited in the element
by the incident field. These current elements establish
fields of the type described earlier in Equations 3-10,
3-11, and 3-12. The radiation from the Huygen's current
source varies with the sine of the angle θ , measured
between its axis and the direction of the radiation. For
signals received at the antenna this variation is given by

$$(3-13) \quad \sin \theta_s = \sqrt{1 - \sin^2 \theta \cos^2 \phi}$$

Now the magnetic field intensity received at the antenna
from a single source on the plane can be expressed as

$$(3-14) \quad H = \frac{K}{r} \sin \theta_s \propto \cos \theta_s \sin \theta_s$$

where "K" is the magnetic field intensity (radiation field)
of the source at unit distance and r is a factor which
accounts for absorption.

The geometry of Figure 3-11 indicates that the normal
component of particle velocity (which is effective in ex-
citing Huygen's sources in the boundary) varies with $\cos \theta$
over the surface. The radiation from the Huygen's velocity
source is isotropic (above the boundary) and therefore does
not vary with angle. Now, in a similar manner, the particle
velocity at the antenna can be expressed as

$$(3-15) \quad V = \frac{V_0}{r} \cos \theta \propto \cos \theta$$

where " u " is the particle velocity (radiation field) of the source at unit distance.

Equation 3-50 can be written as

$$H = \frac{e}{2r} \times \cos \theta \left[\frac{(1 - \sin^2 \theta \cos^2 \phi)}{\cos^2 \theta + \sin^2 \theta \sin^2 \phi} \right]^{1/2} \quad (3-52)$$

where the function outside the brackets corresponds to Equation 3-51 for acoustic particle velocity and the quantity inside the brackets is unity for all values of θ and ϕ . The electromagnetic field intensity at the antenna due to a Huygen's current source is, therefore, the same as the particle velocity at the antenna due to a Huygen's velocity source for the scattering model considered. This particular rough surface model must be considered to be a "scalar model" since polarization effects are not evident.

3.7 Summary of Model Validity

It was shown that the pressure and velocity fields, about several acoustic sources, are analogous to the electric and magnetic field intensities about a short current element, when certain geometric factors are considered. In some cases the analogy applies to terms of order $1/r$ and $1/r^2$; in other cases it applies only to terms of order $1/r$.

The application of the acoustic-electromagnetic wave analogy, using the acoustic simulator, generally requires a directive antenna pattern and only the radiation fields are considered. In addition, it is necessary that the

where " u " is the particle velocity (radiation field) of the source at unit distance.

Equation 3-59 can be written as

$$H = \frac{e}{2c} \left[\frac{(1 - \sin^2 \theta \cos^2 \phi)}{\cos^2 \theta + \sin^2 \theta \sin^2 \phi} \right] \quad (3-59)$$

where the function outside the brackets corresponds to Equation 3-51 for acoustic particle velocity and the quantity inside the brackets is unity for all values of θ and ϕ . The electromagnetic field intensity at the antenna due to a Huygen's current source is, therefore, the same as the particle velocity at the antenna due to a Huygen's velocity source for the scattering model considered. This particular rough surface model must be considered to be a "scalar model" since polarization effects are not evident.

3.7 Summary of Model Validity

It was shown that the pressure and velocity fields about several acoustic sources, are analogous to the electric and magnetic field intensities about a short current element, when certain geometric factors are considered. In some cases the analogy applies to terms of order $1/r$ and $1/r^2$; in other cases it applies only to terms of order $1/r$. The application of the acoustic-electromagnetic wave analogy, using the acoustic simulator, generally requires a directive antenna pattern and only the radiation fields are considered. In addition, it is necessary that the

acoustic fields, scattered from appropriate model targets, have most of the characteristics of electromagnetic waves scattered from terrain or from some other object. The acoustic and electromagnetic fields are compared using a simple scattering model which assumes a distribution of Huygen's sources about a plane that is passed through the irregular surface. The acoustic and electromagnetic waves give the same results for this model, which shows that the model is scalar in nature and does not account for polarization effects. No restrictions are placed on the antenna pattern or on the antenna orientation, except that the acoustic system must use an antenna pattern and orientation that are similar to those in the electromagnetic system.

The acoustic simulator, therefore, gives correct results to the extent that polarization effects can be neglected or can be considered by other means.

acoustic fields, scattered from apertured model targets, have most of the characteristics of electromagnetic waves scattered from terrain or from some other object. The acoustic and electromagnetic fields are compared using a simple scattering model which assumes a distribution of Huygen's sources about a plane that is passed through the irregular surface. The acoustic and electromagnetic waves give the same results for this model, which shows that the model is scalar in nature and does not account for polarization effects. No restrictions are placed on the antenna pattern or on the antenna orientation, except that the acoustic system must use an antenna pattern and orientation that are similar to those in the electromagnetic system. The acoustic simulator, therefore, gives correct results to the extent that polarization effects can be neglected or can be considered by other means.

CHAPTER IV

RADAR SYSTEM SCALE FACTORS

One application of the analogies between electromagnetic and acoustic waves allows a study of the scattering characteristics of a particular type of target using a model system. This is the first problem investigated with the acoustic simulator in this study. A further application involves a model of the complete radar system where circuitry such as duplexers and range gates are involved and the system performance is reproduced in detail. This type of simulation makes it possible to evaluate certain circuit design changes rapidly since full scale tests are not required.

A major characteristic of radar return from terrain is the fading due to interference of many signals of nearly the same frequency and amplitude.¹ At all but the lowest

¹There has been some discussion of the importance of the interference phenomenon in explaining the angle dependence of the backscattering radar cross section of a target, especially over sea surfaces. Katz, I. and Spetner, L. M., "Polarization and Depression Angle Dependence of Radar Terrain Return," Jour. of Res. of N. B. S., Vol. 64D, No. 5, Sept. - Oct. 1960, pp 483-86. While the angular dependence of the scattering pattern may not be classed as an interference phenomenon, the fading which occurs certainly is due to interference and the fading characteristics comprise an important part of the model study.

CHAPTER IV

RADAR SYSTEM SCALE FACTORS

One application of the analogies between electro-

magnetic and acoustic waves allows a study of the scattering

characteristics of a particular type of target using a

model system. This is the first problem investigated with

the acoustic simulator in this study. A further application

involves a model of the complete radar system where circuitry

such as duplexers and range gates are involved and the

system performance is reproduced in detail. This type of

simulation makes it possible to evaluate certain circuit

design changes rapidly since full scale tests are not re-

quired.

A major characteristic of radar return from terrain

is the fading due to interference of many signals of nearly

the same frequency and amplitude. At all but the lowest

¹There has been some discussion of the importance of the interference phenomenon in explaining the angle dependence of the backscattered radar cross section of a target, especially over sea surfaces. Katz, I. and Spetner, I. M., "Polarization and Depression Angle Dependence of Radar Terrain Return," *Journal of Res. of N. S. A.*, Vol. 5, No. 5, Sept. - Oct. 1960, pp. 487-88. While the angular dependence of the scattering pattern may not be classed as an interference phenomenon, the fading which occurs certainly is due to interference and the fading characteristics comprise an important part of the model study.

carrier frequencies the terrain acts principally as a scatterer of energy and the returned signal is therefore composed of a multitude of small signal components from the various scattering elements. The resulting fading in the received signal can be readily modeled by acoustic waves since the interference effects are common to all types of linear wave motion.

4.1 Pulsed Radar

The quantities which must be scaled when modeling a pulsed radar system are listed in Table 4-1.¹ These quantities are based on the fundamental time and distance scales which are related by the basic equations of mechanics. Such factors as the radar cross-section per unit area for the target and antenna pattern are not scaled since their directional characteristics must be the same in the real and model systems. The scale factors represent the ratio of the indicated quantity in the real system in air to the same quantity in the model system in water.

The scale factor, V , is given by

$$V = \frac{V^a}{V^w} \doteq 2 \times 10^5 \quad (4-1)$$

and is fixed by the ratio of the velocity of propagation of electromagnetic waves in air to that of acoustic waves

¹Moore, R. K., Radar Design Using Acoustical Simulation as a Tool, Univ. of New Mexico, Engr. Exp. Sta. Rpt. EE-22, April, 1959. The scale factors for pulse and frequency modulated radar were first presented in this report.

carrier frequencies the carrier wave principally as a
 scatterer of energy and the returned signal is therefore
 composed of a multitude of small signal components from
 the various scattering elements. The resulting fading in
 the received signal can be readily modeled by acoustic waves
 since the interference effects are common to all types of
 linear wave motion.

4.1 Pulsed Radar

The quantities which must be scaled when modeling a
 pulsed radar system are listed in Table 4-1.¹ These quan-
 tities are based on the fundamental time and distance scales
 which are related by the basic equations of mechanics. Both
 factors as the radar cross-section per unit area for the
 target and antenna pattern are not scaled since their di-
 rectional characteristics must be the same in the real and
 model systems. The scale factors represent the ratio of
 the indicated quantity in the real system in air to the
 same quantity in the model system in water.

The scale factor, V , is given by

$$V = \frac{V_a}{V_w} \div 2 \times 10^2 \quad (4-1)$$

and is fixed by the ratio of the velocity of propagation
 of electromagnetic waves in air to that of acoustic waves

¹Moore, R. K., Radar Design Using Statistical Simulation
 as a Tool, Univ. of New Mexico, Eng. Res. Rpt. ER-12,
 April, 1959. The scale factors for pulse and frequency mod-
 ulated radar were first presented in this report.

TABLE 4-1

SCALED PARAMETERS FOR PULSE RADAR

Parameters	Scale Factor (Ratios)
Velocity of propagation	V
Range	R
Time	T
Carrier Frequency	f_c
Wavelength	λ
Pulse Duration	d
Number of Cycles per Pulse	n
Repetition Rate	f_r
Antenna Velocity	\underline{v}
Doppler Frequency	f_D

in water. For most purposes, it is sufficiently accurate to use a value of 2×10^5 for this ratio of velocities.

The range scale factor

$$R = \frac{R^a}{R^w} \quad (4-2)$$

and the time scale factor

$$T = \frac{T^a}{T^w} \quad (4-3)$$

are related to the velocity scale by the basic equation

$$R = VT \quad (4-4)$$

If the range scale is to be adjustable, then the model system cannot operate in real time. There is a definite advantage to scaling both time and range since a realistic range scale generally results in a time scale such that pulse widths

TABLE 4-1

SCALED PARAMETERS FOR PULSE RADAR

Parameter	Scale Factor (Ratio)
Velocity of propagation	V
Range	R
Time	T
Carrier Frequency	f_c
Wavelength	λ
Pulse Duration	δ
Number of Cycles per Pulse	n
Repetition Rate	f_r
Antenna Velocity	v
Doppler Frequency	f_d

in water. For most purposes, it is sufficiently accurate to use a value of 2×10^8 for this ratio of velocities. The range scale factor

$$R = \frac{R^a}{R^w} \quad (4-2)$$

and the time scale factor

$$T = \frac{T^a}{T^w} \quad (4-3)$$

are related to the velocity scale by the basic equation

$$R = VT \quad (4-4)$$

If the range scale is to be adjustable, then the model system cannot operate in real time. There is a definite advantage to scaling both time and range since a realistic range scale generally results in a time scale such that pulse widths

are wider and repetition rates are lower in the model than in the real system. This serves to simplify the model circuitry problem.

The range scale, \mathcal{R} , is selected first, based on the physical size limitation of the acoustic tank. This in turn determines the time scale, \mathcal{T} , according to Equation 4-4. The wavelength of the carrier frequency is scaled using the range scale, if linear modeling is employed. The carrier frequency scale factor, given by

$$f_c = \frac{f^a}{f^w} \quad (4-5)$$

is related to the basic time scale by

$$f_c = \frac{1}{\mathcal{T}} \quad (4-6)$$

for linear modeling. In some cases, especially when the range is large, this form of modeling becomes impractical since an unreasonably high carrier frequency is required in the model. The alternative in this situation is to employ non-linear modeling which scales the wavelength separately from the range. This is equivalent to making

f_c a separate independent scale factor by definition, thus Equation 4-6 will be considered as determining the frequency scale factor f_c only for the special case of linear modeling. In general the factor f_c will be independently chosen to best satisfy the modeling problem.

The wavelength scale is given by

$$\lambda = \frac{\lambda^a}{\lambda^w} \quad (4-7)$$

are wider and repetition rates are lower in the model than in the real system. This serves to simplify the model circuitry problem.

The range scale, λ , is selected first, based on the

physical size limitation of the acoustic tank. This in turn determines the time scale, T , according to Equation 4-4. The wavelength of the carrier frequency is scaled using the range scale, if linear modeling is employed. The carrier frequency scale factor, given by

$$\lambda_c = \frac{f_c}{f} \quad (4-5)$$

is related to the basic time scale by

$$\lambda_c = \frac{1}{T} \quad (4-6)$$

for linear modeling. In some cases, especially when the range is large, this form of modeling becomes impractical since an unreasonably high carrier frequency is required in the model. The alternative in this situation is to employ non-linear modeling which scales the wavelength separately from the range. This is equivalent to making λ_c a separate independent scale factor by definition. Thus Equation 4-6 will be considered as determining the frequency scale factor λ_c only for the special case of linear modeling. In general the factor λ_c will be independently chosen to best satisfy the modeling problem.

The wavelength scale is given by

$$\lambda = \frac{\lambda_c}{\lambda_c} \quad (4-7)$$

which can be written as

$$\lambda = \frac{v^a f^w}{v^w f^a} = \frac{V}{f_c} \quad (4-8)$$

The pulse duration must be scaled so the pulse length in space is the same percentage of the total range in both the real and the model system. This criterion which is a geometric similitude requirement is satisfied when the pulse width is scaled the same as time so the scale factor is written as

$$d = \frac{d^a}{d^w} = J \quad (4-9)$$

The number of cycles of carrier frequency per pulse is of importance since in some cases the model may be poor because of too few carrier cycles per pulse to properly define the pulse shape. The scale factor for the number of cycles per pulse is

$$n = \frac{n^a}{n^w} \quad (4-10)$$

which can be written as

$$n = \frac{d^a f_c^a}{d^w f_c^w} = J f_c \quad (4-11)$$

The repetition rate must be scaled so the distance in space between consecutive pulses is the same percentage of the total range in both the real and model systems. This insures that the signal standing wave in space is sampled at the proper interval. The condition is satisfied when the repetition frequency is scaled as

which can be written as

$$(4-8) \quad \lambda = \frac{v_w f_w}{v_f f_c} = \frac{v_w}{v_f}$$

The pulse duration must be scaled so the pulse length in space is the same percentage of the total range in both the real and the model system. This criterion which is a geometric similitude requirement is satisfied when the pulse width is scaled the same as time so the scale factor is

written as

$$(4-9) \quad b = \frac{b_w}{b_f} = \frac{v_w}{v_f}$$

The number of cycles of carrier frequency per pulse is of importance since in some cases the model may be poor because of too few carrier cycles per pulse to properly define the pulse shape. The scale factor for the number of cycles per pulse is

$$(4-10) \quad n = \frac{n_w}{n_f}$$

which can be written as

$$(4-11) \quad n = \frac{b_w f_w}{b_f f_c} = \frac{v_w}{v_f}$$

The repetition rate must be scaled so the distance in space between consecutive pulses is the same percentage of the total range in both the real and model systems. This insures that the signal standing wave in space is sampled at the proper interval. The condition is satisfied when the repetition frequency is scaled as

$$f_R = \frac{f_R^a}{f_R^w} = \frac{1}{J} \quad (4-12)$$

The scale factor for antenna velocity must be such that the antenna moves the same distance measured in wavelengths in both the real and model system in one unit of time. This requirement establishes the proper fading rate in the model. The antenna velocity scale factor can therefore be written as

$$\underline{U} = \frac{\underline{U}^a}{\underline{U}^w} = \frac{\lambda^a/t^a}{\lambda^w/t^w} \quad (4-13)$$

which becomes

$$\underline{U} = \frac{\lambda}{J} = \frac{V}{J f_c} \quad (4-14)$$

The scale factor for the Doppler frequency is given by

$$f_D = \frac{f_D^a}{f_D^w} \quad (4-15)$$

and since the Doppler frequency is proportional to the product of the carrier frequency and the antenna velocity divided by the velocity of propagation, Equation 4-15 can be written as

$$f_D = \frac{\frac{\underline{U}^a}{V^a} f_c^a}{\frac{\underline{U}^w}{V^w} f_c^w} = \frac{1}{J} \quad (4-16)$$

The complete set of scaling relations for a pulse radar system is compiled in Table 4-2.

The scale factor for the transformation is

first the end of the scale is marked as
wherever it is found in the original
of time. This is done by
the in the original.

It is then found that

which becomes

The scale factor for the original is given by

and since the original is given as the original is the
product of the original and the original is the
divided by the original of the original is the original

be written as

The complete set of values for the original is given

system is contained in the original

TABLE 4-2

SCALING RELATIONS FOR A PULSE RADAR SYSTEM

Parameter	Scale Factor	Relation to Independent Scale Factors
Velocity of Propagation	V	V
Range	R	VJ
Time	J	R/V
Carrier Frequency	f_c	f_c
Wavelength	λ	V/f_c
Pulse Duration	d	J
Number of Cycles per Pulse	n	Jf_c
Repetition rate	f_R	$1/J$
Antenna Velocity	U	V/Jf_c
Doppler Frequency	f_D	$1/J$

As an example of the application of these scaling factors, consider a pulse radar system with the parameters given in Table 4-3. A model carrier frequency of 1 mc/sec and a model range of 1 meter are now selected to use in the acoustic system. The other scaled parameters in the model result from an application of the scaling relations shown in Table 4-2.

In this example, the model carrier frequency is selected in a range convenient for the acoustic simulator. From Equation 4-12 and Table 4-2 it can be seen that an increase in the model carrier frequency will reduce the carrier frequency scale factor f_c , which will in turn

SCALING RELATIONS FOR A PULSE RADAR SYSTEM

Parameter	Scale Factor	Relation to Independent Scale Factors
Velocity of Propagation	V	V
Range	R	V/D
Time	D	R/V
Carrier Frequency	f_c	R/V
Wavelength	λ	V/f_c
Pulse Duration	δ	D
Number of Cycles per Pulse	n	D/δ
Repetition Rate	f_r	$1/D$
Antenna Velocity	V_a	V/V_a
Doppler Frequency	f_d	V/V_a

As an example of the application of these scaling factors, consider a pulse radar system with the parameters given in Table 4-2. A model carrier frequency of 1 mc/sec and a model range of 1 meter are now selected to use in the acoustic system. The other scaled parameters in the model result from an application of the scaling relations shown in Table 4-2.

In this example, the model carrier frequency is selected in a range convenient for the acoustic transmitter. From Equation 4-12 and Table 4-2 it can be seen that an increase in the model carrier frequency will reduce the carrier frequency scale factor f_c , which will in turn

increase the number of cycles per pulse and will reduce the antenna velocity in the model. Parameters such as the pulse duration, repetition rate and Doppler frequency will remain unaffected by this change. An increase in the range in the model will reduce the range scale factor, R , which will in turn reduce the time scale factor T . This change will increase the pulse width, increase the number of cycles per pulse, reduce the repetition rate, reduce the antenna velocity and reduce the Doppler frequency. These changes are generally all desirable so it is advantageous to use the maximum permissible range in the model for many of the typical modeling problems.

TABLE 4-3
EXAMPLE OF PULSE RADAR SCALING

Parameter	Radar (Parameters Given)	Model
Carrier Frequency	10^4 mc/s	1.0 mc/s
Wavelength	3 cm	0.15 cm
Range	2000 m	1 m
Pulse width	0.1 μ s	10 μ s
Cycles per Pulse	10^3	10
Repetition rate	3000 pps	30 pps
Antenna velocity	300 m/s	15 cm/s
Doppler frequency	20 kc/s	20 cps

increase the number of cycles per pulse and will reduce the antenna velocity in the model. Parameters such as the pulse duration, repetition rate and Doppler frequency will remain unaffected by this change. An increase in the range in the model will reduce the range scale factor, R , which will in turn reduce the time scale factor T . This change will increase the pulse width, increase the number of cycles per pulse, reduce the repetition rate, reduce the antenna velocity and reduce the Doppler frequency. These changes are generally all desirable so it is advantageous to use the maximum permissible range in the model for many of the typical modeling problems.

TABLE 4-3
EXAMPLE OF PULSE RADAR SCALING

Parameter	Radar Parameters Given	Model
Carrier frequency	10^4 mc/s	1.0 mc/s
Wavelength	3 cm	0.15 cm
Range	2000 m	1 m
Pulse width	0.1 μ s	10 μ s
Cycles per pulse	10^3	10
Repetition rate	2000 pps	20 pps
Antenna velocity	300 m/s	15 cm/s
Doppler frequency	20 kc/s	20 cps

If linear modeling is used in the previous example, the following situation exists. The range must still be selected to suit the size of the acoustic tank. Therefore the range will remain 1 meter in water. This results in a range scale of

$$R = \frac{R^a}{R^w} = \frac{2000}{1} \quad (4-17)$$

The time scale is determined from

$$J = \frac{R}{V} = 0.01 \quad (4-18)$$

and the frequency scale factor is

$$f_c = \frac{1}{J} = 100 \quad (4-19)$$

In this case linear modeling will require a model frequency of

$$f^w = \frac{f^a}{f_c} = \frac{10^{10}}{10^2} = 10^8 \text{ cps} \quad (4-20)$$

which is unreasonably high for several reasons. In order to improve the situation and retain linear modeling it is required that f_c be larger, perhaps as large as 10^4 . This results in a model carrier frequency of 1 mc/s which is very reasonable. The time scale now becomes 10^{-4} which gives a range scale of

$$R = VJ = 20 \quad (4-21)$$

This would require a scaled range in the tank of 100 meters. The need for non-linear modeling for certain problems should now be evident.

If linear modeling is used in the previous example, the following situation exists. The range must still be selected to suit the size of the acoustic tank. Therefore the range will remain 1 meter in water. This results in a range scale of

$$R = \frac{R_a}{R_w} = \frac{2000}{1} \quad (4-17)$$

The time scale is determined from

$$T = \frac{T_a}{V} = 0.01 \quad (4-18)$$

and the frequency scale factor is

$$f_c = \frac{1}{T} = 100 \quad (4-19)$$

In this case linear modeling will require a model frequency of

$$f'' = \frac{f}{f_c} = \frac{10^5}{100} = 10^3 \text{ cps} \quad (4-20)$$

which is unreasonably high for several reasons. In order to improve the situation and retain linear modeling it is required that f_c be larger, perhaps as large as 10^4 . This results in a model carrier frequency of 1 mc/s which is very reasonable. The time scale now becomes 10^{-4} which gives a range scale of

$$R = VT = 20 \quad (4-21)$$

This would require a scaled range in the tank of 100 meters. The need for non-linear modeling for certain problems should now be evident.

4.2 FM Radar System

In frequency modulated radar systems the carrier frequency is swept in some manner over a portion of the frequency spectrum. The echo signals received from the target will occur at a frequency that is different from the instantaneous carrier frequency by an amount proportional to the time delay involved in making the round trip to the target (linear FM). The resulting difference frequency becomes the signal and is a measure of the range to the target. When the target is terrain, as is the case for a typical altimeter application, the signal consists of a multitude of separate signals received from the many scatterers in the illuminated region. Since the slant ranges to the different scatterers will vary, the return signal will consist of a spectrum of difference frequencies. Also if the altimeter is in motion there is a Doppler frequency shift added to each of the components of the return signal. Salient features of the signal can be scaled and modeled in order to study effects on the system operation.

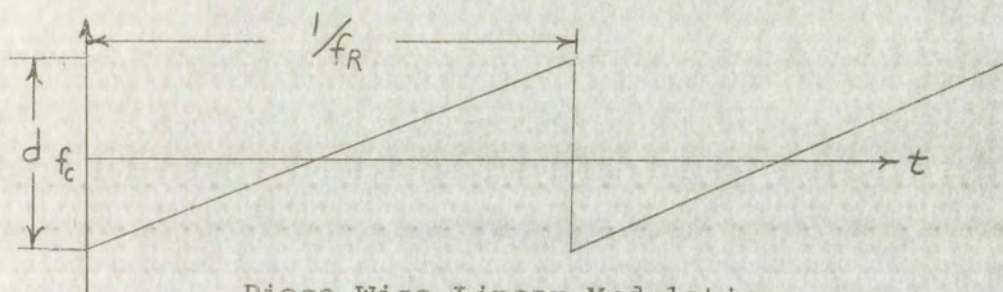
A simple piece-wise linear frequency modulation, such as that shown in Figure 4-1, is considered, although other types are frequently used.

Parameters which must be scaled in modeling a frequency modulated radar are given in Table 4-4.

In frequency modulated radar systems the carrier frequency is swept in some manner over a portion of the frequency spectrum. The echo signals received from the target will occur at a frequency that is different from the instantaneous carrier frequency by an amount proportional to the time delay involved in making the round trip to the target (linear FM). The resulting difference frequency becomes the signal and is a measure of the range to the target. When the target is terrain, as is the case for a typical altimeter application, the signal consists of a multitude of separate signals received from the many scatterers in the illuminated region. Since the slant ranges to the different scatterers will vary, the return signal will consist of a spectrum of difference frequencies. Also if the altimeter is in motion there is a Doppler frequency shift added to each of the components of the return signal. Saliient features of the signal can be scaled and modeled in order to study effects on the system operation.

A simple piece-wise linear frequency modulation, such as that shown in Figure 4-1, is considered, although other types are frequently used.

Parameters which must be scaled in modeling a frequency modulated radar are given in Table 4-1.



Piece-Wise Linear Modulation

Figure 4-1

TABLE 4-4

SCALED PARAMETERS FOR FM RADAR

Parameter	Scale Factor
Velocity of Propagation	V
Range	R
Time	J
Carrier Frequency	f_c
Wavelength	λ
Total Carrier Frequency Deviation	d
Repetition Rate	f_R
Difference Frequency	f_s
Number of Cycles of Difference Frequency per sweep	n
Antenna Velocity	\underline{V}
Doppler Frequency	f_D

Here, as in the case of pulse radar, the scale factor V is fixed by the ratio of velocities of propagation of electromagnetic waves in air and acoustic waves in water. Also, the range scale is selected to accomodate the experiment in the available acoustic tank. The time scale, J , is therefore determined by the basic relation



Figure 4-1
Pulse-Wave Linear Modulation

TABLE 4-1
SCALED PARAMETERS FOR FM RADAR

Parameter	Scale Factor
Doppler frequency	$\frac{V}{c}$
Antenna velocity	$\frac{V}{c}$
Frequency per sweep	$\frac{1}{T}$
Number of cycles of difference	$\frac{1}{T}$
Difference frequency	$\frac{1}{T}$
Repetition Rate	$\frac{1}{T}$
Total Carrier Frequency Deviation	$\frac{1}{T}$
Wavelength	λ
Carrier Frequency	f_c
Time	T
Range	R
Velocity of Propagation	V

Here, as in the case of pulse radar, the scale factor V is fixed by the ratio of velocities of propagation of electromagnetic waves in air and acoustic waves in water. Also, the range scale is selected to accommodate the experiment in the available acoustic tank. The time scale, T , is therefore determined by the basic relation

$$J = R/V \quad (4-22)$$

In certain cases it may be feasible to use linear modeling in which case the carrier frequency in the model is determined by the time scale J so that

$$f_c = \frac{1}{J} \quad (4-23)$$

The general problem, however, will require nonlinear modeling as in the pulse radar case so f_c will be determined by the ratio

$$f_c = \frac{f_c^a}{f_c^w} \quad (4-24)$$

where f_c^w is a convenient carrier frequency to use in the model. The wavelength scale is also given by the same expression as in the pulse radar case and is

$$\lambda = \frac{\lambda^a}{\lambda^w} = \frac{V}{f_c} \quad (4-25)$$

The total carrier frequency deviation, d , has dimensions of $[T]^{-1}$ and is therefore scaled as

$$d = \frac{d^a}{d^w} = \frac{1}{J} \quad (4-26)$$

The repetition rate should scale such that one cycle of the modulating frequency occupies a distance in space that is the same percentage of the range as in the real system. This requires that

$$f_R = \frac{f_R^a}{f_R^w} = \frac{1}{J} \quad (4-27)$$

(4-22)

In certain cases it may be feasible to use linear modeling in which case the carrier frequency in the model is determined by the time scale T so that

(4-23)

The general problem, however, will require nonlinear modeling as in the pulse radar case so f_c will be determined by the ratio

(4-24)

where f_c is a convenient carrier frequency to use in the model. The wavelength scale is also given by the same expression as in the pulse radar case and is

(4-25)

The total carrier frequency deviation, b , has dimensions of $[T]^{-1}$ and is therefore scaled as

(4-26)

The repetition rate should scale such that one cycle of the modulating frequency occupies a distance in space that is the same percentage of the range as in the real system. This requires that

(4-27)

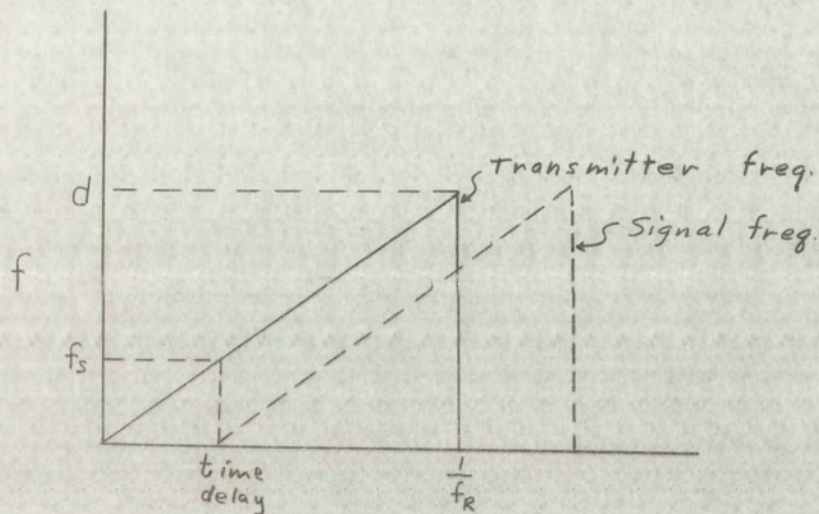
which is in agreement with the dimensions of the corresponding physical equation.

For the case of piece-wise linear modulation the difference frequency can be written as

$$f_s = \frac{f_s^a}{f_s^w} = t d f_r \quad (4-28)$$

as illustrated by the similar triangles in Figure 4-2. The scale factor for the difference frequency can therefore be written as

$$f_s = J d f_r = \frac{1}{J} \quad (4-29)$$



FM Difference Frequency

Figure 4-2

It is important in simulating a frequency modulated radar to maintain the number of cycles of the difference frequency per cycle of the modulation frequency, N , the same in the real and model systems. This requirement is satisfied when

which is in agreement with the dimensions of the corresponding

physical equation.

For the case of piece-wise linear modulation the difference

frequency can be written as

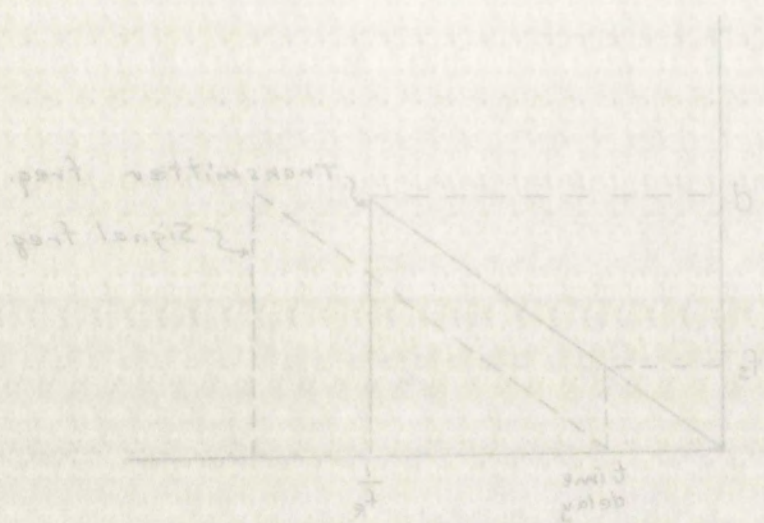
$$f_s = \frac{f_a}{f_w} = f_b f_s \quad (4-28)$$

as illustrated by the similar triangles in Figure 4-2. The

scale factor for the difference frequency can therefore be

written as

$$f_s = \frac{1}{f_w} = \frac{1}{f_b} \quad (4-29)$$



FM Difference Frequency

Figure 4-2

It is important in simulating a frequency modulated radar to maintain the number of cycles of the difference frequency per cycle of the modulation frequency, N , the same in the real and model systems. This requirement is satisfied when

$$N = \frac{f_s}{f_R} \quad (4-30)$$

in both the real and model systems since this relationship results in a scale factor

$$h = \frac{N^a}{N^w} = \frac{f_s^a / f_R^a}{f_s^w / f_R^w} = 1 \quad (4-31)$$

The antenna velocity must be scaled such that the antenna moves through a distance measured in wavelengths that is equivalent in one unit of time in both the real and model systems. The antenna velocity scale factor can be written as

$$\underline{V} = \frac{V^a}{V^w} = \frac{\lambda^a / t^a}{\lambda^w / t^w} \quad (4-32)$$

which reduces to

$$\underline{V} = \frac{V}{J f_c} \quad (4-33)$$

The Doppler frequency shift will change the difference frequency and will thus affect the range indication of the radar. It is important that the ratio of difference frequency to Doppler frequency be the same in the real and model systems in order to obtain correct results. The Doppler frequency is proportional to the product of the antenna velocity and the carrier frequency divided by the phase velocity and can be expressed as

$$f_D \approx \frac{V}{V} f_c \quad (4-34)$$

(4-30)

$$N = \frac{f_s}{f_a}$$

in both the real and model systems since this relationship results in a scale factor

(4-31)

$$N = \frac{N_w}{N_a} = \frac{f_s / f_w}{f_a / f_r} = 1$$

The antenna velocity must be scaled such that the antenna moves through a distance measured in wavelengths that is equivalent in one unit of time in both the real and model systems. The antenna velocity scale factor can be written as

(4-32)

$$V = \frac{V_w}{V_a} = \frac{\lambda_w / f_w}{\lambda_a / f_a}$$

which reduces to

(4-33)

$$V = \frac{V}{c}$$

The Doppler frequency shift will change the difference frequency and will thus affect the range indication of the radar. It is important that the ratio of difference frequency to Doppler frequency be the same in the real and model systems in order to obtain correct results. The Doppler frequency is proportional to the product of the antenna velocity and the carrier frequency divided by the phase velocity and can be expressed as

(4-34)

$$f_d \approx \frac{V}{c} f_c$$

The corresponding scale factor can therefore be written as

$$f_D = \frac{v f_c}{V} \quad (4-35)$$

which is in terms of the antenna velocity scale factor. Now substituting the scale factor for antenna velocity into this relation the result is

$$f_D = \frac{1}{J} \quad (4-36)$$

This result satisfies the requirement that the ratio of difference frequency to Doppler frequency remain constant in the real and model systems since $f_s/f_D = 1$. These results are now tabulated in Table 4-5.

4.3 Doppler Frequency Radar

A Doppler frequency radar can be used to detect relative motion along a line joining the radar and the target. There are a number of variations of this type of radar; however, only one particular kind is considered here. The transmitter operates continuously and transmits a signal toward the target. An echo signal is at the transmitter frequency if there is no relative velocity along the line joining the transmitter and receiver. When relative velocity exists, the echo is shifted in frequency by some amount due to the Doppler effect. When the echo is mixed with the transmitter frequency the beat difference frequency is directly proportional to the relative velocity between the radar and the target along the line which joins them.

The corresponding scale factor can therefore be written as

(4-35)
$$f_d = \frac{v}{c}$$

which is in terms of the antenna velocity scale factor. Now substituting the scale factor for antenna velocity into this relation the result is

(4-36)
$$f_d = \frac{1}{\gamma}$$

This result satisfies the requirement that the ratio of difference frequency to Doppler frequency remain constant in the real and model systems since $f_d = 1$. These results are now tabulated in Table 4-5.

4.5 Doppler Frequency Radar

A Doppler frequency radar can be used to detect relative motion along a line joining the radar and the target. There are a number of variations of this type of radar; however, only one particular kind is considered here. The transmitter operates continuously and transmits a signal toward the target. An echo signal is at the transmitter frequency if there is no relative velocity along the line joining the transmitter and receiver. When relative velocity exists, the echo is shifted in frequency by some amount due to the Doppler effect. When the echo is mixed with the transmitter frequency the beat difference frequency is directly proportional to the relative velocity between the radar and the target along the line which joins them.

TABLE 4-5
SCALING RELATIONS FOR AN FM RADAR SYSTEM

Parameter	Scale factor	Relation to Independent Scale Factors
Velocity of Propagation	V	V
Range	R	VJ
Time	J	R/V
Carrier Frequency	f_c	f_c
Wavelength	λ	V/f_c
Total Carrier Frequency Deviation	d	$1/J$
Repetition Rate	f_R	$1/J$
Difference Frequency	f_S	$1/J$
Number of Cycles of Difference Frequency per Sweep	n	1
Antenna Velocity	$\frac{U}{f_0}$	$V/J f_c$
Doppler Frequency	f_0	$1/J$

When the target is some irregular object such as an aircraft, the signal will fade due to echoes received from different scattering elements which are at slightly different ranges or where velocity components are slightly different. The spectrum of the returned signal gives rise to some ambiguity in the measured velocity. Model studies can show the statistics of the fluctuations of indicated velocity and provide a realistic method of evaluating indicators and read-out devices under controlled conditions.

SCALING RELATIONS FOR AN FM RADAR SYSTEM

TABLE 1-1

Parameter	Scale factor	Relation to independent scale factors
Doppler Frequency	$\propto \frac{1}{\lambda}$	$\propto \frac{1}{\lambda}$
Antenna Velocity	$\propto \frac{1}{\lambda}$	$\propto \frac{1}{\lambda}$
Frequency per Sweep	$\propto \frac{1}{\lambda}$	$\propto \frac{1}{\lambda}$
Number of Cycles of Difference	$\propto \frac{1}{\lambda}$	$\propto \frac{1}{\lambda}$
Difference Frequency	$\propto \frac{1}{\lambda}$	$\propto \frac{1}{\lambda}$
Repetition Rate	$\propto \frac{1}{\lambda}$	$\propto \frac{1}{\lambda}$
Deviation	$\propto \frac{1}{\lambda}$	$\propto \frac{1}{\lambda}$
Total Carrier Frequency	$\propto \frac{1}{\lambda}$	$\propto \frac{1}{\lambda}$
Wavelength	$\propto \frac{1}{\lambda}$	$\propto \frac{1}{\lambda}$
Carrier Frequency	$\propto \frac{1}{\lambda}$	$\propto \frac{1}{\lambda}$
Time	$\propto \frac{1}{\lambda}$	$\propto \frac{1}{\lambda}$
Range	$\propto \frac{1}{\lambda}$	$\propto \frac{1}{\lambda}$
Velocity of Propagation	$\propto \frac{1}{\lambda}$	$\propto \frac{1}{\lambda}$

read-out devices under controlled conditions and provide a realistic method of evaluating indicators and the statistics of the fluctuations of indicated velocity amplitude in the measured velocity. Model studies can show the spectrum of the returned signal gives rise to some ranges or where velocity components are slightly different, different scattering elements which are at slightly different aircraft, the signal will fade due to echoes received from When the target is some irregular object such as an

The parameters to be scaled in modeling this radar are the same as for pulsed radar with a few omissions. It is assumed in this case that the radar is fixed and the target is in motion.

TABLE 4-6

SCALED PARAMETERS FOR A DOPPLER RADAR

Parameter	Scale Factor (Ratios)
Velocity of Propagation	V
Range	R
Time	T
Carrier Frequency	f_c
Wavelength	λ
Target Velocity	U
Doppler Frequency	f_D

The velocity scale factor is again fixed by the properties of the media in which the two wave phenomena propagate. Also, the range scale is selected to suit the physical dimensions of the model facility. The basic relations which are repeated for convenience are

$$V = 2 \times 10^5 \quad (4-37)$$

and

$$T = R/V \quad (4-38)$$

The parameters to be scaled in modeling this radar are the same as for pulsed radar with a few omissions. It is assumed in this case that the radar is fixed and the target is in motion.

TABLE 4-6

SCALED PARAMETERS FOR A DOPPLER RADAR

Parameter Scale factor (Ratio)

Velocity of Propagation	V
Range	R
Time	t
Carrier Frequency	f_c
Wavelength	λ
Target Velocity	V_t
Doppler Frequency	f_d

The velocity scale factor is again fixed by the properties of the media in which the two wave phenomena propagate. Also, the range scale is selected to suit the physical dimensions of the model facility. The basic relations which are repeated for convenience are

(4-57)

$$V = 3 \times 10^8$$

and

(4-58)

$$f = \frac{V}{\lambda}$$

As in prior cases the carrier frequency can be scaled as $1/J$ if linear modeling is to be employed, or it can be scaled independently if the linear model results in an unrealistic value for the model carrier frequency. In either case the wavelength scale factor is

$$\lambda = V/f_c \quad (4-39)$$

which reduces to $\lambda = R$ for linear modeling.

The target velocity must scale in such a manner that the target moves through the distance equivalent to one wavelength in a corresponding amount of time in both the real and the model system. The scale factor for velocity can therefore be written as

$$\underline{V} = \frac{V^a}{\underline{V}^w} = \frac{V}{J f_c} \quad (4-40)$$

which is the same as for the case of pulse radar. The Doppler frequency also scales the same as in the previous model so the scale factor is

$$f_D = \frac{1}{J} \quad (4-41)$$

The complete set of scaling relations for this Doppler radar model are compiled in Table 4-7.

4.4 Forward Scatter Model

Communication links using forward scattering from inhomogeneities in the atmosphere are currently in use. Scattering takes place from the random distribution of "blobs" where the index of refraction is slightly different from

As in prior cases the carrier frequency can be scaled as $\lambda \propto 1/\lambda$ if linear modeling is to be employed, or it can be scaled independently if the linear model results in an unrealistic value for the model carrier frequency. In either case the wavelength scale factor is

$$\lambda = \lambda_0 / \lambda_r \quad (4-39)$$

which reduces to $\lambda = \lambda_0$ for linear modeling. The target velocity must scale in such a manner that the target moves through the distance equivalent to one wavelength in a corresponding amount of time in both the real and the model system. The scale factor for velocity can therefore be written as

$$V = \frac{V_r}{V_0} = \frac{V}{V_0} \quad (4-40)$$

which is the same as for the case of pulse radar. The Doppler frequency also scales the same as in the previous model so the scale factor is

$$f_D = f_{D_0} / f_{D_r} \quad (4-41)$$

The complete set of scaling relations for this Doppler radar model are compiled in Table 4-7.

4.4. Forward Scatter Model

Communication links using forward scattering from inhomogeneities in the atmosphere are currently in use. Scattering takes place from the random distribution of "blobs" where the index of refraction is slightly different from

TABLE 4-7
SCALING RELATIONS FOR A DOPPLER RADAR SYSTEM

Parameter	Scale Factor	Scale Factor in Terms of Independent Scale Factors
Velocity of Propagation	V	V
Range	R	$V\tau$
Time	τ	R/V
Carrier Frequency	f_c	f_c
Wavelength	λ	V/f_c
Target Velocity	V	V/f_c
Doppler Frequency	f_D	$1/\tau$

that in the surrounding medium. The scattering tends to be more directive in the forward direction as the blob size increases with respect to the wavelength. A great deal of theoretical and experimental work has been directed in this area.^{1,2,3} The major interest in this area concerns the propagation of electromagnetic waves in an inhomogeneous

¹Wheelon, A.D., "Radio-Wave Scattering by Tropospheric Irregularities," Jour. of Res. of N.B.S., Vol. 63D, No. 2, Sept-Oct. 1959, pp 205-33. This is an excellent review article on the subject of tropospheric scattering and contains an additional 81 references.

²Chernov, L.A., "Wave Propagation in a Turbulent Medium," McGraw-Hill Book Co., New York, 1960. (Russian Translation).

³Tatarski, V.I., "Wave Propagation in a Turbulent Medium," McGraw-Hill Book Co., New York, 1961. (Russian Translation).

TABLE 2-7

SCALING RELATIONS FOR A COPIER RADAR SYSTEM

Parameter	Scale Factor	Scale Factor in Terms of Independent Scale Factors
Doppler Frequency	V/λ_0	V/λ_0
Target Velocity	V/λ_0	V/λ_0
Wavelength	λ_0	λ_0
Carrier Frequency	V/λ_0	V/λ_0
Time	V/λ_0	V/λ_0
Range	V/λ_0	V/λ_0
Velocity of Propagation	V/λ_0	V/λ_0

propagation of electromagnetic waves in an inhomogeneous area.^{1,2,3} The major interest in this area concerns the theoretical and experimental work has been directed in this increases with respect to the wavelength. A great deal of be more directive in the forward direction as the blob size that in the surrounding medium. The scattering tends to

¹Wheeler, A.P., "Radio-Wave Scattering by Tropospheric Irregularities," *Journal of Res. of N.B.S.*, Vol. 57D, No. 2, Sept-Oct. 1953, pp. 205-21. This is an excellent review article on the subject of tropospheric scattering and contains an additional 81 references.

²Chernov, L.A., "Wave Propagation in a Turbulent Medium," McGraw-Hill Book Co., New York, 1960. (Russian Translation)

³Tatarski, V.I., "Wave Propagation in a Turbulent Medium," McGraw-Hill Book Co., New York, 1961. (Russian Translation)

medium. The basic problem, however, is generally based on the use of the scalar wave equation, as in the case of acoustics, and appropriate modifications are then introduced to account for polarization.¹

It is felt that a considerable amount of experimental work can be performed in the area of forward scattering in an inhomogeneous medium using high frequency acoustic waves in water. Although no serious experimental work on this subject was performed in this study, an investigation of the propagation of short sonic pulses through a column of air bubbles in water indicated that the equipment is ideally suited for this type of work.

A full scale experiment in this area would make use of multiple receivers in order to record signals simultaneously over a region in the tank. This would allow various autocorrelations, crosscorrelations, and time correlations to be obtained from the received signals. Investigations of this type hold promise of describing the nature of the inhomogeneities from an analysis of the signal correlation functions.

There are a variety of methods of introducing the irregularities into the propagation path. A simple procedure already mentioned involves use of a column of air bubbles in water to scatter the sonic waves. Turbulence in the atmosphere could perhaps be better represented by a

¹This approach is taken by Chernov, op. cit.

medium. The basic problem, however, is generally based on the use of the scalar wave equation, as in the case of acoustics, and appropriate modifications are then introduced to account for polarization.

It is felt that a considerable amount of experimental work can be performed in the area of forward scattering in an inhomogeneous medium using high frequency acoustic waves in water. Although no serious experimental work on this subject was performed in this study, an investigation of the propagation of short sonic pulses through a column of air bubbles in water indicated that the equipment is ideally suited for this type of work.

A full scale experiment in this area would make use of multiple receivers in order to record signals simultaneously over a region in the tank. This would allow various autocorrelations, crosscorrelations, and time correlations to be obtained from the received signals. Investigations of this type hold promise of describing the nature of the inhomogeneities from an analysis of the signal correlation functions.

There are a variety of methods of introducing the inhomogeneities into the propagation path. A simple procedure already mentioned involves use of a column of air bubbles in water to scatter the sonic waves. Turbulence in the atmosphere could perhaps be better represented by a

¹This approach is taken by Caernov, op. cit.

distribution of heat sources on the bottom of the tank. The rising columns of heated water will provide an inhomogeneous medium with many of the characteristics found in the atmosphere. Stratified layers can easily be obtained by using thin mylar film in the tank to separate the different temperature or turbulent conditions. The thin film is essentially transparent to the sonic waves.

distribution of heat sources on the bottom of the tank.
The rising column of heated water will provide an
inhomogeneous medium with many of the characteristics
found in the atmosphere. Stratified layers can easily
be obtained by using thin Mylar film in the tank to
separate the different temperature or turbulent conditions.
The thin film is essentially transparent to the sonic waves.

CHAPTER V

THE ACOUSTIC SIMULATOR

The acoustic simulator consists of a complete radar system using acoustic waves in a large tank of water to simulate electromagnetic waves in air. The simulator is designed to model several types of radar equipment such as pulsed and frequency modulated altimeters, Doppler frequency navigators and proximity fuse radars. It is only necessary to substitute certain of the equipment components when changing from one type of operation to another. In many cases where signal statistics from a particular type of target are required the pulsed radar can be used to obtain the information which is then interpreted in terms of the appropriate modulation scheme.

Certain of the equipment items are common to all of the forms of the acoustic simulator. These include components such as the piezoelectric transducers and pattern-forming devices, the antenna motion mechanism, amplifiers, and, of course, the water tank. The simulator is composed of commercially available equipment except for such special purpose devices as the duplexer which allows a single transducer to be used for both transmitting and receiving signals.

CHAPTER V

THE ACOUSTIC SIMULATOR

The acoustic simulator consists of a complete radar

system using acoustic waves in a large tank of water to

simulate electromagnetic waves in air. The simulator is

designed to model several types of radar equipment such

as pulsed and frequency modulated simulators, Doppler

frequency navigators and proximity fuse radars. It is only

necessary to substitute certain of the equipment components

when changing from one type of operation to another. In

many cases where signal statistics from a particular type

of target are required the pulsed radar can be used to obtain

the information which is then interpreted in terms of the

appropriate modulation scheme.

Certain of the equipment items are common to all of

the forms of the acoustic simulator. These include com-

ponents such as the piezoelectric transducers and pattern-

forming devices, the antenna motion mechanism, amplifiers

and, of course, the water tank. The simulator is composed

of commercially available equipment except for such special

purpose devices as the duplexer which allows a single

transducer to be used for both transmitting and receiving

signals.

Specific details are given for the various radar systems that have been modeled. In addition, problems associated with reverberation in the water tank and methods of obtaining different antenna patterns are discussed. The descriptions of experimental procedures using the photographic data recording process are generally associated with investigations of scattering from rough surfaces. In this case the acoustic simulator is used as a research tool. Chapter VII gives an illustration of the use of the acoustic simulator as an analog computer for system design.

5.1 Pulsed Radar Simulator

A block diagram for the pulsed radar simulator is shown in Figure 5-1. The transmitter is a variable frequency, pulse modulated radio frequency oscillator capable of delivering 300 volts peak-to-peak value to a 93 ohm load.¹ The push-pull oscillator circuit provides a very stable pulse output with a minimum of phase and frequency distortion. Because consecutive pulses are phase coherent, multiple exposure photographs can be made of the transmitted pulse without noticeable blurring of the carrier frequency cycles in the pulse. This stability makes it possible to detect very low Doppler frequencies in an echo signal. The pulsed oscillator is shown in Figure 5-2.

¹The pulsed oscillator is a Model PG-650, manufactured by the Arenberg Ultrasonic Laboratory, Inc., Jamaica Plain, Mass.

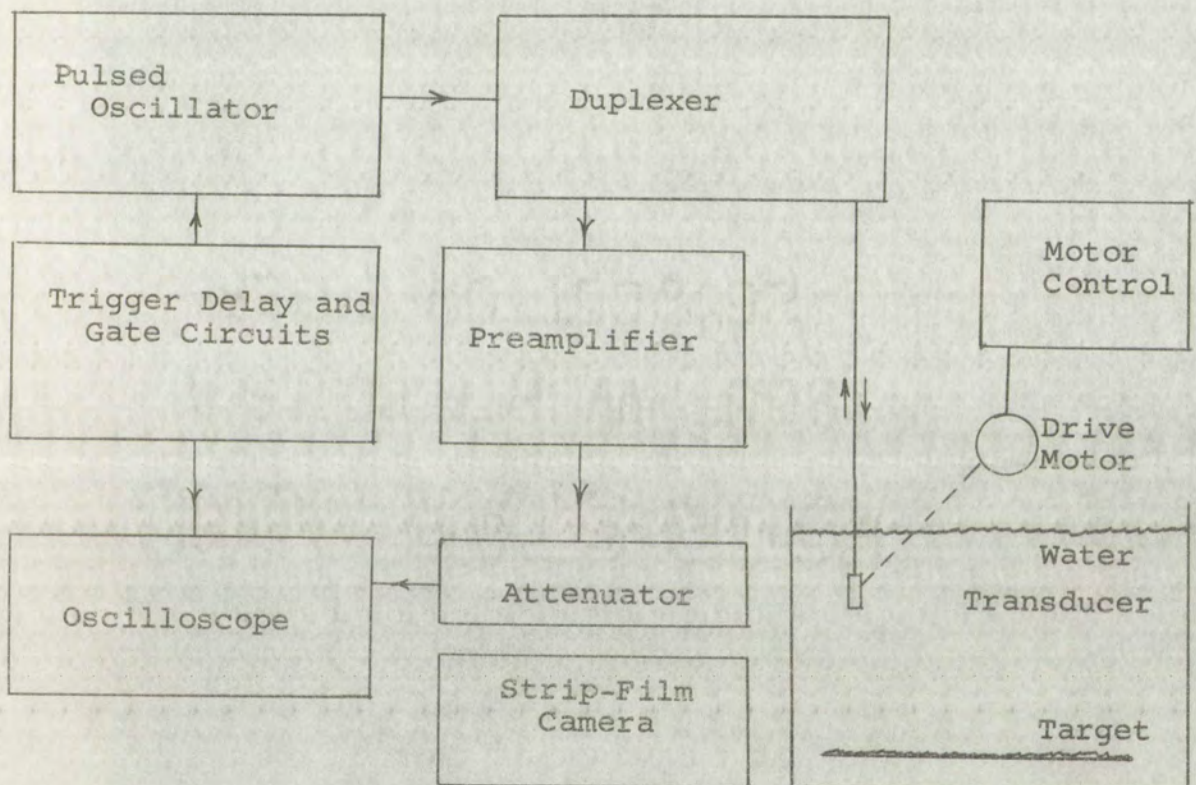
Specific details are given for the various radar systems that have been modeled. In addition, problems associated with reverberation in the water tank and methods of obtaining different antenna patterns are discussed. The descriptions of experimental procedures using the photographic data recording process are generally associated with investigations of scattering from rough surfaces. In this case the acoustic simulator is used as a research tool. Chapter VII gives an illustration of the use of the acoustic simulator as an analog computer for system design.

5.1 Pulsed Radar Simulator

A block diagram for the pulsed radar simulator is shown in Figure 5-1. The transmitter is a variable frequency, pulse modulated radio frequency oscillator capable of delivering 500 volts peak-to-peak value to a 50 ohm load.¹ The push-pull oscillator circuit provides a very stable pulse output with a minimum of phase and frequency distortion. Because consecutive pulses are phase coherent, multiple exposure photographs can be made of the transmitted pulse without noticeable blurring of the carrier frequency cycles in the pulse. This stability makes it possible to detect very low Doppler frequencies in an echo signal. The pulsed oscillator is shown in Figure 5-2.

¹The pulsed oscillator is a Model PG-650, manufactured by the Ardenberg Ultrasonic Laboratory, Inc., Jamaica Plain, Mass.

The pulsed oscillator will deliver output pulses that vary in width from 2 to 100 μ s over a frequency range from 0.5 to 5 mc/sec, with the exception of the low-frequency narrow-pulse combination where about 1-1/2 cycles is the minimum number of cycles per pulse. The minimum usable pulse width is determined by the bandwidth of the transducer in most cases.



Pulsed Radar Acoustic Simulator Block Diagram

Figure 5-1

The oscillator will operate from an internal trigger over a frequency range of 50 to 2,500 cps with provisions for synchronizing with the power line frequency; or external

The pulsed oscillator will deliver output pulses that vary in width from 2 to 100 μ s over a frequency range from 0.5 to 5 mc/sec, with the exception of the low-frequency narrow-pulse combination where about 1-1/2 cycles is the minimum number of cycles per pulse. The minimum usable pulse width is determined by the bandwidth of the transducer in most cases.



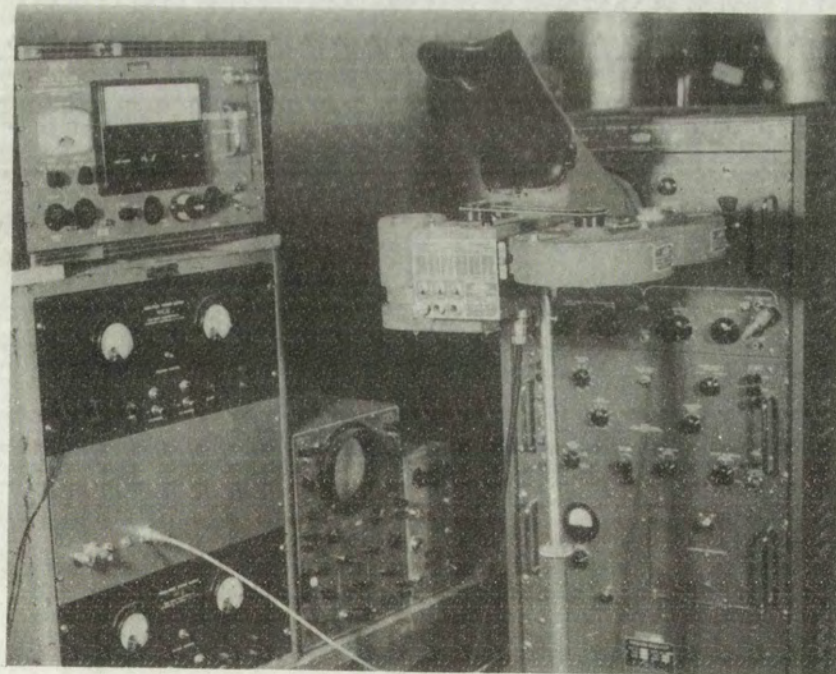
Pulsed Radar Acoustic Transducer Block Diagram

Figure 5-1

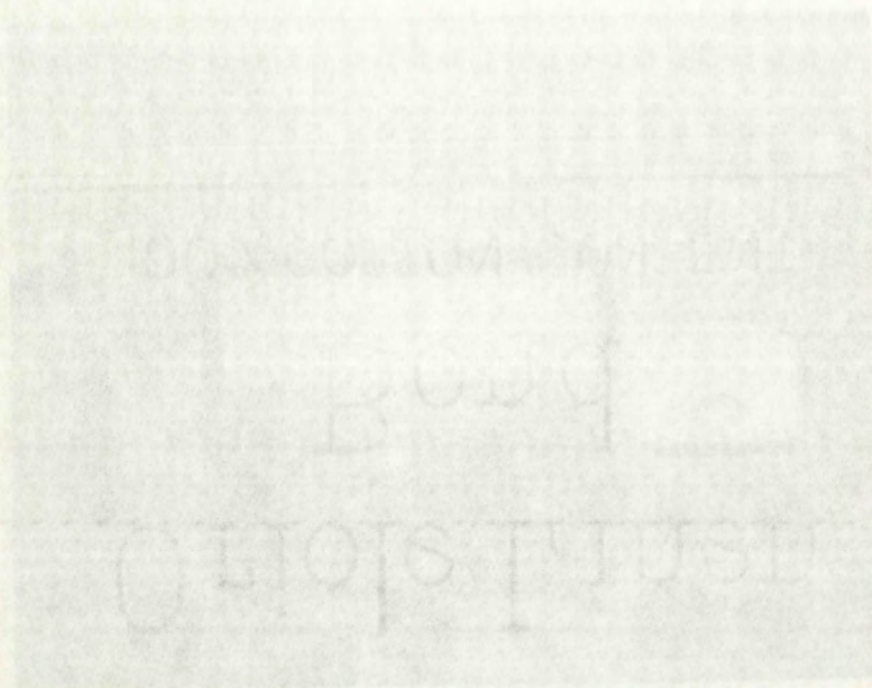
The oscillator will operate from an internal trigger over a frequency range of 50 to 2,500 cps with provisions for synchronizing with the power line frequency or external



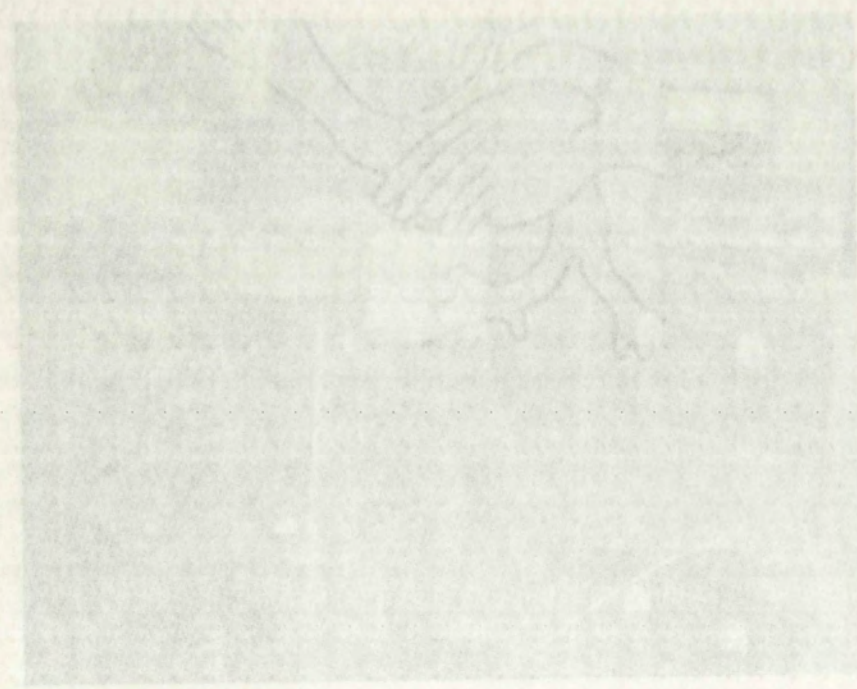
Pulsed Oscillator
Fig. 5-2



Acoustic Simulator Equipment Setup
Fig. 5-3



Trilobite Oscillator
Fig. 5-2



Acoustic Stimulator Equipment Setup
Fig. 5-3

triggering can be used. By synchronizing with the power line frequency, the disturbing effects of stray field pickup are eliminated from the system. The stray field pickup is troublesome only in cases where maximum system gain is required. An external trigger source can be used to reduce the repetition rate to zero. Also, trigger output with a variable time delay is available for synchronizing an oscilloscope with the pulsed oscillator.

A ladder type attenuator with a 41 db range in steps of $\frac{1}{2}$ db is used for purposes of calibration. The attenuator matches the 93 ohm coaxial cable that is used throughout the system. The high impedance system is desirable because the ceramic transducers are "voltage actuated" devices and it is necessary to operate at a relatively high voltage level.

The transmit-receive (TR) circuit or duplexer is used to isolate the transmitter from the receiver during the transmitting period and to direct the received signal into the receiver preamplifier. The duplexer consists of a transformer connected in the form of a bridge circuit as shown in Figure 5-4.

The transformer has three windings on a 2 inch diameter ferrite core. The primary winding consists of 40 turns of number 28 enameled, stranded, cotton covered wire close wound on one side of the core. The secondary consists of two 40-turn coils of the same size wire wound with the two coils together to improve the balance. The dummy load consists of a shielded, adjustable RC combination to match the

triggering can be used, by synchronizing with the power

line frequency, the disturbing effects of stray fields

pickup are eliminated from the system. The stray field

pickup is troublesome only in cases where maximum system

gain is required. An external trigger source can be used

to reduce the repetition rate to zero. Also, trigger output

with a variable time delay is available for synchronizing

an oscilloscope with the pulsed oscillator.

A ladder-type attenuator with a 51 db range in steps

of $\frac{1}{2}$ db is used for purposes of calibration. The attenuator

matches the 95 ohm coaxial cable that is used throughout

the system. The high impedance system is desirable because

the ceramic transducers are "voltage activated" devices and

it is necessary to operate at a relatively high voltage level.

The transmit-receive (TR) circuit or duplexer is used

to isolate the transmitter from the receiver during the

transmitting period and to direct the received signal into

the receiver preamplifier. The duplexer consists of a

transformer connected in the form of a bridge circuit as

shown in Figure 5-4.

The transformer has three windings on a 2 inch diameter

ferrite core. The primary winding consists of 40 turns of

number 28 enameled, stranded, cotton covered wire close

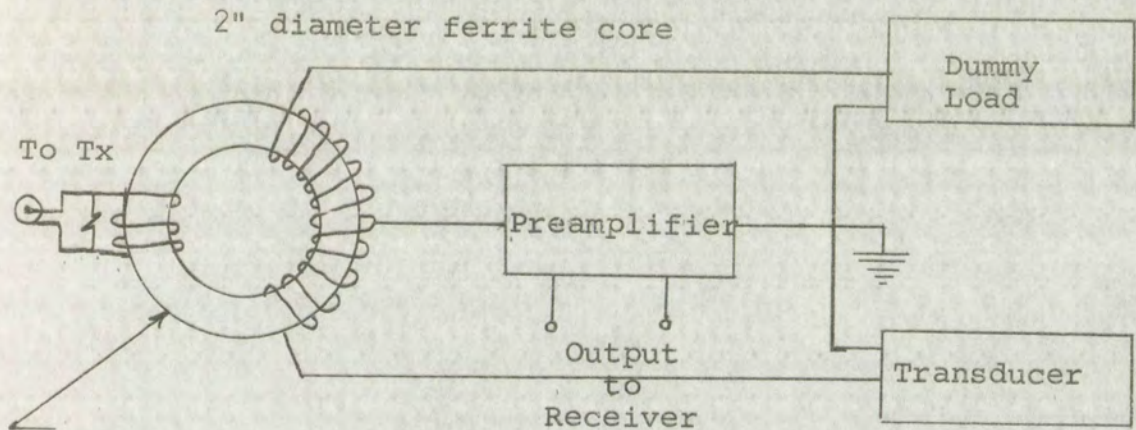
wound on one side of the core. The secondary consists of

two 40-turn coils of the same size wire wound with the

two coils together to improve the balance. The dummy load con-

sists of a shielded, adjustable, RC combination to match the

impedance of the transducer. The transducer and dummy load are connected to the transformer through equal lengths of coaxial cable to improve the balance of the bridge circuit.



Duplexer

Figure 5-4

When a high voltage is impressed on the primary winding of the transformer equal voltages appear across the transducer and the dummy load. The signal on the input of the preamplifier is caused by unbalance in the bridge circuit. The output signal level (while the transmitter is operating) is about 60 db below the source level when the bridge is properly balanced. This amount of isolation is adequate for low levels of transmitted signal. The transducer is a nonlinear capacitor which will cause a certain amount of unbalance in the bridge circuit. Better balance can be realized using an identical transducer as a dummy

impedance of the transducer. The transducer and dummy load are connected to the transformer through equal lengths of coaxial cable to improve the balance of the bridge circuit.

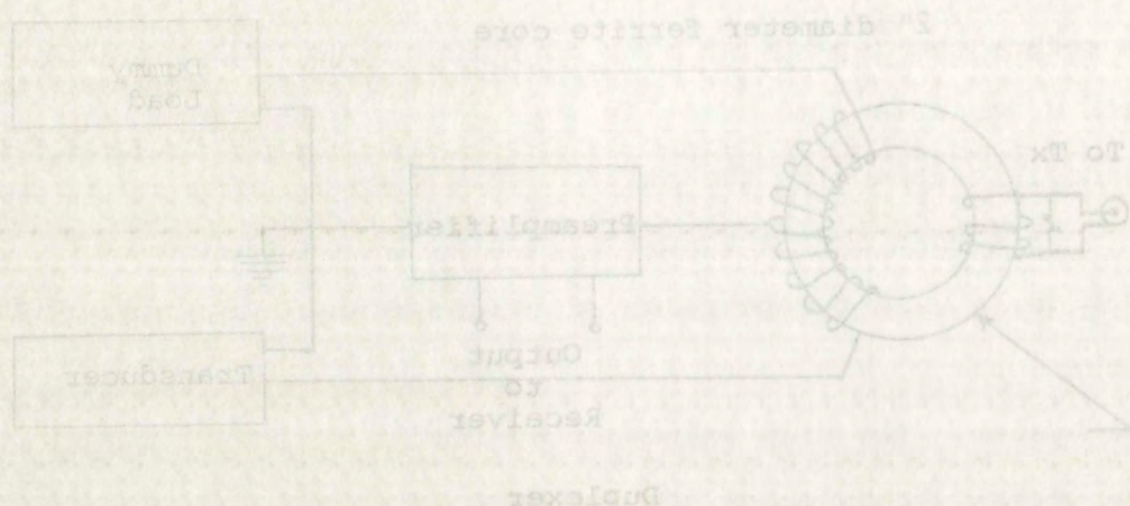


Figure 2-4

When a high voltage is impressed on the primary winding of the transformer equal voltages appear across the transducer and the dummy load. The signal on the input of the pre-amplifier is caused by unbalance in the bridge circuit. The output signal level (while the transmitter is operating) is about 60 db below the source level when the bridge is properly balanced. This amount of isolation is adequate for low levels of transmitted signal. The transducer is a nonlinear capacitor which will cause a certain amount of unbalance in the bridge circuit. Better balance can be realized using an identical transducer as a dummy

load in the circuit. The received signal which is generated in the transducer is applied to the preamplifier terminals with about 6 db loss.

Pulsed radar normally has a very low duty cycle. In the acoustic simulator which is shown in Figure 5-3, it is desirable to keep the oscilloscope blanked except when a received pulse is present. In certain situations it is desirable to photograph an entire received pulse, in which case a triggered sweep is used on the oscilloscope. In other cases it is desired to photograph only a short sample at a particular delay time in the received pulse. For this purpose a gating circuit is used, which blanks the oscilloscope except during the desired sampling period.

A triggered oscilloscope and 35 mm "strip film" camera are used for recording the data when theoretical experiments are being performed. The return signals are photographed in two different ways depending upon what information is desired. The first method of recording data is to photograph individual return pulses on a pulse-by-pulse basis. The camera is mounted so the film moves continuously in the vertical direction. The film speed is then adjusted so individual return pulses are separated by an adequate distance on the film. The time base on the film is provided by the sweep duration on the oscilloscope and the separation between consecutive pulses is provided by the film velocity. This method of recording data is illustrated in Figure 5-5

load in the circuit. The received signal which is generated

in the transducer is applied to the preamplifier terminals

with about 6 db loss.

Pulsed radar normally has a very low duty cycle. In

the acoustic stimulator which is shown in Figure 2-3, it is

desirable to keep the oscilloscope blanked except when a

received pulse is present. In certain situations it is

desirable to photograph an entire received pulse, in which

case a triggered sweep is used on the oscilloscope. In

other cases it is desired to photograph only a short

sample at a particular delay time in the received pulse.

For this purpose a gating circuit is used, which blanks

the oscilloscope except during the desired sampling period.

A triggered oscilloscope and 35 mm "strip film" camera

are used for recording the data when theoretical experiments

are being performed. The return signals are photographed

in two different ways depending upon what information is

desired. The first method of recording data is to photo-

graph individual return pulses on a pulse-by-pulse basis.

The camera is mounted so the film moves vertically in

the vertical direction. The film speed is then adjusted

so individual return pulses are separated by an adequate

distance on the film. The time base on the film is provided

by the sweep duration on the oscilloscope and the separation

between consecutive pulses is provided by the film velocity.

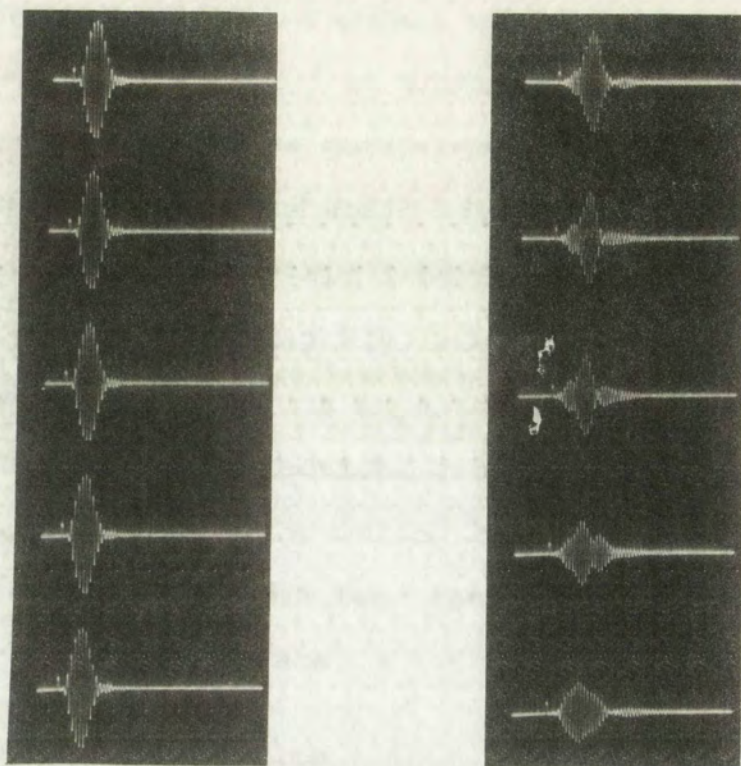
This method of recording data is illustrated in Figure 2-3.

and requires a relatively large amount of film. Approximately 2,500 return pulses can be recorded on 100 feet of film. This corresponds to three ordinary data runs for most of the experiments performed. This method of recording data is used when it is required to measure the amplitude of the return pulse at a number of different time delays in the pulse or when the statistics of the delay time to the leading edge of the pulse are being studied.

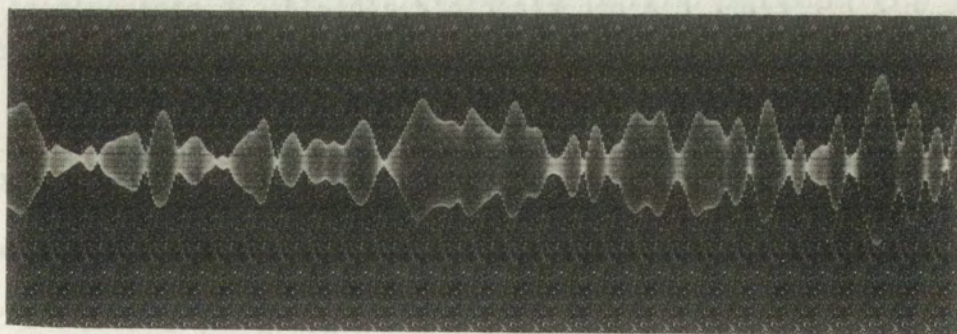
The second method of recording data makes use of a gating circuit to blank out the trace except for a short interval of time when the sample is taken. When adjusting the equipment to take data in this manner, the gate width and position are adjusted using the triggered sweep. After making this adjustment the sweep time is increased so the signal appears to converge to a single vertical line on the oscilloscope. The camera is now positioned so the motion of the film in the horizontal direction provides the separation between consecutive received pulses. No other time base is present in this case since only one point in each return pulse is recorded. This method of taking data, illustrated in Figure 5.6, requires a very slow film speed since the film needs to move only far enough between pulses to avoid overlap of the parallel signal lines. An ordinary data run containing 900 points can be recorded on about three feet of film by this method. Measuring the signal amplitudes is considerably faster with this second method of recording data.

and requires a relatively large amount of film. The first method of recording data is to use a camera to record the return pulses on a film. This corresponds to the method of recording data on a film. The second method of recording data is to use a camera to record the return pulses on a film. This corresponds to the method of recording data on a film. The third method of recording data is to use a camera to record the return pulses on a film. This corresponds to the method of recording data on a film.

The second method of recording data is to use a camera to record the return pulses on a film. This corresponds to the method of recording data on a film. The third method of recording data is to use a camera to record the return pulses on a film. This corresponds to the method of recording data on a film. The fourth method of recording data is to use a camera to record the return pulses on a film. This corresponds to the method of recording data on a film. The fifth method of recording data is to use a camera to record the return pulses on a film. This corresponds to the method of recording data on a film. The sixth method of recording data is to use a camera to record the return pulses on a film. This corresponds to the method of recording data on a film. The seventh method of recording data is to use a camera to record the return pulses on a film. This corresponds to the method of recording data on a film. The eighth method of recording data is to use a camera to record the return pulses on a film. This corresponds to the method of recording data on a film. The ninth method of recording data is to use a camera to record the return pulses on a film. This corresponds to the method of recording data on a film. The tenth method of recording data is to use a camera to record the return pulses on a film. This corresponds to the method of recording data on a film.



Sample Film Strip Showing Successive Pulses
Fig. 5-5



Sample Film Strip Showing Fading Record
Fig. 5-6

The acoustic experiments have been performed in a water tank 2' x 5' x 20' as shown in Figure 2-4. Many experiments can be performed satisfactorily in a much smaller tank. The acoustic waves are almost completely reflected at the water-air interface and the reflection coefficient is only slightly less than unity at the tank wall. When performing an experiment using relatively short pulses, the reflections from the various surfaces are easily eliminated by making the distance from the transducer to the target less than the distance from the transducer to the surface.

2.2 Doppler Radar Device

The Doppler frequency effects are present in all radar return signals where relative motion exists between the radar and the target. The device described here is called a Doppler frequency radar because this phenomenon is used to detect the relative motion between the radar and the target and does not supply range information. The simulator consists of an unmodulated oscillator power amplifier, duplexer, transducer, preamplifier and indicating device. The block diagram is shown in Figure 2-5.

The duplexer serves to isolate the receiver from the transmitter and to direct any signals into the receiver. A balanced bridge network of the same type as used in the

pulsed radar system is adequate. It is desirable to use a duplicate transducer as a dummy load on the bridge circuit in order to improve the balance. About 60 db isolation can be obtained with the bridge circuit between the transmitter and receiver. This is adequate for operation at low signal levels; however, more isolation is desirable when large transmitter voltages are employed.

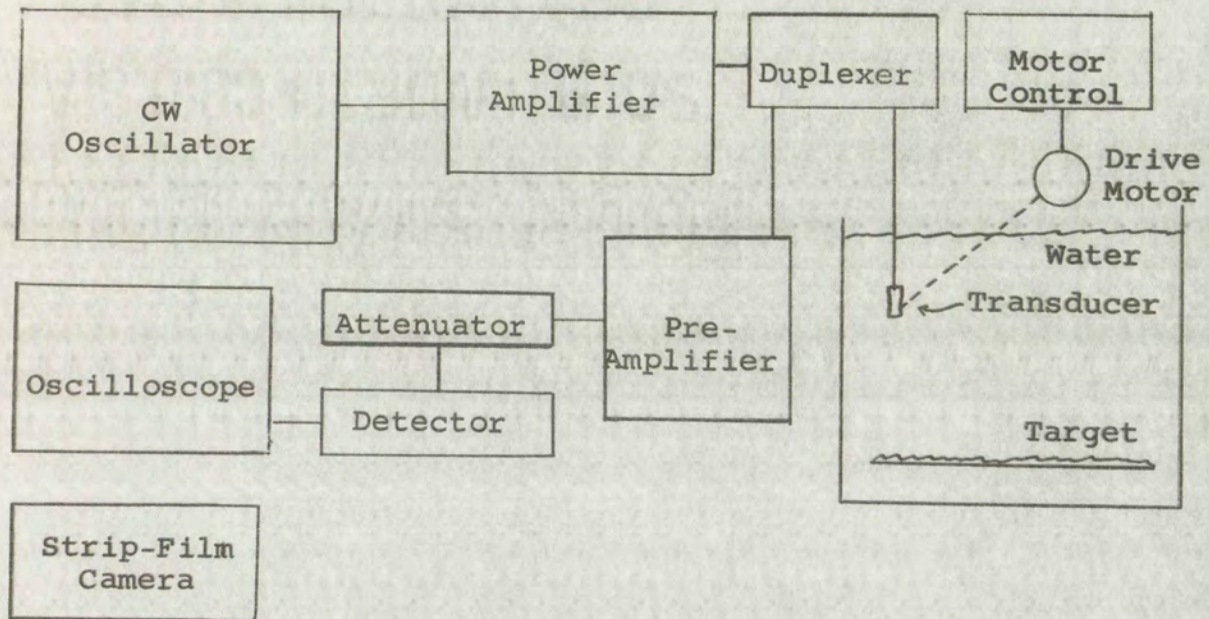
A small component of the transmitter signal comes through the duplexer and is amplified along with the echo signal. When the echo signal is from a stationary target it will be at the same frequency as the carrier frequency and no output will be obtained from the detector. When the target has a component of velocity along the line joining it to the radar, the echo signal will shift in frequency due to the Doppler effect. The resulting Doppler frequency shift will appear as an output signal through the low pass filter in the detector.

When the target returns a specular signal the Doppler shift is a single frequency and the velocity component is directly proportional to the Doppler frequency. When the target is irregular in shape, so the echo is composed of a number of separate components, the Doppler shift exists over a range of frequencies. In this case the velocity component is proportional to some average frequency in the spectrum. The proper method of determining this average has been investigated theoretically and can be studied experimentally using the simulator.



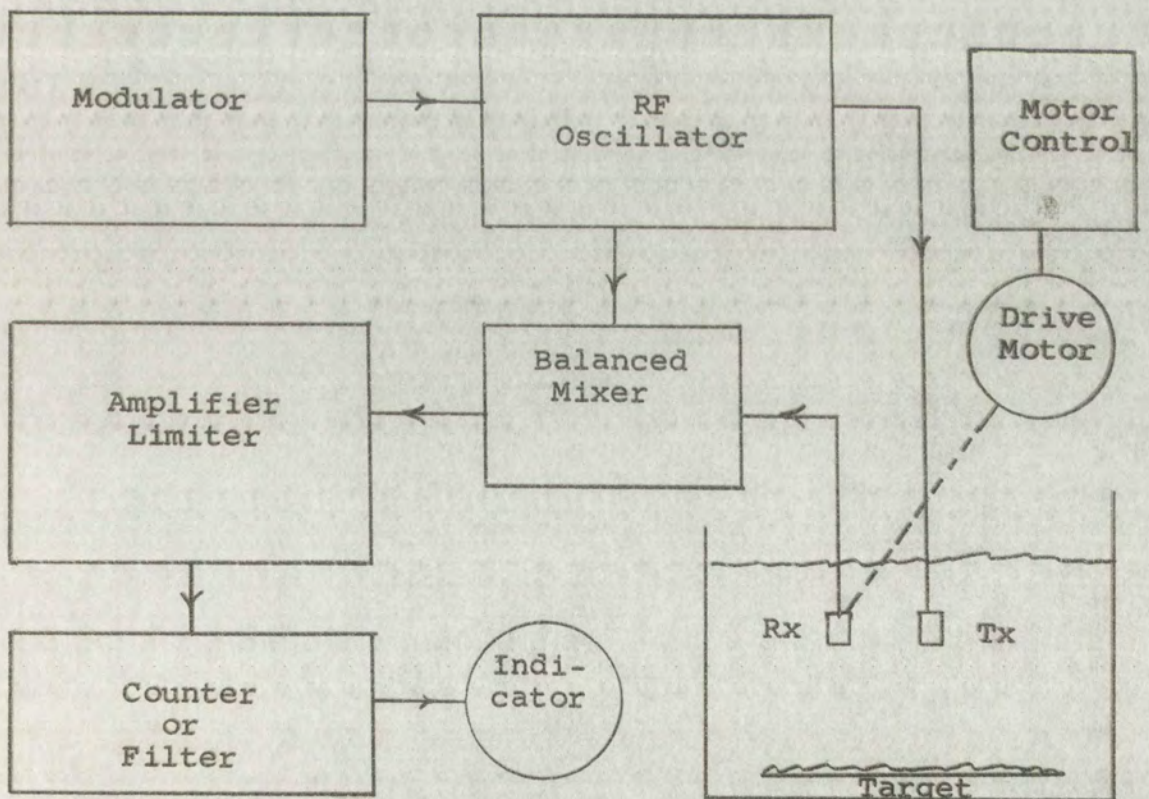
1955 JUL 15

...a number of ...
...in ...
...can be ...
...miller and ...
...low signal ...
...when large ...
...A ...
...through the ...
...slightly ...
...it will ...
...and no ...
...the carrier has ...
...joining is ...
...frequency ...
...Gosling ...
...through ...
...When the ...
...shift is ...
...is directly ...
...the carrier is ...
...of a number ...
...over a ...
...component is ...
...the spectrum ...
...has been ...
...experimentally ...



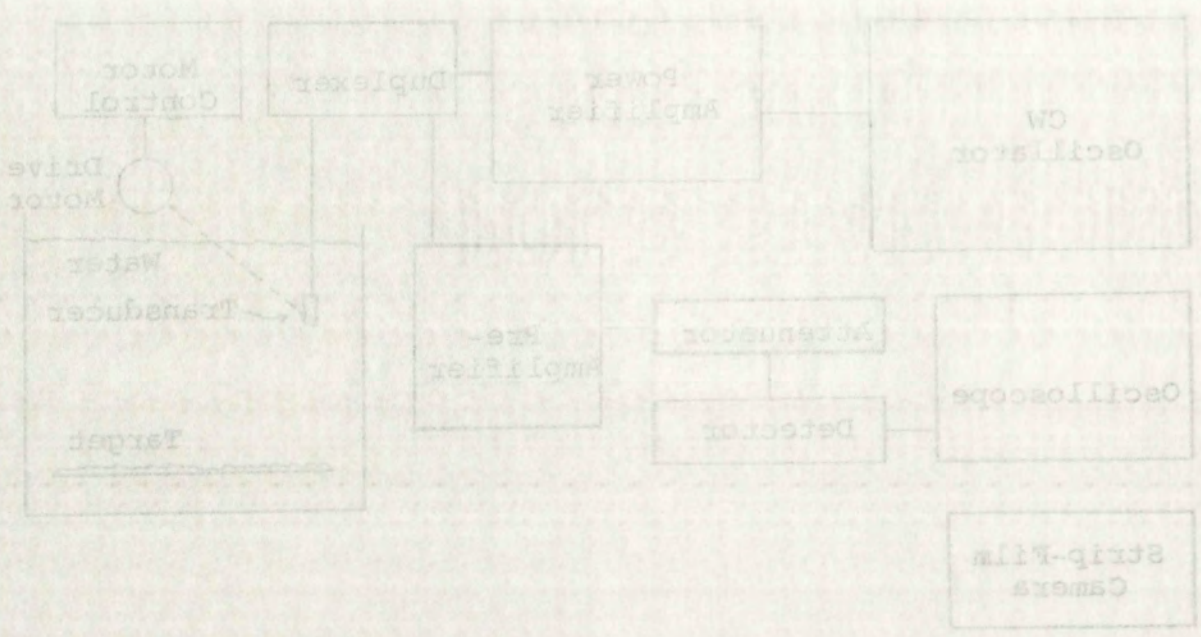
Doppler Frequency Radar Block Diagram

Figure 5-7



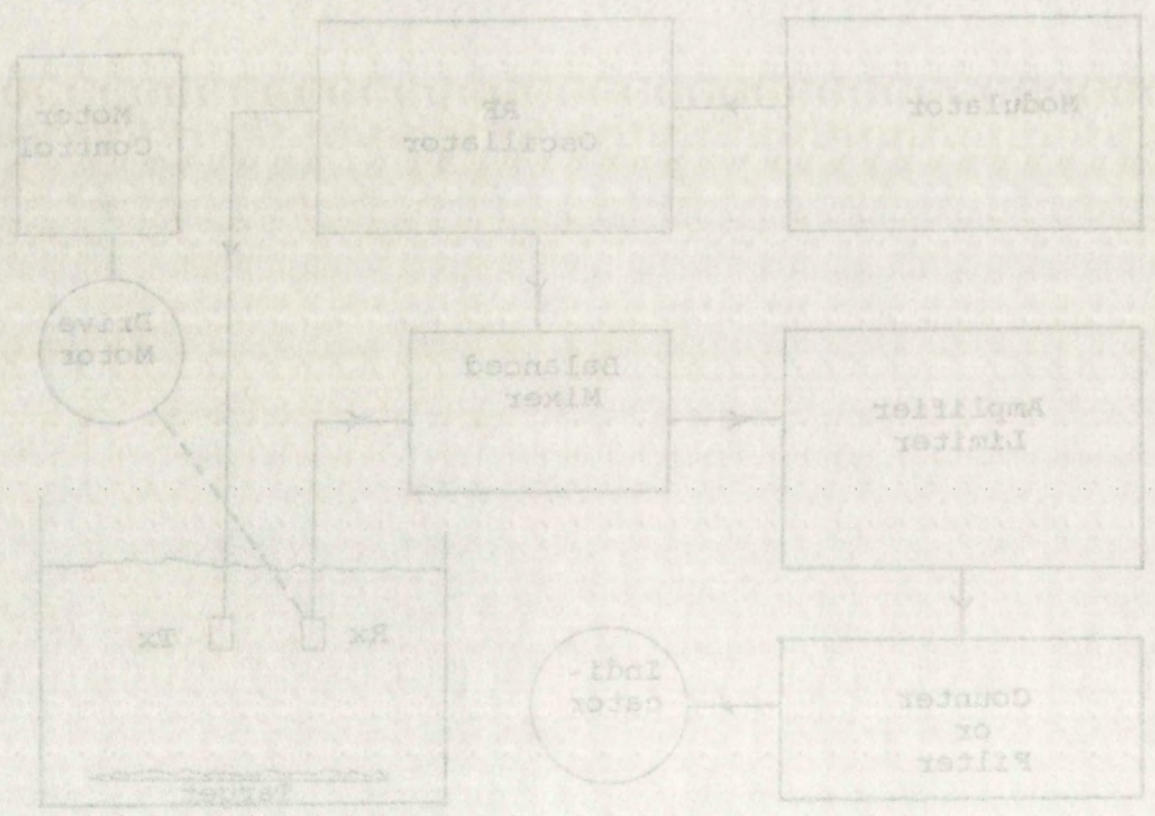
Frequency Modulated Radar Block Diagram

Figure 5-8



Doppler Frequency Radar Block Diagram

Figure 5-7



Frequency Modulated Radar Block Diagram

Figure 5-8

Satisfactory signal records can be made using only the vertical amplifier in an oscilloscope and a strip film camera which provides the time base. A continuous record of the difference frequency is then available for analysis. Other forms of readout device can readily be adapted to this system model.

5.3 Frequency Modulated Radar Device

A typical frequency modulated radar device is shown in Figure 5-8. The system consists of an rf oscillator, modulator, balanced mixer, amplifier, limiter and counter or filter. The oscillator and amplifier requirements are the same as for the Doppler frequency radar and the counter or filter are standard items. The balanced mixer compares the transmitter frequency with the frequency of the received signal and delivers the difference frequencies to the amplifier.

When the radar is moving over a rough target the signal consists of a spectrum of frequencies rather than just a single difference frequency. This spectrum will cause an erroneous range measurement to be indicated by either the counter or the filter output. Model studies can result in methods for minimizing this error by providing large amounts of data for situations where the range is accurately known.

Satisfactory signal results can be obtained by the use of the vertical amplifier in an oscilloscope and a video camera which provides the time base. A comparison of the difference frequency is not available for analysis. Other forms of readout device are being developed for this system model.

5.3 Frequency Modulated Radar Device

A typical frequency modulated radar system is shown in Figure 5-8. The system consists of an oscillator, modulator, balanced mixer, amplifier, filter and counter or filter. The oscillator and amplifier are connected the same as for the Doppler radar. The filter and counter or filter are standard items. The difference between the transmitter frequency with the frequency of the received signal and delivers the difference frequency to the amplifier.

When the radar is moving over a given target the received signal consists of a spectrum of frequencies. The spectrum will cause a single difference frequency. This spectrum will cause an erroneous range measurement to be indicated by the counter or the filter output. Methods for minimizing this error are result in methods for minimizing this error. Large amounts of data for situations where the range is accurately known.

Satisfactory operation of the frequency modulated system requires the transducers to pass a band of frequencies. The Q of a transducer depends on a number of factors including the method of mounting and the loading. A typical pair of lead zirconate, $3/8$ inch diameter, flat plate transducers can be mounted so the overall Q is about 4 when the transducers are submerged in water. The transducers, therefore, have a broad enough frequency pass band to be useful for operating with frequency modulation.

5.4 Sound Absorbing Materials for Tank Walls

An ideal tank for use in performing ultrasonic experiments should be very large so that edge effects can be neglected. One must be realistic, however, and accept the limited size of tanks that are available. When short pulses are employed it is generally an easy matter to position the transducers so the unwanted echoes are separated in time from the desired signal and can therefore be ignored. The reverberation time of most tanks is sufficiently short so it does not cause any difficulty.

There are cases when it is desirable to operate CW or perhaps to use long pulses, in which case reflections from the walls of the tank and the water-air interface may be troublesome. A great deal of experimental work, with varying degrees of success, has been done on methods

- 134 -

Satisfactory operation of the frequency modulated system requires the transducers to pass a band of frequencies. The Q of a transducer depends on a number of factors including the method of mounting and the loading. A typical pair of lead wiretype, 5/8 inch diameter, flat plate transducers can be mounted so the overall Q is about 4 when the transducers are submerged in water. The transducers, therefore, have a broad enough frequency pass band to be useful for operating with frequency modulation.

5.4 Sound Absorbing Materials for Tank Walls

An ideal tank for use in performing ultrasonic experiments should be very large so that edge effects can be neglected. One must be realistic, however, and accept the limited size of tanks that are available. When short pulses are employed it is generally an easy matter to position the transducers so the unwanted echoes are separated in time from the desired signal and can therefore be ignored. The reverberation time of most tanks is sufficiently short so it does not cause any difficulty. There are cases when it is desirable to operate CW or perhaps to use long pulses, in which case reflections from the walls of the tank and the water-air interface may be troublesome. A great deal of experimental work with varying degrees of success, has been done on methods

of dissipating sound energy at the tank walls.^{1,2,3} An attenuation of 20 db can be attained quite easily using two inches of rubberized horse hair and about 25 db can be achieved using a layer of rubber mats with small rubber prongs on the surface.

The methods of dissipating sound can be classified as: (1) flow viscosity, (2) an elasticity of the material, and (3) absorption by air bubbles.⁴ The methods making use of flow viscosity generally employ small wedge shaped structures on a pressure release surface or some porous material which exposes a great deal of area to the sound waves thereby absorbing energy and reducing the reflection. The anelastic properties of rubber make it very useful as an absorbing material, especially in the megacycle region. The rubberized horsehair mat makes some use of flow viscosity; however, the attenuation is largely due to the presence of large quantities of tiny air bubbles held in the rubber. These air bubbles both attenuate and scatter the incident energy and thus reduce

¹Mason, W.P. and Hibbard, F.H., "Absorbing Media for Underwater Sound Measuring Tanks and Baffles," Jour. Acoust. Soc. of Am., Vol. 20, 1948, pp. 476-82.

²Weinstein, M.S., "Some Design Considerations for High Frequency Anechoic Tanks," Jour. Acoust. Soc. of Am., Vol. 25, 1953, pp. 101-05.

³Tamarkin, P. and Eby, R.K., "Tank Wall Lining for Underwater Sound Use," Jour. Acoust. Soc. of Am., Vol. 27, 1955, pp. 692-

⁴Tamarkin, Ibid.

of dissolving sound energy in the medium. The
attenuation of 10 db was obtained in the
two inches of rubber. This result could
be achieved using a layer of rubber 1/2 inch
thick on the surface.

The methods of damping were compared with
as: (1) flow viscosity, (2) absorption by
and (3) absorption by a porous medium.

Use of flow viscosity was found to be
shaped structures on a porous medium. The
porous material which was used was of the
the sound waves thereby causing a large
reflection. The analysis showed that it
very useful as an absorbing material.

mesocycle region. The results showed that
some use of flow viscosity was found to be
largely due to the presence of small particles
air bubbles held in the water. These
attenuate and scatter the sound energy.

¹Mason, W.P. and Hill, R.M. "Acoustics of Solids"
Underwater Sound Measurement Handbook, Chapter 1, 1956.

²Weinstein, M.S. "The Theory of Acoustics"
High Frequency Acoustics, Vol. 1, 1956.

³Tamarkin, P. and S. "Acoustics of Solids"
Underwater Sound Use, Vol. 1, 1956.

⁴Tamarkin, P. "Acoustics of Solids", 1956.

the reflection from the wall. After continual submersion in water, the bubble density diminishes and the effectiveness of the lining is reduced. The use of rubber material is better in this respect since its absorbing properties are relatively unaffected by long and continued submersion.

The concepts of impedance can be used to analyze the behavior of absorbing materials when propagation in the materials is coherent. In this case, an attempt is made to line the tank with a material which presents an impedance equal to that of the water at the water-lining interface so that no signal is reflected. The air-bubble lining must be analyzed from the standpoint of energy scattering and absorption in a volume distribution of microscopic bubbles.

When a tank is lined with a sound absorbing material that gives an attenuation of 20 db. it has the effect on the signal level of moving the tank wall back about ten times as far from the transducer, based on an inverse square signal variation with distance.

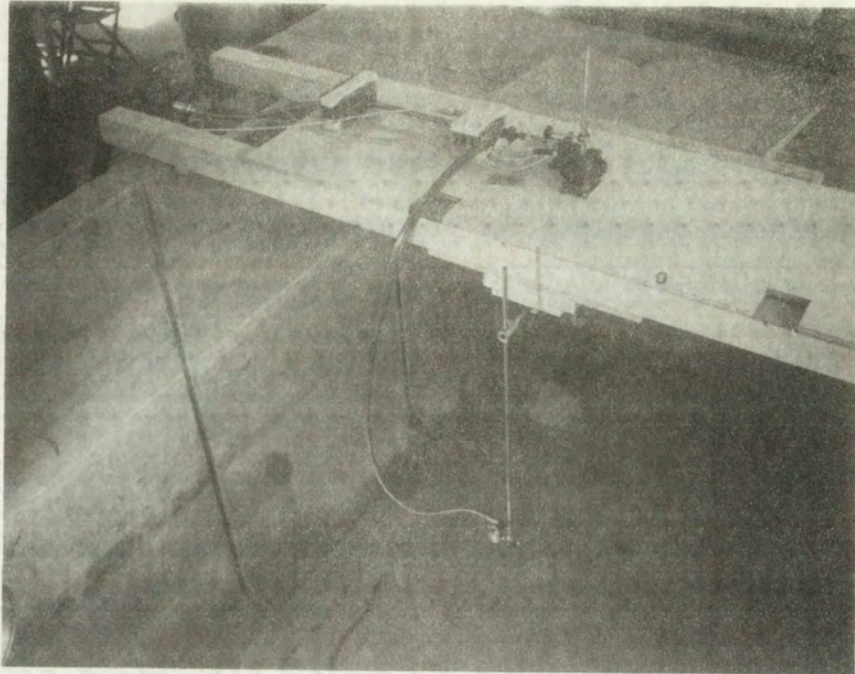
5.5 Acoustic Tank and Targets

The tank is equipped with a mechanism for moving the transducer at a constant velocity in a path parallel to a plane surface containing the target, as illustrated in Figures 5-9 and 5-10. This type of motion simulates the motion of an airborne radar in a horizontal flight path over the earth. In some instances, it is desired to have

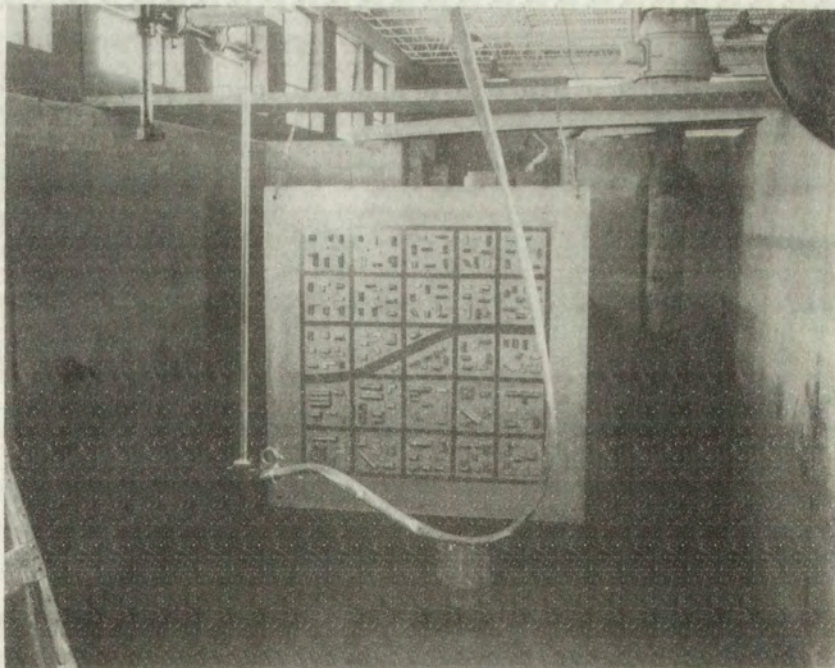
the reflection from the wall. After continual submergence in water, the bubble density diminishes and the effectiveness of the lining is reduced. The use of rubber material is better in this respect since the absorbing properties are relatively unaffected by long and continued submergence. The concept of impedance can be used to analyze the behavior of absorbing materials when propagation in the material is coherent. In this case, an attempt is made to line the tank with a material which presents an impedance equal to that of the water at the water-lining interface so that no signal is reflected. The air-bubble lining must be analyzed from the standpoint of energy scattering and absorption in a volume distribution of microscopic bubbles. When a tank is lined with a sound absorbing material that gives an attenuation of 30 db it has the effect on the signal level of moving the tank wall about ten times as far from the transducer, based on an inverse square signal variation with distance.

5.2. Acoustic Tank and Targets

The tank is equipped with a mechanism for moving the transducer at a constant velocity in a path parallel to a plane surface containing the target, as illustrated in Figures 4-9 and 5-10. This type of motion simulates the motion of an airborne radar in a horizontal flight path over the earth. In some instances, it is desired to have

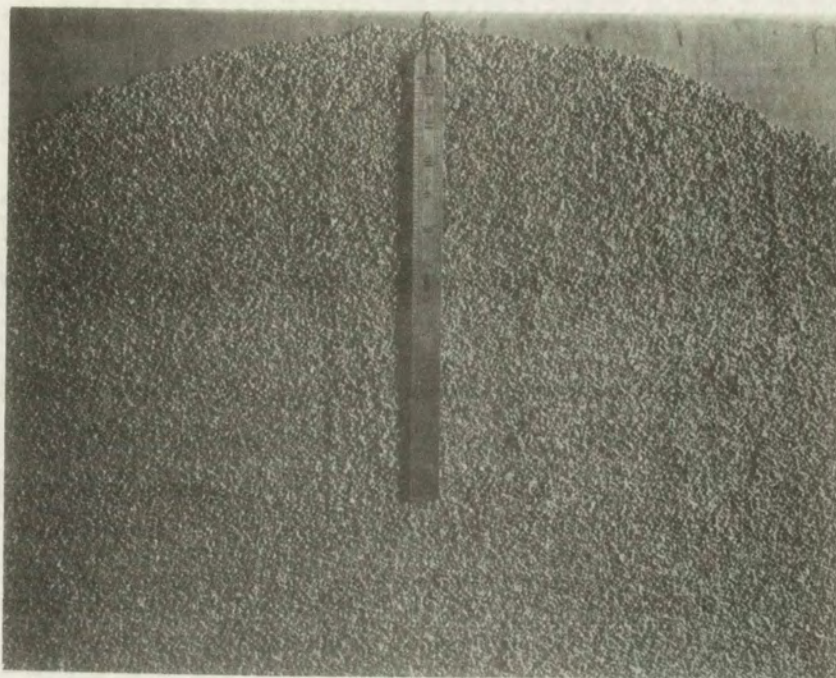


Water Tank, Platform, and Transducer
Fig. 5-9

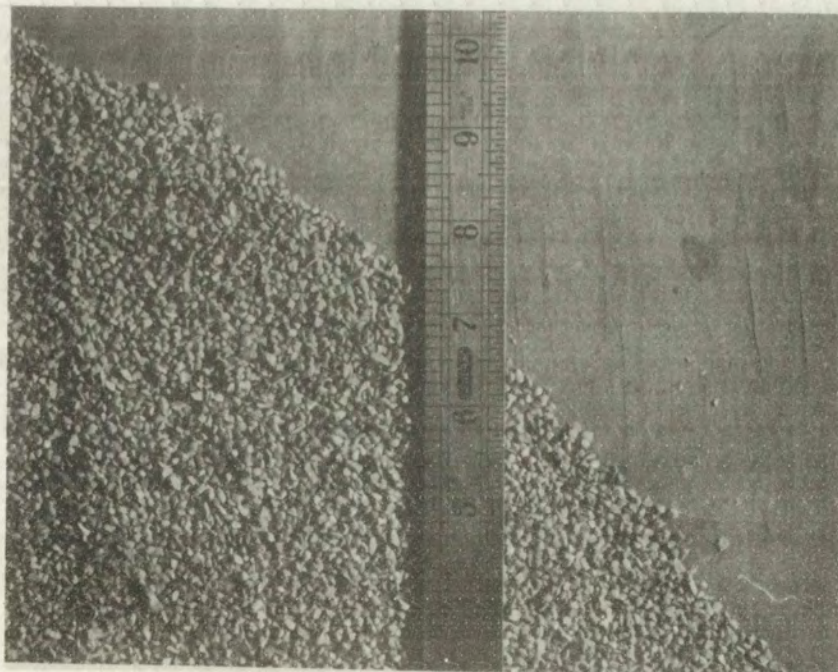


City Target in the Tank
Fig. 5-10

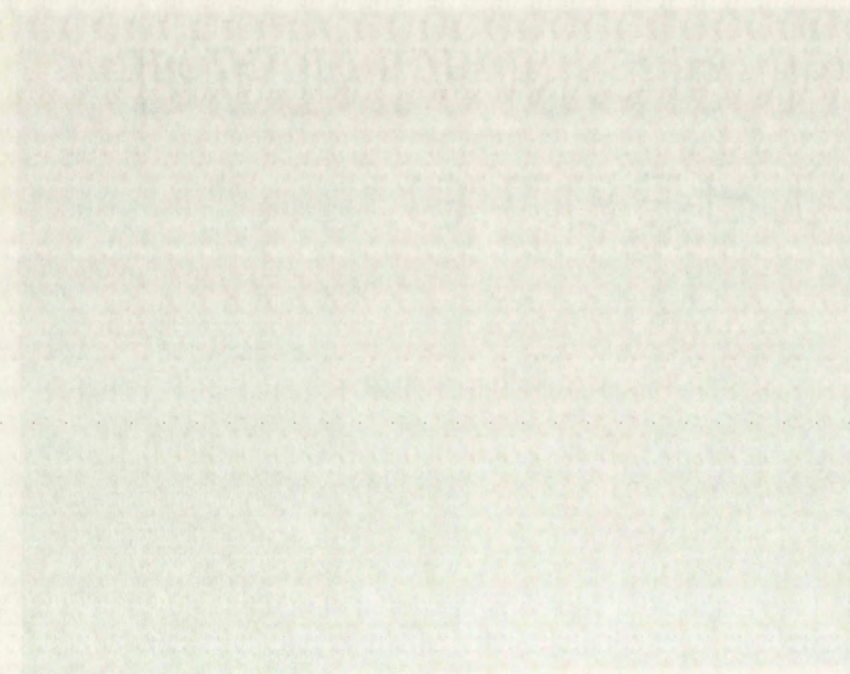
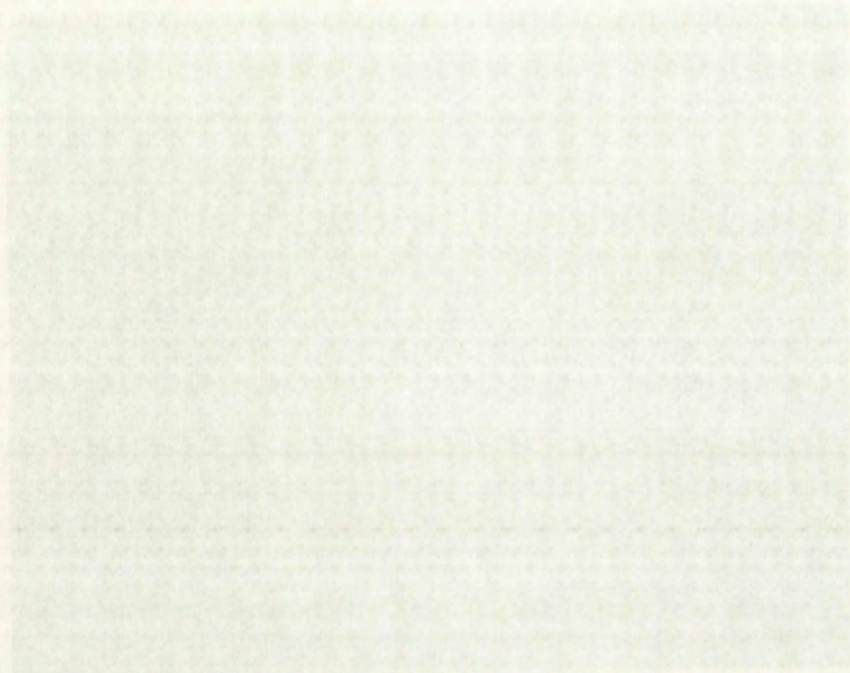
the most common... can be seen... by reflection... Numerous... the tank... involves... such as the... separated... same... samples of... It is possible... certain... type of... aimed with... to account... should be... provide... of particles... appears to... and particles... surface... the wood... A smooth... calibration... once level... reflection...



Rough Sand Target
Fig. 5-11



Close-up of Rough Sand Target
Fig. 5-12



signal to the antenna. A specular signal is defined as one that does not fade when the antenna moves in a horizontal path over the surface. The signal obeys the inverse square law over the steel, and therefore provides a convenient reference.

Another type of target is constructed using a sheet of galvanized steel fastened to a sheet of plywood. This target provides a uniform impedance background on which a roughening agent is applied. When sand particles are glued on the surface to provide roughness, no appreciable difference in fading characteristics is noticed from those provided by the plywood-sand targets. One metal target has been formed into a surface representing a range of mountains where the small scale roughness is provided by a wrinkle finish paint on the surface. This type of target which is shown in Figure 5-13 is satisfactory when modeling hilly or mountainous terrain. The impedance of the target is uniform everywhere and only the physical shape of the large size irregularities is modeled. This target maintains the proper shape of return pulse because the gross time delays for various scattering areas in the target are preserved properly. The time delays on the order of one period of the carrier frequency are of a random nature and are modeled by the randomly located small scale irregularities on the surface.

THEORY OF THE

... of the ...
... of the ...
... of the ...
... of the ...
... of the ...

... of the ...
... of the ...
... of the ...
... of the ...
... of the ...

... of the ...
... of the ...
... of the ...
... of the ...
... of the ...

... of the ...
... of the ...
... of the ...
... of the ...
... of the ...

... of the ...
... of the ...
... of the ...
... of the ...
... of the ...

... of the ...
... of the ...
... of the ...
... of the ...
... of the ...

... of the ...
... of the ...
... of the ...
... of the ...
... of the ...

... of the ...
... of the ...
... of the ...
... of the ...
... of the ...

Modeling a target area such as that presented by typical terrain presents a difficult problem. The physical characteristic shapes involve so much detail that an exact model is hopelessly complicated. In addition, the impedance variation over the area is random in nature which further complicates the situation. The radar return signal is influenced by all of this detail and some attempt must be made to account for it in the model. There are several practical alternatives that can be used. The simplest of these is to model the large scale detail carefully and to represent the small scale detail with a random distribution of scattering facets. The effects of the impedance variations are assumed to be included in the random distribution of scattering facets. This form of model assumes that the physical shape of the target is the most important single feature as far as the scattering is concerned. A refinement can be made by using a variety of materials in the target in order to take advantage of different impedances. A typical city area model is shown in Figure 5-14.

5.6 Transducers

Measurements in the acoustic system are made by means of piezoelectric transducers. These transducers are generally molded in a variety of shapes from barium titanate, lead zirconate, or some other piezoelectric material. The simple flat disk transducer has proven to be very satisfactory for most applications. One surface of the disk is

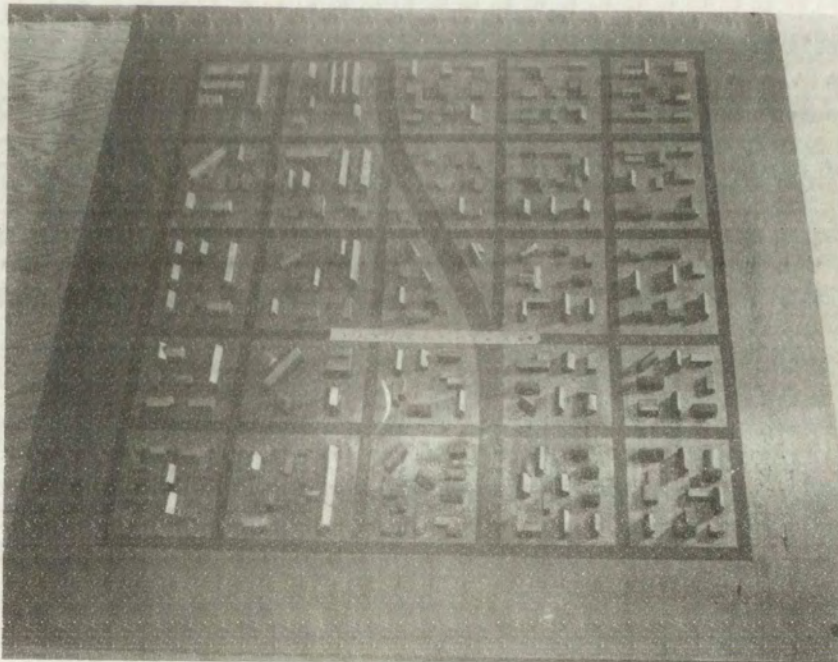
Modeling a target area such as that presented by typical terrain presents a difficult problem. The physical characteristic shapes involve so much detail that an exact model is hopelessly complicated. In addition, the impedance variation over the area is random in nature which further complicates the situation. The radar return signal is influenced by all of this detail and some attempt must be made to account for it in the model. There are several practical alternatives that can be used. The simplest of these is to model the large scale detail carefully and to represent the small scale detail with a random distribution of scattering facets. The effects of the impedance variations are assumed to be included in the random distribution of scattering facets. This form of model assumes that the physical shape of the target is the most important single feature as far as the scattering is concerned. A refinement can be made by using a variety of materials in the target in order to take advantage of different impedances. A typical city area model is shown in Figure 5-14.

5.6 Transducers

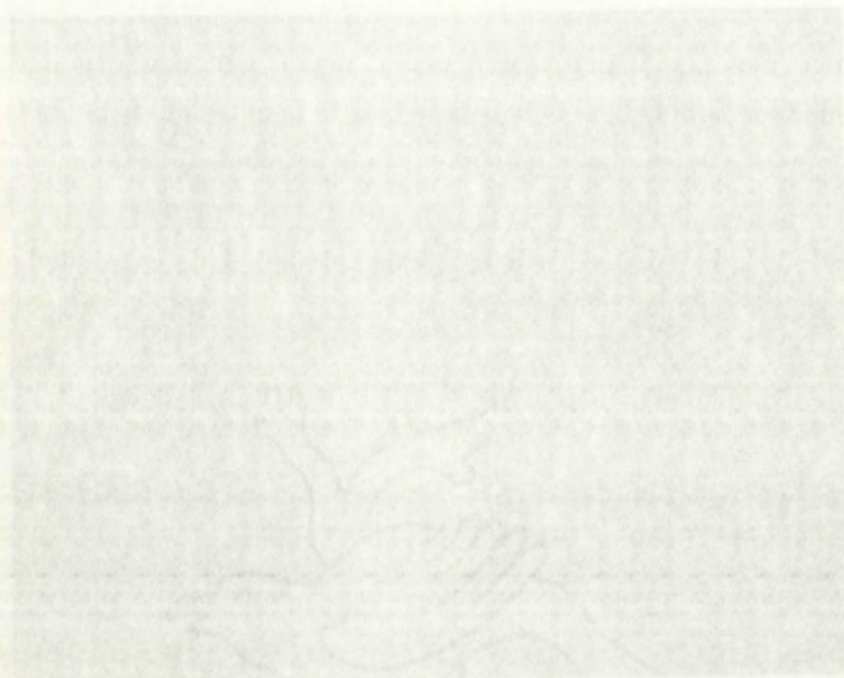
Measurements in the acoustic system are made by means of piezoelectric transducers. These transducers are generally molded in a variety of shapes from barium titanate, lead titanate, or some other piezoelectric material. The simple flat disk transducer has proven to be very satisfactory for most applications. One surface of the disk is



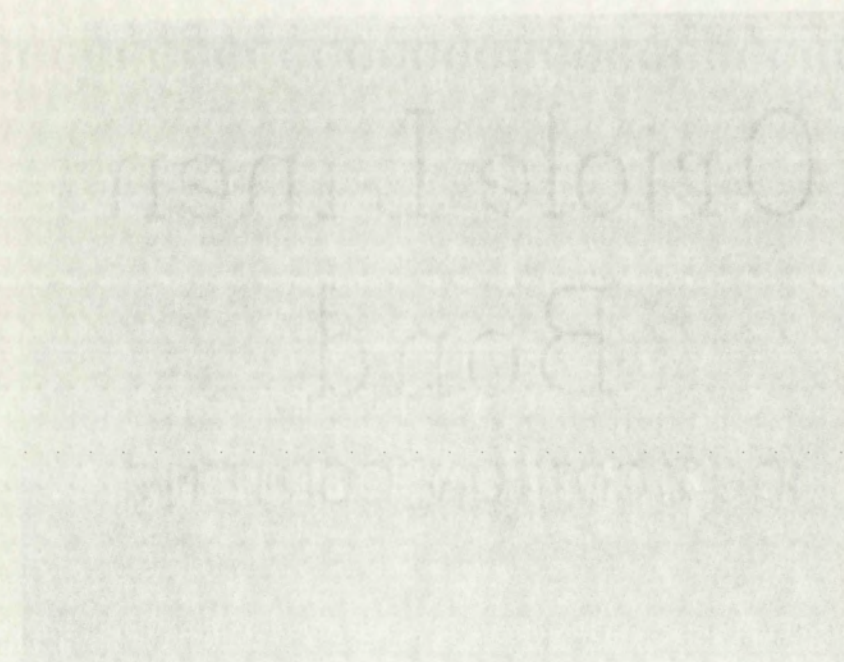
Mountain Target
Fig. 5-13



City Target
Fig. 5-14



Mountain Target
1/10 8-13



City Target
1/10 8-13

exposed to the water so the transducer acts like a piston source while the other surface is glued to a high impedance, lossy material to lower the mechanical Q .¹ When relatively high frequencies are considered, the active area of the flat disk may be several wavelengths across so a directive antenna pattern is obtained, through the interference principle. The transducer is a pressure sensitive device; however, the fact that it is not infinitely small makes it necessary to investigate what parameter is being measured.

A theoretical pressure transducer consisting of an elementary sphere as a detecting element could measure the dynamic pressure at a point in the medium. The direction of travel of the acoustic wave would have no effect on the pressure measurement. Since the physically realizable transducer does have an antenna pattern that is generally quite directive, the pressure measurements are made only for those waves arriving from the proper directions. The transducer acts as an integrating device which determines the resultant pressure due to the plane wave components incident on its surface, and each plane wave component is weighted according to the gain of the transducer. The transducer, therefore, measures a partial pressure selected from a group of plane waves traveling in the directions preferred by the antenna pattern.

¹Hueter, op. cit., p. 109.

exposed to the... source while... lossy material... high frequency... flat disk... antenna pattern... the fact that... to investigate... A theoretical... elementarily... dynamic pressure... of level of the... pressure measurement... transducer... cause distortion... for those... transducer... the resultant... incident on... weighted... transducer... from a group of... preferred by the...

When the antenna pattern is very directive, the transducer can be used to measure the magnitude and direction of the particle velocity as well as the pressure. In reality this merely requires a proper calibration to give the magnitude of the particle velocity. The direction, is, of course, determined by the orientation of the transducer which results in a maximum received signal.

The transducers function better when operated at mechanical and electrical resonance.¹ The mechanical resonant frequency of interest in this application is determined by the thickness of the disk for a given transducer material. Electrically the transducer appears to be capacitive with a shunt conductance in parallel. Electrical resonance is therefore achieved by adding the proper inductance in parallel to cancel the total capacitive reactance. The tuned transducer can be used in this form as a receiver. Maximum power transfer will occur when the input resistance of the preamplifier is equal to the resistive component of the transducer. When the transducer is used for transmitting, it is necessary to add another resistor in parallel so the transmitter output impedance is matched. This allows proper operation of the transmitter by eliminating standing waves from the transmission line.

¹Op. cit., Chap. 4.

When the antenna pattern is very directive, the transducer can be used to measure the magnitude and direction of the particle velocity as well as the pressure. In reality this merely requires a proper calibration to give the magnitude of the particle velocity. The direction is, of course, determined by the orientation of the transducer which results in a maximum received signal.

The transducer function is better when operated at mechanical and electrical resonance. The mechanical resonant frequency of interest in this application is determined by the thickness of the disk for a given transducer material. Electrically the transducer appears to be capacitive with a shunt conductance in parallel. Electrical resonance is therefore achieved by adding the proper inductance in parallel to cancel the total capacitive reactance. The tuned transducer can be used in this form as a receiver. Maximum power transfer will occur when the input resistance of the preamplifier is equal to the resistive component of the transducer. When the transducer is used for transmitting, it is necessary to add another resistor in parallel so the transmitter output impedance is matched. This allows proper operation of the transmitter by eliminating standing waves from the transmission line.

A piezoelectric transducer has a capacitance given by

$$C = \epsilon_r \epsilon_o \frac{A}{d} \quad (5-1)$$

where C is the capacitance,

ϵ_r is the relative dielectric constant of the material,

ϵ_o is the dielectric constant of a vacuum,

A is the cross-sectional area of the transducer, and

d is the distance between the plates.

The mechanical properties of the transducer are described to a first approximation by

$$S = \frac{F d}{A \delta} \quad (5-2)$$

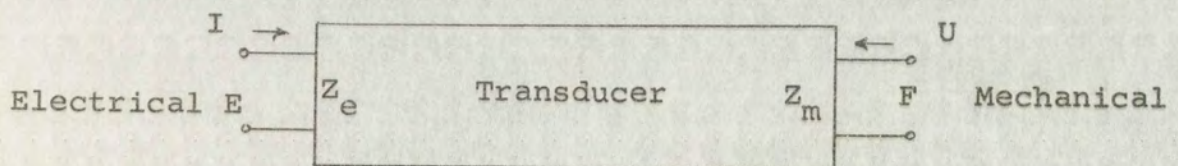
where:

S is the stiffness constant,

F is the total force on one face of the transducer, and

δ is the incremental displacement caused by the force F .

The transducer can be described in terms of a four-terminal network where the left port is designated as the electrical terminals and the right port is designated as the mechanical terminals. The quantity, Z_e , refers to the electrical impedance and the quantity, Z_m , refers to the mechanical impedance of the transducer as shown in Figure 5-15.



Electro-Mechanical Transducer Diagram

Figure 5-15

A piezoelectric transducer is a device which converts mechanical energy into electrical energy.

$$C = \frac{Q}{V}$$

where C is the capacitance

ϵ_0 is the permittivity of free space

ϵ_r is the dielectric constant of the material

A is the area of the plates

d is the distance between the plates

The mechanical properties of the transducer are given by

to a first approximation by

$$S = \frac{F}{\Delta L}$$

where:

S is the stiffness constant

F is the force on one end of the transducer and

ΔL is the incremental displacement of the transducer

The transducer can be modeled in terms of a

terminal network where the left terminals are connected to the

electrical terminals and the right terminals are connected to the

mechanical terminals. The diagram of the transducer is shown in

electrical impedance and the diagram of the transducer is shown in

mechanical impedance of the transducer is shown in Figure 5-15.

5-15

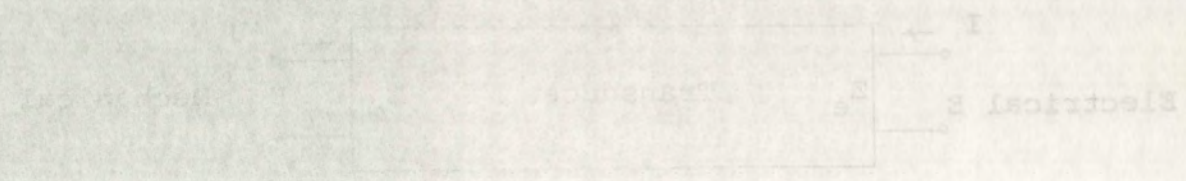


Figure 5-15 Electro-mechanical transducer model

Figure 5-15

The mechanical impedance, Z_m , is essentially pure resistance when plane waves are transmitted into a low viscosity medium such as water. For this case the mechanical impedance is given by

$$Z_m = \frac{F}{u} = \rho_0 v A \quad (5-3)$$

where F is the phasor value of force on the transducer surface,

u is the phasor value of particle velocity at the surface,

v is the phase velocity in the medium,

ρ_0 is the density of the liquid, and

A is the cross sectional area of the transducer.

Since Z_m is real, the acoustic power requirement can be taken into account by a resistor in the equivalent electrical circuit. The total electrical input impedance of the transducer can now be expressed as

$$Z_e = \frac{E}{I_c + I_m} \quad (5-4)$$

where Z_e is the electrical input impedance

I_c is the phasor current in the transducer capacitance, and

I_m is the phasor current in the resistor representing radiation resistance.

Now the electrical impedance can be written as

$$Z_e = \frac{1}{G_e + j B_c} \quad (5-5)$$

The mechanical impedance, Z_m , is essentially pure resistance when plane waves are transmitted into a low viscosity medium such as water. For this case the mechanical impedance is given by

$$Z_m = \frac{F}{v} = \rho v A \quad (2-3)$$

where F is the phase value of force on the transducer

surface

v is the phase value of particle velocity at the

surface

ρ is the phase velocity in the medium

A is the cross sectional area of the transducer

Since Z_m is real, the acoustic power requirement can

be taken into account by a resistor in the equivalent elec-

trical circuit. The total electrical input impedance of

the transducer can now be expressed as

$$Z_e = \frac{1}{\frac{1}{Z_0} + \frac{1}{Z_m}} \quad (2-4)$$

where Z_0 is the electrical input impedance

$\frac{1}{Z_0}$ is the phase current in the transducer capacitance

and

$\frac{1}{Z_m}$ is the phase current in the resistor representing

radiation resistance.

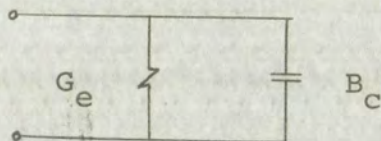
Now the electrical impedance can be written as

$$Z_e = \frac{1}{\frac{1}{Z_0} + \frac{1}{Z_m}} \quad (2-5)$$

where G_e is the input conductance, and

B_c is the input susceptance.

The equivalent electrical circuit is shown in Figure 5-16. When transducer losses are considered, and additional conductance is introduced which can be combined with G_e .



Transducer Equivalent Circuit

Figure 5-16

A barium titanate flat disk transducer $\frac{1}{2}$ inch in diameter and resonant at 1 mc/sec has a capacitance of about 550 μmf . The equivalent parallel resistance is on the order of 250 ohms, and the reactance at 1 mc/sec is about 300 ohms. This transducer will properly match the 93-ohm output impedance of the pulsed oscillator when a 150-ohm resistor and a 48 μh inductor are connected in parallel with the transducer. When the oscillator output is set near its maximum level, 100 volts rms is developed across the transducer during the pulse interval. The acoustic power density is then about 25 w/cm^2 and the transducer and matching network efficiency is on the order of 32%. The power density in the water is well below the point where cavitation begins at this frequency.

where θ is the angle between the
B is the magnetic field
The enthalpy of the system
2-1 When the system is at equilibrium
conductance is zero

A barium fluoride crystal is used as
diameter and thickness of 1.2 cm. It is a
about 500 μ m. The electrode potential is
the order of 100 mV. The electrode is
about 500 μ m. The electrode is
25-cm diameter. The electrode is
150-cm diameter. The electrode is
parallel with the crystal. The
is at the maximum level. The
developed across the electrode. The
The acoustic power density is 100
the transducer and the acoustic
order of 100. The power density is
below the point where the acoustic

5.7 Antenna Pattern for Flat Disk Transducer

The directivity of a transducer is a function of its physical dimensions measured in terms of the wavelength and of the amplitude distribution over the surface. The flat disk transducers used in these experiments are mounted so the amplitude distribution is uniform over the transducer face. This is demonstrated by observing the good agreement between a theoretical antenna pattern for a circular disk acting as a piston-like source and the actual measured patterns. Several transducers are shown in Figure 5-17.

The far field antenna pattern for a flat disk transducer operating in an infinite baffle is given by¹

$$\frac{2J_1(ka \sin \theta)}{ka \sin \theta} \quad (5-6)$$

where J_1 is a Bessel function of first kind and first order,
 k is the wave number,
 a is the radius of the piston source, and
 θ is the angle measured from the normal to the surface.

The value of θ at the first zero of the Bessel function is given by

$$\theta = \sin^{-1} \frac{0.61\lambda}{a} \quad (5-7)$$

which determines the angular limits on the major lobe. A few calculated values for the full angle of the major lobe, 2θ , at different frequencies and for different size disks

¹Hueter, op. cit., p. 64.

are given in Table 5-1. (The transducers are assumed to be submerged in water.) It is customary to give the antenna pattern in terms of the included angle between the half-power points. For the flat disk transducer the angle measured from the normal to the surface to the half-power point on the major lobe is given by

$$\alpha = \sin^{-1} \frac{1.60 \lambda}{2\pi a} \quad (5-8)$$

Values of the total included angle, between the half-power points, 2α , are also tabulated in Table 5-1.

The calculated values for the beamwidth to the half-power points on the pattern agree well with measured values on the 1 mc/sec, 3/8 inch transducers used in the experimental work. It should be pointed out that the 3/8 inch disk is covered with an aluminum oxide disk 1/2 inch in diameter, which governs the antenna pattern.

The antenna patterns available from various sizes of flat plate transducers are seen to be rather narrow at frequencies near one mc/sec. It is desirable to be able to use a single transducer for the experimental work and to obtain a variety of antenna patterns. There are several methods available for controlling the antenna pattern. A few of these methods are considered as a means of broadening a normal pattern obtained from a flat disk transducer.

ASTROPHYSICAL JOURNAL

Published by the American Astronomical Society

Volume 150, Number 1, January 1999

Editor: J. K. O'Neil

Editorial Board: J. K. O'Neil, J. H. Kuhn, J. L. Linsky, J. M. O'Neil, J. R. O'Neil, J. S. O'Neil, J. T. O'Neil, J. W. O'Neil, J. X. O'Neil, J. Y. O'Neil, J. Z. O'Neil

Editorial Office: American Astronomical Society, 475 Williamstown Avenue, Cambridge, MA 02142

Subscription Information: Single copies \$10.00; Annual subscription \$30.00; Institutional subscription \$100.00

Advertising Information: For advertising rates and information, contact the American Astronomical Society, 475 Williamstown Avenue, Cambridge, MA 02142

Copyright © 1999 American Astronomical Society

Printed in the United States of America

Postmaster: Send address changes to the American Astronomical Society, 475 Williamstown Avenue, Cambridge, MA 02142

Second-class postage paid at Cambridge, MA

Postage paid at other mailing offices

Postage paid at New York, NY

Postage paid at Washington, DC

Postage paid at Los Angeles, CA

Postage paid at San Francisco, CA

Postage paid at Seattle, WA

Postage paid at Portland, OR

Postage paid at Denver, CO

Postage paid at Phoenix, AZ

Postage paid at Salt Lake City, UT

Postage paid at Albuquerque, NM

Postage paid at Santa Fe, NM

Postage paid at Las Vegas, NV

Postage paid at Reno, NV

Postage paid at Sacramento, CA

Postage paid at San Jose, CA

Postage paid at San Diego, CA

Postage paid at San Francisco, CA

Postage paid at Seattle, WA

TABLE 5-1
BEAMWIDTHS FOR FLAT DISK TRANSDUCERS

f_{mc}	Diameter of Transducer, in.	Full-lobe angle	Angle [°] Between Half-Power Points
0.2	1/4		74.0
	3/8	149.1	47.5
	1/2	92.1	35.0
	3/4	57.2	23.1
	1	42.3	17.3
0.5	1/4	70.4	27.9
	3/8	45.2	18.5
	1/2	33.5	13.8
	3/4	22.1	9.2
	1	16.6	6.9
1.0	1/4	33.5	13.8
	3/8	22.1	9.2
	1/2	16.6	6.9
	3/4	11.0	4.6
	1	8.3	3.4
2.25	1/4	14.7	6.1
	3/8	9.8	4.1
	1/2	7.3	3.1
	3/4	4.9	2.0
	1	3.7	1.5

5.8 Pattern Shaping Devices

Antenna patterns for acoustic waves can be controlled by the following methods:

- (1) lenses, which redirect the sonic ray paths by refraction to give the desired pattern.

BEAMWIDTHS FOR FLAT DISK TRANSDUCERS
TABLE 2-1

Angle Between Foli- Power Points	Foli- angle	Diameter of Transducer, in.	f mc
74.0		1/8	0.2
47.5	149.1	1/8	
33.0	92.1	1/2	
23.1	57.2	3/4	
17.3	42.3	1	
17.9	70.4	1/4	0.5
18.5	45.2	3/8	
15.8	33.5	1/2	
9.2	22.1	3/4	
6.9	16.6	1	
13.8	33.2	1/4	1.0
9.2	22.1	3/8	
6.9	16.6	1/2	
4.6	11.0	5/8	
3.4	8.7	1	
6.1	14.7	1/4	2.25
4.1	9.8	3/8	
3.1	7.3	1/2	
2.0	4.9	3/4	
1.5	3.7	1	

5.8. Pattern Shaping Devices

Antenna patterns for acoustic waves can be controlled by the following methods:

- (1) lenses, which redirect the acoustic ray paths by refraction to give the desired pattern.

- (2) reflectors, which redirect the sonic ray paths by reflection to give the desired pattern,
- (3) aperture control, which alters the effective cross sectional area of the source by changing the aperture of the transducer,
- (4) shaped transducers, which use a preformed piezoelectric element to give a particular pattern, and
- (5) combinations of sources, which makes use of the principle of wave interference to establish a pattern.

Each of these methods of pattern control is discussed briefly.

5.81 Lenses - Polystyrene is a satisfactory lens material for the following reasons: (1) the impedance is only about 1.7 times the impedance of water so interface reflections are small, (2) the velocity of propagation of acoustic waves is about 1.6 times greater than in water so the angle of refraction is fairly large, (3) the material has very low acoustic loss, and (4) it is very easy to machine and polish.

A polystyrene lens with a hemispherical surface will approximately double the beamwidth of a $\frac{1}{2}$ inch diameter transducer when used at a frequency of 1 mc/sec. The expected beamwidth from such a lens can be estimated by assuming ray theory to apply. This assumption is reasonable since the transducer is about 8.45 wavelengths in diameter.

(5) reflector with a diameter of 10 cm.

by the reflector of the same diameter.

(6) acoustic beam of 1 cm diameter.

cross section of 1 cm.

the aperture of the reflector.

(7) shaded reflector of 10 cm diameter.

cross section of 1 cm.

and

(8) combination of acoustic and reflector of 10 cm diameter.

principles of wave interaction in reflector.

pattern.

Each of these methods of reflector is described in detail.

5.81 lenses - polyethylene is a transparent material.

for the following reasons: (1) the refractive index is 1.5.

1.7 times the impedance of water and acoustic reflector.

are small, (2) the velocity of propagation is 1.5.

waves is about 1.5 times greater than water and acoustic reflector.

of refraction is fairly large, (3) the refractive index is 1.5.

low acoustic loss, and (4) it is very easy to cut and polish.

polish.

A polyethylene lens with a refractive index of 1.5.

approximately double the beamwidth of a beam reflector.

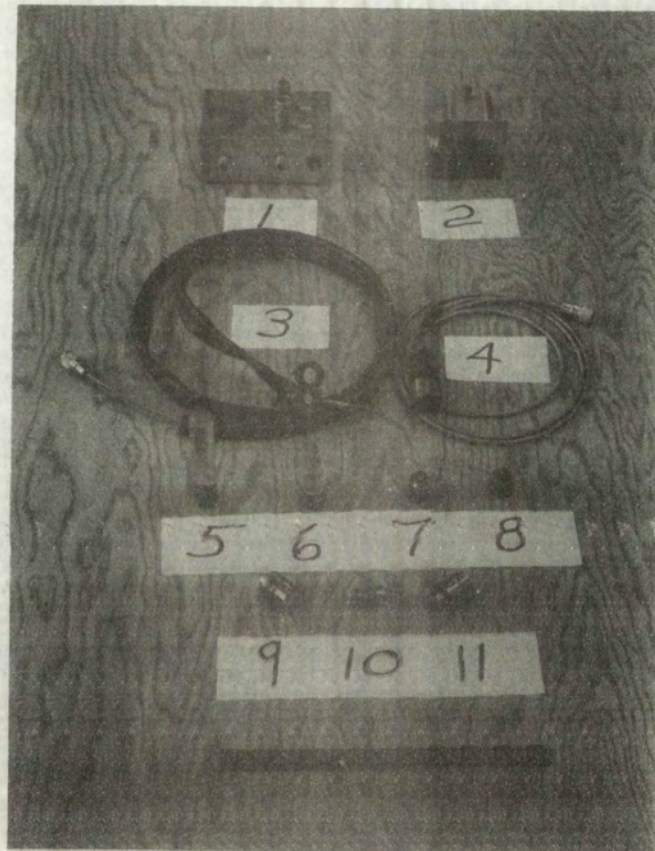
transducer when used at a frequency of 100 kHz.

expected beamwidth from such a lens can be estimated by

assuming ray theory to apply. This assumption is reasonable.

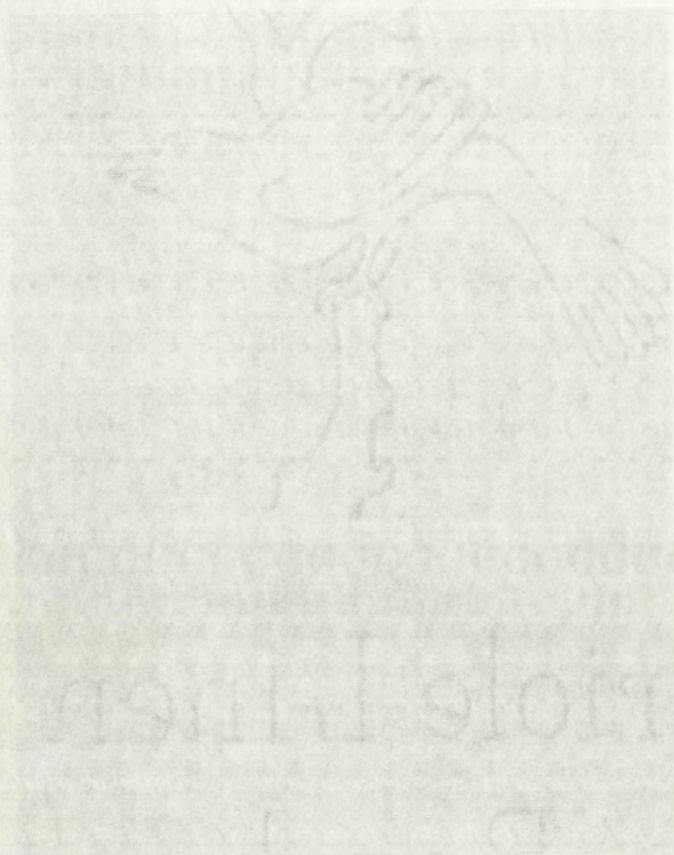
able since the transducer is about 1 cm in diameter.

diameter.



- | | |
|----------------------------|----------------------|
| 1. Duplexer | 6. Point Source Lens |
| 2. Dummy Load | 7. 1" Diameter Lens |
| 3. 3/8" Transducer & Cable | 8. 3/4" Dia. Lens |
| 4. 3/4" Transducer & Cable | 9. 1" Transducer |
| 5. Extended Lens | 10. 3/4" Transducer |
| | 11. 1" Transducer |

Fig. 5-17



1. Duplek
2. Duplek
3. Duplek
4. Duplek
5. Duplek
6. Duplek

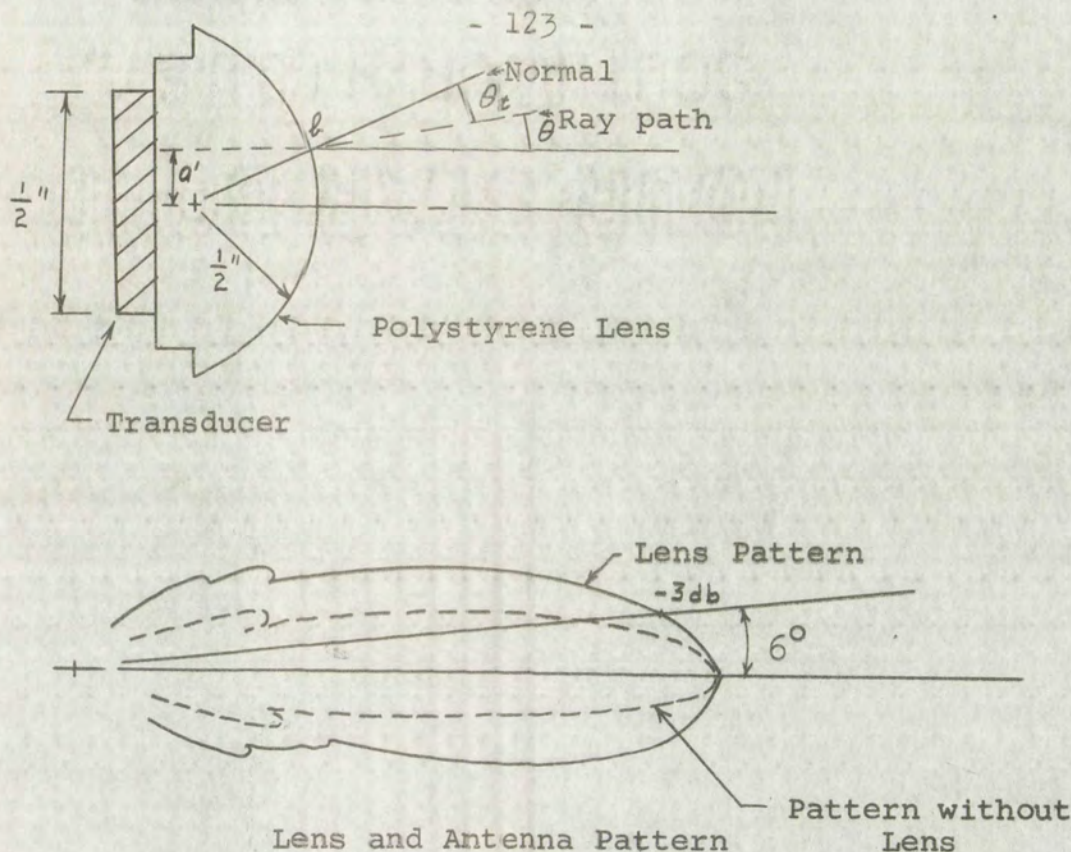


Figure 5-18

Figure 5-18 shows the geometry involved in the calculation of the antenna pattern beamwidth between the half-power points. The distance a' is the radius of a circle enclosing half the area of the active transducer surface. A ray from a point on this circle intercepts the lens surface at a point b as shown. The angle of incidence, θ_i , is determined by the radius a' and radius of the lens. The angle of transmission, θ_t , is determined by Snell's Law which can be written as

$$\theta_t = \sin^{-1} \left(\frac{V_w}{V_p} \sin \theta_i \right) \quad (5-9)$$

where V_w and V_p are the velocities of propagation of sonic waves in water and polystyrene respectively. For this

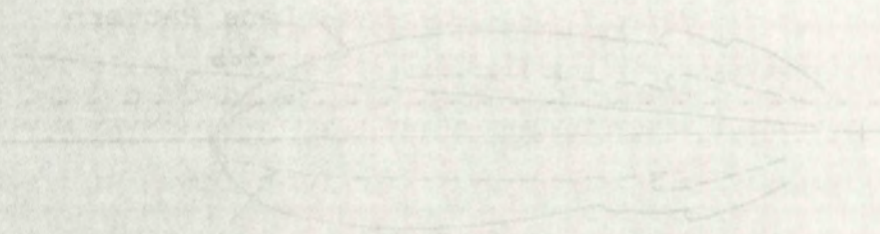
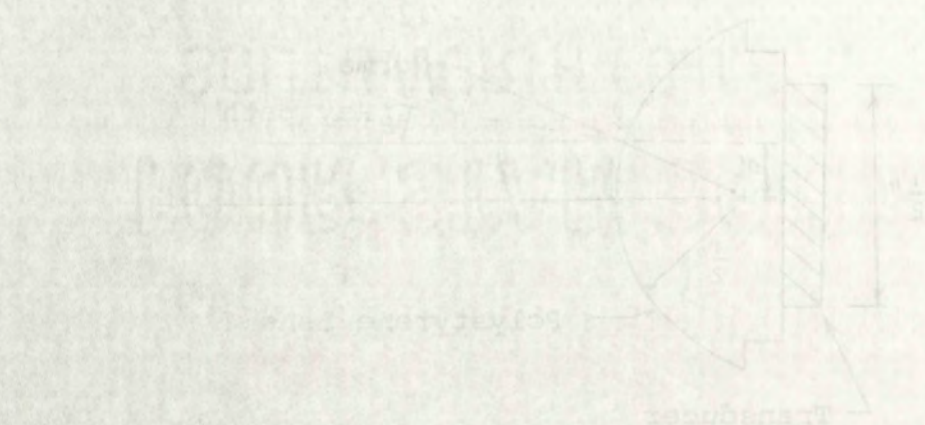


Figure 5-16 shows the geometry involved in the calculation of the antenna and lens parameters. The half-power points, the distance a , is the radius of a circle enclosing half the area of the active element surface. A ray from a point on the circle intersects the lens surface at a point b as shown. The angle of incidence θ_i is determined by the radius a and radius of the lens. The angle of refraction θ_r is determined by Snell's law which can be written as

$$\theta_i = \sin^{-1} \left(\frac{v_w}{v_p} \sin \theta_r \right) \quad (5-1)$$

where v_w and v_p are the velocities of propagation of sound waves in water and polyethylene respectively.

particular lens-transducer combination, the angle θ measured from the centerline to the half-power point on the transducer is

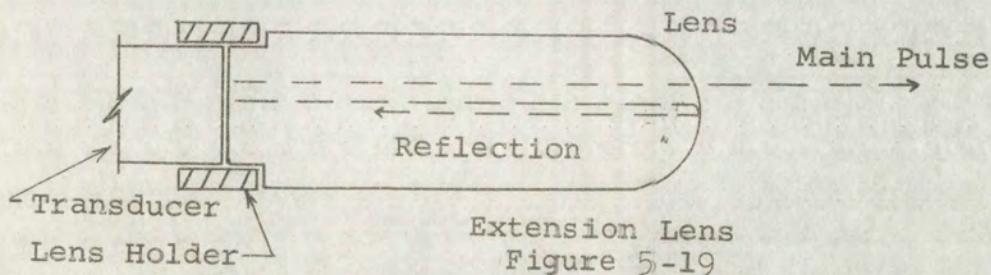
$$\theta = 7.87^\circ$$

which gives a total included angle between half-power points of

$$2\theta = 15.74^\circ$$

Antenna pattern measurements made at a frequency of 1 megacycle per second gave a pattern with a total included angle between the half-power points of 13.2 degrees for this lens-transducer combination. The agreement is adequate to demonstrate the usefulness of this simple calculation in estimating the antenna pattern for the lens.

The impedance ratio between polystyrene and water is about 1.7/1, so some reflection will occur inside of the lens. This reflection is troublesome if short pulses are being transmitted, since the reflected wave inside the lens reappears after a time delay, Δt , equal to the time required for the wave to make a round trip in the lens. This difficulty can be overcome by using a long lens as shown in Figure 5-19. In this case, the internal reflection is delayed long enough so as not to interfere with the main transmitted pulse.

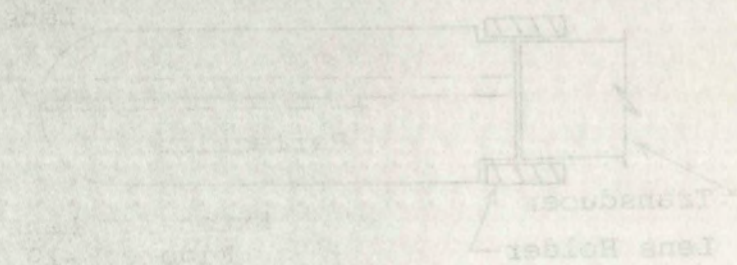


particular lens... measured from the... the transducer is

which gives a... points of

Antenna pattern... megacycles per second... angle between the... this lens-transducer... adequate to demonstrate... calculation in estimating the

The impedance... is about 1.7... the lens. This... are being transmitted... lens response... required for the wave to... This difficulty... shown in Figure... election is delayed... with the main transducer



Photographs of these polystyrene lenses are shown as Items 5 through 8 in Figure 5-17.

There is a slight power advantage gained in using a larger transducer and the polystyrene lens of this type, compared with a smaller transducer element which will give the same beamwidth. For example, consider a 1/2 inch diameter, 1 mc/sec flat disk transducer operating in water with the 1 inch diameter polystyrene lens described above. The half-power beamwidth is about 13 degrees as determined by measurement. A corresponding half-power beamwidth is obtained with a flat disk transducer 0.278 inch in diameter. Now, if both transducers are connected across the same impedance, have equivalent driving voltages, and have equivalent antenna patterns (the patterns are nearly the same) there will be a 5.1 db power advantage using the larger transducer. It is necessary to subtract the losses in the lens due to reflections which amount to about 0.6 db for a round trip through the lens. This leaves a net advantage of 4.5 db for the larger transducer and lens as compared to the smaller transducer.

5.82 Reflectors - Several different reflectors were constructed using 18 gauge copper. It was found that a pressure release substance such as a plastic or rubber tape on the back side of the reflector greatly improved the efficiency of operation. In each case the antenna pattern was measured using a long transmitter pulse to

Photographs of these polystyrene lenses are shown as

items 5 through 8 in Figure 5-17.

There is a slight power advantage gained in using

a larger transducer and the polystyrene lens of this type,

compared with a smaller transducer element which will give

the same beamwidth. For example, consider a 1/2 inch

diameter, 1 mc/sec flat disk transducer operating in

water with the 1 inch diameter polystyrene lens described

above. The half-power beamwidth is about 15 degrees as

determined by measurement. A corresponding half-power

beamwidth is obtained with a flat disk transducer 0.278

inch in diameter. Now, if both transducers are connected

across the same impedance, have equivalent driving voltages,

and have equivalent antenna patterns (the patterns are

nearly the same) there will be a 5.1 db power advantage

using the larger transducer. It is necessary to subtract

the losses in the lens due to reflections which amount

to about 2.5 db for a round lens through the lens. This

leaves a net advantage of 2.6 db for the larger transducer

and lens as compared to the smaller transducer.

5.82 Reflectors - Several different reflectors were

constructed using 18 gauge copper. It was found that a

pressure release substance such as a plastic or rubber

tape on the back side of the reflector greatly improved

the efficiency of operation. In each case the antenna

pattern was measured using a long transmitter pulse to

obtain steady state conditions. The transient response was also observed by using a short transmitter pulse. Figure 5-20 illustrates a reflector which produces a fan shaped beam.

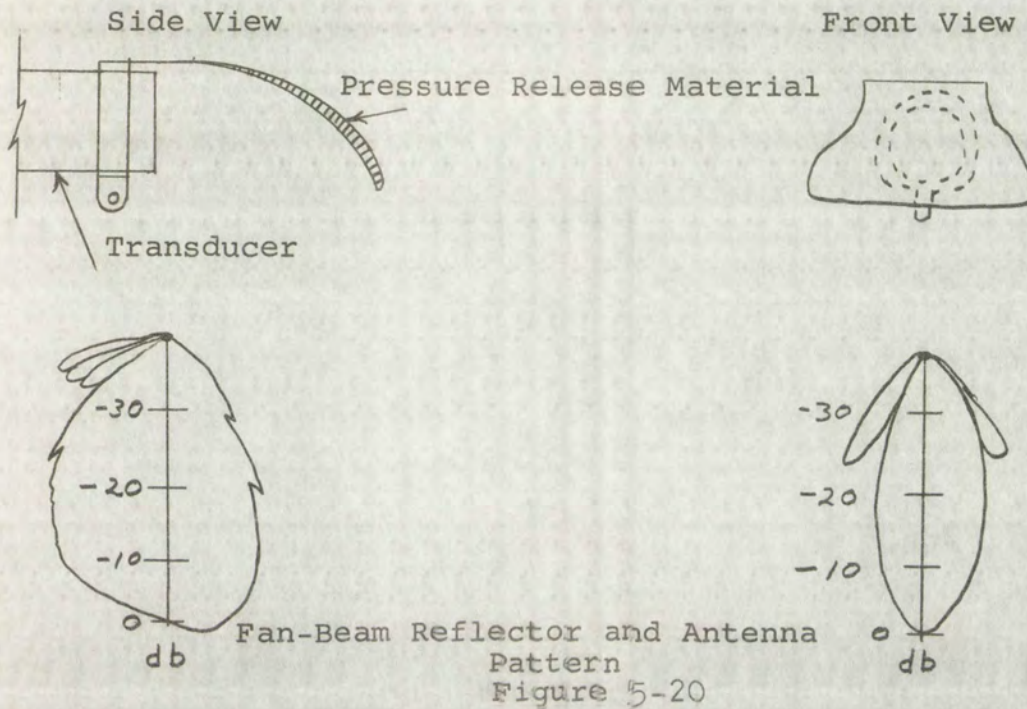


Figure 5-21 shows another reflector of smaller size which is designed to spread the beam in all directions by use of a convex reflecting surface.

A wide variation in the pattern is obtained by making small changes in the shape of the reflector. The reflectors are satisfactory for long pulses and for cw waves; however, their size is large compared to a short pulse length so transient effects are troublesome. This effect may be used to advantage in another manner, however, as a means of studying effects of very short electromagnetic pulses in a large antenna structure.

obtain steady state conditions.

was also observed by using a fan shaped beam.

Figure 5-10 illustrates the results of the experiment.

fan shaped beam.

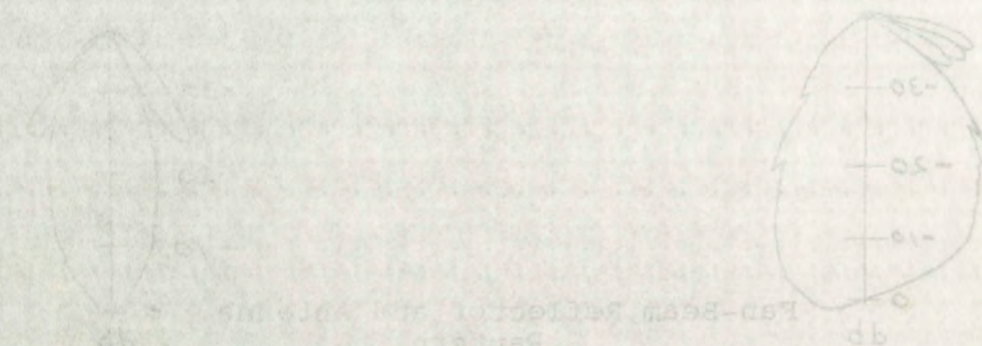
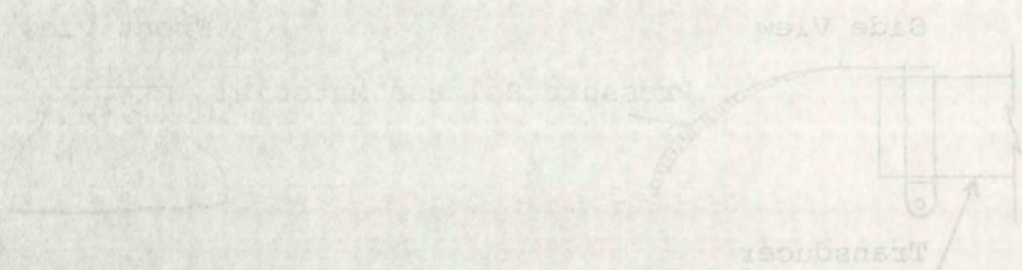


Figure 5-11 shows another reflection of the fan beam.

which is designed to spread the beam in all directions by

use of a convex reflecting surface.

A wide variation in the output is obtained by

making small changes in the shape of the reflector. The

reflectors are satisfactory for long pulses and for

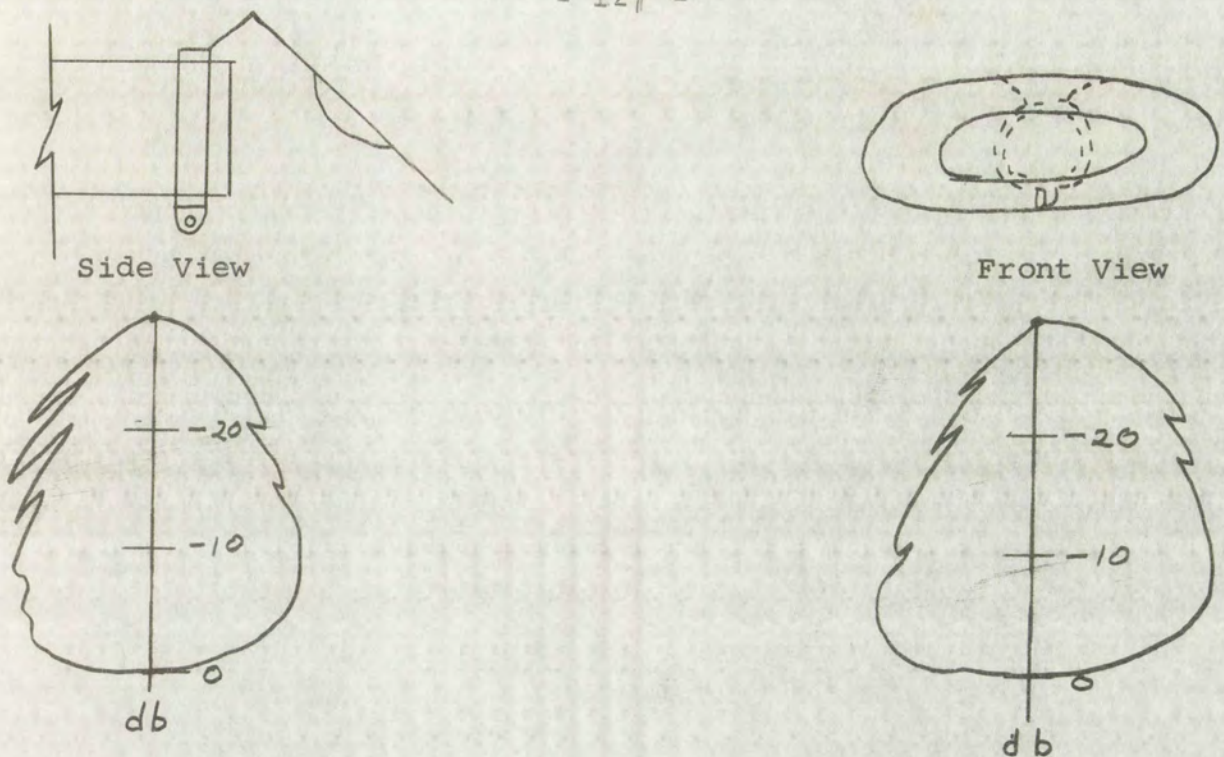
waves; however, there are some problems for a short

pulse length as the length of the pulse is increased. This

effect may be used to advantage in a certain manner, however.

as a means of studying the effects of the pulse length on

pulses in a large antenna system.

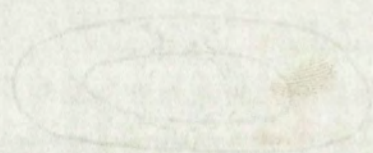


Broad-Beam Reflector and Antenna Pattern

Figure 5-21

5.83 Aperture Control - Flat disk transducers on the order of $\frac{1}{2}$ inch in diameter have relatively narrow antenna patterns at frequencies near 1 mc/sec. A broader pattern can be obtained by reducing the size of the transducer. It is possible to use a mask over the face of the disk to give an effective reduction in the size of transducer. This allows one transducer to provide several different patterns just by changing the size of the hole in the aperture mask.

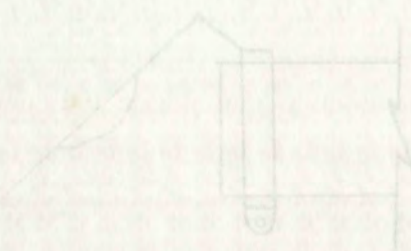
Figure 5-22 shows a cross sectional view of an aperture mask using a cork washer and a brass plate. The wave front is distorted as it passes into the piezoelectric material as shown in the figure. This is undesirable



Front View



Side View



Front View



Side View

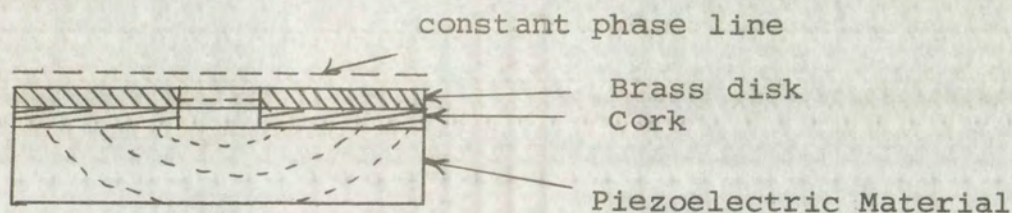
Figure 5-22 Broad-Beam Reflector and Antenna Pattern

5.3 Aperture Control - This disc transducer on the

order of $\frac{1}{8}$ inch in diameter has a relatively narrow antenna pattern at frequencies near 1 megacycle. A broader pattern can be obtained by reducing the size of the transducer. It is possible to use a mask over the face of the disk to give an effective reduction in the size of transducer. This allows the transducer to provide several different patterns just by changing the size of the hole in the acoustic mask.

Figure 5-23 shows a cross sectional view of an aperture mask using a cork washer and a brass plate. The wave front is distorted as it passes into the transducer material as shown in the figure. This is undesirable

since it introduces some distortion in the received signal. A similar effect occurs when the transducer acts as a transmitter. In this case the cork restrains the disk slightly and prevents the surface velocity from being uniform.



Aperture Mask

Figure 5-22

Aperture masks have been used successfully at a frequency of 200 kc/sec by experimenters at Melpar, Incorporated.¹

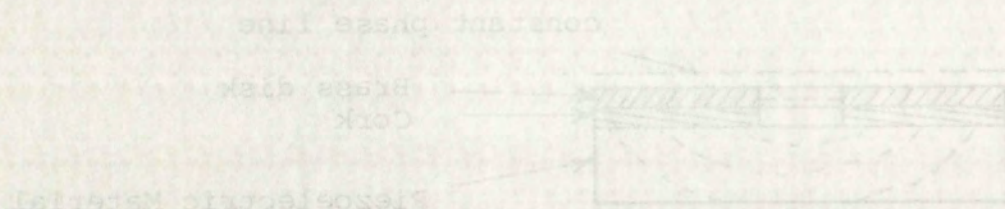
An alternate method of aperture control consists of using a collimator to concentrate the radiated waves into a small aperture. Two devices of this type were investigated. The first collimator was machined from brass using an exponential taper along the length of the device. The second collimator was constructed of 18 gauge copper and was conical in shape except near the transition region to the aperture. These collimators are shown in cross sectional view in Figure 5-23.

¹Maestri, op. cit.

since it introduces some distortion in the received signal.

A similar effect occurs when the transmitter acts as a transmitter. In this case the cork resists the disk slightly and prevents the surface velocity from being

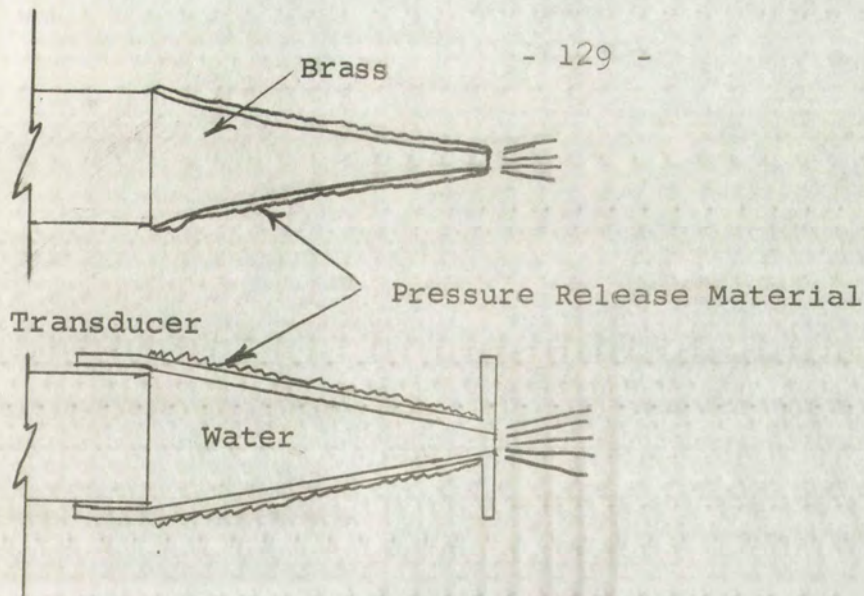
uniform.



Aperture Mask

Figure 5-12

Aperture masks have been used successfully at a frequency of 200 Mc/sec by experimenters at Melpar, Incorporated. An alternate method of aperture control consists of using a collimator to concentrate the radiated waves into a small aperture. Two devices of this type were investigated. The first collimator was machined from brass and was conical in shape except near the transition region and was conical in shape except near the transition region. The second collimator was constructed of 18 gauge copper and was conical in shape except near the transition region to the aperture. These collimators are shown in cross sectional view in Figure 5-13.



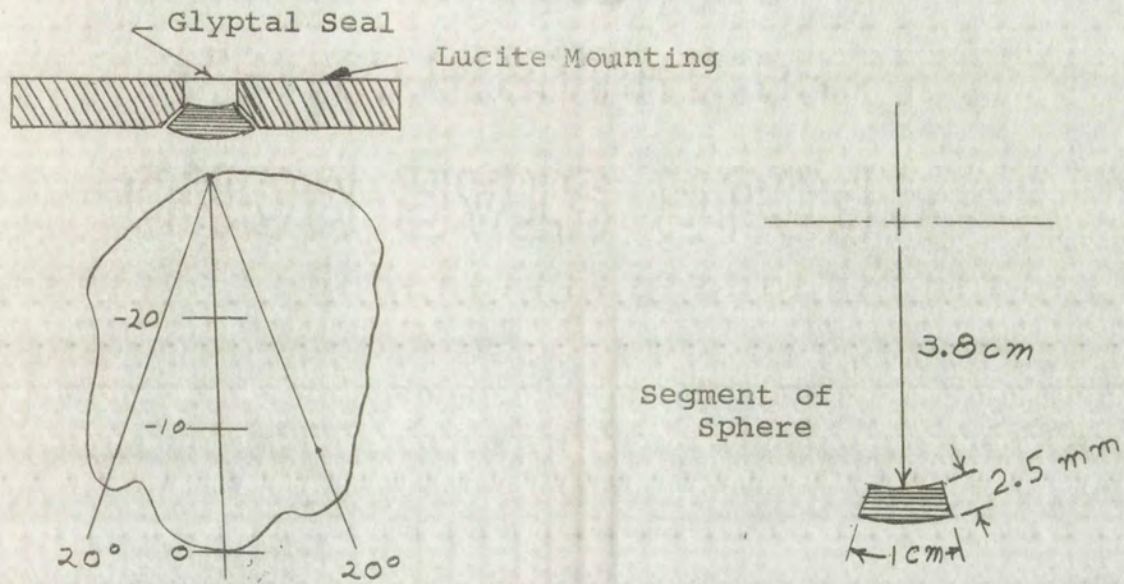
Collimators

Figure 5-23

Both collimators are unsatisfactory for pulse work because of reflections which occur at the aperture; however, they can be used successfully for cw transmission. The brass collimator has a large impedance mismatch to water which results in a pressure transmission coefficient of less than 0.1.

5.84 Shaped Transducers¹ - The most satisfactory method of obtaining a specific antenna pattern without the usual troublesome transient effects is to use a shaped transducer. In this case the piezoelectric material is molded into a specific shape before being mounted. Satisfactory broad beam patterns can be obtained using a segment of a spherical shell for the transducer element.

¹Lane, A.L., "Design Techniques for a High Frequency Transducer with a Wide-Beam Searchlight Pattern," Jour. Acoust. Soc. of Am., Vol. 25, 1953, p. 697.



Antenna Pattern at 1 mc.

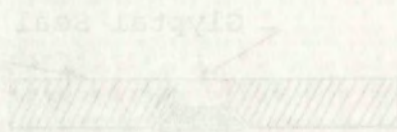
Shaped Transducers

Figure 5-24

A small shaped transducer was prepared using a segment from a barium titanate hemispherical shell as shown in Figure 5-24.¹ This transducer has a pattern that is considerably broader than would be obtained by a flat disk of similar dimensions. Also the deviations from a flat surface are small enough compared to a short pulse length that transient effects are negligible.

5.85 Combinations of Sources - This method of pattern control works well and is frequently used in situations where the total size of the antenna is not an important

¹This work was performed by Ray Tillery at the University of New Mexico in 1961 and will appear in a report at a later date.



Antenna pattern at 1 mc.

Shaped Transducer

Figure 5-11

A small shaped transducer was prepared using a segment from a barium chloride piezoelectric shell as shown in Figure 5-11. This transducer has a pattern that is considerably broader than would be obtained by a flat disk of similar dimensions. Also the deviations from a flat surface are small enough compared to a short pulse length that transient effects are negligible.

5.65 Comparison of sources - The method of pattern control works well and is frequently used in situations where the total size of the antenna is not so important.

¹This work was performed by Ray Willett at the University of New Mexico in 1951 and will appear in a report at a later date.

factor. In the modeling experiments considered in this investigation, however, the target must be in the radiation field of the antenna in order to obtain proper results. Since the size of the water tank is limited, the overall antenna size must remain small so combinations of sources have not been used.

5.9 Recommendations for an Acoustic Simulator

The acoustic simulator can be designed as a special purpose analog device for a particular radar system, or it can be designed to model a wide variety of systems. Naturally the special purpose device can be less elaborate since it models only a particular type of radar.

An acoustic simulator for general use is restricted by the size of the water tank and by the power limitations of the equipment. Geometrical conditions of similitude require that the physical dimensions of a pulse packet be linearly scaled in the model system. This means that pulse length in space will be the same percentage of the total range as in the real system. The geometrical similitude requirements insure that a properly shaped wave front impinges on the target and that the proper return pulse shape is maintained (this assumes of course that a properly modeled target is used).

A tank that measures 4' x 4' x 3' can be used satisfactorily for many model experiments. This tank size is adequate for such experiments as:

- (1) making scatter patterns from objects with different geometric shapes,
- (2) measuring the reflection coefficient of different materials,
- (3) measuring the absorption coefficient of materials,
- (4) measuring antenna patterns,
- (5) studying the propagation characteristics of an inhomogeneous medium, and
- (6) performing many radar system model experiments.

The total attenuation experienced in the transducer is on the order of 60 db so it is desirable to use a large source voltage. The transducers are "voltage actuated" devices and much of the available transmitter power is lost in the impedance matching network. It is desirable to drive the transducers with a hundred volts or more when they are matched to the transmission line impedance. When a 93-ohm system is used a pulse power of 242 watts is required to establish a potential of 150 volts rms on the transducer. In a short pulse system the average power is, of course, much lower in value. The attenuation due to losses in the water is not appreciable at frequencies below 1 mc/sec. When using a typical rough target, an antenna beamwidth of six degrees, a range of 1 meter in water and a long transmitter pulse, the overall attenuation will be on the order of 100 db at a frequency of 1 mc/sec. This value, of course, will vary considerably with different targets, pulse widths and antenna patterns.

(1) making scatter patterns from objects with different

geometric shapes,

(2) measuring the reflection coefficient of different

materials,

(3) measuring the absorption coefficient of materials,

(4) measuring antenna patterns,

(5) studying the propagation characteristics of an

inhomogeneous medium, and

(6) performing many radar system model experiments.

The total attenuation experienced in the transducer

is on the order of 60 db so it is desirable to use a large

source voltage. The transducers are "voltage actuated"

devices and much of the available transmitter power is lost

in the impedance matching network. It is desirable to drive

the transducers with a hundred volts or more when they are

matched to the transmission line impedance. When a 95-ohm

system is used a pulse power of 741 watts is required to

establish a potential of 150 volts rms on the transducer.

In a short pulse system the average power is of course much

lower in value. The attenuation due to losses in the water

is not appreciable at frequencies below 1 mc/sec. When

using a typical rough target, an antenna beamwidth of six

degrees, a range of 1 meter in water and a 100 transmitter

pulse, the overall attenuation will be on the order of 100

db at a frequency of 1 mc/sec. This value, of course, will

vary considerably with different targets, pulse widths and

antenna patterns.

The desirable frequency range for use in the acoustic model is between 0.2 and 2 mc/sec. At these frequencies the wavelengths are approximately 7.5 mm and 0.75 mm, respectively. At the lower frequencies wide beam antenna patterns can be obtained from flat disk transducers while at the high frequencies the patterns are generally quite narrow. When modeling short-pulse radar the lower model carrier frequencies frequently do not provide enough cycles per pulse to define the pulse shape. In this case it is necessary to use a higher carrier frequency.

The "strip-film" camera and oscilloscope provide a convenient method of recording data for theoretical investigations. The film records the maximum amount of information that is available and provides a permanent record. It would be advantageous, however, to have automatic readout devices that would indicate mean values of a series of pulses at a particular delay time in the pulse, as well as to make autocorrelations and probability distribution curves. These devices would greatly speed up the data reduction process and would increase the usefulness of the acoustic simulator.

Provisions must be made for providing linear transducer motion over the target. An appropriate device would be capable of moving the transducer on a straight line path in a plane at a uniform velocity that is adjustable between a few mm per second and 15 cm per second. The length of

The following is a description of the model as shown in Figure 1. The model is a rectangular block with a width of 10 cm and a height of 10 cm. The top surface is a square with a side length of 10 cm. The front face is a rectangle with a width of 10 cm and a height of 10 cm. The right side face is a rectangle with a width of 10 cm and a height of 10 cm. The bottom surface is a square with a side length of 10 cm. The left face is a rectangle with a width of 10 cm and a height of 10 cm. The model is shown in a perspective view. The top surface is a square with a side length of 10 cm. The front face is a rectangle with a width of 10 cm and a height of 10 cm. The right side face is a rectangle with a width of 10 cm and a height of 10 cm. The bottom surface is a square with a side length of 10 cm. The left face is a rectangle with a width of 10 cm and a height of 10 cm. The model is shown in a perspective view.

a typical path in the model is 100 cm. It is necessary to be able to reproduce a particular path to within less than a tenth of a wavelength. This allows fading records to be duplicated by making another identical run over the target.

a typical path in the model is 100 cm. It is necessary to
be able to reproduce a particular path to within less than
a tenth of a wavelength. This allows fading records to
be duplicated by making another identical run over the
target.

CHAPTER VI

EXPERIMENTAL RESULTS

Experimental results, obtained using the acoustic simulator, are tabulated and compared in this chapter with theoretical and experimental results for radar and altimeter systems. Certain characteristics of pulse radar return signals are caused by a combination of geometrical factors involving the antenna pattern, altitude, and pulse width. These characteristics are demonstrated in Section 6.1 by several pulse-by-pulse photographic records.¹

The most outstanding characteristic of electromagnetic signals scattered from a rough surface is the fading that occurs in nearly all cases. Fading is defined as the fluctuation in the envelope of the signal which is caused by interference between the signal components. The fluctuations in the signal envelope are classified as "intrapulse fading" and "interpulse fading" for the case of pulsed radar.²

¹See Appendix A for a discussion of the effects of pulse and antenna geometry.

²"Intrapulse fading" is defined here as the fluctuation which occurs in the envelope of a single return pulse when the target is irregular. It is an effect caused by the pulse spreading over the target. "Interpulse fading" is defined here as the fluctuations which occur in the envelopes of consecutive return pulses and is caused by relative motion between the target and the radar.

EXPERIMENTAL RESULTS

Experimental results, obtained by means of a pulse simulator, are presented and compared with theoretical and experimental results for various systems. Certain characteristics of pulse propagation signals are caused by the combination of various factors involving the antenna pattern, distance, and pulse width. These characteristics are demonstrated in section 3.1. Several pulse-by-pulse propagation results are presented. The most outstanding characteristics of electromagnetic signals scattered from a rough surface are the following: occurs in nearly all cases; fading is defined as the fluctuation in the envelope of the signal which is caused by interference between the signal components. The fluctuations in the signal envelope are characterized as "fading" and "interference fading" for the case of "interference fading" and "interference fading" for the case of "interference fading".

¹See Appendix A for a discussion of the effect of pulse and antenna geometry.

²Interference fading is defined here as the fluctuation which occurs in the envelope of a signal which is caused by the interference of two or more signals. The term "interference fading" is used here as the fluctuations which occur in the envelope of a signal which is caused by the interference of two or more signals. The term "interference fading" is used here as the fluctuations which occur in the envelope of a signal which is caused by the interference of two or more signals.

It has been shown that the returned scatter power for the case of antenna beam-width limiting of the illuminated area varies as the inverse square of the altitude, while for the case of pulse-width limiting of the illuminated area, the peak-returned scatter power varies as the inverse cube of the altitude.¹ Experimental results which are in agreement with these predictions are shown in Figures 6-10 and 6-11.

The mean backscattering radar cross section per unit area, as a function of the angle of incidence, is determined by the nature of the scattering surface at a particular frequency. The scattering cross sections for different terrains have been modeled using sand-covered plywood targets. Some results of these experiments are shown in Figure 6-15.

6.1 Geometrical Effects

A series of photographs, made using a "strip-film" camera, can best illustrate the effects of pulse and antenna geometry on the return signal. The photographs are samples of return signals for runs made over a rough target at a model altitude of 1/2 meter, which scales to a real system altitude of 330 wavelengths for the particular target used (based on linear modeling). A photograph

¹Moore and Williams, op. cit.

It has been shown that the returned scatter power

for the case of constant pulse width lighting of the illumin-

ated area varies as the inverse square of the altitude,

while for the case of pulse-width limiting of the illuminated

area, the peak-returned scatter power varies as the inverse

cube of the altitude. Experimental results which are in

agreement with these predictions are shown in Figures 6-10

and 6-11.

The mean backscatter radar cross section per unit

area, as a function of the angle of incidence, is determined

by the nature of the scattering surface at a particular

frequency. The scattering cross sections for different

targets have been modeled using sand-covered plywood car-

pets. Some results of these experiments are shown in

Figure 6-12.

6.1 Geometrical Effects

A series of photographs, made using a "strip-film"

camera, can best illustrate the effects of pulse and

antenna geometry on the return signal. The photographs

are samples of return signals for runs made over a rough

target at a model altitude of 1/2 meter, which scales to

a real system altitude of 350 wavelengths for the parti-

cular target used (based on linear modeling). A photograph

of the target is shown in Figure 5-11. The model carrier frequency is 1 mc/sec with a wavelength of about 1.5 mm in water. The sweep time on the oscilloscope is 50 μ s for the short transmitter pulse and is 150 μ s for all the other pulses shown in this section. The peak transmitter power is constant for all cases. Three separate amplitude scales apply to the pulses when they are grouped as follows:

- (1) All transmitter pulses,
- (2) All received pulses using the narrow-beam antenna, and
- (3) All received pulses using the wide-beam antenna.¹

In all cases the antenna is oriented with the axis normal to the plane of the target area. The narrow-beam and wide-beam antenna patterns are shown in Figures 5-18 and 5-21, respectively.

The transmitter pulses are shown in Figure 6-1 for pulses of width 10 μ s and 100 μ s.² In both cases the signals are obtained by photographing reflections from a smooth glass target. Since the target is smooth, the reflections are specular in nature and show the correct

¹The terms "narrow-beam" and "wide-beam" antenna, as used in this chapter, refer to the antennas with a 6 degree beam width and a 15 degree beam width, respectively (measured between the -3db points on the pattern).

²The 10 μ s and 100 μ s pulses are referred to as the "narrow pulse" and the "wide pulse" respectively in this chapter.

of the crystal is shown in Figure 1. The crystal is
frequency is 100 MHz. The crystal is
water. The crystal is 100 MHz. The crystal is
the short circuit. The crystal is 100 MHz. The crystal is
pulses show in Figure 2. The crystal is 100 MHz. The crystal is
is constant for all values of the crystal. The crystal is 100 MHz. The crystal is
apply to the crystal. The crystal is 100 MHz. The crystal is

(1) All values of the crystal are 100 MHz. The crystal is
(2) All values of the crystal are 100 MHz. The crystal is
antenna and
(3) All values of the crystal are 100 MHz. The crystal is
In all cases the antenna is 100 MHz. The crystal is
to the plane of the antenna. The antenna is 100 MHz. The antenna is
beam antenna patterns are shown in Figure 3. The antenna is 100 MHz. The antenna is
respectively.

The antenna is 100 MHz. The antenna is
pulses of width 100 MHz. The antenna is 100 MHz. The antenna is
signals are shown in Figure 4. The antenna is 100 MHz. The antenna is
smooth glass surface. The antenna is 100 MHz. The antenna is
reflections are shown in Figure 5. The antenna is 100 MHz. The antenna is

The antenna is 100 MHz. The antenna is
used in this experiment. The antenna is 100 MHz. The antenna is
beam width and a 100 MHz. The antenna is 100 MHz. The antenna is
between the two points. The antenna is 100 MHz. The antenna is
The antenna is 100 MHz. The antenna is
"narrow pulse" and "wide pulse". The antenna is 100 MHz. The antenna is
Chapter

pulse shape. The short pulse described in this section is narrow enough to illustrate the effects of pulse width limiting of the illuminated area on the rough target and the wide pulse is broad enough to show effects of beam width limiting.

Figure 6-2 illustrates the appearance of a typical series of return pulses using a short transmitter pulse and a narrow beam antenna. There is no antenna motion so all pulses are of the same shape. Intrapulse fading is evident, however, and is caused by the changing population of scatterers as the pulse spreads over the target. The amount of pulse-stretching observed for this example is limited by the narrow antenna pattern.

Figure 6-3 shows return pulses under the same conditions as those described for Figure 6-2 except for relative motion between the antenna and target. The intrapulse fading is still evident as in the preceding case, and in addition interpulse fading exists. The continuing intrapulse fading which exists throughout the received pulse is characteristic of a short-pulse radar.

Figure 6-4 illustrates the return signals when wide transmitter pulses and a narrow beam antenna are used. In this case the illuminated region is limited by the antenna pattern so the term "beam-width limiting" is applied. The intrapulse fading is limited in this case to the leading and trailing edges of the received pulse where the population of scatterers is changing. The

relatively flat middle portion of the pulse exists for the interval during which the group of scatterers contributing to the return is not changing. Here, as in Figure 6-2, there is no interpulse fading since there is no relative motion between the antenna and the target.

Figure 6-5 shows return pulses under the same conditions as for Figure 6-4 except the antenna is in motion. The obvious effect on the broad pulse of the interpulse fading is to cause the flat portion in the middle of the pulse to fade as a unit. This is again characteristic of beam-width limiting of the illuminated area.

The return pulses, shown in Figure 6-6, were made using a wide beam antenna, narrow pulses and no relative antenna velocity with respect to the target. The noticeable effect of the wide beam antenna is to lengthen or stretch the received pulse. The intrapulse fading is of the same character as that observed with the narrow beam antenna and indicates the effect of the illuminated region spreading over the target area. Figure 6-7 shows a similar situation except interpulse fading is introduced by antenna motion.

Figure 6-8 shows a series of return pulses using the wide beam antenna and wide transmitter pulse. In this case the received pulse is stretched a great deal because of the wide antenna pattern. Intrapulse fading, however, still

relatively flat signal pattern in the interval during which the signal is not changing. To the extent that there is no interference between the antenna and the signal, motion between the antenna and the signal.

Figure 0-5 shows a series of plots of the received pulse as for Figure 0-4, but with the antenna moving.

The obvious effect of the motion is that the received pulse is no longer a single pulse, but is spread out over a range of beam-width limits of the antenna. The result is a spread-out pulse, and the spread-out pulse is wider than the original pulse.

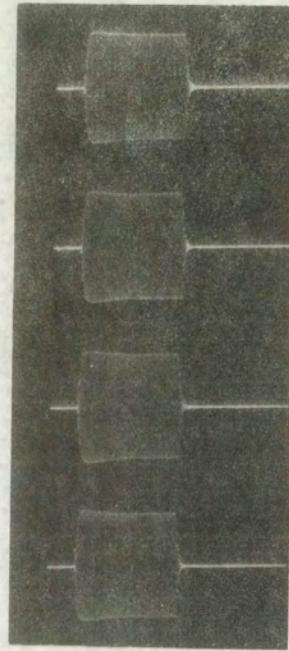
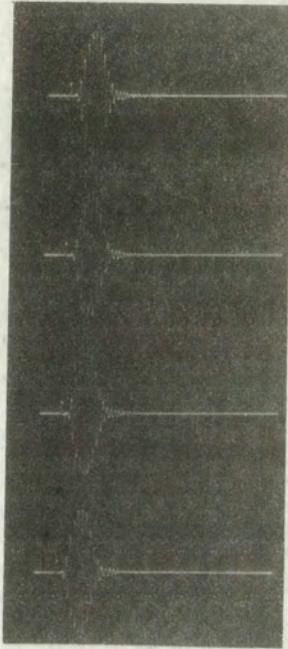
Using a wide beam antenna, the spread-out pulse is wider than the original pulse, and the spread-out pulse is wider than the original pulse. The spread-out pulse is wider than the original pulse, and the spread-out pulse is wider than the original pulse.

attenuation the received pulse, the spread-out pulse is wider than the original pulse, and the spread-out pulse is wider than the original pulse. The spread-out pulse is wider than the original pulse, and the spread-out pulse is wider than the original pulse.

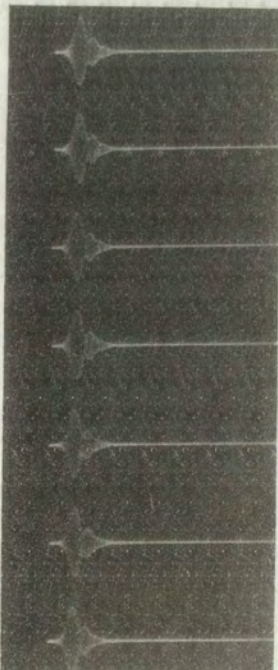
spreading over the larger area, the spread-out pulse is wider than the original pulse, and the spread-out pulse is wider than the original pulse. The spread-out pulse is wider than the original pulse, and the spread-out pulse is wider than the original pulse.

Figure 0-5 shows a series of plots of the received pulse as for Figure 0-4, but with the antenna moving. The spread-out pulse is wider than the original pulse, and the spread-out pulse is wider than the original pulse. The spread-out pulse is wider than the original pulse, and the spread-out pulse is wider than the original pulse.

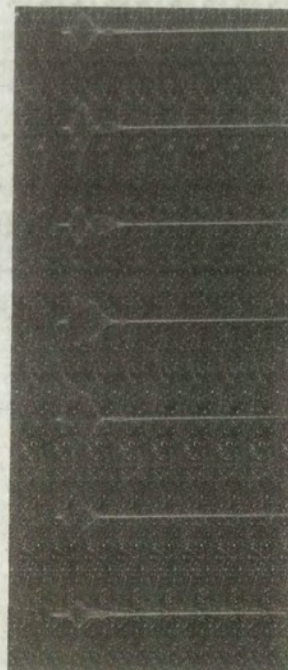
the received pulse is spread out over a range of beam-width limits of the antenna pattern. The spread-out pulse is wider than the original pulse, and the spread-out pulse is wider than the original pulse.



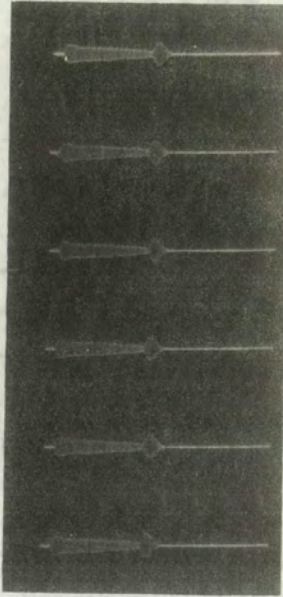
Transmitter Pulses
Fig. 6-1



Short Pulse
Narrow Beam
No Motion
Fig. 6-2



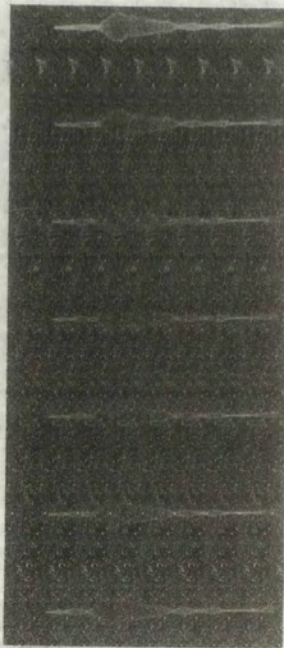
Short Pulse
Narrow Beam
Motion
Fig. 6-3



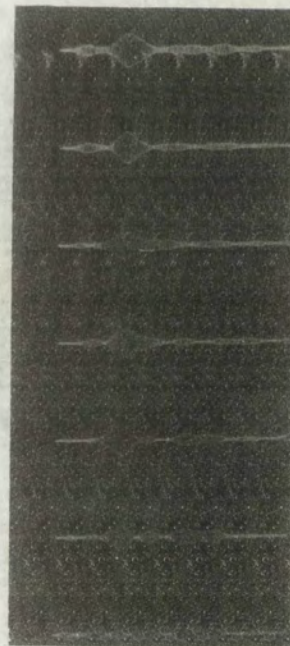
Wide Pulse
Narrow Beam
No Motion
Fig. 6-4



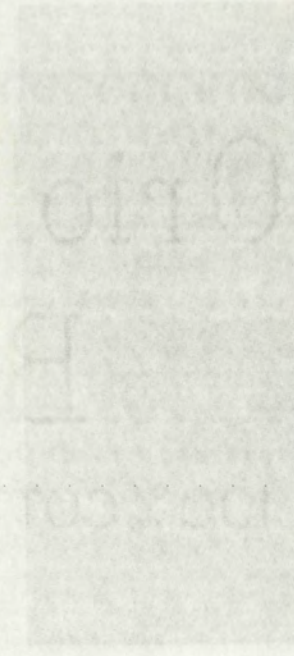
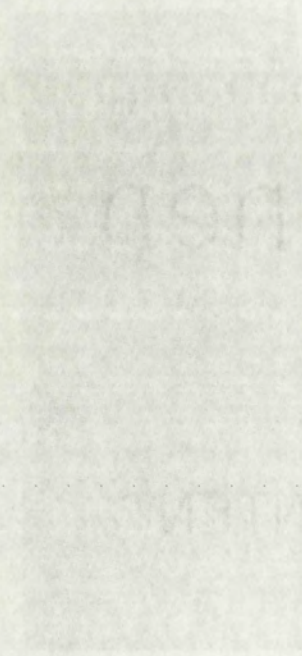
Wide Pulse
Narrow Beam
Motion
Fig. 6-5



Narrow Pulse
Wide Beam
No Motion
Fig. 6-6

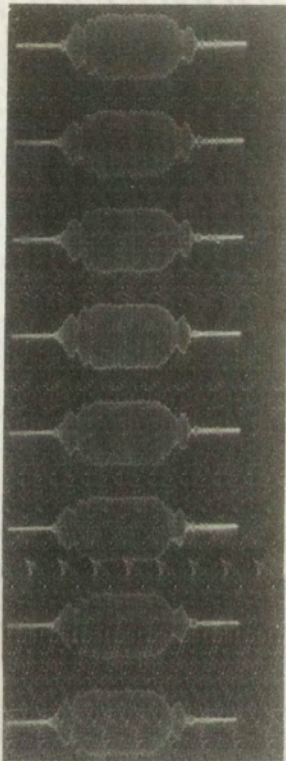


Narrow Pulse
Wide Beam
Motion
Fig. 6-7

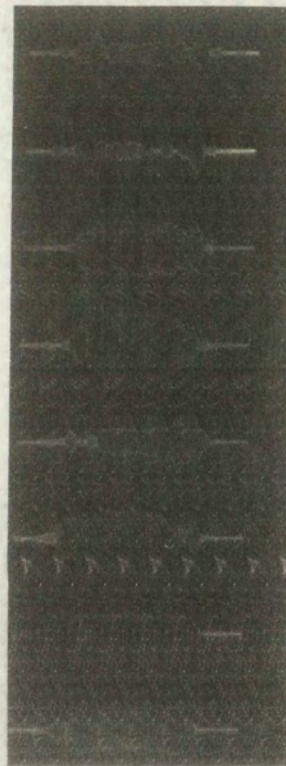


Wide Pulse
Narrow Band
No Motion
File 8-4

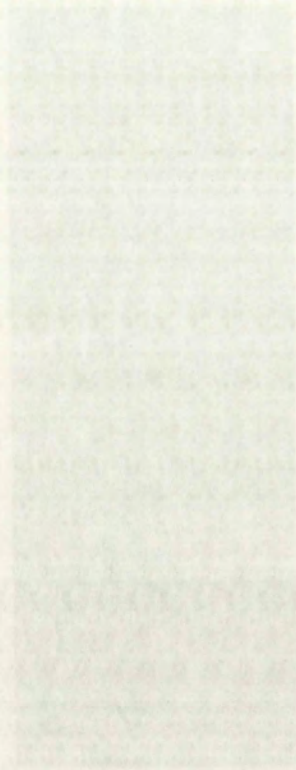
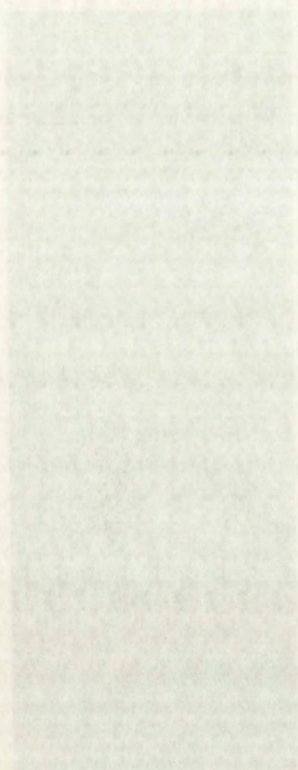
Narrow Pulse
Wide Band
No Motion
File 8-6



Wide Pulse
Wide Beam
No Motion
Fig. 6-8



Wide Pulse
Wide Beam
Motion
Fig. 6-9



W. de B. de
W. de B. de
W. de B. de
W. de B. de

W. de B. de
W. de B. de
W. de B. de
W. de B. de

shows the effects of beam width limiting. There is no interpulse fading since the antenna is stationary for this series of signals.

Figure 6-9 represents similar conditions to those described for Figure 6-8 except antenna motion is included. The interpulse fading is characteristic of beam width limiting again, since the transmitter pulse is wide.

Another aspect of the geometrical effects on the returned signal concerns the variation of signal with altitude. The return power varies inversely as the square of the altitude when the reflection is from a smooth surface and the altitude is great enough for the antenna to be treated as a point source. This result, which depends on the spherical geometry, can be used as a check on the accuracy of the measurements made with the acoustic simulator. A typical experimental curve is shown in Figure 6-10.

When scattering from a rough surface is considered, the return signal will not vary inversely with the square of the altitude for all cases. It has been shown by Moore and Williams¹ that the scattered signal power varies inversely with the square of the altitude for the case of beam-width-limited illumination and varies inversely as the cube of the altitude for the case of pulse-length-

¹Moore, R.K. and Williams, C.S., "Radar Terrain Return at Near-Vertical Incidence," Proc. IRE, Vol. 45, No. 2, Febr. 1957, pp. 228-28. The signal power is measured at the delay time in the pulse where the mean returned pulse has peak amplitude.

show the effect of the pulse rate on the signal
of signals

Figure 1 shows the effect of the pulse rate on the signal
The signal is shown as a function of the pulse rate

Figure 2 shows the effect of the pulse rate on the signal
The signal is shown as a function of the pulse rate

Figure 3 shows the effect of the pulse rate on the signal
The signal is shown as a function of the pulse rate

Figure 4 shows the effect of the pulse rate on the signal
The signal is shown as a function of the pulse rate

Figure 5 shows the effect of the pulse rate on the signal
The signal is shown as a function of the pulse rate

Figure 6 shows the effect of the pulse rate on the signal
The signal is shown as a function of the pulse rate

limited illumination. The distinction between beam-width and pulse-length limiting of the illuminated area is a function of altitude¹ and is given by

$$1 + \frac{v\tau}{2h} = \sec \theta_0 \quad (6-1)$$

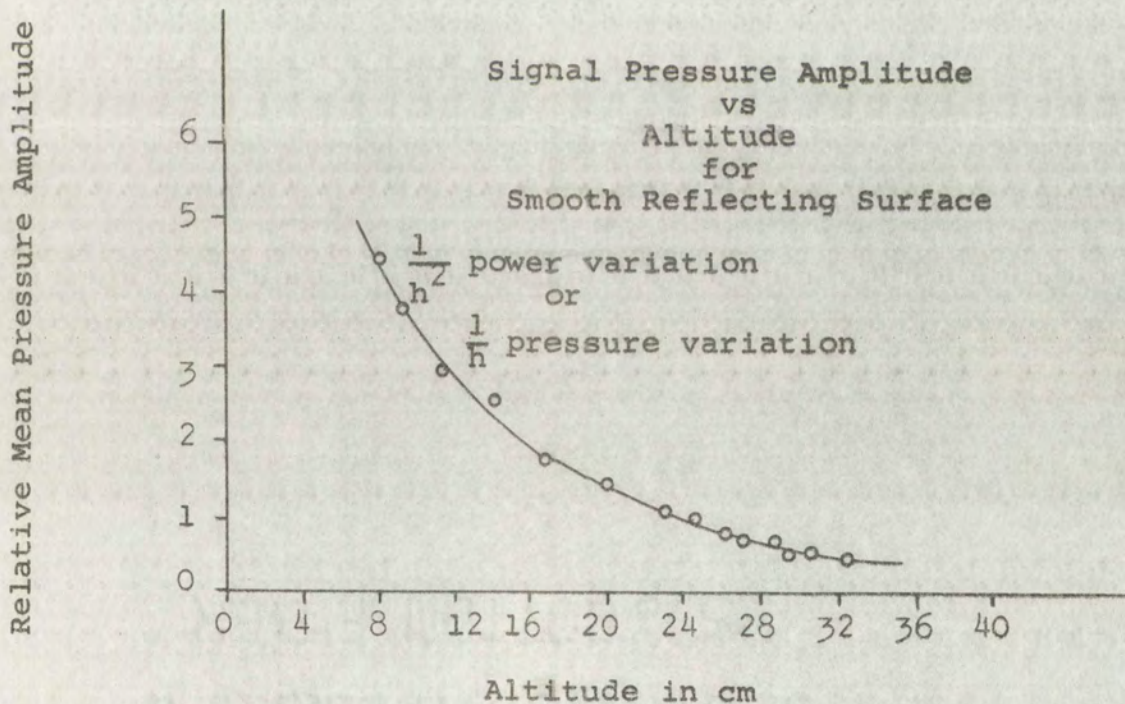
where

v is the velocity of propagation,

τ is the pulse width,

h is the altitude, and

θ_0 is the effective half-angle of the antenna pattern.



Signal vs Altitude over Smooth Surface

Figure 6-10

¹Ibid.

limited illumination. The distinction between beam-width

and pulse-length limiting of the illuminated area is a

function of altitude¹ and is given by

$$(6-1) \quad 1 + \frac{vT}{2h} = \sec \theta$$

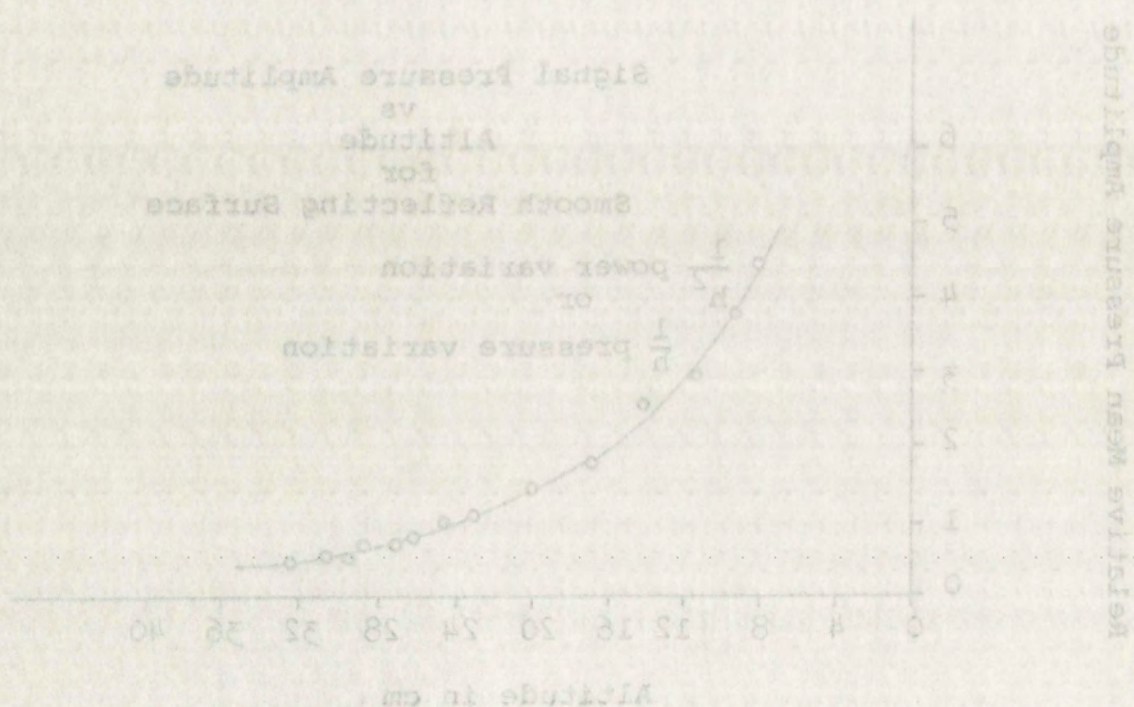
where

v is the velocity of propagation,

T is the pulse width,

h is the altitude, and

θ is the effective half-angle of the antenna pattern.



Signal vs Altitude over Smooth Surface

Figure 6-10

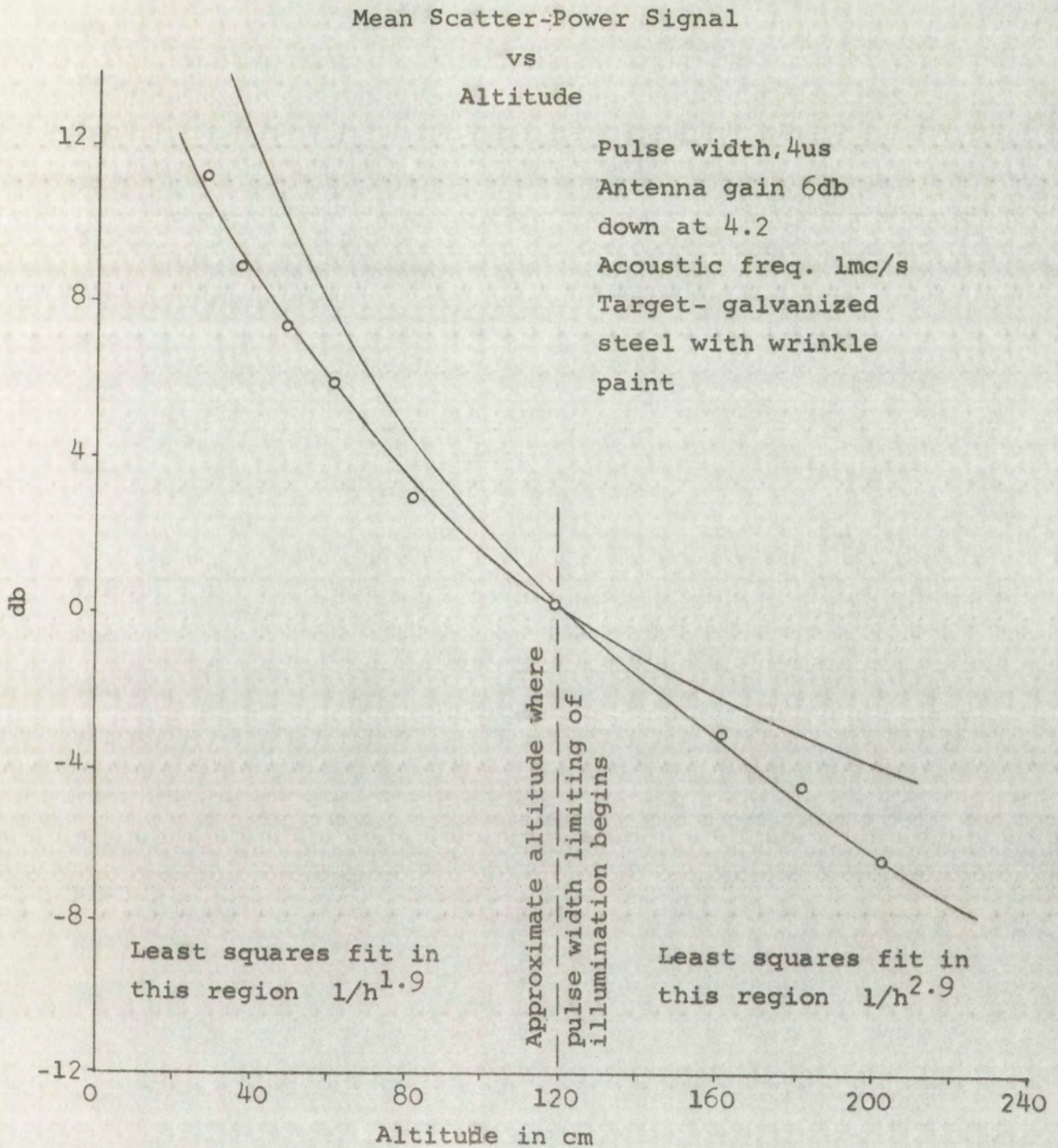


Fig. 6-11

LONG-TERM EFFECTS

Mean body weight (g)

Age (days)

Experiment 1

Least squares fit to this region $r^2 = 0.99$
 Least squares fit to this region $r^2 = 0.99$
 Least squares fit to this region $r^2 = 0.99$
 Least squares fit to this region $r^2 = 0.99$
 Least squares fit to this region $r^2 = 0.99$
 Least squares fit to this region $r^2 = 0.99$

Least squares fit to this region $r^2 = 0.99$
 Least squares fit to this region $r^2 = 0.99$
 Least squares fit to this region $r^2 = 0.99$
 Least squares fit to this region $r^2 = 0.99$
 Least squares fit to this region $r^2 = 0.99$
 Least squares fit to this region $r^2 = 0.99$

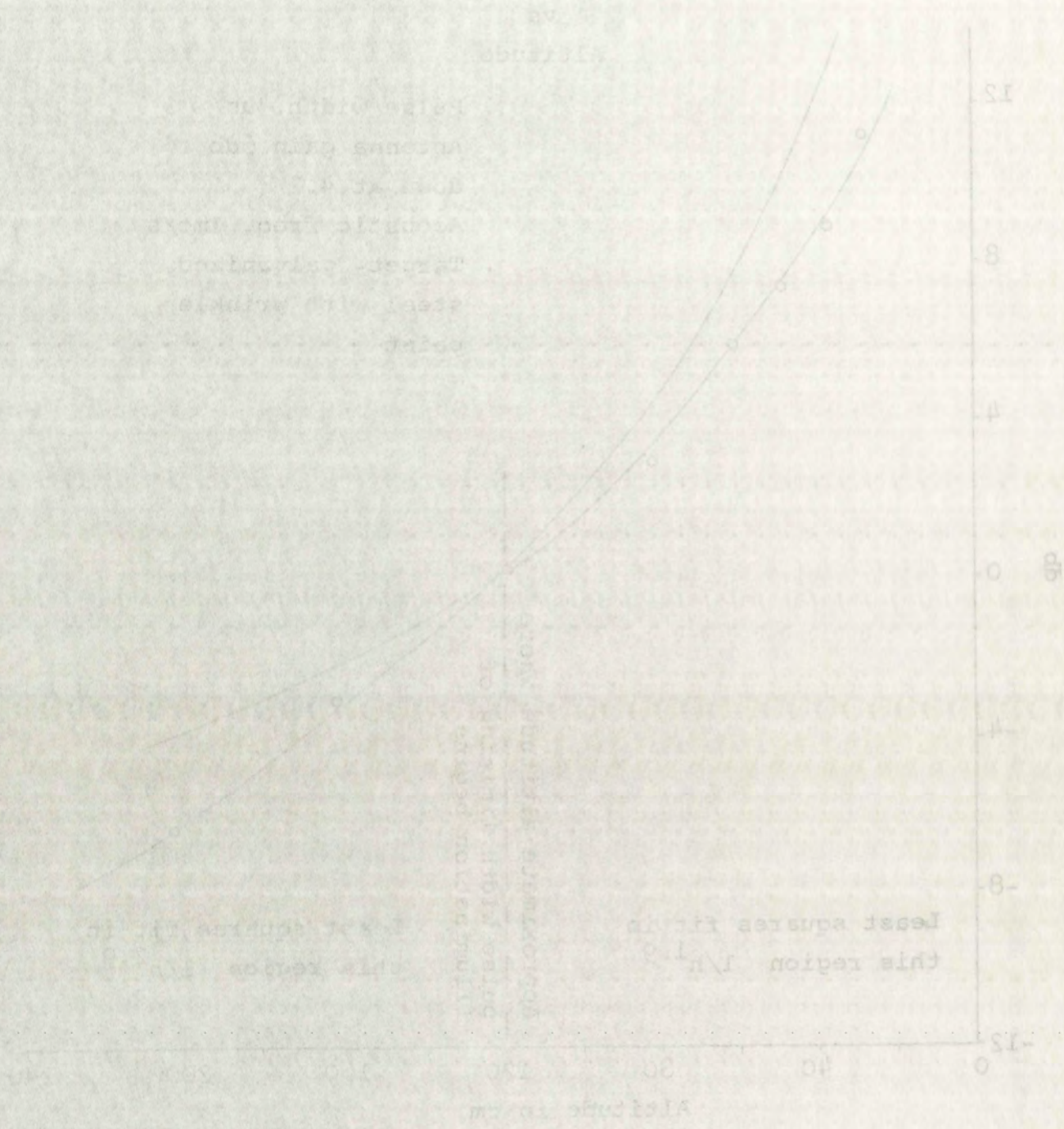


Fig. 1.1

An experiment was performed to demonstrate the change in altitude dependence from $1/h^2$ to $1/h^3$ as the illuminated region changed from the beam-width-limited to the pulse-length-limited case. A smooth steel target with a wrinkle paint surface was used in the experiment which was performed with a carrier frequency of 1 mc/sec and a pulse width of 4 μ s. The experimental points are plotted in Figure 6-11 along with curves showing a $1/h^2$ and $1/h^3$ signal variation with altitude.

6.2 Fading Statistics

The return signal, to an altimeter or other radar type device, fades because the population of scatterers in the illuminated region changes in some manner. The fading can be described in terms of two functions: (1) the probability distribution function of amplitudes,¹ and (2) The distribution over frequency of the mean squared fluctuating power in the signal (the variance or fading spectrum).² The probability distribution function for returned power can be used to obtain the probability density function, the median value, and the range of fading between two specified probability levels. The variance spectrum can be used to estimate the rate of fading of

¹Power, as used here, refers to the average value over 1 cycle of the carrier frequency.

²See Appendix A for more detail on fading and fading spectra.

the radar signal.¹

A number of comparisons is made in order to demonstrate the similarity between radar signal statistics from terrain and signal statistics from rough targets used in the acoustic simulator. In Table 6-1 the range of fading between the 5 and 95 percent levels on the first probability distribution curve is shown for several terrain targets. These data were taken from altitudes ranging from 2,000 to 12,000 feet using a wide beam antenna (about 50 degrees between half-power points) oriented vertically and using a short transmitter pulse (about 0.2 μ s).² The following figures were obtained by measuring the amplitudes of the received pulses at the point where the mean pulse had peak amplitude. This occurred when the illuminated region was within about 15 degrees of vertical at the lower altitude and within about 10 degrees of vertical at the higher altitude.³ Table 6-2 shows similar range of fading data obtained using the acoustic simulator.

The fading rate of a radar signal is determined by several factors, such as (1) the carrier frequency, (2) the antenna velocity, (3) the antenna pattern,

¹Edison, A.R., Radar Terrain Return Statistics at Near-Vertical Incidence, Univ. of New Mexico Engineering Exp. Stn. Rept. EE-35, Oct., 1960.

²Edison, A.R., Moore, R.K. and Warner, B.D., "Radar Terrain Return Measured at Near-Vertical Incidence," IRE Trans. PGAP, Vol. AP-8, No. 3, May 1960, pp. 246-54.

³Edison, A.R., Moore, R. K. and Warner, B.D., Radar Return at Near-Vertical Incidence, Univ. of New Mexico Engr. Exp. Stn. Report EE-24, Sept., 1959.

the radar signal.¹

A number of comparisons is made in order to demonstrate the similarity between radar signal statistics from terrain and signal statistics from rough targets used in the acoustic simulator. In Table 6-1 the range of fading between the 5 and 95 percent levels on the first probability distribution curve is shown for several terrain targets. These data were taken from altitudes ranging from 2,000 to 12,000 feet using a wide-beam antenna (about 50 degrees between half-power points) oriented vertically and using a short transmitter pulse (about 0.2 μ s).² The following figures were obtained by measuring the amplitudes of the received pulses at the point where the mean pulse had peak amplitude. This occurred when the illuminated region was within about 15 degrees of vertical at the lower altitudes and within about 10 degrees of vertical at the higher altitudes.³ Table 6-1 shows similar range of fading data obtained using the acoustic simulator.

The fading rate of a radar signal is determined by several factors, such as (1) the carrier frequency, (2) the antenna velocity, (3) the antenna pattern,

¹Edison, A.R., "Radar Terrain Return Statistics at Near-Vertical Incidence," Univ. of New Mexico Engineering Exp. Sta. Rept. EE-55, Oct., 1960.

²Edison, A.R., Moore, R.K., and Warner, E.D., "Radar Terrain Return Measured at Near-Vertical Incidence," IRE Trans. PGAP, Vol. AP-8, No. 3, May 1960, pp. 246-54.

³Edison, A.R., Moore, R.K., and Warner, E.D., "Radar Return at Near-Vertical Incidence," Univ. of New Mexico Eng. Exp. Sta. Report EE-57, Sept., 1963.

(4) the antenna orientation, and (5) the mean backscattering radar cross section of the target. Therefore, the fading rate is controlled by a combination of system parameters, geometrical factors, and target characteristics.

TABLE 6-1
RADAR TERRAIN RETURN DATA

Target	90% range of fading in db	
	415 mc/sec	3800 mc/sec
Desert	15.9	16.9
Ocean	15.6	17.2
Lakes	7.0	9.5
Farmland (summer)	14.7	14.2
Farmland (winter)	18.1	15.9
Forests	14.7	17.5
Residential area	16.4	15.8

An interpulse fading record is obtained by recording the value of the returned power at a particular delay time (measured from the beginning of each received pulse) in successive received pulses. The delay time is again selected to correspond to the peak of the mean return pulse. This fading record, of finite length, consists of uniformly spaced samples of a hypothetical standing wave pattern of

(A) the average of the values of the
 target cross section of the
 rate is controlled by the
 geometrical factors and the

Table 1. Geometrical factors and the

Target	
Desert	
Ocean	
Lakes	
Farmland (winter)	
Farmland (winter)	
Forests	
Residential areas	

the value of the rate of the
 (measured from the beginning of the
 successive recorded values
 selected to determine the value of
 This table shows the values of the
 spaced samples of a given value of the

power in space. The hypothetical standing wave can be "Fourier analyzed" to give a spectrum which shows how rapidly the standing wave varies in space. The spectrum can also be expressed in terms of frequency, f , by assuming an antenna velocity, v , and using the relation

$$T = \frac{S}{v} = \frac{1}{f} \quad (6-2)$$

where T is time, and S is distance. This is the variance or fading spectrum.¹

TABLE 6-2
ACOUSTIC SIMULATOR FADING DATA

Target	90% range of fading in db 1 mc/sec
Smooth galvanized steel	0
Smooth plywood	10
Plywood with sparse covering of sand particles	14
Plywood with dense covering of sand particles	17
Residential area model (lower simulated altitude than for radar data)	20

A practical method of calculating the fading spectrum from a series of data samples is: (1) to find the approximate autocorrelation of the data, and then (2) to find the

¹For more detail on fading spectra see, Edison, op. cit., EE-35. Also see Appendix A.

power is applied, the antenna is
excited and the antenna is
excited by the antenna and the
antenna is excited by the antenna
an antenna is excited by the antenna

where T is time, ω is angular frequency
of the antenna

TABLE I
Properties of the antenna

Target
Smooth polarization
Smooth polarization
Plywood with a layer of plywood
Plywood with a layer of plywood
Resonant frequency of the antenna
than for the antenna

A proposed method for the
from a series of data points
made and calculated for the antenna

The antenna is excited by the antenna
on the antenna

ANTENNA

Fourier transform of the autocorrelation function. Blackman and Tukey¹ have covered this procedure in detail, so no further comment will be made here.

A typical autocorrelation function for radar return signals from a flat, heavily wooded area, is shown in Figure 6-12 along with the corresponding variance spectrum.² It should be observed that a straight line approximation can be found that will fit the experimental variance curve reasonably well. This is generally true for experimental variance spectra for terrain targets.³ A typical autocorrelation function for acoustic signals from a flat, sand covered, plywood target is shown in Figure 6-13 along with the corresponding variance spectrum.

A difference is observed between the variance spectrum for radar return signals from woods and acoustic signals from the rough sand target. This difference is, for the most part, due to the size of the illuminated region in the two cases. The illuminated region is circular and extends 13 degrees from vertical for the radar data while it extends only 3 degrees from vertical for the acoustic data.

¹Blackman, R.B. and Tukey, J.W., The Measurement of Power Spectra, Dover Publication, S507, 1959, p. 7.

²The variance spectrum is plotted in terms of a frequency unit called the yule. By definition, a yule is π/m radians per sampling interval where m is the greatest lag for which the autocorrelation function is computed. The yule can be considered as a form of normalized frequency.

³Edison, et al, op. cit., EE-24.

Fourier transform of the autocorrelation function. Blackman and Tukey have covered this procedure in detail, so no further comment will be made here.

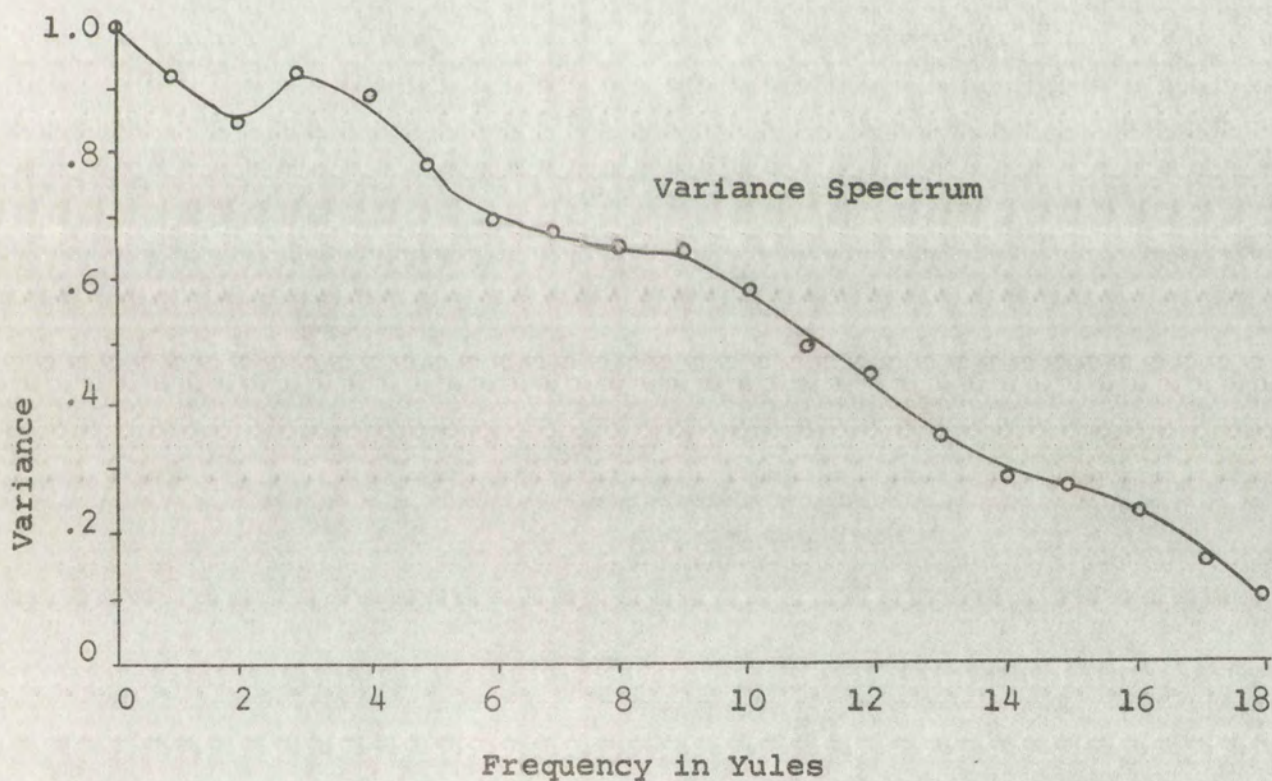
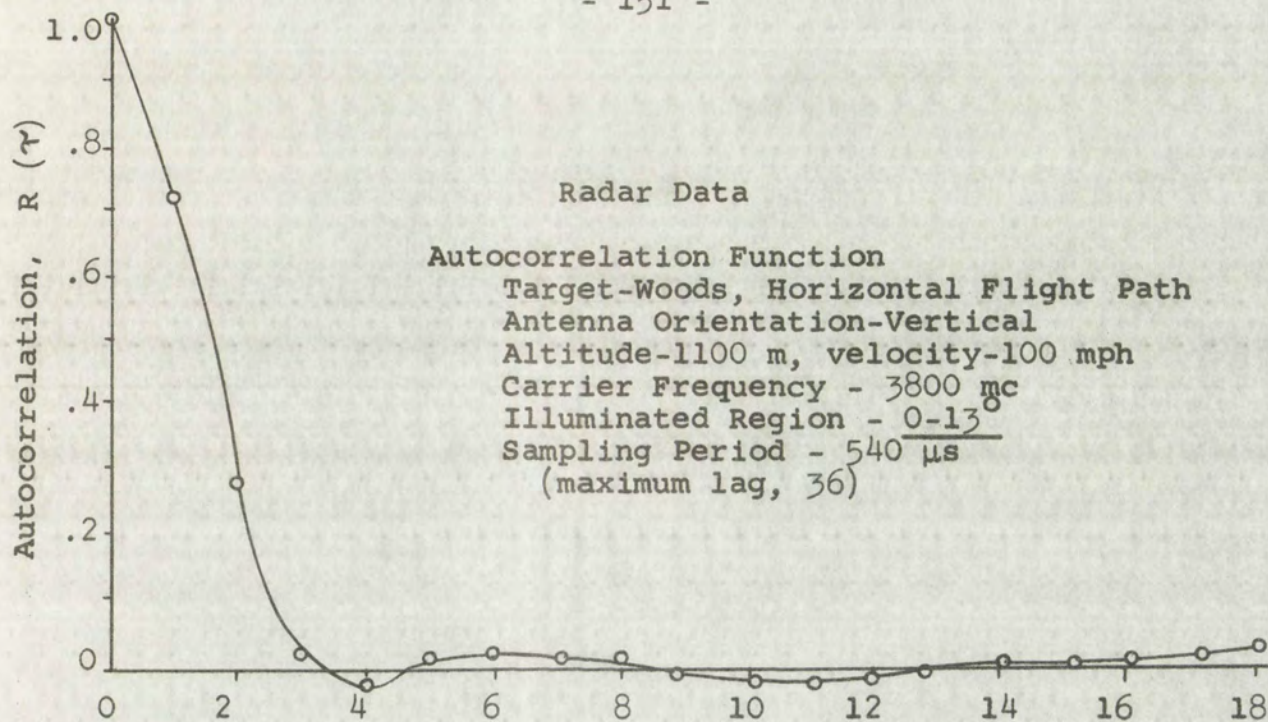
A typical autocorrelation function for radar return signals from a flat, heavily wooded area is shown in Figure 5-12 along with the corresponding variance spectrum. It should be observed that a sharp peak in the approximation can be found that will fit the experimental variance curve reasonably well. This is generally true for experimental variance spectra for certain targets. A typical autocorrelation function for acoustic signals from a flat, sandy covered, plywood target is shown in Figure 5-13 along with the corresponding variance spectrum.

A difference is observed between the variance spectrum for radar return signals from woods and acoustic signals from the rough sand target. This difference is for the most part, due to the size of the illuminated region in the two cases. The illuminated region is circular and extends 1.5 degrees from vertical for the radar data while it extends only 3 degrees from vertical for the acoustic data.

¹Blackman, R.B. and Tukey, J.W., The Measurement of Power Spectra, Dover Publications, 1959, p. 100.

²The variance spectrum is plotted in terms of a target unity unit called the yule. By definition, a yule is 1/2 radian per sampling interval where π is the greatest lag for which the autocorrelation function is computed. The yule can be considered as a form of normalized frequency.

³Blackman, et al., op. cit., p. 100.

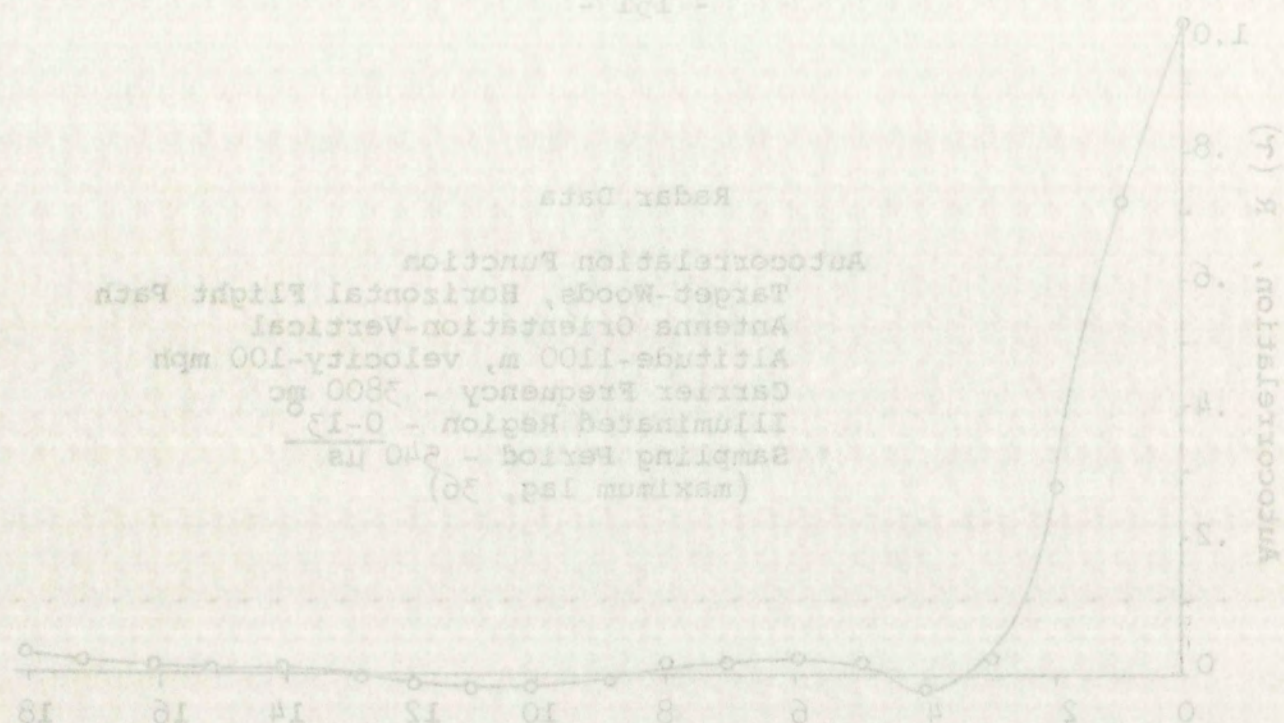


Variance Spectrum for Wooded Terrain

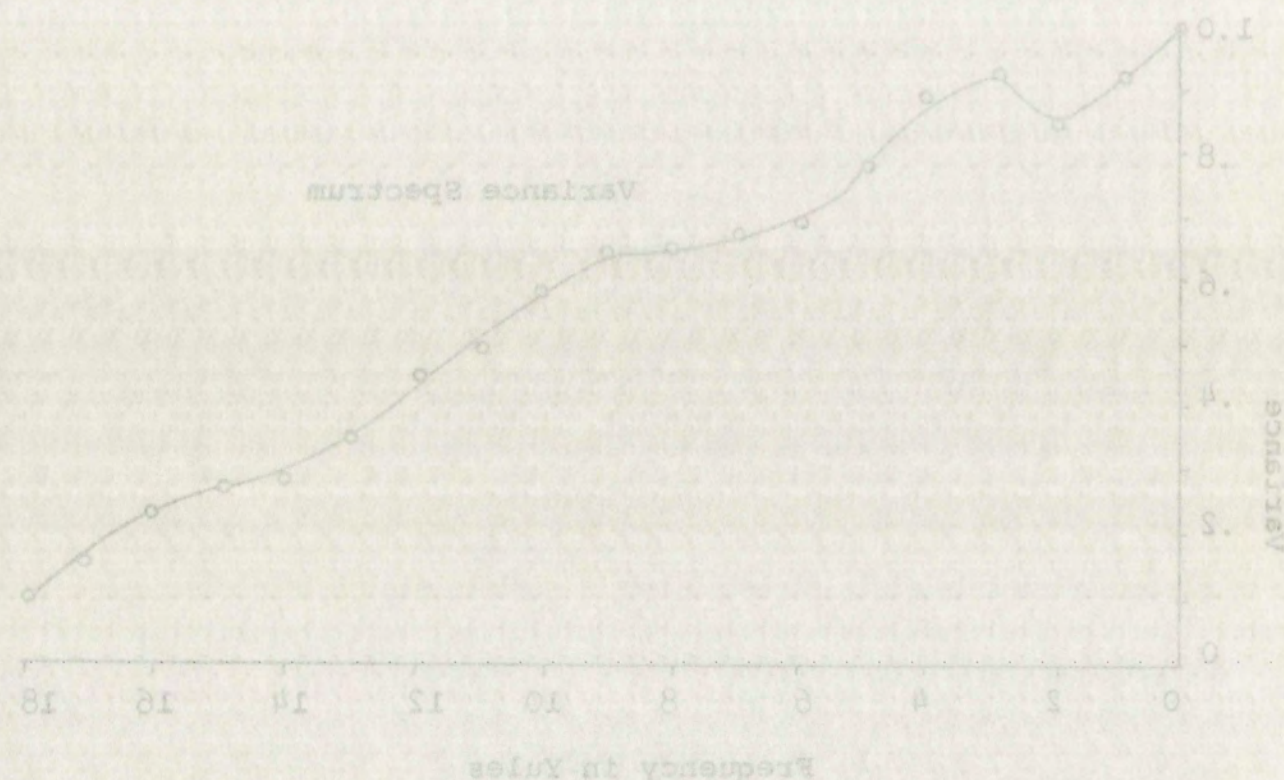
Figure 6-12

Autocorrelation Function

Target-Woods, Horizontal Flight Path
Antenna Orientation-Vertical
Altitude-1100 m, velocity-100 mph
Carrier Frequency - 5800 mc
Illuminated Region - 0-15
Sampling Period - 240 μ s
(Maximum lag, 36)

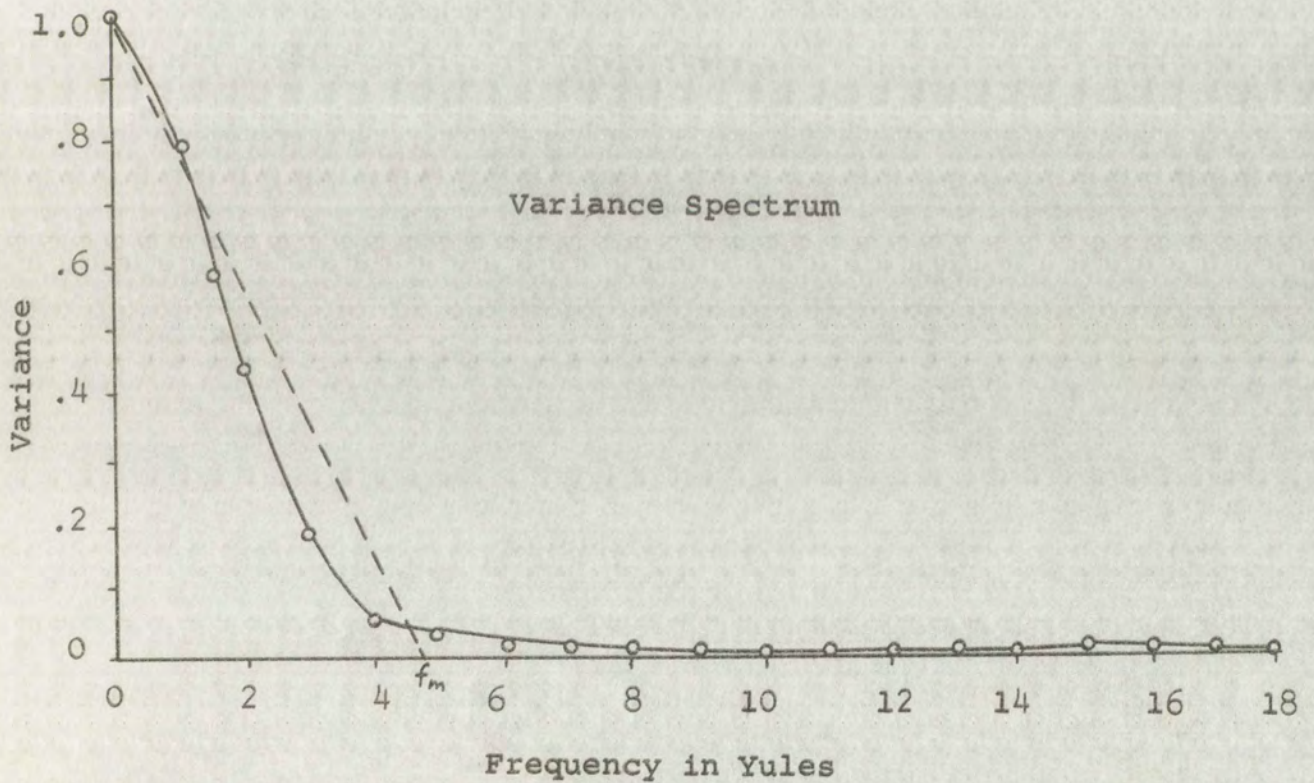
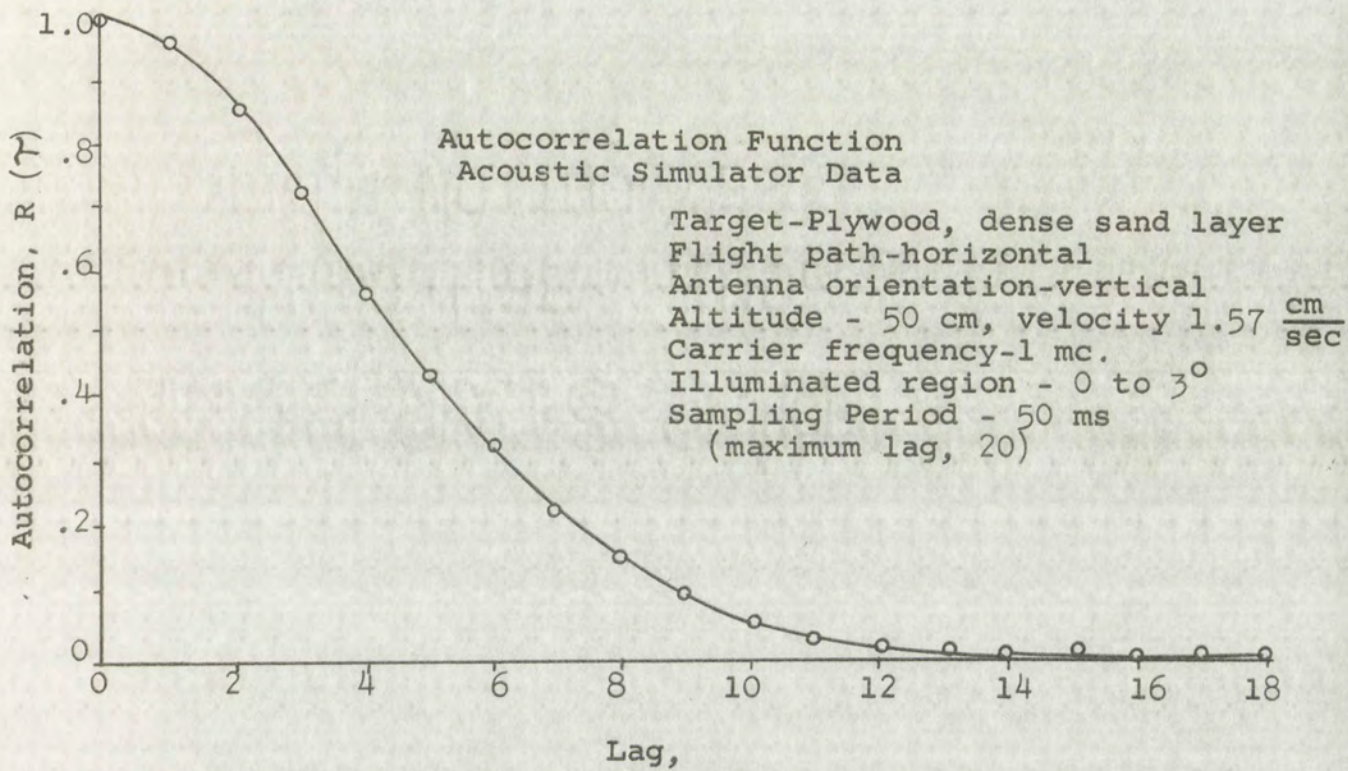


Variance Spectrum



Variance Spectrum for Woods Terrain

Figure 5-12

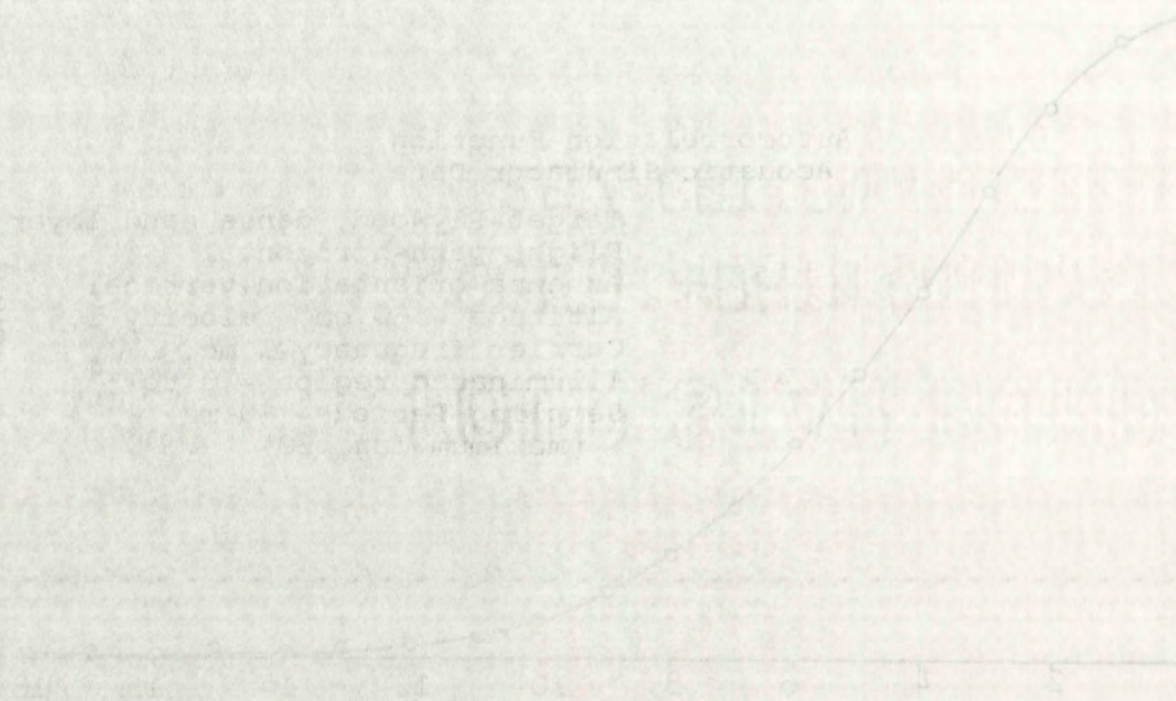


Variance Spectrum for Rough Sand

Figure 6-13

Aspirin, %

0 0.2 0.4 0.6 0.8 1.0



Aspirin

0 2 4 6 8 10



It has been shown that an effective maximum fading frequency can be determined from the carrier frequency, antenna velocity and the antenna pattern geometry.¹ This maximum frequency is given by

$$f_{MAX} = \frac{2 f_c v}{v_p} (\cos \alpha_{min} - \cos \alpha_{max}) \quad (6-3)$$

where f_c is the carrier frequency,

v is the antenna velocity,

v_p is the phase velocity,

α_{min} is the minimum angle between the antenna velocity vector and a contributing scatterer which lies within or on the half power pattern of the antenna, and

α_{max} is the maximum angle between the antenna velocity vector and a contributing scatterer which lies within or on the half power pattern of the antenna.

Equation 6-3 is used to locate the maximum effective frequency which controls the straight line approximation to the variance spectra shown in Figures 6-12 through 6-13. Now an effective fading frequency, which is really a single representative frequency from the spectrum, can be found from

$$f_e = 0.36 f_{MAX} \quad (6-4)$$

for horizontal radar motion and

$$f_e = 0.22 f_{MAX} \quad (6-5)$$

¹Edison, op. cit., EE-35.

It has been shown that the frequency of the antenna velocity is proportional to the maximum frequency of the antenna velocity.

$$f_{\max} = \frac{1}{2\pi} \left(\frac{v}{r} \right)$$

where f is the frequency of the antenna velocity.

v is the velocity of the antenna velocity.

r is the radius of the antenna velocity.

θ_{\min} is the minimum angle of the antenna velocity.

vector and the antenna velocity.

With the antenna velocity, the antenna velocity is proportional to the antenna velocity.

and the antenna velocity is proportional to the antenna velocity.

θ_{\max} is the maximum angle of the antenna velocity.

vector and the antenna velocity.

With the antenna velocity, the antenna velocity is proportional to the antenna velocity.

Equation (1) is the antenna velocity.

frequency of the antenna velocity is proportional to the antenna velocity.

to the antenna velocity, the antenna velocity is proportional to the antenna velocity.

Now an effective antenna velocity is proportional to the antenna velocity.

representative of the antenna velocity.

for horizontal antenna velocity.

UNITED STATES BUREAU OF AERONAUTICS

WRIGHT PATTENSON AIR FORCE BASE, OHIO

RESEARCH REPORT

for vertical radar motion.¹ Similar estimators have been used for determining the fading rate of moon echo signals.² The validity of Equation 6-4 has been checked for a number of targets in the acoustic simulator. The procedure is to obtain a fading record such as that shown in Figure 5-6; then to count the maxima and minima in the record, divide this number by 2 and divide the result into the length of the fading record in seconds. The result is a representative fading frequency for the record. This experimental result is then compared to the theoretical result using the estimator defined in Equations 6-3 and 6-4. A few results for effective fading frequencies in the acoustic system are shown in Table 6-3.

TABLE 6-3
EFFECTIVE FADING FREQUENCIES

Target	Angle of Incidence ^o	Experimental Fading Freq. cps	Theoretical Fading Freq. cps
City Target 1	0	2.5	2.7
	10 ^o	3.4	4.0
	20	4.9	4.9
	30	4.5	5.6
City Target 2	0	3.0	3.2
	10	3.9	3.7
	20	3.6	4.2
	30	3.9	4.9

¹Ibid. These equations are developed in the above reference.

²Fricker, S.J., et al., "Computation and Measurement of the Fading Rate of Moon-Reflected VHF Signals," N.B.S. Jour. of Research, Vol. 64D, No. 5, Sept.-Oct. 1960, pp. 455-65.

for vertical target motion. The following relationships have been used for determining the testing time of each angle stimulus. The velocity of rotation (RPM) has been checked for a number of targets in the acoustic simulator. The procedure is to obtain a testing record such as that shown in Figure 5-6. Then we count the axials and divide the result by the length of this number by 1 and divide the result by the length of the testing record in seconds. The result is a representative testing frequency for the record. This experimental result is then compared to the theoretical result using the estimator defined in Equations 5-3 and 5-4. A few results for effective testing frequencies in the acoustic system are shown in Table 5-2.

TABLE 5-2

EFFECTIVE TESTING FREQUENCIES

Target	Angle of Inclination	Testing Time, sec	Experimental Frequency
City Target 1	0	2.5	4.0
	10°	3.4	4.0
	20	4.3	4.2
	30	5.2	4.0
City Target 2	0	3.0	3.3
	10	3.8	3.3
	20	4.6	3.3
	30	5.5	3.3

1. Ibid. These equations are developed in the above reference.
 2. Eichen, G. J., et al., "Composition and Measurement of the Firing Rate of Mood-Related WII Animals," Research, Vol. 612, No. 2, Sept. 1968, pp. 11-15.

Range measurements using a pulsed radar are based upon the time required for the wave packet to make the round trip from the radar to the target. When great accuracy is required it becomes necessary to locate with precision a particular point in the return pulse.

The leading edge of the return pulse is frequently selected since it supposedly contains the best range information. The determination of the leading edge of the pulse is a difficult matter since the return signal from an irregular target is generally subject to considerable fading. The accuracy of a radar altimeter is of course affected by the fading.¹

The acoustic simulator can be used to obtain range fading statistics from various targets such as cities or mountainous areas. It is expected that these statistics will compare favorably with similar statistics obtained from radar experiments over cities or mountains.

A typical "range fading" curve is shown in Figure 6-14. This curve was obtained by measuring the delay time to the first sign of signal on the leading edge of consecutive return pulses. The target area is a model city, scaled 500/1, the equivalent radar altitude is 820 feet, and the equivalent radar carrier frequency using linear modeling is 400 mc. The antenna is oriented vertically and has a 6° beamwidth between half power points on the major lobe. The radar path is horizontal over the city.

¹ Lyytikainell, H.E., "An Analysis of Radar Profiles over Mountainous Terrain, "Photogrammetric Engineering, Vol. 26, No. 3, June 1960, pp. 403-12.

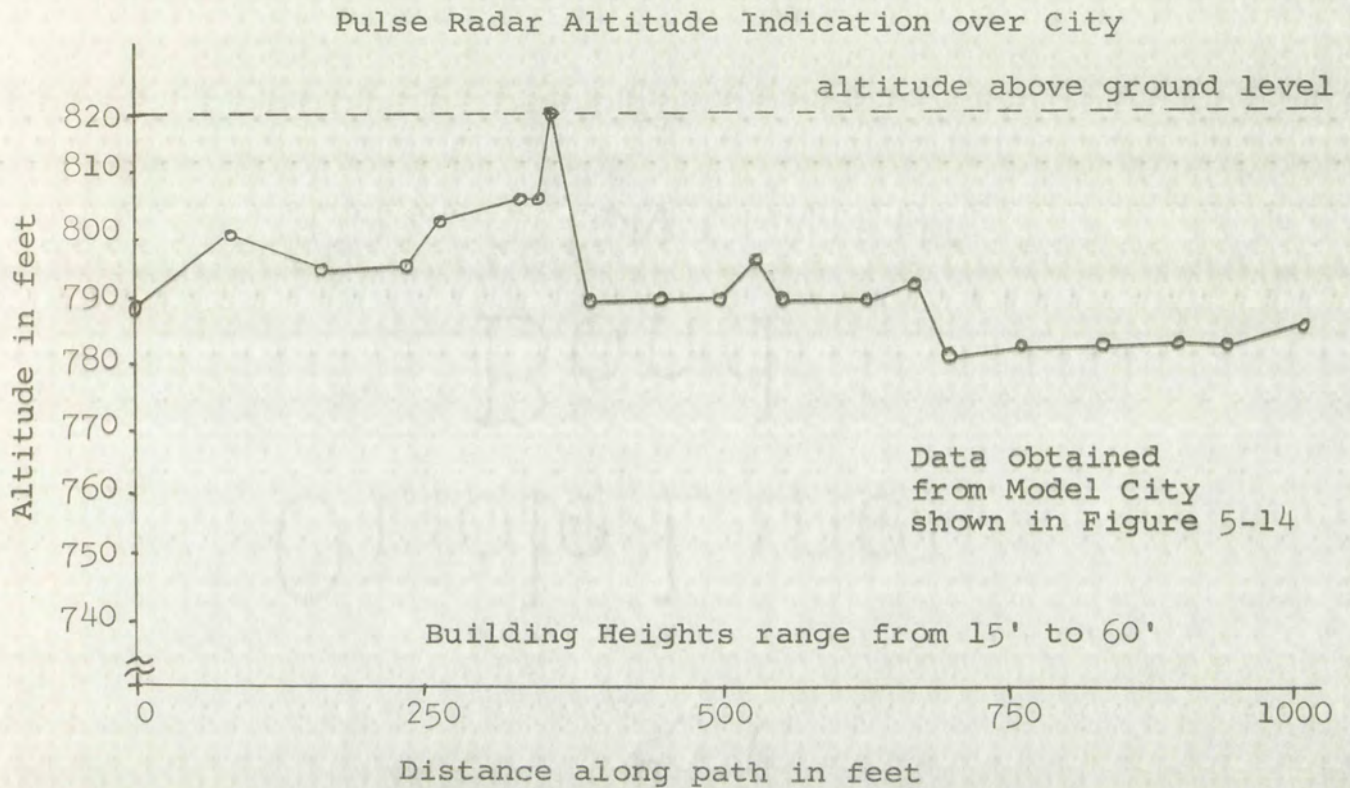


Figure 6-14

6.3 Radar Cross Sections

Satisfactory modeling of an altimeter system requires a model target with a backscattering radar cross section per unit area that is similar to that of terrain. For this application the antenna will be oriented in the vertical direction and will have a fairly broad beam. The backscattering cross section varies quite rapidly at near-vertical incidence for many types of terrain. This variation with angle must be correctly reproduced in the model in order to simulate the return signal characteristics.

Figure 1. Altitude above ground level versus distance along path in feet.

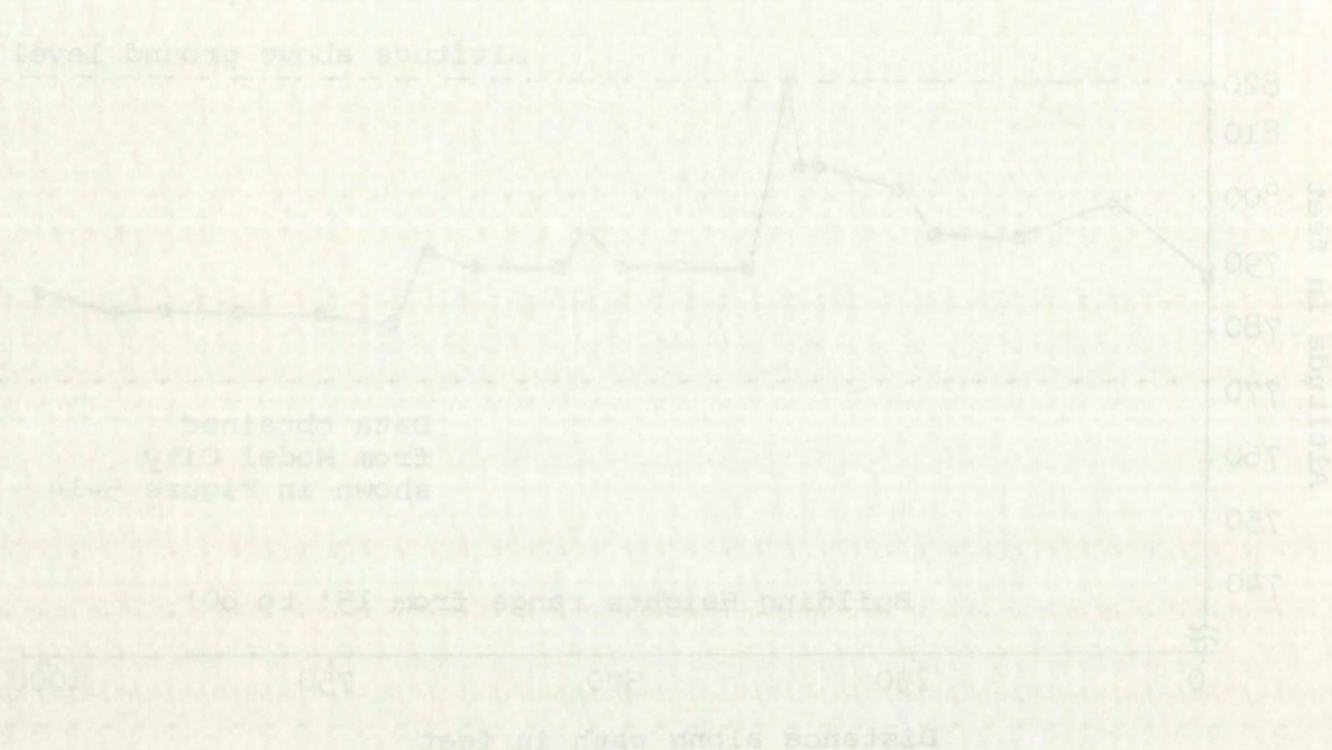


Figure 1-1

3.3. Radar Cross Section

Satisfactory modeling of an altimeter system requires

a model target with a backscattered radar cross section

per unit area that is similar to that of terrain. For this

application the antenna will be oriented in the vertical

direction and will have a fairly broad beam. The back-

scattered cross section varies quite rapidly as beam

vertical incidence for many types of terrain. This variation

with angle must be correctly reproduced in the model in order

to simulate the terrain signal characteristics.

Many experiments have been performed to obtain radar backscattering cross sections of terrain as a function of the angle of incidence.^{1,2,3,4} The shape of the backscattering curve for targets used in the acoustic simulator can be controlled over a wide range by changing the target roughness. This is done by increasing or decreasing the density of sand particles on the surface. Three backscattering cross section curves for typical model targets are shown in Figure 6-15 together with actual X-Band backscattering curves for water and woods.⁵ These curves illustrate the good agreement that can be attained in the model for certain types of terrain. The woods appear to be a very rough surface so the signal remains quite constant out to 30° . This backscattering cross section is duplicated in the model by a dense sand layer on plywood. The slightly rough sand target and bare plywood target have the same general characteristics as the rough water target. The model requirement is that the shape of the curve be correct since the relative level can be adjusted by scaling.

¹Edison, A.R., et al., Ref. 7 (this chap.)

²Cosgriff, R.F., Peake, W.H., and Taylor, R.C., Terrain Scattering Properties for Sensor System Design, Engr. Exp. Stn., Ohio State, Bulletin 181, May 1961.

³Dye, Jack E., "Ground and Sea Return Signal Characteristics of Microwave Pulse Altimeters," Trans. of 1959 Symposium on Radar Return, Part 1, Sponsored by U.S. Naval Ordnance Test Station, China Lake, Calif. and Univ. of New Mexico, NOTS TP 2338.

⁴Campbell, J.P., "Backscattering Characteristics of Land and Sea at X-Band," Ibid.

⁵The X-Band back-scattering characteristics are taken from Reference 3 above.

background of the study is the fact that the

the authors have not been able to find any

other studies which have been published

in the literature on this subject

It is to be noted that the study was

and the results of the study are

shown in the following table

Table 1. Results of the study

water and wood

that can be seen in the following

The work of the

remains quite similar to that of

analysis as described in the following

glycerol. The following table

table have been published in the

water, and the results of the study

the curve be shown in the following

by scaling

Table 2. Results of the study

Table 3. Results of the study

Table 4. Results of the study

Table 5. Results of the study

Table 6. Results of the study

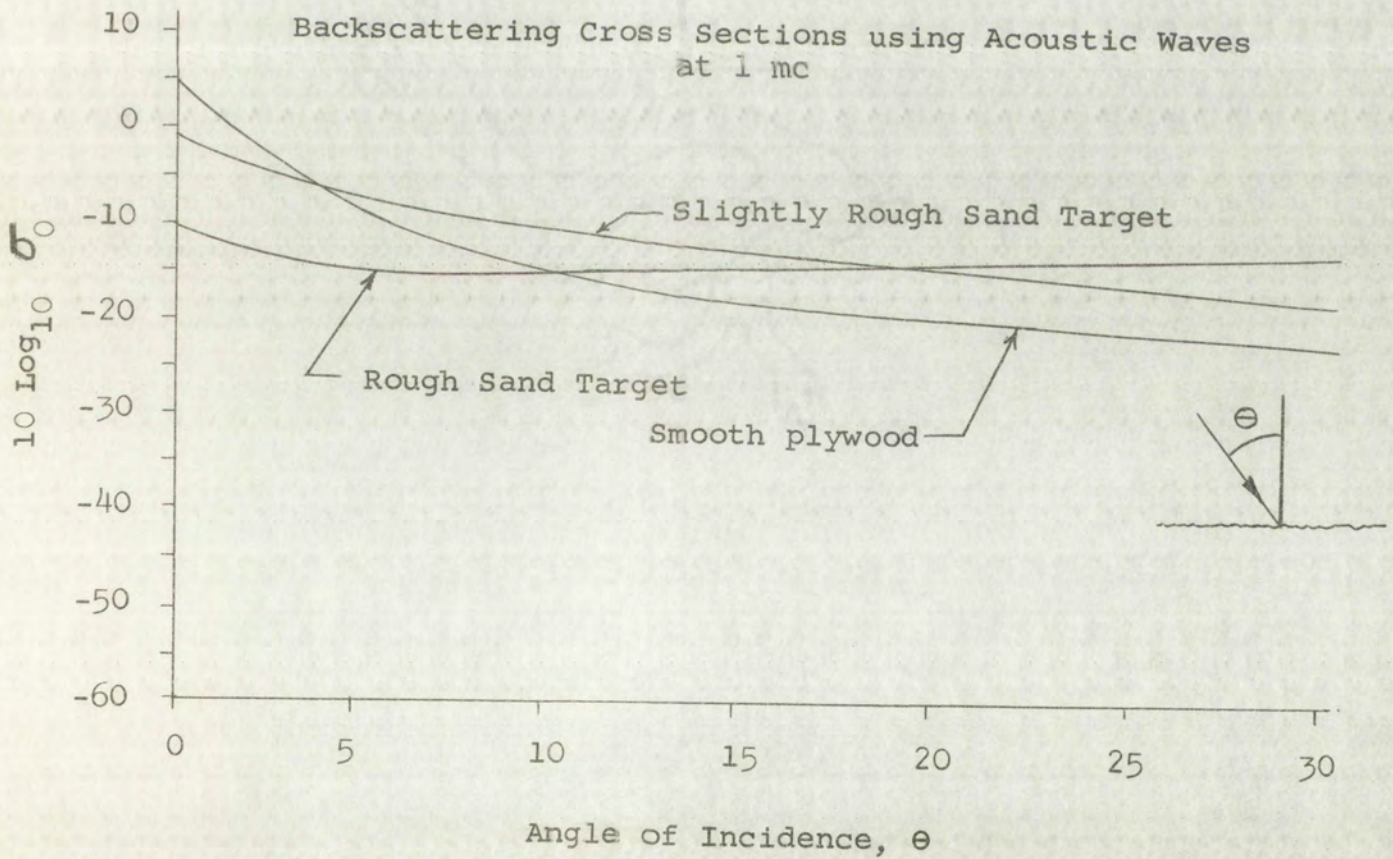
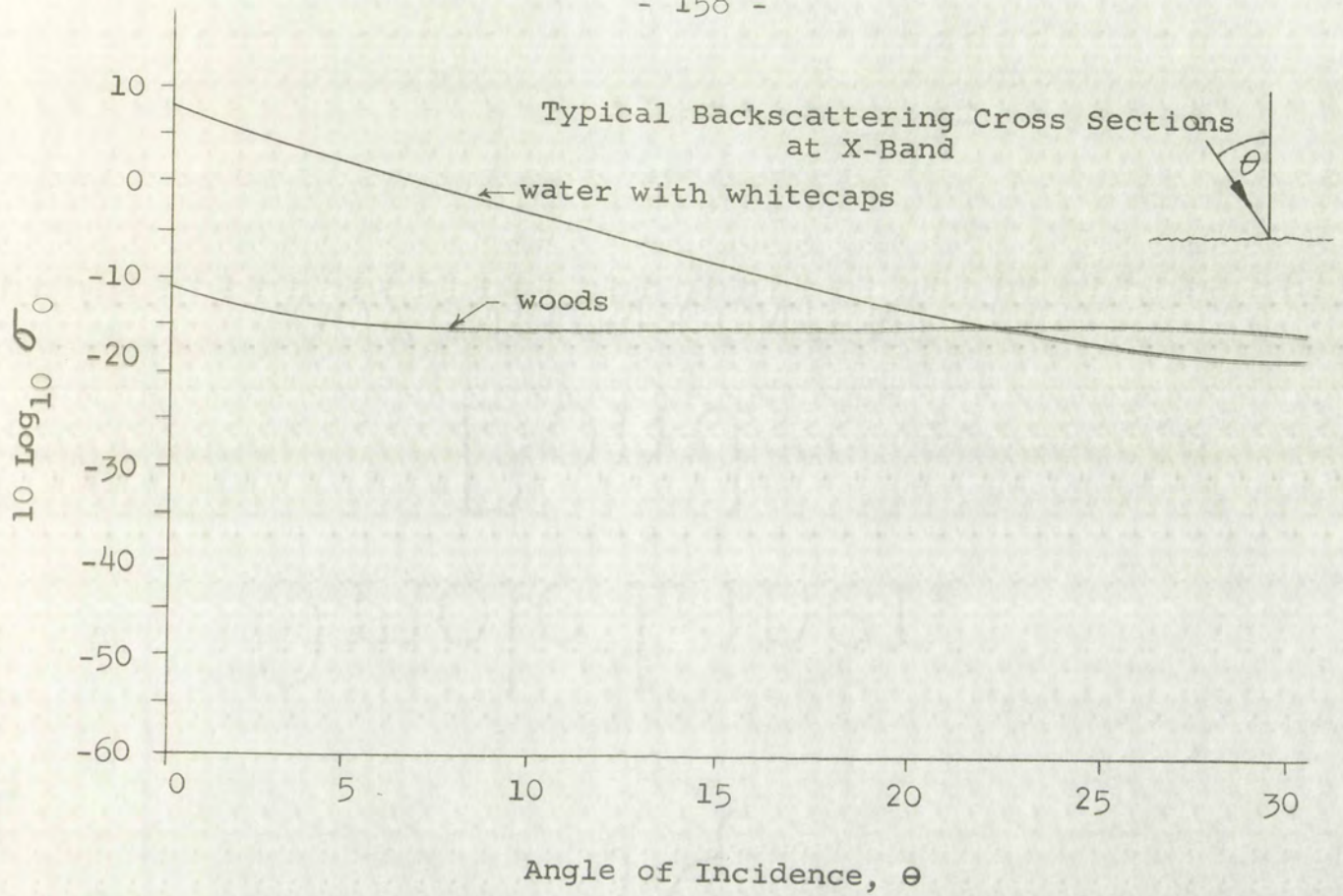
Table 7. Results of the study

Table 8. Results of the study

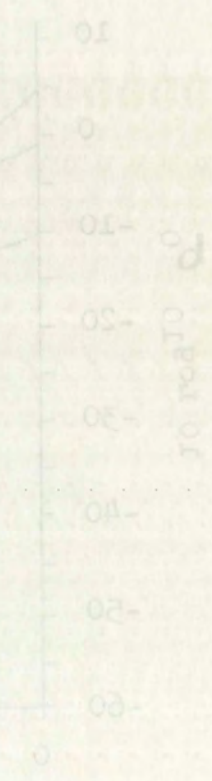
Table 9. Results of the study

Table 10. Results of the study

Table 11. Results of the study



Typical Radar Back-Scattering Cross Sections
Figure 6-15



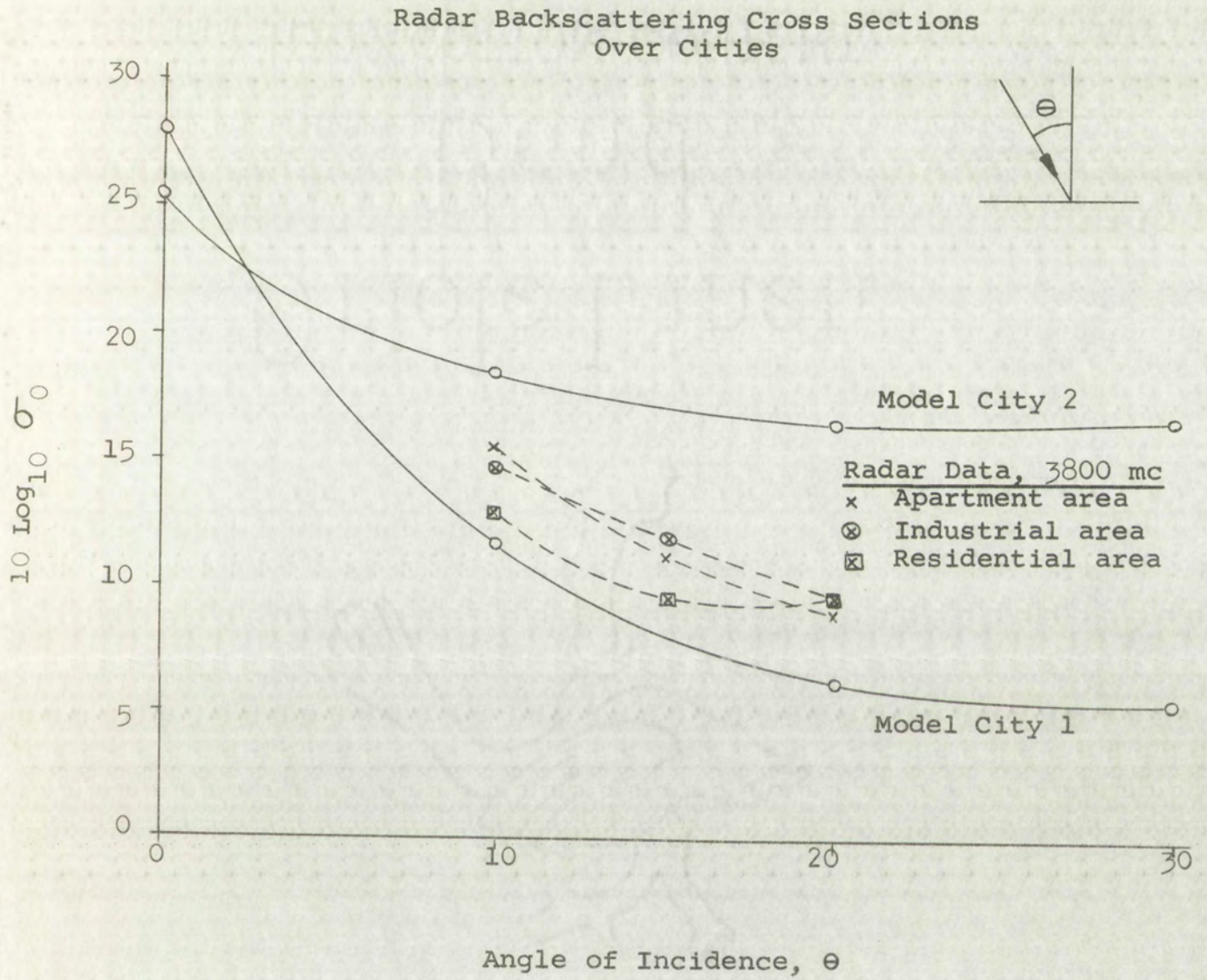


Figure 6-16

Radar Backscattering Cross Sections Over Cities

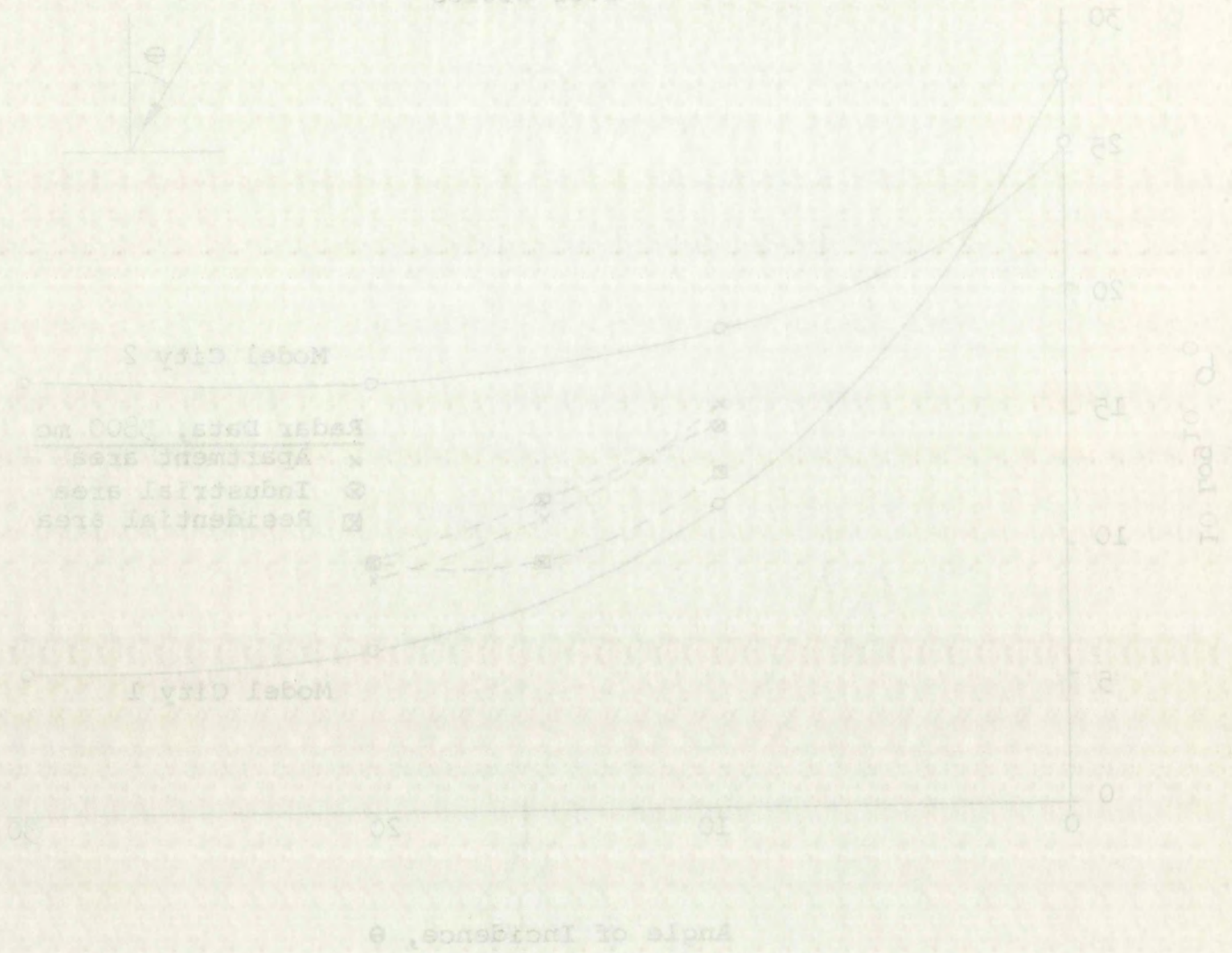


Figure 6-16

Additional radar backscattering cross sections were obtained for the city target shown in Figure 6-16. City targets number 1 and number 2 are actually the same model, except for a layer of sand which was added to the off-street areas on target number 2. The addition of scatterers to the surface had the effect of reducing the backscattering cross section at vertical incidence and of increasing it at angles of incidence greater than about 10 degrees. Actual radar backscattering curves over city areas are shown in the figure for comparison purposes.¹ These data are limited to angles between 10 and 20 degrees from vertical; however, they do show a trend that fits the model data.

6.4 Recommendations

The success of the acoustic simulator as an analog computer depends upon the use of appropriate targets. Results of the tests described in this chapter show that many terrain targets, such as woods, farmland, cities, and water can be adequately represented by models.

The evaluation of signal processing circuitry, with the acoustic simulator, requires that certain signal statistics have the same characteristics in the model as in the real system. As an example, consider the case of pulse return signals from mountainous terrain. The return signals from different parts of the illuminated region will appear

¹Actual radar backscattering curves for cities are taken from reference; Edison, et al, op. cit., EE-24.

in the proper time sequence if the mountains are properly scaled. On the other hand, the fading which exists in the component signals from specific areas in the illuminated region must be provided by small scale roughness on the target. Sand particles on the order of a fraction of a wavelength for the carrier frequency are satisfactory for these scattering agents. This approach to modeling assumes that physical shape is important for objects (on the order of a wavelength in size). This, of course, assumes that the illuminated region is large enough to include many of the small scattering elements.

The proper density for small scatterers on the target can usually be determined by making a preliminary test on a flat target. It is relatively easy to obtain a back-scattering cross section as a function of the angle of incidence and also to obtain fading statistics. This information, from the flat target, is usually adequate to decide whether or not the small scale roughness is correct for the particular problem.

Recommendations for several terrain targets are made in Table 6-4. These targets use a flat, 3/4 inch, exterior grades plywood base and in some cases the plywood is covered with galvanized steel. Sand particles are glued to the surface to provide small scale roughness. The surfaces recommended have been found to give suitable acoustic signals for modeling altimeter systems.

in the proper time sequence of the measurements are properly scaled. On the other hand, the testing which exists in the component signals from specific areas in the illuminated region must be provided by small scale roughness on the target. Sand particles on the order of a fraction of a wavelength for the carrier frequency are satisfactory for these scattering systems. This approach to modeling assumes that physical shape is important for objects (on the order of a wavelength in size). Thus, of course, assumes that the illuminated region is large enough to include many of the small scattering elements.

The proper density for small scatterers on the target can usually be determined by making a preliminary test on a flat target. It is relatively easy to obtain a back scattering cross section as a function of the angle of incidence and also to obtain fading statistics. This information, from the flat target, is usually adequate to decide whether or not the small scale roughness is correct for the particular problem.

Recommendations for several terrain targets are made in Table 3-4. These targets use a flat, 3/4 inch, exterior grade plywood base and in some cases the plywood is covered with galvanized steel. Sand particles are glued to the surface to provide small scale roughness. The surfaces recommended have been found to give suitable acoustic signals for modeling altimeter systems.

TABLE 6-4

TARGET RECOMMENDATIONS

Terrain	Target Base	Sand Particle size, wavelengths	Distance Between Particles, Wavelengths
Woods	Plywood	1-2	0 - 1/2
Farmland	"	1-2	1 - 5
Desert	"	---	-----
Cities	" (buildings) ^a	$\frac{1}{2}$ -1	1 - 5
Water (smooth)	galv. steel	$< \frac{1}{2}$	3 - 5
Water (rough)	" "	$\frac{1}{2}$ -1	1 - 2
Mountains	" " (shaped) ^b	$\frac{1}{2}$ -1	1 - 2

^aBuildings are pine blocks cut to size.

^bSteel can be formed into appropriate contours.

It should be observed that the slope of the radar backscattering cross section curves is important in modeling practice. The absolute level of the curves can be increased or decreased by proper scaling.

Terrain	
Woods	
Farmland	
Desert	
Cities	
Water (smooth)	
Water (rough)	
Mountains	

buildings are
 steel can be
 If should be
 cross section
 face level of
 scaling

CHAPTER VII

THE ACOUSTIC SIMULATOR AS AN ANALOG COMPUTER

The acoustic simulator can be used as an analog device to simulate radar and altimeter system performance by using model targets and acoustic waves in water. The appropriate signal characteristics are provided by the scattering of acoustic waves from the target, and the system response is simulated using circuits which perform in a similar manner to those in the real system. It is easy to observe, in the model system, the effects of changing pulse shapes or modulation frequencies. The behavior of the real system is then inferred from the model system results. A fading record, obtained using the acoustic simulator and a rough target, can be exactly reproduced (for practical purposes) because the transducer path can be easily duplicated from one run to the next.¹ Thus a more exact comparison between systems is possible than the actual flight tests.

¹ Examples of reproducible fading records for pulse and FM radars are shown in Appendix B.

CHAPTER VII

THE ACOUSTIC SIMULATOR AS AN ANALOG

COMPUTER

The acoustic simulator can be used as an analog device to simulate radar and altimeter system performance by using model targets and acoustic waves in water. The appropriate signal characteristics are provided by the scattering of acoustic waves from the target, and the system response is simulated using circuits which perform in a similar manner to those in the real system. It is easy to observe, in the model system, the effects of changing pulse shapes or modulation frequencies. The behavior of the real system is then inferred from the model system results. A fading record, obtained using the acoustic simulator and a rough target, can be exactly reproduced (for practical purposes) because the transducer path can be easily duplicated from one run to the next.¹ Thus a more exact comparison between systems is possible than the actual flight tests.

¹ Examples of reproducible fading records for pulse and FM targets are shown in Appendix B.

A frequency modulated radio altimeter was selected as the system to be used in illustrating the application of the acoustic simulator as an analog computer.¹ The altimeter under consideration is intended to provide a continuous record of the altitude of the antenna above the terrain and is, therefore, provided with a strip chart recorder to indicate altitude. The altimeter modeled is similar in indicator circuitry to the formerly widely used AN/AFN-1, but other parameters are different.

In nearly all cases terrain acts primarily as a scatterer at frequencies above a few hundred megacycles per second. The signal returned to the altimeter is therefore subject to considerable fading because of interference. When the altimeter is in motion the return signal consists of a number of frequencies because the relative velocity between the radar and each individual scatterer is different. This results in a different Doppler frequency shift for the signal from each scatterer. It broadens the signal spectrum. A frequency modulated radio altimeter measures altitude by measuring the difference frequency between the transmitted and received signals. Since the received signal will generally consist of a number of frequencies which fade in a random manner, the altitude indication of the altimeter is expected to fluctuate in some manner. This acoustic simulator

¹Quinlan, David L., Comparison of Pulse and FM Radar Altimeters Based on Terrain Return Theory, Univ. of N. Mex., Engr. Exp. Stn. Rpt. EE-56, May, 1961.

study is intended to demonstrate these fading effects on the accuracy of the altimeter indication for a number of different situations.

7.1 The FM Altimeter Analog

The altimeter system selected for study is intended to operate at altitudes below 3000 meters and uses a sinusoidal modulating frequency. Table 7-1 shows the desired altimeter parameters, a selected operating altitude of 2450 meters (about 8000 feet), and an antenna velocity of 250 m/sec (about 560 mph). The corresponding acoustic system parameters are determined using the scaling relations obtained from Table 4-5.

TABLE 7-1
Frequency Modulated Altimeter Model

Parameter	Altimeter	Acoustic Model
Carrier Frequency	1500 mc	1 mc
Wavelength	20 cm	0.15 cm
Altitude	2450 m	0.5 m
Modulation frequency	612 cps	15 cps
Total Deviation	735 kc	18 kc
Difference frequency	23 kc	565 cps
No. cycles diff. freq. per cycle mod.	37.7	37.7
Antenna velocity	250 m/s	4.6 cm/sec
Doppler frequency ^a	217 cps	5.33 cps

^aThe Doppler frequency is based upon a signal received from an angle of 85 degrees from the antenna velocity vector.

any is assumed to determine these fading errors on
the accuracy of the statistical calculation for a number of
different situations.

7.1 The M-Statistic Method

The statistic method selected for study is assumed
to operate at a distance below 1000 meters and with a
statistical averaging frequency. Table 7-1 shows the
desired statistical parameters, a selected operating distance
of 1000 meters (about 800 feet), and an antenna velocity
of 250 m/sec (about 800 mph). The corresponding statistical
system parameters are determined using the scaling relations
obtained from Table 4-5.

TABLE 7-1

Frequency Modulated Altimeter Model

Parameter	Altimeter	Acoustic Model
Carrier frequency	150 kHz	100 kHz
Wave length	2 m	3.4 m
Altitude	1000 m	1000 m
Modulation frequency	15 cps	15 cps
Total Deviation	15 cps	15 cps
Difference frequency	15 cps	15 cps
No. cycles diff. freq.	15 cps	15 cps
Antenna velocity	250 m/sec	250 m/sec
Doppler frequency	250 cps	250 cps

The Doppler frequency is added upon a signal received
from an angle of 5 degrees from the antenna velocity vector.

An important advantage of the acoustic simulator is that relatively low frequencies are employed so experimental circuits can be used in "breadboard" form. This makes it relatively easy to modify the circuits and thus change the operating characteristics. Many of the system components for the altimeter model can be commercial units such as amplifiers, oscillators, and pulse circuits; these are used without modification.

The block diagram for the frequency modulated altimeter is shown in Figure 7-1.

The basic unit in the transmitter section is a signal generator with provisions for frequency modulation. The signal generator includes a modulation meter which directly indicates the frequency deviation. Sine wave modulation is supplied by a low frequency oscillator. The frequency modulated 1 mc/sec carrier signal is amplified and used to drive a power amplifier which in turn drives the transmitting transducer.

It is desirable to drive the transmitting transducer with about 25 volts or more in order to obtain an adequate output signal. This requires a power amplifier since the transducer with its impedance matching network has an impedance near 93 ohms. A 6L6 beam-power tube was used in a "breadboard" circuit for this application. Class A operation was used and a ferrite core transformer was

An important part of the system is the

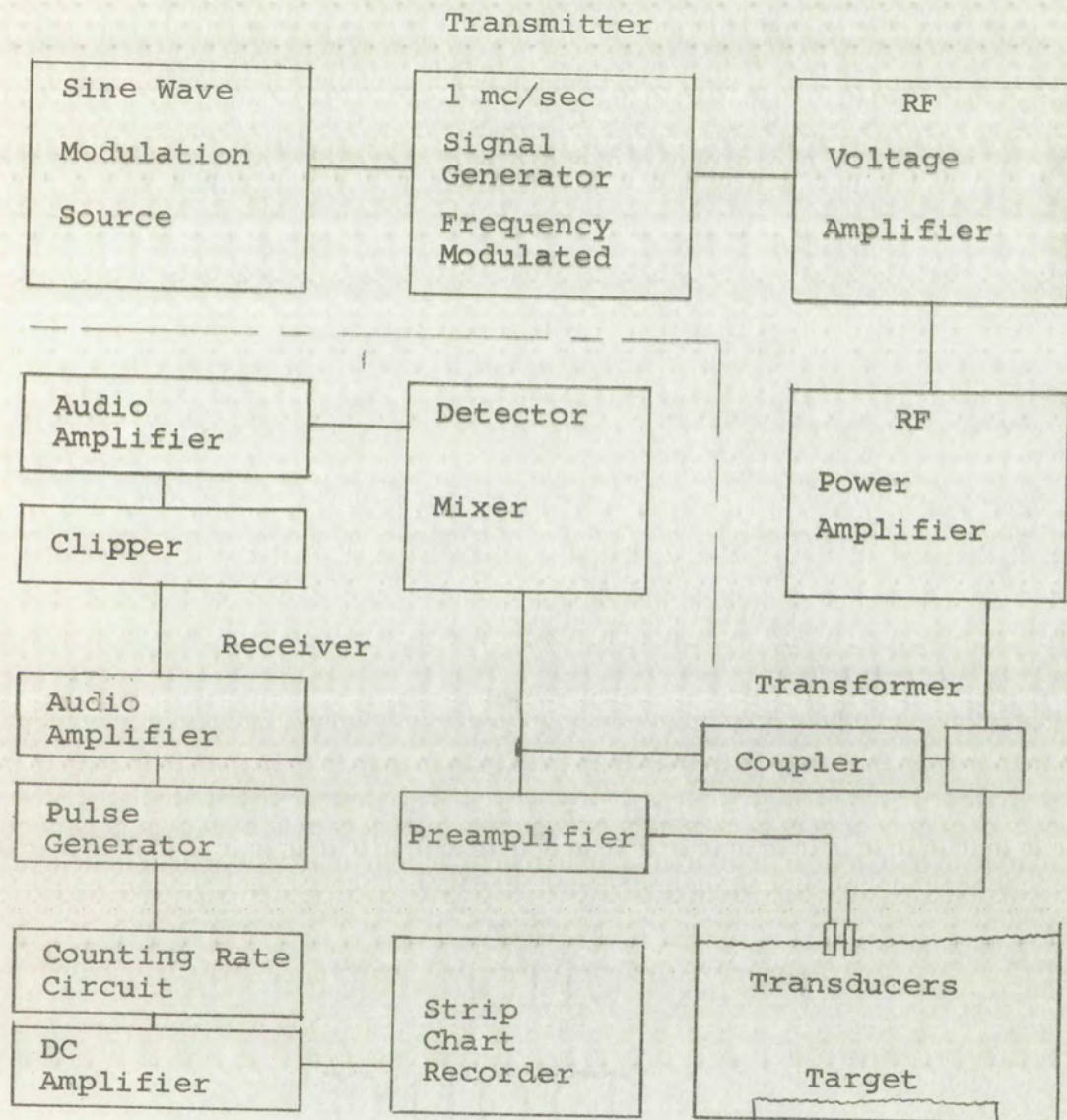
that relatively low frequency is employed in the
mental circuit. The system is designed to
make it relatively easy to change the operating
components for the system. The system is
such as amplifiers, oscillators, and
are used without modification.

The block diagram of the system is shown in Figure 1.

The basic block diagram of the system is shown in Figure 1. The system consists of a generator with a variable frequency, a signal generator, and a power supply. The signal generator is connected to the generator and the power supply. The power supply is connected to the generator and the signal generator. The signal generator is connected to the generator and the power supply. The power supply is connected to the generator and the signal generator. The signal generator is connected to the generator and the power supply. The power supply is connected to the generator and the signal generator.

It is desirable to have a power supply with about 15 volts or more. The power supply is connected to the generator and the signal generator. The signal generator is connected to the generator and the power supply. The power supply is connected to the generator and the signal generator. The signal generator is connected to the generator and the power supply. The power supply is connected to the generator and the signal generator. The signal generator is connected to the generator and the power supply. The power supply is connected to the generator and the signal generator.

employed for coupling to the transducer.¹ Using this power amplifier it is possible to develop 100 volts rms across the primary of the matching transformer.



FM ALTIMETER SYSTEM
BLOCK DIAGRAM

Figure 7-1

¹A 2" diameter ferrite core was wound with 40 turns of No. 28 stranded wire for the primary coil and 10 turns for the secondary coil.

employed for coupling to the transducer. Using this power amplifier it is possible to develop 100 volts rms across the primary of the matching transformer.

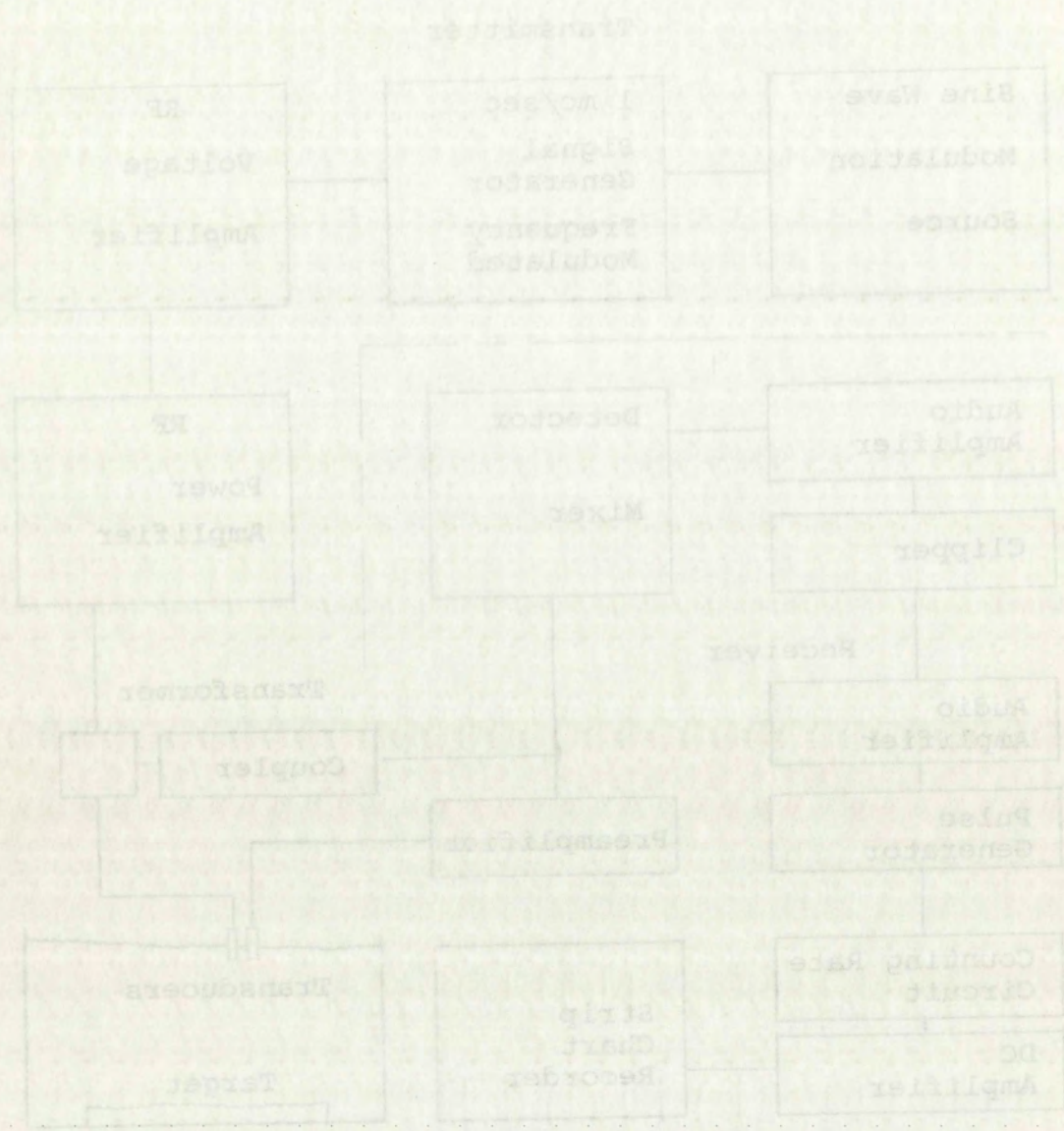
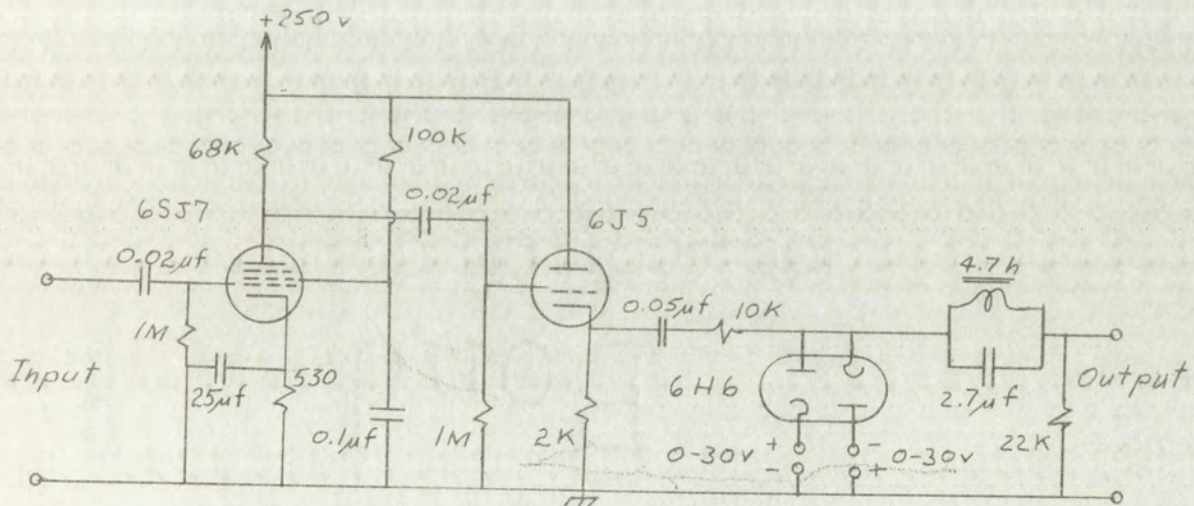


FIGURE 1-1
BLOCK DIAGRAM OF THE AUDIO SYSTEM

A 3" diameter ferrite core was wound with 30 turns of No. 18 stranded wire for the primary coil and 18 turns for the secondary coil.

A portion of the transmitter frequency which is used as a reference is fed through a coupler and mixed with the received signal in the detector mixer. The preamplifier is used to raise the received signal to about the same level as the reference signal before mixing. The detector mixer consists of an 1N34 crystal diode and a low pass filter. The difference frequency is below 1 kc for the application considered so the remaining amplifiers operate at low frequencies.

The clipper circuit shown in Figure 7-2 was constructed on a "breadboard" and consists of a voltage amplifier, cathode follower, and positive and negative peak clipper circuits. Small adjustable power supplies were



AMPLIFIER AND CLIPPER CIRCUIT

Figure 7-2

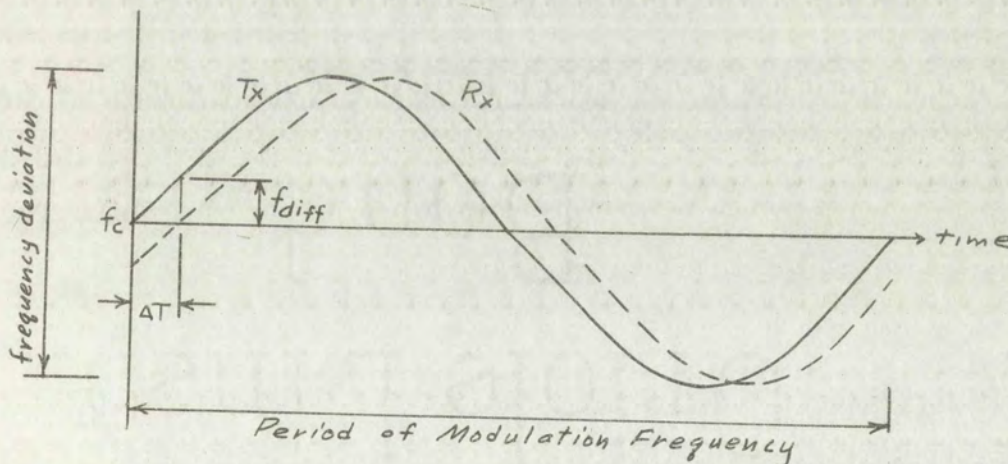
A portion of the received signal is used as a reference in the circuit. The received signal is the received signal is used to raise the received signal as the reference signal. The reference signal consists of an input signal. The difference frequency is considered as the remaining signal. The clipper circuit shown is attached on a "breadboard" with amplifier, cathode follower, and clipper circuit. Small adjustment.



AMPLIFIER AND CLIPPER

used to control the level of clipping on the positive and negative peaks. The output signal was fed through a power line frequency rejection filter to a second audio amplifier. This filter is necessary because the "breadboard" circuits are completely unshielded. The received signal is subject to considerable fading which introduces amplitude modulation along with the frequency modulation in the difference frequency signal. There are brief intervals, over a rough target, where the signal fades to zero (for practical purposes). The clipper circuits are set to remove as much as possible of this amplitude modulation from the difference frequency signal.

Figure 7-3 illustrates how a difference frequency is obtained for sinusoidal frequency modulation.

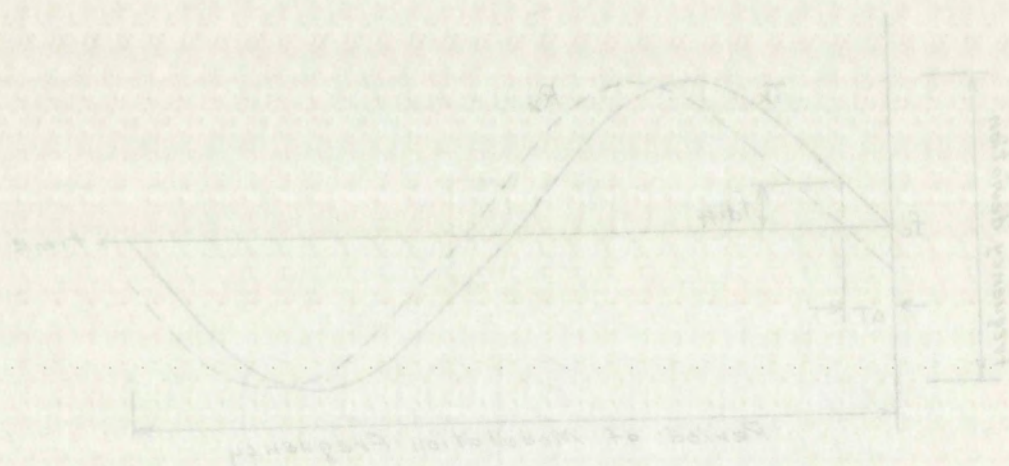


TRANSMITTED AND RECEIVED FREQUENCIES AS A
FUNCTION OF TIME

Figure 7-3

need to control the level of clipping on the positive and
 negative peaks. The output signal was fed through a power
 line frequency rejection filter to a second audio amplifier.
 This filter is necessary because the "breadboard" circuit
 are completely unshielded. The received signal is subject
 to considerable fading which introduces amplitude modulation
 along with the frequency modulation in the difference fre-
 quency signal. There are brief intervals, over a rough
 target, where the signal fades to zero (for practical
 purposes). The clipper circuits are set to remove as much
 as possible of this amplitude modulation from the difference
 frequency signal.

Figure 7-5 illustrates how a difference frequency is
 obtained for sinusoidal frequency modulation.



TRANSMITTED AND RECEIVED FREQUENCIES AS A
 FUNCTION OF TIME

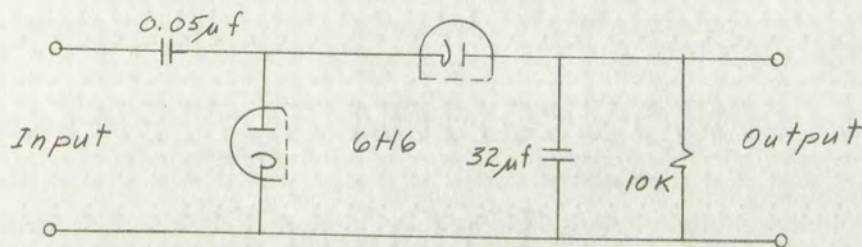
Figure 7-5

The transmitter frequency varies in a sinusoidal manner at a rate determined by the modulating frequency. The frequency of a received signal from a smooth target will also vary in a sinusoidal manner except it will be shifted in phase an amount determined by the time increment, ΔT , required for the signal to make a round trip to the target. It is necessary that ΔT remain less than about 2% of the modulation frequency period for proper operation. When the transmitted and received signals are mixed in the detector mixer the difference frequency appears at the output. It can be seen in Figure 7-3 that the difference frequency will remain fairly constant with time, except near the cross-over points which occur twice during each period of the modulation frequency. The difference frequency goes to zero at each cross-over point for any altitude.

The difference frequency which varies almost directly with altitude (when over a smooth target) is amplified and used to drive a pulse generator. The pulse generator gives one output pulse for each positive half cycle of the input waveform. The difference frequency is therefore replaced by a series of pulses of uniform width and amplitude and with a frequency that is determined by the altitude.

The output pulses are fed into a counting rate circuit shown in Figure 7-4, which integrates the signal and provides an output voltage that corresponds to the average value of the series of pulses. This average signal is amplified and

used to drive a strip-chart recorder which plots an altitude record for the radar. The entire system is capable of plotting a target profile when the altimeter moves in a horizontal path over the target. The target profile must be interpreted in terms of the antenna radiation characteristics, target roughness, and altimeter velocity since these factors contribute to the altitude indication of the equipment.



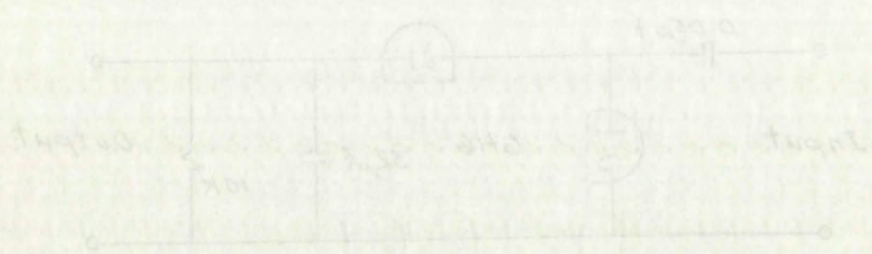
COUNTING RATE CIRCUIT

Figure 7-4

7.2 FM Altimeter Results

A number of experimental runs were made over several different targets to ascertain the main features of the system performance. This was done to demonstrate that the characteristics of FM altimeters can be studied in modeled form in the laboratory. A 6-degree antenna beamwidth (measured between the -3db points on the major lobe) was used in all cases except where otherwise specified.

used to drive a strip-chart recorder which plots an altitude record for the radar. The entire system is capable of plotting a target profile when the altimeter beam is in a horizontal path over the target. The target profile must be interpreted in terms of the known radiation characteristics, target roughness, and altimeter velocity since these factors contribute to the altitude indication of the equipment.



2.2 VM Altimeter Results

A number of experimental runs were made over several different ranges to ascertain the main features of the system performance. It was not to demonstrate that the characteristics of the altimeter can be studied in model form in the laboratory. A 6-degree antenna beamwidth (measured between the -3db points on the major lobe) was used in all cases except where otherwise specified.

The first run was used for calibration purposes. A smooth galvanized steel target, 1 x 1.2 meters in size was used since this target gives a specular reflection that does not fade. A small steel plate, 40 x 50 cm in size was supported on the large target at a distance of 2.8 cm from the surface. This small plate provided a known step change in altitude as the antennas moved over the surface. A model altitude between 40 and 60 cm was used in all cases.

The radar parameters were adjusted as shown in Table 7-1 for this experiment. The strip chart recording for this calibration run is shown in Figure 7-5. Measurements show that one division on the strip chart corresponds to 1.12 cm of altitude in the model system and to 54.8 m of altitude in the real system. The maximum fluctuation of indicated altitude in the model system is 0.58 cm (27.4 m in the real system) which is about 1% of the total altitude. This fluctuation represents the level of the instabilities in the system. Since this run over a smooth target was used for calibration purposes, the mean error is taken as zero.

The altimeter traveled a total of about 1.3 cm in the model system (64 m in the real system) in making the transition from the large target to the small target. This distance is determined by the antenna beamwidth and the threshold level of the receiver. Signals below a certain level will not actuate the pulse generator and will, therefore, not be counted. This level must be maintained sufficiently high so that noise does not actuate the counter circuit.

The sand-covered target shown in Figure 5-11 was used to illustrate the effects of a rough surface on the altimeter indication.¹ A run was made with the antenna tilted about 5 degrees away from the vertical position to show effects of the Doppler frequency shift on the altitude indication. The results from the chart, shown in Figure 7-6, show a slight increase in altitude when the antenna moves in the direction which raises the Doppler frequency, and an apparent decrease in altitude when the antenna moves in the opposite direction. The error in altitude for each of the runs is about 0.08 cm or 0.16% of the true altitude.²

The average expected per unit shift in the altitude indication can be calculated from the ratio

$$\delta h = \frac{f_D}{f_s} \quad (7-1)$$

where f_D is the Doppler frequency and f_s is the difference frequency.

The Doppler frequency is given by

$$f_D = \frac{2v f_c}{V} \sin 5^\circ \quad (7-2)$$

¹The rough sand target gives acoustic signals that are statistically similar to radar signals from heavily wooded areas.

²This result, while of the proper order of magnitude, is too small to be measured with accuracy with the equipment used.

The band-pass filter ranges from 5-11 was used to eliminate the effects of a rough surface on the distance indication. A run was made with the antenna tilted about 5 degrees away from the vertical position to show effects of the Doppler frequency shift on the altitude indication. The results from the chart show in Figure 1-3, show a slight increase in altitude when the antenna moves in the direction which raises the Doppler frequency, and an apparent decrease in altitude when the antenna moves in the opposite direction. The error in altitude for each of the runs is about 0.05 cm or 0.10% of the true altitude.

The average expected per unit shift in the altitude indication can be calculated from the ratio

$$\frac{\Delta h}{h} = \frac{v}{c} \quad (1-1)$$

where Δh is the Doppler frequency and h is the distance

frequency. The Doppler frequency is given by

$$f_D = \frac{2v}{\lambda} \quad (1-2)$$

The rough and raised surface, stochastic signals that are essentially random in nature, signals from heavily wooded areas.

This results in the order of magnitude is too small to be measured with accuracy with the equipment used.

and the difference frequency is given by

$$f_s = \frac{f_{dev}}{2} \sin \left(\frac{\Delta T}{T} 360 \right) \quad (7-3)$$

where

f_{dev} is the total frequency deviation,

ΔT is the time required for the signal to make a round trip to the target, and

T is the period of the modulation frequency

The resulting per unit shift in the altitude indication is found to be 0.0047 which results in a total expected deviation of 0.19 cm in the model (10 m in the real system).

The accuracy of the altimeter indication is affected by the Doppler frequencies in the received signal and is therefore dependent upon the antenna pattern. When the altimeter is moving in a horizontal path with the antenna oriented in the vertical direction, energy is received from scatterers that are ahead and behind the altimeter. The signal spectrum, therefore, spreads out around the transmitted frequency. The altitude indication on the altimeter is based on some type of average frequency in this spectrum. Since the signal fluctuates in a random manner, the altitude indication also fluctuates.

Horizontal runs were made over the rough sand target using two different antenna patterns in order to demonstrate the effect of antenna beamwidth on the altitude indication. The first run was made with an antenna beamwidth of 6 degrees (measured between - 3db points) and with the antenna oriented vertically. The chart record is shown in Figure 7-7.

and the difference between the two

$$\Delta f = \frac{v}{\lambda}$$

where

Δf is the difference in frequency

λ is the wavelength

v is the velocity

f is the frequency

The results

is found to be 0.0

deviation of 0.1

The accuracy

by the Doppler principle

therefore depends

altimeter is moving

oriented in the

from scatterers

The signal spectrum

transmitted frequency

altimeter is based

spectrum. Since

the altitude

Horizontal

using two different

the effect of

The first was

measured between

vertically. The

Measurements from the record indicate that the signal fluctuated over a total range of 6.7 cm from the mean value in the model (328 m in the real system), which is about 14%. The variance is about 2.2 percent of the mean altitude. The expected error in the mean altitude for this case is on the order of 0.5% and is too small to detect (with confidence) in this experiment. A second similar run was made using an antenna beamwidth of 12 degrees. The altitude record is shown in Figure 7-8. The maximum fluctuation from the mean indicated altitude is 5 cm (245 m in the real system). The variance of the indicated altitude is about 4% of the total altitude for this case as compared to 2.2% for the 6-degree antenna pattern. The mean error in altitude in this case was + 2.2% which is the same as the error introduced by a signal returned from an angle of 12 degrees from vertical.

A theoretical calculation for the expected error in an FM altimeter indication has been developed.¹ The theoretical mean difference frequency power spectrum for a linearly modulated FM signal, which is scattered from a rough surface, is approximated by

$$\overline{B(f)} = c f^{-8}, \quad f_1 \leq f \leq f_2 \quad (7-4)$$

where c is a constant.

Now, f_1 is the difference frequency obtained at vertical incidence and f_2 is the difference frequency

¹Quinlan, op. cit.

Measurements from the second indicate that the signal fluctuates over a total range of 5 cm from the mean value in the model (2.5 m in the real system) which is about 1.5. The variance is about 2.2 percent of the mean altitude. The expected error in the mean altitude for this case is on the order of 0.5 m and is too small to detect (with confidence) in this experiment. A second similar run was made using an antenna beamwidth of 12 degrees. The altitude vector is shown in Figure 9-8. The maximum fluctuation from the mean indicated altitude is 5 cm (2.5 m in the real system). The variance of the indicated altitude is about 4% of the total altitude for this case as compared to 2.2% for the 6-degree antenna pattern. The mean error in altitude in this case was + 1.2% which is the same as the error introduced by a signal returned from an angle of 12 degrees from vertical. A theoretical calculation for the expected error in an FM altimeter indication has been developed. The theoretical mean difference frequency spectrum for a linearly modulated FM signal, which is scattered from a rough surface, is approximated by

$$S(f) = \frac{1}{2} [J_0^2(f/f_1) + J_1^2(f/f_1)] \quad (9-1)$$

where c is a constant, f_1 is the difference frequency obtained at vertical incidence and f_2 is the difference frequency

obtained from the largest angle of incidence for which a usable signal level is received. This angle is taken as 16 degrees where the round-trip antenna gain, for the antenna used in the experiment, is down 24 db. The upper frequency limit can now be written in terms of the lower frequency limit as

$$f_2 = \frac{f_1}{\cos 16^\circ} \doteq 1.040 f_1 \quad (7-5)$$

Rice's formula,¹ for the expected number of zero crossings, can now be used to determine the expected frequency which determines the indicated altitude. The result is

$$\bar{f} = \left[\frac{\int_{f_1}^{f_2} f^2 \overline{B(f)} df}{\int_{f_1}^{f_2} \overline{B(f)} df} \right]^{1/2} = 1.016 f_1 \quad (7-6)$$

Since f_1 is the frequency corresponding to the correct altitude, the expected error is 1.6% which compares well with the measured error of 2.2%.

The frequency modulated altimeter was also tested while operating on an inclined path over the rough sand target. The results of runs where the altitude was increasing and decreasing are shown in Figure 7-9. The mean altitude changes from 46 cm to 49.9 cm in the model (2250 m to 2440 m in the real system) and the maximum indicated fluctuation from the mean path is 3.4 cm (166 m in the real system).

¹Rice, S.O., "Mathematical Analysis of Random Noise," Dover Publication, S262, Section 3.3, edited by Nelson Wax.

obtained from the observation of a visible signal from the target as it passes within the range of the antenna used in the experiment. The frequency limit of the system is 2000 m in the case of the system.

The frequency limit of the system is 2000 m in the case of the system. The frequency limit of the system is 2000 m in the case of the system. The frequency limit of the system is 2000 m in the case of the system.

The frequency limit of the system is 2000 m in the case of the system. The frequency limit of the system is 2000 m in the case of the system. The frequency limit of the system is 2000 m in the case of the system.

The frequency limit of the system is 2000 m in the case of the system. The frequency limit of the system is 2000 m in the case of the system. The frequency limit of the system is 2000 m in the case of the system.

The city target shown in Figure 5-14 provides a rough surface where altitude fluctuations and the effects of Doppler frequencies are combined. The results of a run using a horizontal path over the target are shown in Figure 7-10. The maximum deviation from the true altitude above the target surface is 6.7 cm (328 m in the real system). These results are summarized in Table 7-2.

TABLE 7-2
FM ALTIMETER EXPERIMENTAL RESULTS

Target	Antenna Beamwidth	Antenna Orientation	Altitude Variance	% of Total Altitude	Max. Deviation From Mean
Smooth steel	6°	Vert.	0 cm	<< 1%	0.56 cm
Rough Sand	6°	Vert.	1.12	2.2	6.72
Rough Sand	6°	5° (+Dopp.)	1.0	2.0	2.00
Rough Sand	6°	5° (-Dopp.)	0.6	1.2	2.50
Rough Sand	12°	Vert.	2.0	4.0	5.00
City	6°	Vert.	2.6	5.2	6.70

This series of tests does not exhaust the possibilities of evaluating the altimeter performance using the acoustic simulator, but merely indicates the kinds of experiments that can be performed. Other experiments that are of interest include:

- (1) the effects of changing the modulation rate and frequency deviation,
- (2) the results of using a variety of model targets,

- (3) the effects of following different trajectories over the targets,
- (4) a comparison with other FM schemes, and
- (5) the errors introduced by the use of wide beam antennas.

- (3) the effects of following different trajectories over the targets,
- (4) a comparison with other FM schemes, and
- (5) the errors introduced by the use of wide beam antennas.

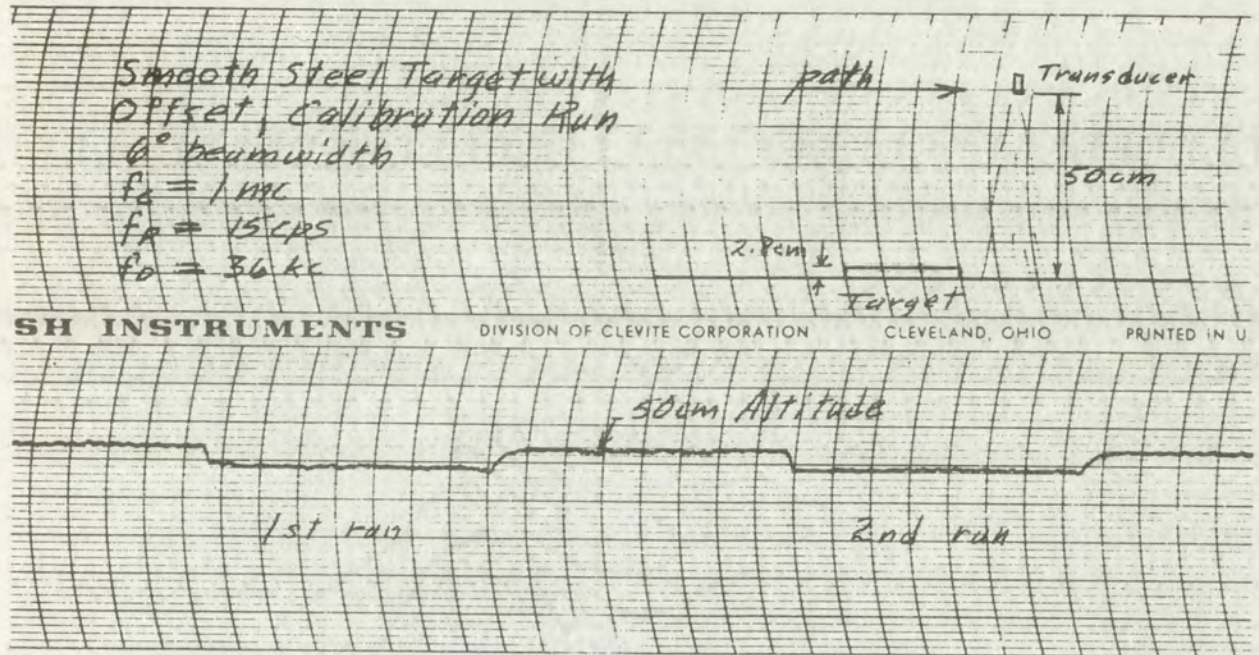


Fig. 7-5

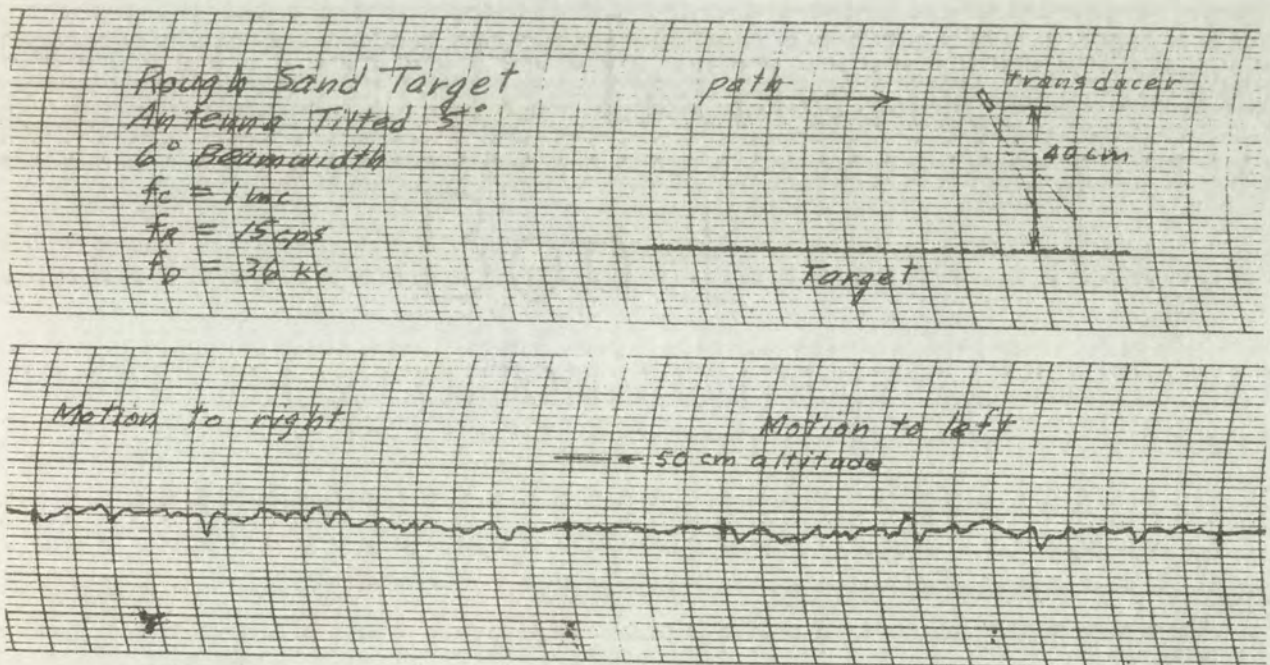


Fig. 7-6

INSTRUMENTS

[Faint handwritten notes and scribbles on graph paper]

[Faint handwritten notes]

[Faint handwritten notes]

[Faint handwritten notes]

[Faint handwritten notes]

[Faint handwritten notes]

[Faint handwritten notes]

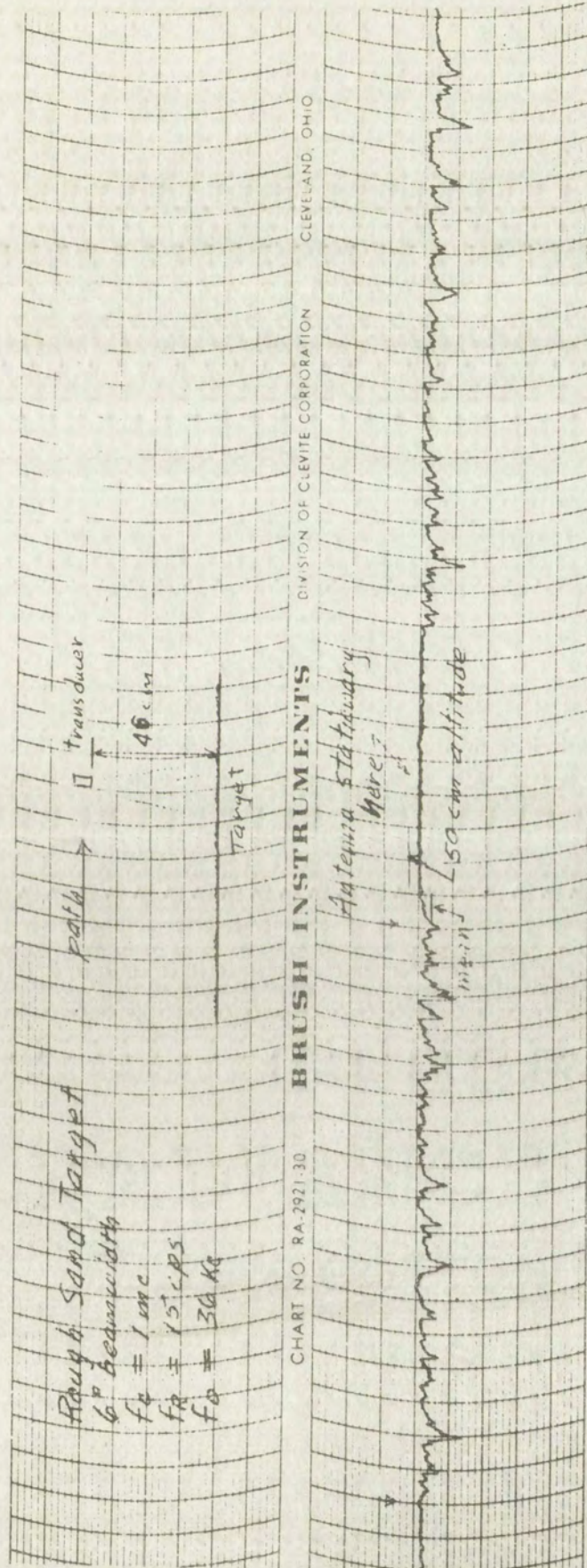


Fig. 7-7

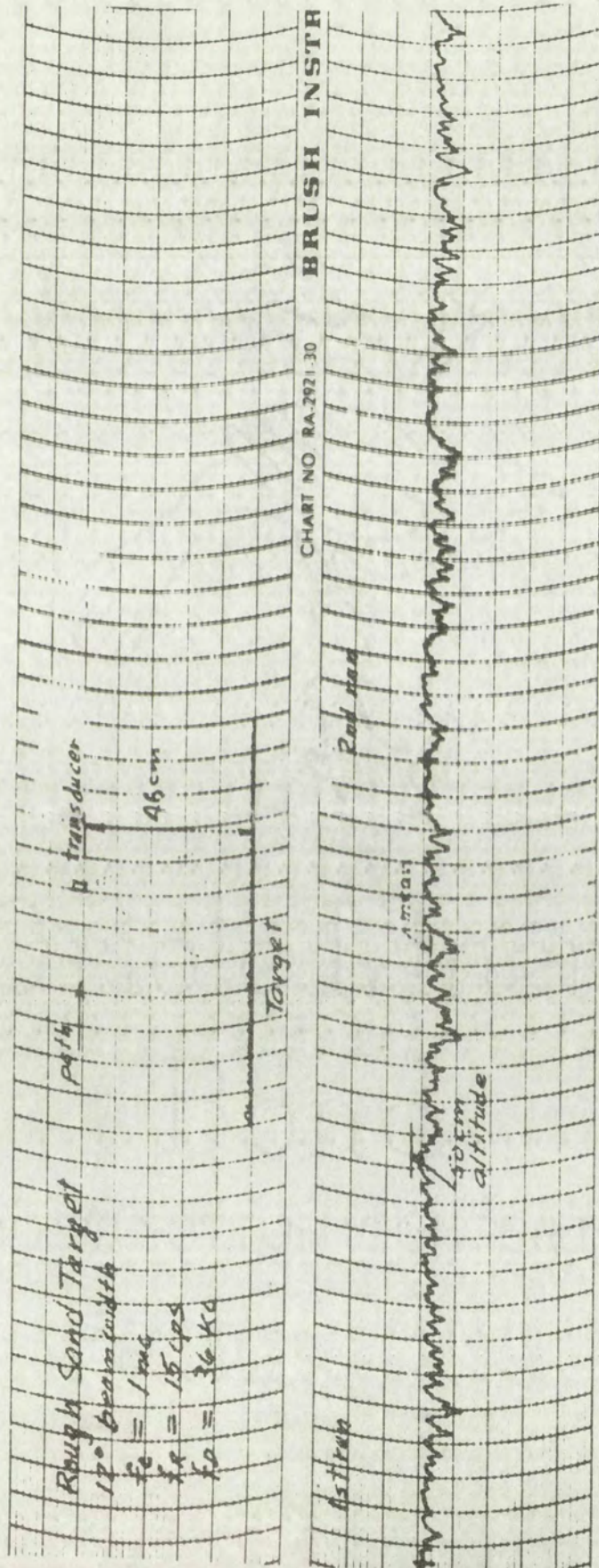
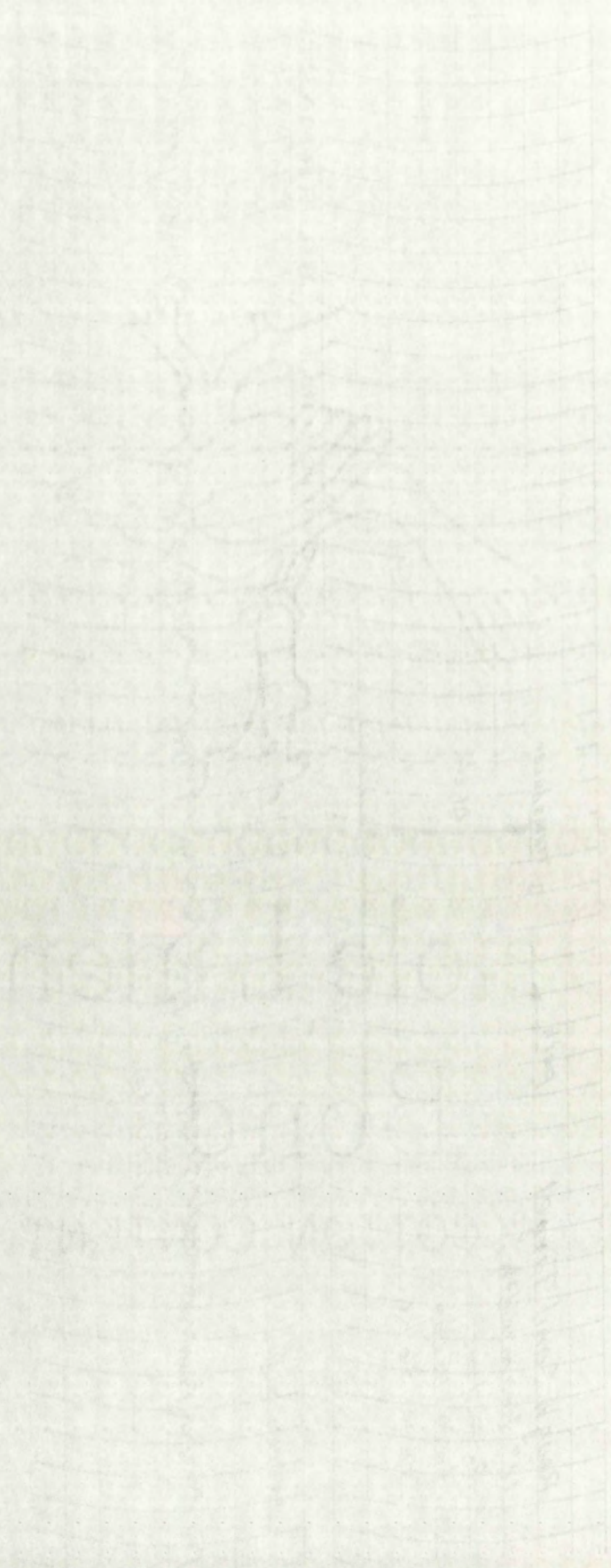


Fig. 7-8



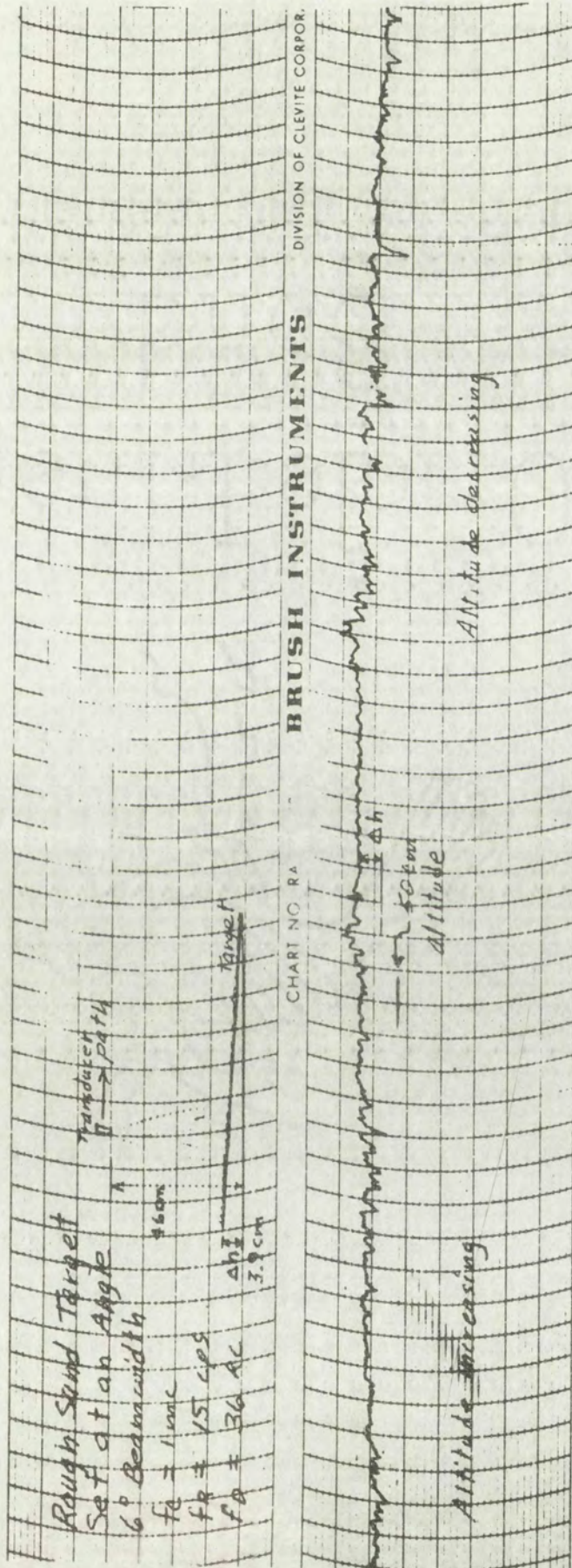


Fig. 7-9

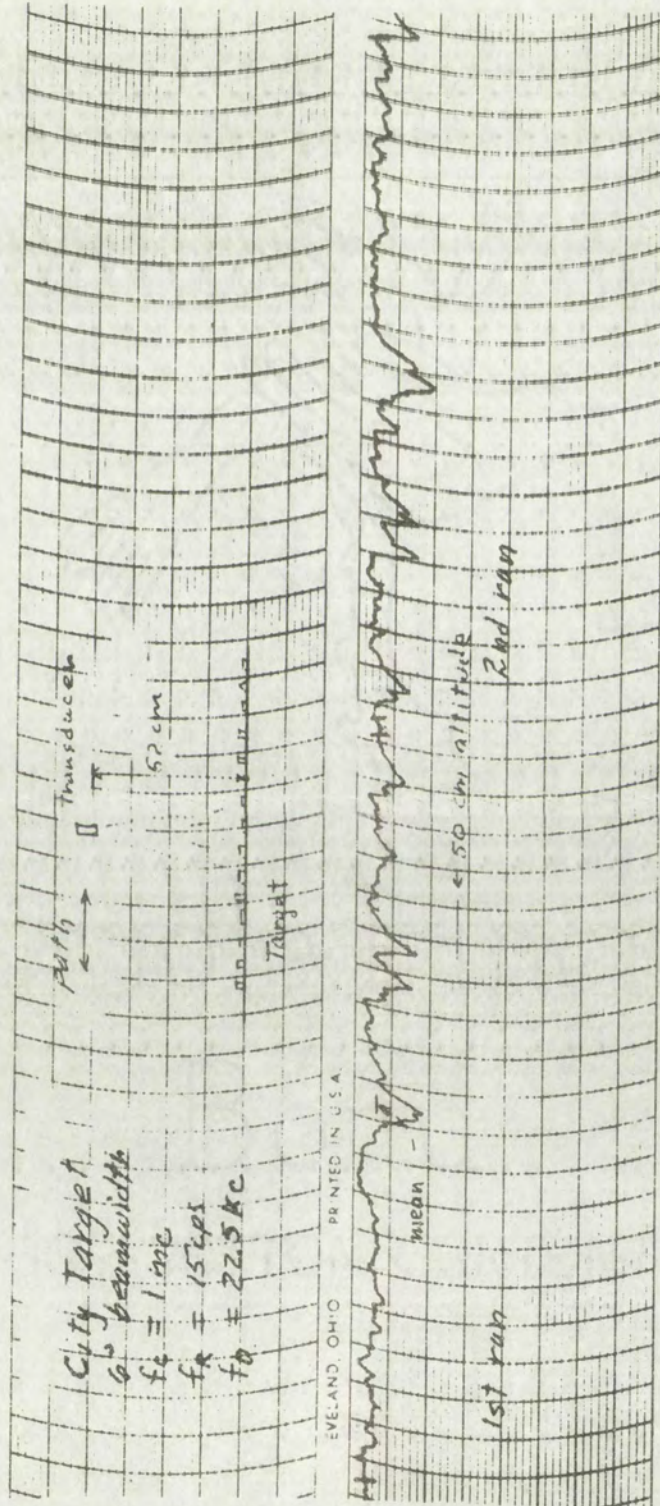


Fig. 7-10

CHAPTER VIII

CONCLUSIONS

The use of linear and nonlinear modeling and the analogy between acoustic and electromagnetic waves make it feasible to simulate radar type systems and propagation problems in the laboratory. It has been determined that many of the statistical characteristics of electromagnetic waves scattered from terrain, such as: (1) the angular dependence of the mean backscattered intensity, (2) the range of fading, and (3) geometrical effects, can be duplicated using appropriate targets and acoustic waves in water. It is therefore possible to perform model experiments using acoustic waves, which aid in evaluating the operating behavior of radar type systems under controlled laboratory conditions.

An investigation of the feasibility of a radar type device, such as an altimeter or Doppler frequency navigator, is aided by the performance of certain preliminary experiments. It is always advantageous to complete these preliminary experiments before a large development program is established; therefore, modeling techniques are desirable. A scaled system experiment using the acoustic simulator can be set up in the laboratory in a few days time to

The use of linear and nonlinear models and the analogy between acoustic and electromagnetic waves make it feasible to consider the problem of wave propagation in the form of a boundary value problem in the theory of linear and nonlinear waves. The many of the physical processes of electromagnetic waves scattered from objects, such as antennas, angular dependence of the mean field, etc., can be duplicated using appropriate models and wave propagation in water. It is therefore possible to perform model experiments using water as a medium for investigation of the operating behavior of antennas in water. The excited laboratory model is a scaled model of the actual device. An investigation of the behavior of a device, such as an antenna or a hydrophone, is aided by the performance of model experiments. It is also possible to perform preliminary experimental tests of the elements of a system is established; therefore, modeling techniques are possible. A scaled system experiment during the experimental work can be set up in the laboratory in a few days time.

investigate the effects of parameter changes in the system. A properly designed target model can provide acoustic signals which simulate the real signals and help in the evaluation of the system performance under a variety of conditions. Design programs which normally require many months can therefore be accelerated because some of the problems can be solved rapidly using modeling techniques.

The factors, which transform the parameters of the real system into the parameters of the model system, scale both time and distance in the model. This is desirable in that the environment of a propagation or backscattering experiment can be confined to a water tank in the laboratory. The range and wavelength are shortened, and pulse width and rise time are lengthened. The modulation frequency, Doppler frequency, and radar antenna velocity are greatly reduced in the model. This simplifies the problem of building the model system since "breadboard" circuits are usually satisfactory.

The acoustic simulator can also be used to study theoretical problems associated with the scattering of waves from different surfaces. It is always desirable to check theoretical predictions with appropriate experiments. The analogy between linearly polarized plane waves and acoustic waves makes it possible to check certain electromagnetic scattering theories involving the scattering properties of different surfaces. The similarities, between a spherical

investigate the effect of parameter changes in the system.

A properly designed target model can provide accurate results.

It also allows the user to help in the evaluation

of the system performance under a variety of conditions.

Design programs which normally require many months can

therefore be accelerated because some of the problems can

be solved rapidly using modeling techniques.

The designer, which represents the parameters of the

real system, into the parameters of the model system, can

both time and distance in the model. This is desirable

in that the environment of a propagator or backscattering

experiment can be confined to a water tank in the laboratory.

The range and wavelength are selected as 4, 5 and 6 pulses

width and rise time are determined. The modulation frequency

frequency, Doppler frequency, and radar antenna velocity are

greatly reduced in the model. This simplifies the problem

of building the model system with "bandwidth" circuits

are usually satisfactory.

The acoustic simulator can also be used to study

theoretical problems associated with the scattering of waves

from different surfaces. It is always desirable to check

theoretical predictions with appropriate experiments. The

analogy between linearly polarized plane waves and acoustic

waves makes it possible to check certain electromagnetic

scattering theories involving the scattering properties of

different surfaces. The similarities between a spherical

acoustic wave and the field about a short current element, extend through terms which vary as $1/r$ and $1/r^2$ for the analogy between particle velocity and magnetic field intensity. Other possible analogies, between the variables in the acoustic system and the electric and magnetic field components, are valid only at large distances from the source and, in some cases, do not exist. Boundary conditions are also similar in that tangential components of the electric and magnetic fields are continuous across the boundary, as are the pressure and the normal component of particle velocity.

A simplified model, for the scattering of polarized electromagnetic waves from a rough surface, was investigated. A distribution of excited scattering elements, located above and below a mean plane surface, was shown to give the same resultant field at the receiving antenna as for the case of acoustic waves. The model is, therefore, essentially scalar in nature and does not exhibit polarization effects.

The frequency range between 200 kc/sec and 5 mc/sec is best suited to acoustic modeling experiments. The attenuation in the water and the effects of foreign particles such as dust become significant at frequencies above a few megacycles per second. On the other hand when the frequencies become too low, the wave length is large and proper scaling is impractical for a small water tank. When non-linear modeling is used with experiments involving short pulses, it is desirable to use a high carrier frequency

in order to maintain an adequate number of cycles of the carrier frequency to define the pulse shape.

The size of tank required depends considerably upon the type of experiments to be performed. A small tank, on the order of 4 feet in each dimension, is quite adequate for many experiments, such as:

- (1) making scatter patterns from objects with different geometric shapes,
- (2) measuring antenna patterns,
- (3) investigating propagation characteristics in a nonhomogeneous medium, and
- (4) performing some system experiments. A tank capable of accommodating a plywood target measuring 4 x 6 feet, at a range of 6 feet, is desirable for high altitude modeling problems.

The addition of rubberized horsehair or a resilient rubber lining on the interior of the tank will reduce the echoes on the order of 20 db. This absorbing material is generally more effective at the higher acoustic frequencies. A wooden tank is better than a steel tank from the standpoint of reflections from the walls since the reflection coefficient from wood is on the order of 0.5 as compared to nearly unity for the steel tank. When using directional antennas the undesired signal is generally reflected several times in the tank before arriving at the receiving antenna. The inverse square variation of intensity with distance will

in order to make a...
earlier...
The...
the type of...
on the order of...
for many experiments...

- (1) ...
- (2) ...
- (3) ...
- (4) ...

The addition of...
lining on the...
on the order of...
more effective...
tank is better...
reflections...
from wood as...
only for the...
the undesired...
in the tank...
investigate...

usually reduce this signal to a negligible value compared to the desired signal when the tank is several feet in each dimension.

Terrain such as heavily wooded areas has a back-scattering radar cross section per unit area that remains fairly constant with angles of incidence out to 30 degrees from the vertical (at frequencies above a few hundred megacycles per second). Flat wooded terrain is properly modeled by a flat plywood target with a dense covering of sand particles that are on the order of a wavelength in size. The wavelength in water is about 1.5 mm at a typical model frequency of 1 mc/sec, therefore, sand particles on the order of 1 to 2 mm in size are suitable for use on the targets. Other terrain areas, such as farmland, can be represented by using a sparse covering of sand particles with a separation of from 1 to 5 wavelengths between particles. The smooth plywood gives return signals with statistics similar to those for certain flat areas where vegetation is sparse. The range of fading, defined here as the range between the level exceeded by 95% of the returned signals and the level exceeded by only 5% of the returned signals, is about 18 db for the wooded areas and about 8 to 12 db for the relatively smooth areas.

The essential components for an acoustic simulator, in addition to the water tank, include several submersible

piezo electric transducers, an oscillator, amplifiers and pulse circuits. A special purpose high powered pulsed oscillator is desirable if pulse work is anticipated. For theoretical investigations a "strip film" camera is desirable so pulse-by-pulse photographs can be made. When specific systems are being modeled it is necessary to use special signal processing circuitry to duplicate the system performance. For general purposes, the majority of the simulator components are standard electronics laboratory items. "Breadboard" circuitry can be used for special purpose applications. Because of the low frequency range involved, the wiring is not as critical as in the full scale equipment.

In summary, the acoustic simulator is useful as an analog computer for modeling radar type systems. The model does not provide all the answers since the acoustic wave is longitudinal in nature and can be described by a vector and a scalar quantity; while the electromagnetic wave is transverse and can be specified by two vector quantities. Polarization effects are, therefore, not present in the acoustic model. The acoustic simulator is of value, however, because it provides a means of studying experimentally the scattering of waves from different surfaces and it answers many questions concerning the design and application of radar type systems.

phase electric transients, an oscillator, amplifiers and
pulse circuits. A special purpose high powered pulsed
oscillator is desirable if pulse work is anticipated. For
theoretical investigations a "strip film" camera is desir-
able so pulse-by-pulse photographs can be made. When
specific systems are being modeled it is necessary to use
special signal processing circuitry to duplicate the
system performance. For general purposes, the majority
of the standard components are standard electronic
laboratory items. "Breadboard" circuitry can be used for
special purpose applications. Because of the low frequency
range involved, the wiring is not as critical as in the
full scale equipment.

In summary, the acoustic simulator is useful as an
analog computer for modeling radar type systems. The model
does not provide all the answers since the acoustic wave
is longitudinal in nature and can be described by a vector
and a scalar quantity; while the electromagnetic wave is
transverse and can be specified by two vector quantities.
Polarization effects are, therefore, not present in the
acoustic model. The acoustic simulator is of value, however,
because it provides a means of studying experimentally
the scattering of waves from different surfaces and its
answers many questions concerning the design and appli-
cation of radar type systems.

APPENDIX A

FADING OF RADAR SIGNALS

Fading is defined as the fluctuation in the envelope of the received signal, which is due to interference between the components of the total signal. When considering a pulse radar, the fading can be considered as being: (1) intrapulse, and (2) interpulse fading. Intrapulse fading is the fluctuation which occurs in the envelope of a single received pulse and is caused by a "wavepacket" spreading over an irregular target, which introduces a changing population of scatterers into the illuminated region. Interpulse fading is the fluctuation in the pulse envelope at a particular delay time (measured from the leading edge of the received pulse) which occurs between successive pulses. It is caused by small changes in range to the different illuminated scatterers because of a relative velocity between the radar and the target.

Fading will be discussed briefly in two categories; with and without relative motion between the radar and the target. In each case three schemes will be considered: (1) CW unmodulated, (2) short-pulse, and (3) long-pulse radar. In addition, the method of determining the variance spectrum is considered.

CW Unmodulated Radar - No Relative Motion

Consider first the situation where the CW unmodulated radar is operating with a single point isotropic scatterer in the illuminated region. The echo consists of a single frequency since the target and radar are stationary. Now, when a second similar scatterer is introduced into the illuminated region, the total signal depends upon the relative amplitude and phase of the two components.

Consider now a situation where many scatterers are distributed over a surface that is generally flat, except for irregularities on the order of a wavelength in size. The total signal received from an illuminated region on this target is composed of a large number of separate components of nearly equal magnitudes but with random phases determined by the irregular surface. When no relative motion exists, the received signal is a sine wave at the carrier frequency and has an amplitude corresponding to one member of an ensemble having statistics of a random walk. This situation is the steady state case.

Short-Pulse Radar - No Relative Motion

When a very short pulse is used, the illuminated area at a given time is always limited by the pulse width, except at very short ranges. Fading occurs continuously during the received pulse for this "pulse-width limited" situation.

CW Unmodulated Radar - No Relative Motion

Consider first the situation where the CW unmodulated radar is operating with a single point isotropic scatterer in the illuminated region. The echo consists of a single frequency since the target and radar are stationary. Now, when a second similar scatterer is introduced into the illuminated region, the total signal depends upon the relative amplitude and phase of the two components.

Consider now a situation where many scatterers are distributed over a surface that is generally flat, except for irregularities on the order of a wavelength in size. The total signal received from an illuminated region on this target is composed of a large number of separate components of nearly equal magnitudes but with random phases determined by the irregular surface. When no relative motion exists, the received signal is a sine wave at the carrier frequency and has an amplitude corresponding to one member of an ensemble having statistics of a random walk. This situation is the steady state case.

Short Pulse Radar - No Relative Motion

When a very short pulse is used, the illuminated area at a given time is always limited by the pulse width, except at very short ranges. Fading occurs continuously during the received pulse for this "pulse-width limited" situation.

It should be observed that relative motion between the radar and target is not involved in this fading; only the illuminated region is changing. When consecutive pulses are observed they are all identical. This intra-pulse fading is caused by the spreading of the advancing spherical wave over the target, which changes the population of scatterers that are contributing to the return signal at a particular instant of time. All components of the signal are at the carrier frequency since no relative velocity exists between the target and the radar.

Long-Pulse Radar - No Relative Motion

Assume now that a long-pulse radar with a directional antenna is used. The pulse propagates from the antenna toward the target as a spherical wave. The target is first illuminated at the point closest to the antenna. From this point the illuminated region as "seen" by the radar is smaller than the actual region on the target where incident energy exists. The number of scatterers in the illuminated region continually increases as the spherical wave expands over the target and the signal at the antenna continues to fade as some of the added scatterers give signals in-phase with the resultant and some give signals out of phase. When the leading edge of the pulse, as seen from the antenna location, reaches the edge of the antenna pattern no new scatterers are added. This corresponds

to the steady state condition previously discussed. The signal level remains constant until the trailing edge of the pulse reaches the target, at which time another transient period starts. As the trailing edge of the pulse moves out over the target, scatterers are removed from the illuminated area and fading again occurs in the signal. This situation is called the "beamwidth limited" case.

CW Unmodulated Radar - Relative Motion

Now consider the situation where an unmodulated CW radar is moving with respect to the target. The signal fades since the relative distances to the various scatterers change continuously. As the antenna moves to a new position the relative phases of the many signal components change so the phasor sum changes, resulting in a new magnitude. Also a few new scatterers are continually being added to the illuminated area on one side of the pattern and a few others are being removed from the illuminated region on the other side.

The fading that exists in this situation can be analyzed in two different ways. First one can observe that the radar occupies a slightly different position in space after a small elapsed time. This means that the distribution of scatterers, with respect to the radar, is slightly altered and the relative phase shifts are somewhat displaced from what they were at the earlier time. This results in a different magnitude for the signal at each successive interval

to the steady state condition previously discussed. The signal level remains constant until the trailing edge of the pulse reaches the target, at which time another transient period starts. As the trailing edge of the pulse moves out over the target, scatterers are removed from the illuminated area and fading again occurs in the signal. This situation is called the "complementary fading" effect.

CW Unmodulated Radar - Relative Motion

Now consider the situation where an unmodulated CW radar is moving with respect to the target. The signal fades since the relative distances to the various scatterers change continuously. As the antenna moves to a new position the relative phases of the many signal components change as the phase sum changes, resulting in a new magnitude. Also a few new scatterers are continuously being added to the illuminated area on one side of the pattern and a few others are being removed from the illuminated region on the other side. The fading that exists in this situation can be analyzed in two different ways. Either one can observe that the radar occupies a slightly different position in space after a small elapsed time. This means that the distribution of scatterers, with respect to the radar, is slightly altered and the relative phase shifts are somewhat displaced from what they were at the earlier time. This results in a different magnitude for the signal at each successive interval.

of time. From another viewpoint the signal returned from each scatterer is shifted in frequency by an amount determined by the relative velocity between the antenna and the scatterer along the line joining them. The various scattered signals therefore make up a spectrum of frequencies about the carrier frequency. When these signals are combined to give a single resultant signal they "beat" together and therefore fade at a rate equal to the individual difference frequencies. Since there are many difference frequencies present a fading spectrum exists which describes the fading in the envelope of the resultant signal.

Short-Pulse Radar - Relative Motion

The short-pulse radar signals have both intrapulse and interpulse fading when relative motion exists between the radar and the target. The intrapulse fading occurs throughout the pulse because the narrow illuminated region spreads over the target, as before, and the interpulse fading occurs because the orientation of the scatterers changes with respect to the radar, between successive pulses.

The discrete interpulse fading record, which occurs at a particular delay time (as measured from the leading edge of each pulse) in successive received pulses, corresponds to samples taken from an unmodulated CW fading record over the same illuminated region.

Long-Pulse Radar - Relative Motion

The long-pulse radar signals will also have both intrapulse and interpulse fading when relative motion exists between the radar and the target and a directive antenna is used. In this case, however, the intrapulse fading will exist only near the leading edge and near the trailing edge of the pulse, since antenna beam-width limiting of the illuminated area exists (except for very high altitudes). The middle portion of the received pulse which corresponds to the unmodulated CW case, fades as a unit from one pulse to the next.

Variance Spectrum - Unmodulated CW Radar

The maximum frequency component in the envelope of the return signal fading record is determined by the maximum difference frequency between signals from various scatterers. The difference frequency can be written as

$$f_{diff} = \frac{2f_c v}{c} (\cos \alpha_{min} - \cos \alpha_{max}) \quad (1)$$

where

f_c is the carrier frequency,

c is the velocity of propagation,

v is the antenna velocity

α_{min} is the minimum angle between the antenna velocity vector and a contributing scatterer, and

α_{max} is the maximum angle between the antenna velocity vector and a contributing scatterer.

Long-Pulse Radar - Relative Motion

The long-pulse radar signal will also have both intrapulse and interpulse fading when relative motion exists between the radar and the target and a directive antenna is used. In this case, however, the intrapulse fading will exist only near the leading edge and near the trailing edge of the pulse, since antenna beam-width limiting of the illuminated area exists (except for very high frequencies). The middle portion of the received pulse which corresponds to the unmodulated CW case, fades as a unit from one pulse to the next.

Variance Spectrum - Unmodulated CW Radar

The maximum frequency component in the envelope of the return signal fading record is determined by the maximum difference frequency between signals from various scatterers. The difference frequency can be written as

$$f_{\text{diff}} = \frac{2c}{\lambda} \left(\cos \alpha_{\text{min}} - \cos \alpha_{\text{max}} \right) \quad (1)$$

where

- f_c is the carrier frequency,
- c is the velocity of propagation,
- v is the antenna velocity
- α_{min} is the minimum angle between the antenna velocity vector and a contributing scatterer, and
- α_{max} is the maximum angle between the antenna velocity vector and a contributing scatterer.

For the usual case, where the antenna illuminates a region on the rough target, there will be scatterers distributed over the entire range of angles

$$\alpha_{min} \leq \alpha \leq \alpha_{max}$$

This establishes a pre-detection spectrum which describes the fluctuations in the envelope of the signal.

It is convenient to study this spectrum after square-law detection by specifying the variance at each frequency in the spectrum. The variance is defined as the mean squared value of the fluctuating component of power about the mean.^{1,2} The variance can be expressed as

$$Var = \overline{(P - \bar{P})^2} \quad (2)$$

where

P is the average power over a single cycle of the carrier frequency, and

\bar{P} is the mean power for the entire record.

The variance spectrum shows the distribution over frequency of the fluctuating component of power in the interpulse fading record, and is used to estimate the fading rate for the radar.

¹Edison, A.R., Radar Terrain Return Statistics at Near Vertical Incidence, Univ. of New Mexico, Engr. Exp. Stn. Rpt. EE-35, Oct. 1960.

²"Power" refers to the average power over 1 cycle of the carrier frequency.

For the usual case, the signal is assumed to be a constant amplitude, A , and the noise is assumed to be a constant amplitude, N . The signal is assumed to be a constant amplitude, A , and the noise is assumed to be a constant amplitude, N .

This section discusses the detection of a signal in the presence of noise. The signal is assumed to be a constant amplitude, A , and the noise is assumed to be a constant amplitude, N . The signal is assumed to be a constant amplitude, A , and the noise is assumed to be a constant amplitude, N .

where P is the average power of the signal, N is the average power of the noise, and S is the average power of the signal plus noise. The signal is assumed to be a constant amplitude, A , and the noise is assumed to be a constant amplitude, N .

the carrier frequency is f_c , the signal frequency is f_s , and the noise frequency is f_n . The signal is assumed to be a constant amplitude, A , and the noise is assumed to be a constant amplitude, N .

The variance spectra given in Chapter VI were calculated from pulse radar data. The information on the interpulse fading record is available in the form of a series of discrete samples from an infinite population, which places certain limitations on the validity of the estimated variance spectrum. The sampling theorem stated that samples must be taken at least twice per cycle in order to identify a particular frequency. This requirement places an upper frequency limit on the estimated variance spectrum, which is given by

$$f_u = \frac{1}{2\Delta t} \quad (3)$$

where Δt is the time interval between samples. It is therefore necessary to use a high enough pulse repetition rate to get essentially all of the high frequency fading information in the standing wave pattern when obtaining data for a variance spectrum. Any power in frequencies above f_u in the standing wave pattern is aliased to frequencies above f_u .¹ Two frequencies beating together must be observed for at least one half of a beat period in order to be distinguished. Actually the frequency resolution is somewhat less than indicated by this criterion.

If the time series is assumed to be stationary, then it has been shown that the autocovariance function, ϕ , and

¹Blackman, R.B., and Tukey, J.W., The Measurement of Power Spectra, Dover Publications, New York, S507, 1958

The first of these is the fact that the
calculated from the observed data
interference pattern is not a simple
series of discrete maxima and minima
which places upon the theory of
estimated interference pattern
that samples must be taken in
order to identify the pattern
places an upper limit on the number of
spectrum, which is the number of
in the spectrum, which is the number of
where it is the number of
force necessary to produce the pattern
to get essentially all of the
in the spectrum, which is the number of
since spectrum, which is the number of
standing wave pattern, which is the number of
Two frequencies, which is the number of
least one half of the
Actually the frequency, which is the number of
indicated by the spectrum, which is the number of
It is the frequency, which is the number of
it has been shown that the frequency, which is the number of

Power Spectra
Jackson, R. W.
The frequency, which is the number of

the power spectrum, g , are Fourier transforms of each other.¹
The fading spectrum can therefore be expressed as

$$g(\omega) = 2 \int_0^{\infty} \phi(\tau) \cos \omega \tau d\tau \quad (4)$$

where ω is the angular frequency, and τ is the lag time.
The autocovariance is a function of the lag time, τ , and can be expressed as

$$\phi(\tau) = \lim_{T \rightarrow \infty} \frac{1}{T} \int_{-\frac{T}{2}}^{\frac{T}{2}} p(t) p(t+\tau) dt \quad (5)$$

where $p(t)$ is the random power function obtained from the pulse samples at a fixed delay time in each pulse. The fading spectrum (sometimes called the variance spectrum) can be calculated by taking the cosine transform of the autocovariance function. The fading spectrum shows the distribution of variance over frequency.

¹Ibid.

The power spectrum of the random process is given by

The fading spectrum can be expressed as

$$S(f) = \frac{1}{2} S(f_c)$$

where f_c is the carrier frequency and f is the fading frequency.

The autocorrelation function of the fading process can be expressed as

can be expressed as

$$R(f) = \frac{1}{2} S(f_c)$$

where $R(f)$ is the autocorrelation function of the fading process.

pulse samples at t_1 and t_2 are independent. The fading process is

spectrum (sometimes called the fading spectrum) can be

calculated by taking the Fourier transform of the autocorrelation function.

covariance function. The fading process is a random process with

function of variance over the fading frequency.

role of fading

Bond

of fading

APPENDIX B

REPEATABILITY OF FADING RECORDS

The ability to duplicate a fading record by making a return over the same path is illustrated in Figure 1. The strip charts were made using the frequency modulated radar simulator described in Chapter VII. A rough sand-covered target was used, and the antenna (6 degree beamwidth) moved over the target in a path that was parallel to the surface of the target. The sharp rise in altitude at the left end of the chart indicates the point where the transducers entered the water. The altitude fading record continued until the transducer motion was stopped at the right side of the chart. The close agreement between the two fading records is easily observed in the figure.

The pulse radar simulator, as described in Chapter V, was used in a similar manner over the same rough target. The resulting fading records for two identical runs over the same path are shown in Figure 2. In this case each vertical line represents a sample taken from a pulse at a fixed delay time in the pulse. The photographs are nearly identical, which indicates the ability of the acoustic simulator to reproduce fading records accurately. This makes it possible to vary a single parameter and observe the effects on the signal, thus giving better control over the experiment.

The ship's log... return over the same path... strip charts were used... amplifier... target was used... over the target... of the target... of the chart... entered the water... until the transducer... of the chart... records as easily... The pulse... was used in a... The resulting... same path... line represents... time in the pulse... which indicates... reproduce fading... to vary a single... signal, thus giving...

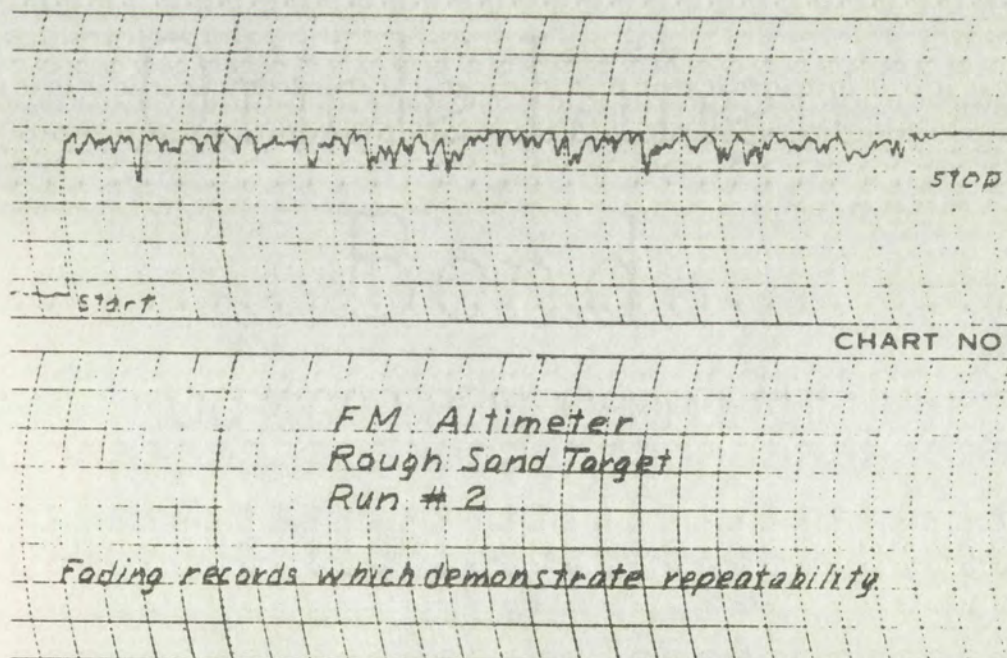
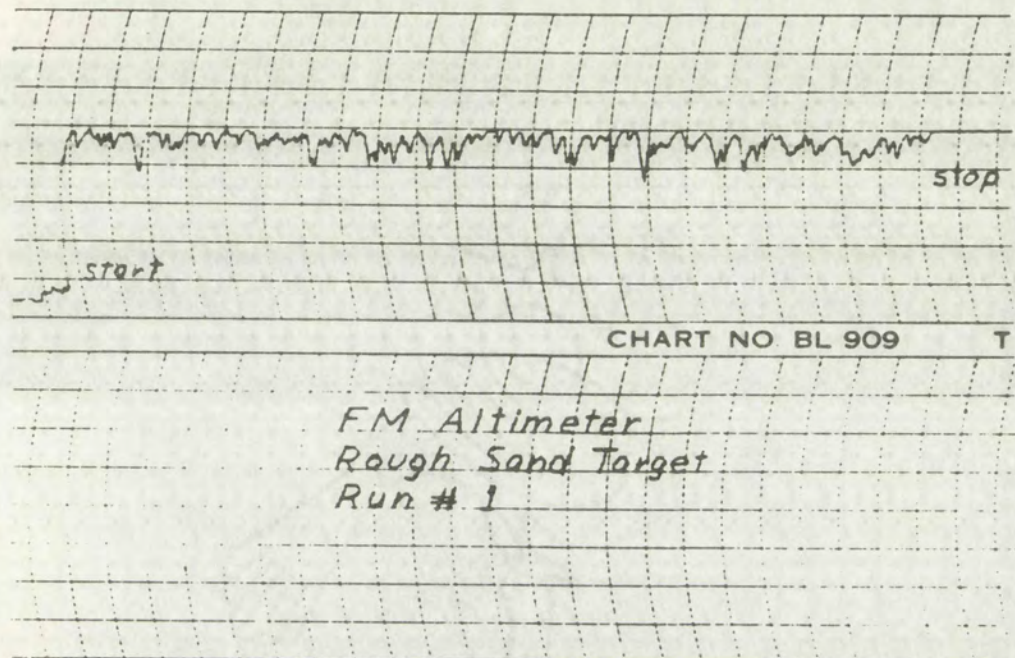
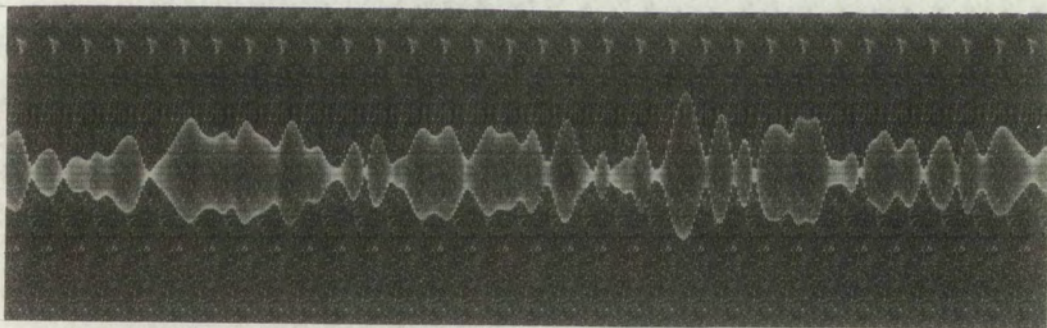
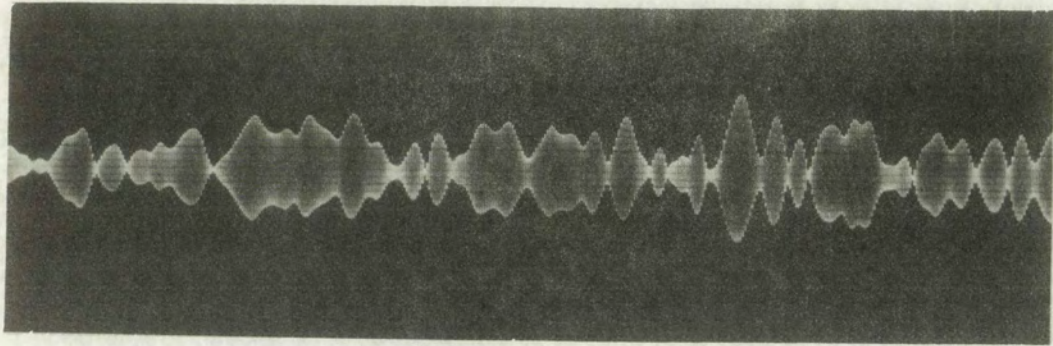
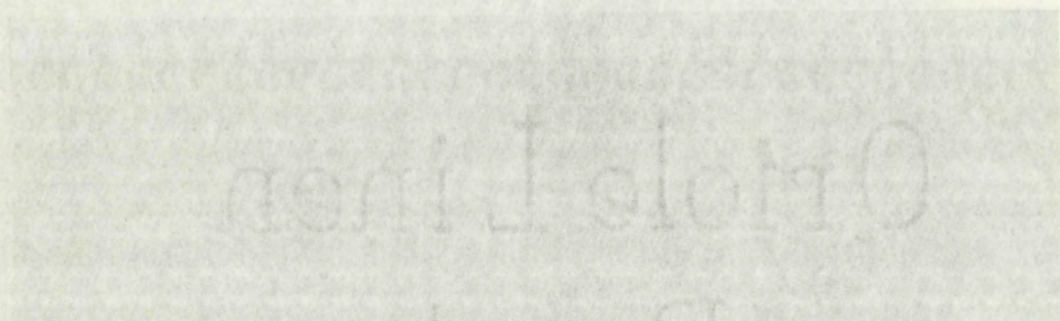
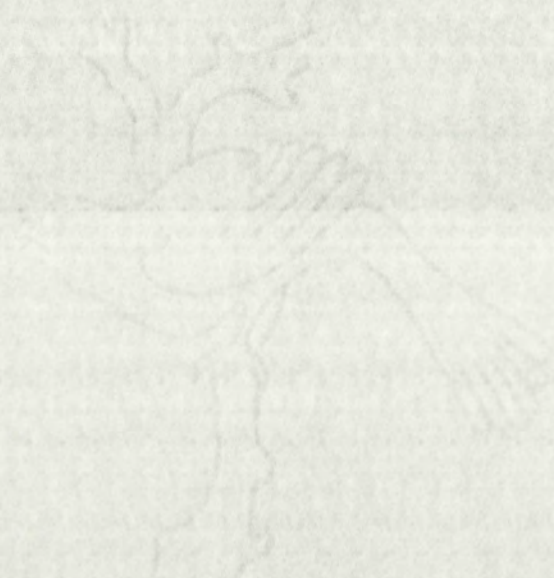
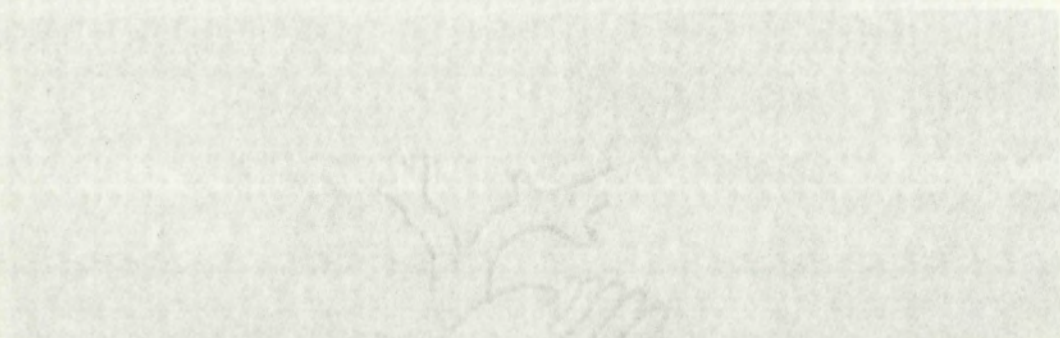


Fig. B-1



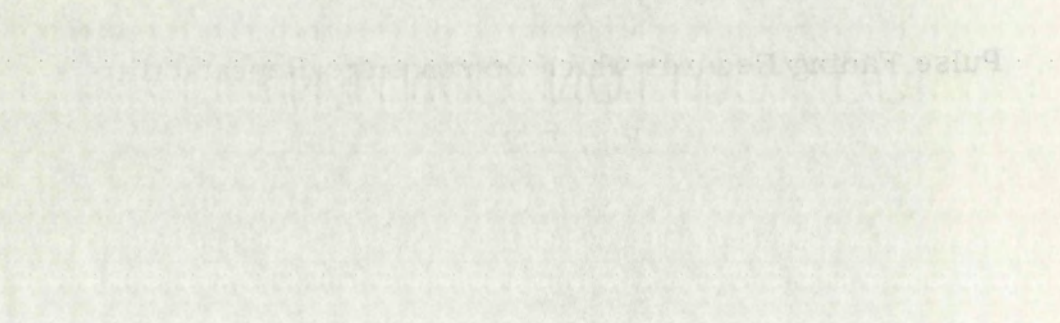
Pulse Fading Records which Demonstrate Repeatability

Fig. B-2



Orion's Line

Board



BIBLIOGRAPHY

A. BOOKS AND REPORTS

- Belyea, J. E., Low, R.D., and Siegel, K. M. Non-Linear Modeling of Maxwell's Equations. University of Michigan, Radiation Laboratory Report, No. 38, December, 1959.
- Birkhoff, G. Hydrodynamics. Dover Publication, New York, 1955.
- Blackman, R. B. and Tukey, J. W. The Measurement of Power Spectra. Dover Publication, New York, 1958.
- Bridgman, P. W. Dimensional Analysis. New Haven, 2nd ed., 1931.
- Chernov, L. A. Wave Propagation in a Turbulent Medium. Translated from Russian by R. A. Silverman. McGraw-Hill Book Company, New York, 1960.
- Cosgriff, R. F., Peake, W. H., and Taylor, R. C. Terrain Scattering Properties for Sensor System Design. Ohio State Engineering Experiment Station, Bulletin 181, May, 1960.
- Dye, J. E. Ground and Sea Return Signal Characteristics of Microwave Pulse Altimeters. Transactions of Symposium on Radar Return, Part 1. Sponsored by U.S. Naval Ordnance Test Station, China Lake, Calif. and Univ. of N. Mex., NOTS TP 2338, 1959.
- Edison, A. R., Moore, R. K., and Warner, B. D. Radar Return at Near-Vertical Incidence - Summary Report. University of New Mexico, Engineering Experiment Station Report EE-24, September, 1959.
- _____. Radar Terrain Return Statistics at Near-Vertical Incidence. University of New Mexico, Engineering Experiment Station Report EE-35, October, 1960.
- Focken, C. M. Dimensional Methods and Their Applications. Edward Arnold and Company, London, 1953.

BIBLIOGRAPHY

BOOKS AND REPORTS

- Beiser, S. E., Low, E. D., and Riebel, K. M. Non-linear Modeling of Maxwell's Equations. University of Michigan, Radiation Laboratory Report, No. 38, December, 1959.
- Birkhoff, G. Hydrodynamics. Dover Publications, New York, 1955.
- Blackman, R. B., and Jukay, J. W. The Measurement of Power Spectra. Dover Publications, New York, 1958.
- Bridgman, P. W. Dimensional Analysis. New Haven, and ed., 1931.
- Chernov, L. A. Wave Propagation in a Turbulent Medium. Translated from Russian by R. A. Silverman. Moscow: Hill Book Company, New York, 1950.
- Goodrich, R. F., Paske, W. B., and Taylor, R. C. Terrain Scattering Properties for Radar System Design. Radio Systems Engineering Experiment Station, Billerica, Mass., May, 1960.
- Gye, J. E. Ground and Sea Return Signal Characteristics of Microwave Pulse Altimeters. Translations of Symposium on Radar Return, Part I. Sponsored by U.S. Naval Ordnance Test Station, China Lake, Calif. and Univ. of N. Mex., Note TP 2528, 1959.
- Edmon, A. R., Moore, R. K., and Warner, R. D. Radar Return at Near-Vertical Incidence - Summary Report. University of New Mexico, Engineering Experiment Station Report EE-24, September, 1959.
- Radar Terrain Return Statistics at Near-Vertical Incidence. University of New Mexico, Engineering Experiment Station Report EE-25, October, 1960.
- Fecken, C. M. Dimensional Methods and Their Applications. Edward Arnold and Company, London, 1957.

- Hueter, T. F. and Bolt, R. H. Sonics. John Wiley and Sons, New York, 1955.
- Jordan, E. C. Acoustic Models of Radio Antennas. Ohio State University, Engineering Experiment Station Bulletin 108, May, 1941.
- Langhaar, H. L. Dimensional Analysis and Theory of Models. John Wiley and Sons, New York, 1951.
- Maestri, A. Hydroacoustic Simulation of Antenna Radiation Characteristics. Melpar, Inc., Falls Church, Virginia, Technical Report TP-1-26, 1961.
- Moore, R. K. Normal Incidence Reflection of Dipole Radiation from a Plane Interface. Sandia Corp. Tech. Memo 199-56-14, Sept., 1956.
- _____. Radar Design Using Acoustical Simulation as a Tool. University of New Mexico, Engineering Experiment Station Report EE-22, April, 1959.
- Morse, P. M. Vibration and Sound. McGraw-Hill Book Company, New York, 1948.
- Quinlan, D. L. Comparison of Pulse and FM Radar Altimeters Based on Terrain Return Theory. University of New Mexico, Engineering Experiment Station Report EE-56, May, 1961.
- Randall, R. H. An Introduction to Acoustics. Addison-Wesley, Cambridge, Mass., 1951.
- Rice, S. O. Mathematical Analysis of Random Noise. Selected papers on noise and stochastic processes, edited by Nelson Wax. Dover Publication, S262, 1954.
- Schelkunoff, S. A. and Friis, H. T. Antennas, Theory and Practice. John Wiley and Sons, New York, 1952.
- Tatarski, V. I. Wave Propagation in a Turbulent Medium. Russian translation by R. A. Silverman. McGraw-Hill Book Company, New York, 1961.

Hunter, J. B. 1891-1900
Jordan, E. 1891-1900

Langhans, J. 1891-1900
Mearns, J. 1891-1900

Moore, J. 1891-1900
Newcomb, J. 1891-1900

Orin, J. 1891-1900
Rice, J. 1891-1900

Schubert, J. 1891-1900
Tate, J. 1891-1900

Wells, J. 1891-1900
Zeller, J. 1891-1900

Adams, J. 1891-1900
Baker, J. 1891-1900

Cole, J. 1891-1900
Foster, J. 1891-1900

Gibson, J. 1891-1900
Harris, J. 1891-1900

Kimball, J. 1891-1900
Lambert, J. 1891-1900

Mason, J. 1891-1900
Nelson, J. 1891-1900

Oliver, J. 1891-1900
Parker, J. 1891-1900

Reynolds, J. 1891-1900
Stewart, J. 1891-1900

Tucker, J. 1891-1900
Vanderbilt, J. 1891-1900

Wright, J. 1891-1900
Young, J. 1891-1900

Allen, J. 1891-1900
Brown, J. 1891-1900

Clark, J. 1891-1900
Davis, J. 1891-1900

Evans, J. 1891-1900
Fisher, J. 1891-1900

B. PERIODICALS

- Booker, H. G. and Gordon, W. E. "A Theory of Radio Scattering in the Troposphere," Proc. IRE, No. 38, 1950, p. 401-412.
- Buckingham, E. "On Physically Similar Systems; Illustrations of the Use of Dimensional Equations," Phy. Rev., Vol. 4, No. 4, 1914, pp. 345-76.
- Campbell, N. "Dimensional Analysis," Phil. Mag., Vol. 47, 1924, pp. 481-94.
- Edison, A. R., Moore, R. K., and Warner, B. D. "Radar Terrain Return Measured at Near-Vertical Incidence," IRE Trans PGAP, Vol. AP-8, No. 3, May, 1960, pp. 246-54.
- Fricker, S. J., et al. "Computation and Measurement of the Fading Rate of Moon-Reflected VHF Signals," N.B.S. Jour. of Res., Vol. 64D, No. 5, Sept.-Oct., 1960, pp. 455-65.
- Katz, I. and Spetner, L. M. "Polarization and Depression Angle Dependence of Radar Terrain Return," N.B.S. Jour. of Res., Vol. 64D, No. 5, Sept.-Oct., 1960, pp. 483-86.
- Lane, A. L. "Design Techniques for a High Frequency Transducer with a Wide-Beam Searchlight Pattern," Jour. Acoust. Soc. of Am., Vol. 25, 1953, p. 697.
- Lyytikainen, H. E. "An Analysis of Radar Profiles over Mountainous Terrain," Photogrammetric Engineering, Vol. 26, No. 3, June, 1960, pp. 403-12.
- Meyer, E. "Experiments on CM Waves with Acoustic Techniques Made in Gottingen," Jour. Acoust. Soc. of Am., Vol. 30, No. 7, July, 1958, pp. 624-32.
- Moore, R. K. and Williams, C. S., Jr. "Radar Terrain Return at Near-Vertical Incidence," Proc. IRE, Vol. 45, February, 1957, pp. 228-38.
- Ritt, R. K. "The Modeling of Physical Systems," IRE Trans. PGAP, Vol. AP-4, No. 3, July, 1956.
- Ruark, A. E. "Inspectional Analysis: A Method which Supplements Dimensional Analysis," Jour. Elisha Mitchell Sci. Soc., Vol. 51, 1935, pp. 127-33.

Bockert, H. G. and ...
 in the ...
 Backingham, E. ...
 of the ...
 No. ...
 Campbell, W. ...
 1924 ...
 Eason, A. R. ...
 Return ...
 1924 ...
 Flicker, S. J. ...
 Flying ...
 Jour. of ...
 pp. ...
 Katz, I. and ...
 Andie ...
 Jour. ...
 pp. ...
 Lane, A. I. ...
 Transacted ...
 Jour. ...
 Lyster, H. ...
 Monks ...
 1924 ...
 Meyer, E. ...
 Made in ...
 No. ...
 Moore, R. K. ...
 at ...
 February ...
 Rice, R. K. ...
 1924 ...
 Rusk, A. E. ...
 Spoken ...
 Mitchell ...

Sinclair, G. "Theory of Models of Electromagnetic Systems,"
Proc. IRE, Vol. 36, No. 11, Nov., 1948, pp. 1364-70.

Tolman, R. C. "The Principle of Similitude," Phy. Rev.,
Vol. 3, No. 4, 1914, pp. 244-55.

Weinstein, M. S. "On the Failure of Plane Wave Theory
to Predict the Reflection of a Narrow Ultra Sonic
Beam," Jour. Acoust. Soc. of Am., Vol. 24, No. 3,
May, 1952, pp. 284-87.

Wheelon, A. D., "Radio-Wave Scattering by Tropospheric
Irregularities," N.B.S. Jour. of Res., Vol. 63D,
No. 2, Sept.-Oct., 1959, pp. 205-33.

Standard Oil Co. of New York
From 1911

Thomas, R. C. 1911-1912
Vol. 1, No. 1, 1911

Wheeler, W. D. 1911-1912
No. 1, 1911
May, 1911

Wheeler, W. D. 1911-1912
No. 1, 1911
May, 1911

Wheeler, W. D. 1911-1912
No. 1, 1911
May, 1911

Wheeler, W. D. 1911-1912
No. 1, 1911
May, 1911

Wheeler, W. D. 1911-1912
No. 1, 1911
May, 1911

Wheeler, W. D. 1911-1912
No. 1, 1911
May, 1911

Wheeler, W. D. 1911-1912
No. 1, 1911
May, 1911

Wheeler, W. D. 1911-1912
No. 1, 1911
May, 1911

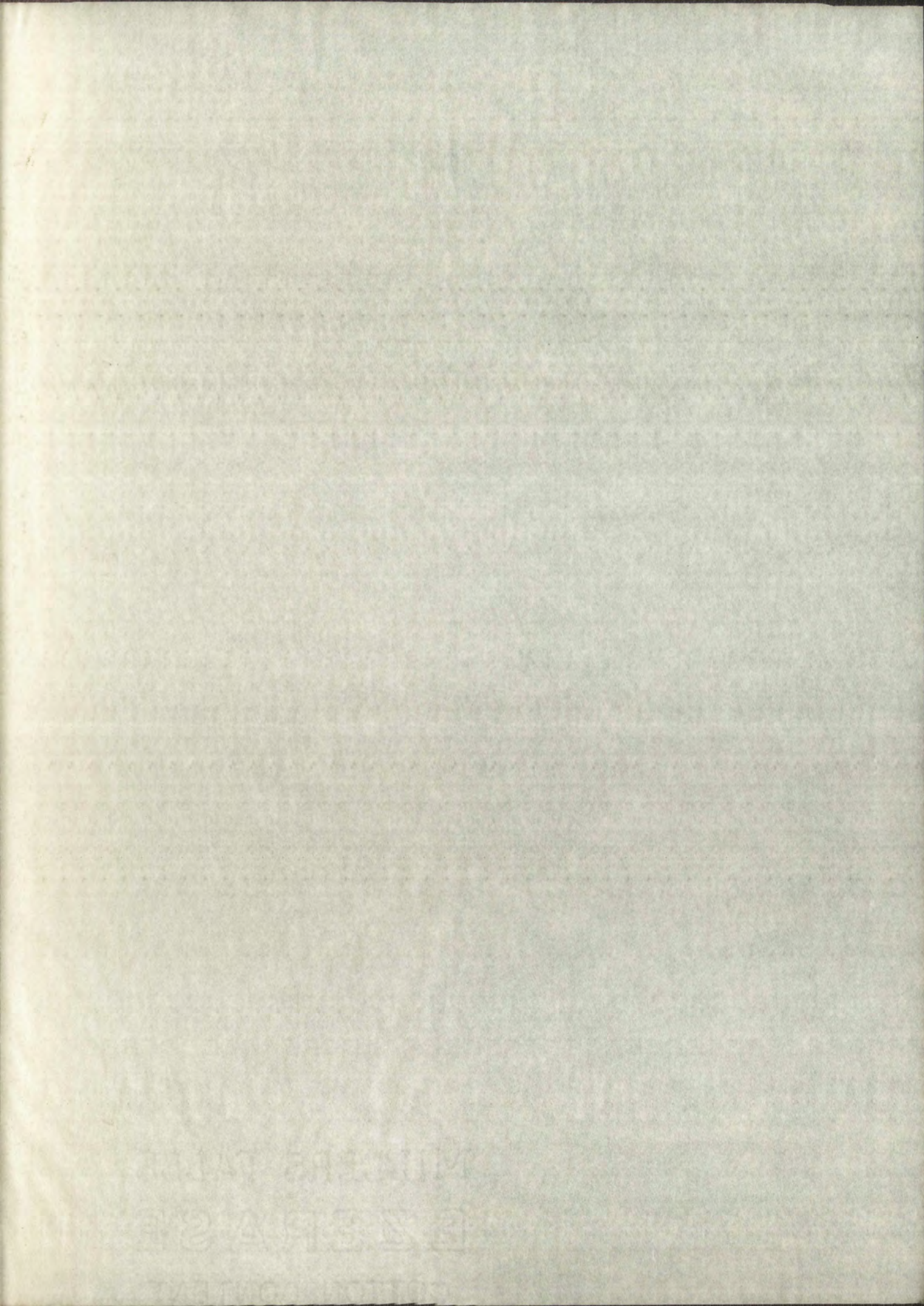
Wheeler, W. D. 1911-1912
No. 1, 1911
May, 1911

Wheeler, W. D. 1911-1912
No. 1, 1911
May, 1911

Wheeler, W. D. 1911-1912
No. 1, 1911
May, 1911

Wheeler, W. D. 1911-1912
No. 1, 1911
May, 1911

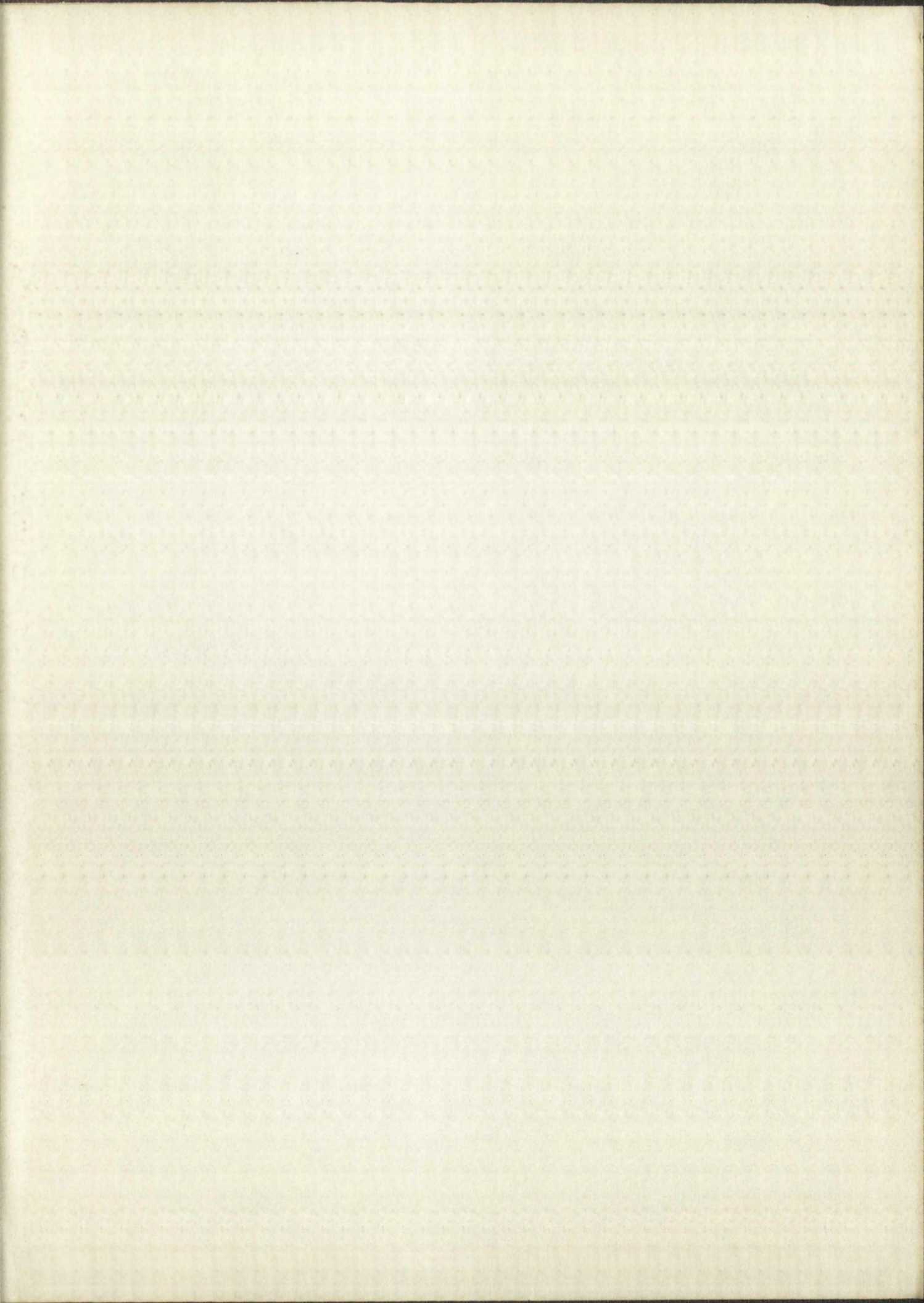
Wheeler, W. D. 1911-1912
No. 1, 1911
May, 1911

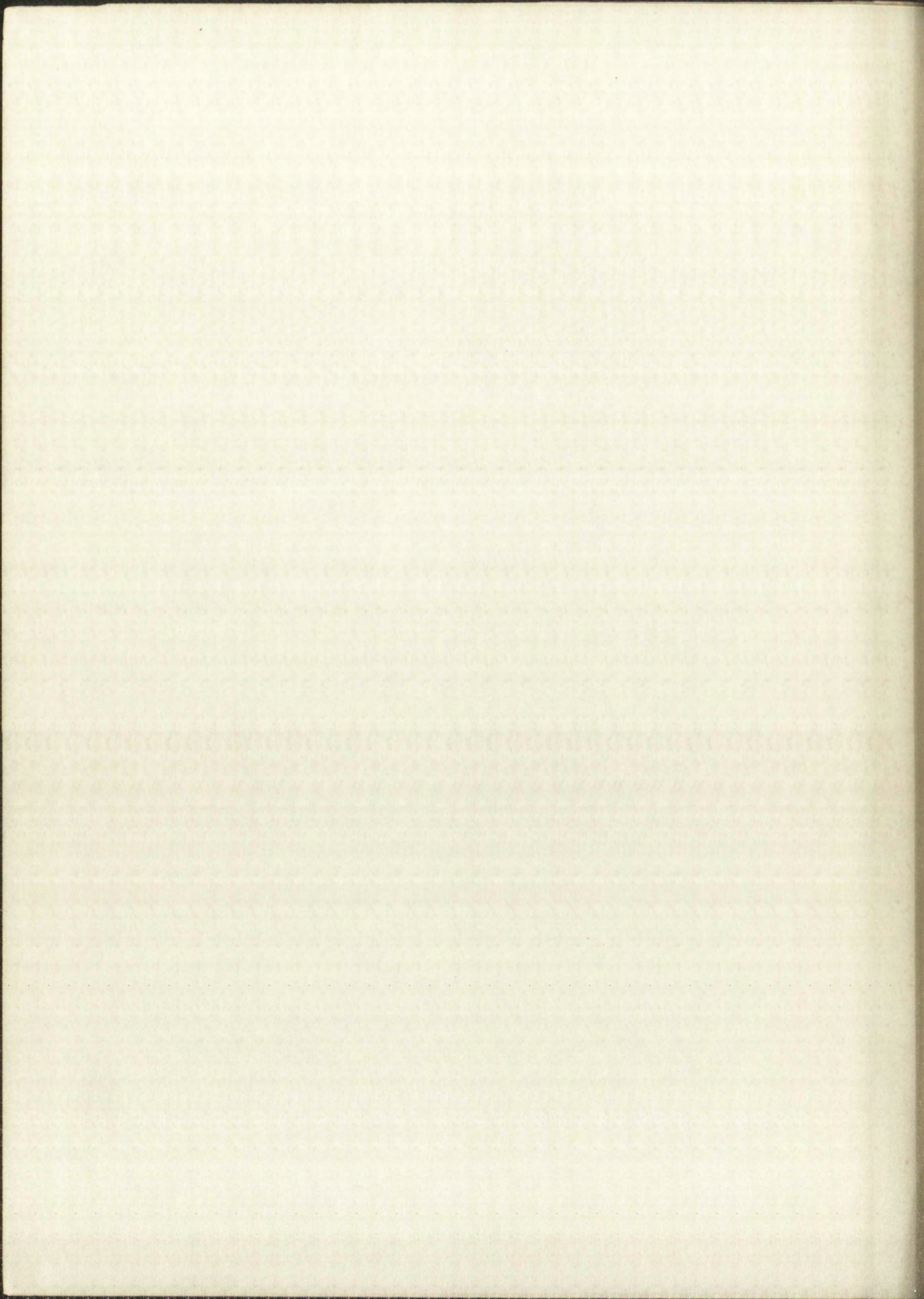


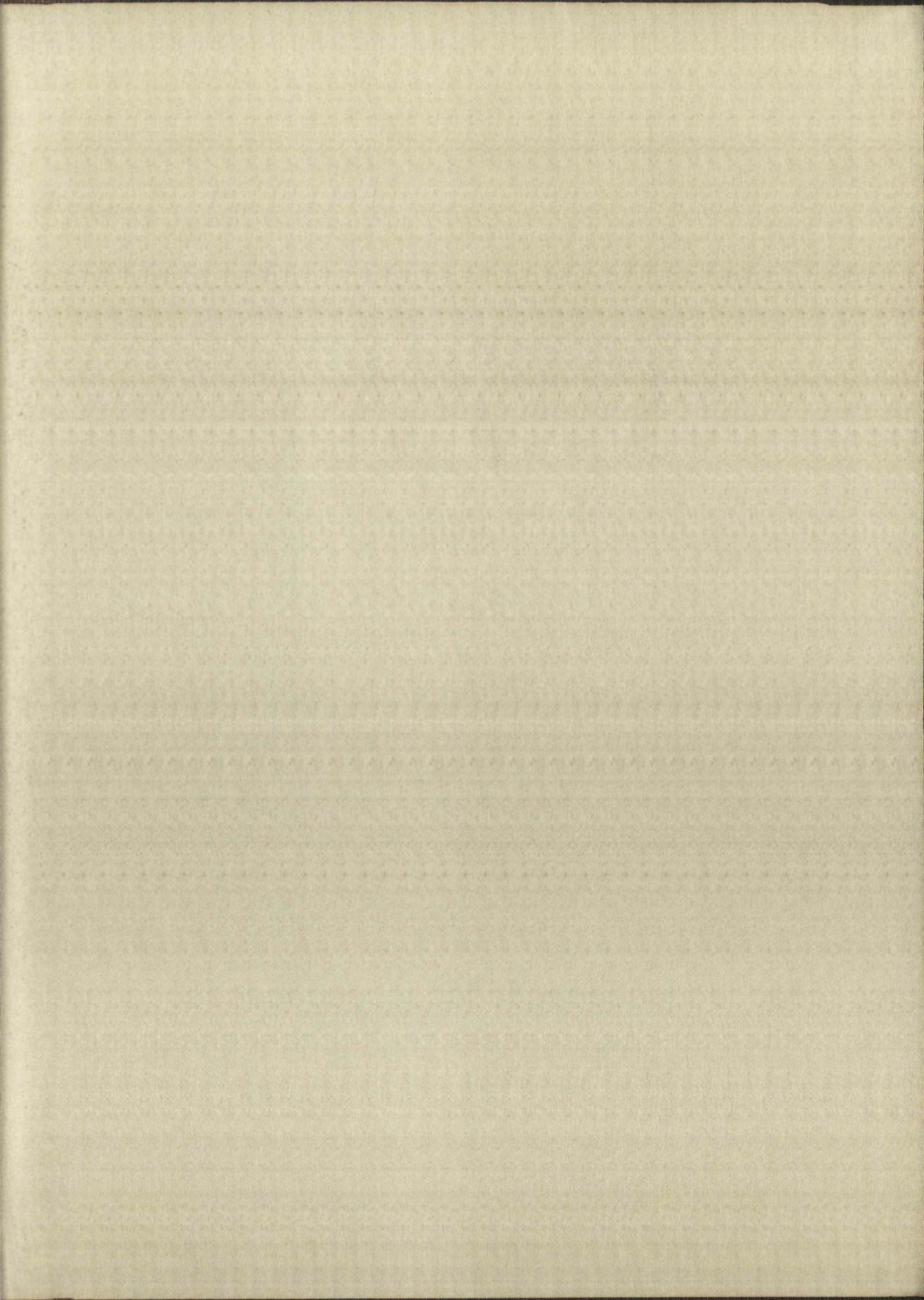
MILLERS FALLS

ERASER

COTTON







IMPORTANT!

Special care should be taken to prevent loss or damage of this volume. If lost or damaged, it must be paid for at the current rate of typing.

DATE DUE					
AUG - 6 RECD					
FEB 28 1985					
MAR - 2 RECD					
DEC 17 1965					
NOV 29 RECD					
GAYLORD					PRINTED IN U.S.A.

